BIOCHEMICAL BASIS OF TEXTURAL SOFTENING IN MANGO DURING RIPENING

A Thesis submitted to the

UNIVERSITY OF MYSORE

for the award of the degree of

Doctor of Philosophy

in

BIOTECHNOLOGY

by

H. M. YASHODA, M.Sc.

Department of Biochemistry and Nutrition

CENTRAL FOOD TECHNOLOGICAL RESEARCH INSTITUTE

Mysore - 570013, India

July 2003

SOFTENING IN MANGO DURING RIPENING

A Thesis submitted to the

UNIVERSITY OF MYSORE

for the award of the degree of

DOCTOR OF PHILOSOPHY

in

BIOTECHNOLOGY

by

H. M. YASHODA, M.Sc.

Department of Biochemistry and Nutrition

CENTRAL FOOD TECHNOLOGICAL RESEARCH INSTITUTE

Mysore-570013, India.

July 2003

DECLARATION

I hereby declare that the thesis entitled **"BIOCHEMICAL BASIS OF TEXTURAL SOFTENING IN MANGO DURING RIPENING",** submitted to the **University of Mysore** for the award of degree of **Doctor of Philosophy** in **Biotechnology**, is the result of research work carried out by me initially under the guidance of Late **Dr. T. N. Prabha**, and subsequently under **Dr. R. N. Tharanathan,** Scientist, Department of Biochemistry and Nutrition, Central Food Technological Research Institute (CFTRI), Mysore-570013, India, during the period 1998 – 2003. I further declare that the results presented in this thesis have not been submitted for the award of any other degree or fellowship.

Date: **(H. M. YASHODA)**
Place: Mysore

Dr. R. N. Tharanathan, PhD
Deputy Director,
Department of Biochemistry and Nutrition

CERTIFICATE

This is to certify that the thesis entitled **"BIOCHEMICAL BASIS OF TEXTURAL SOFTENING IN MANGO DURING RIPENING",** submitted to the **University of Mysore** by **Miss. H.M. Yashoda** for the award of **Doctor of Philosophy** in **Biotechnology,** is the result of research work carried out by her in the Department of Biochemistry and Nutrition, initially under the guidance of Late **Dr. T. N. Prabha,** and subsequently under my guidance during the period 1998 – 2003.

Date:
Place: Mysore

(R. N. THARANATHAN)
Guide

Dedicated to..

my beloved parents and

my research mentor Dr. T. N. Prabha

Acknowledgements

I would like to express my deep sense of gratitude to my research guide, Dr. R. N. Tharanathan, Deputy Director, Department of Biochemistry and Nutrition, C.F.T.R.I., Mysore, for his inspiring guidance, constructive criticism and unstinted cooperation. His constant support and encouragement was invaluable in successfully completing this PhD program.

The major part of this research work was carried out under the guidance of Late Dr. T. N Prabha, Scientist, Department of Biochemistry and Nutrition, C.F.T.R.I. I wish to express immense gratitude and mournful tribute to her. Her motherly attitude, excellent guidance, constant help and encouragement made this work a reality. I will always cherish the academic freedom and friendly atmosphere I enjoyed in her laboratory.

I wish to express my sincere thanks to Dr. V. Prakash, Director, CFTRI, for providing me an opportunity to work in this institute.

I sincerely thank Dr. S. G. Bhat, Head, Department of Biochemistry and Nutrition, C.F.T.R.I., for providing the department facilities, and also for his advise and encouragement throughout this research work.

I am highly indebted to Dr. N. Bhagyalakshmi, for her invaluable help and guidance with the tissue culture work. I am also thankful to Dr. G. A. Ravishankar, Head, Plant Cell Biotechnology, for allowing me to use the departmental facilities for tissue culture studies. Thanks are also due to Dr. P. Srinivas and Mrs. Vijayalakshmi for their help.

I am grateful to the staff of Central Instruments and Facilities Services (CIFS) for all their help and assistance. Special mention is due to Mr. Kumar, Mr. Mukund, Mr. Shivaswamy and Miss Asha. I

would like to express my thanks to the staff of Horticulture Department, Mysore, for their help in providing fruit samples. Special thanks to the staff of SIF, IISc, Bangalore for NMR facility.

I am extremely thankful to all teachers and staff of our department for making my stay here a fruitful and memorable experience. Special thanks to Dr. K. Srinivasan, Dr. Jagannath Rao, Dr. Bhaskaran, Dr. Prasad Rao, Dr. Muralikrashna, Dr. Kalpana and Dr. Shylaja Dharmesh. Thanks are also due to Mr. Vijayakumar for the help in office work.

I extend my warm gratitude to all my friends and well wishers. I will always cherish their company and friendship. It gives me great pleasure to extend my thanks to my lab mates Mr. Prasanna, Mr. Jagdeesh. Special thanks to Nagamani, Beena, Indu, Sangeetha, Nirmala, Saby, Subba Rao, Harish, Bettadaiah and Kumaraswamy. Words cannot suitably express my sense of gratitude and indebtedness towards Mr. Venkatesh Hegde and Mr. Muralidhar Hegde for all the help and support.

Pranamas to my father Late H. M. Madaiah, whose blessings are the source of strength to me. I am privileged to have my mother Manjula and my family sharing my dreams and supportive throughout. Warm thanks to my sisters Jaya, Maheshswari, Sowbhagya, and my brothers Mahesh and Krishna, and my cousin Lakshmi for their patience and moral support.

Finally, I gratefully acknowledge the financial support in the form of junior research fellowship from the University of Mysore and senior research fellowship from the Council of Scientific and Industrial Research (CSIR), New Delhi.

H. M. Yashoda

CONTENTS

Abbreviations

ABA	abscisic acid
Ac	Acetyl
ACC	α-amino-2-cyclopropane carboxylic acid
AG	arabinogalactan
AIP	acetone insoluble powder
AIR	alcohol insoluble residue
Amu (m/Z)	atomic mass unit (mass/charge)
AT	*Agrobacterium tumefaciens*
BAP	benzylaminopurine
BP	boiling point
BSA	bovine serum albumin
CBB	Coomassie brilliant blue
CDTA	1,2-cyclohexaminediaminetetraacetic acid
CE	capillary electrophoresis
CM	carboxymethyl
cv.	cultivar
CWS	cold water solubles
2,4-D	2,4-dichlorophenoxyacetic acid
Da	daltons
DEAE	diethylaminoethyl
DMSO	dimethyl sulfoxide
DNS	dinitrosalicylic acid
EDTA	ethylene diamine tetraacetic acid
EFE	ethylene forming enzyme
FID	flame ionization detector
FT-IR	Fourier Transform detector
FW	fresh weight
GA	gibberilic acid
GalA	galacturonic acid
GC (GLC)	gas (liquid) chromatography
GC-MS	gas chromatography-Mass spectrometry
GPC	gel permeation chromatography
GUS	β-glucuronidase
HPLC	high performance liquid chromatography

HPSEC	high performance size exclusion chromatography
HWS	hot water solubles
IEC	ion exchange chromatography
kDa	kilo Daltons
Km	Michealis-Menten constant
LB	liquid broth
LEM	liquid embryogenesis medium
LMM	liquid maturation medium
Me	methyl
MEM	mango embryogenesis medium
meq	milli equivalents
MGM	mango germination medium
MMM	mango maturation medium
MMT	million metric tones
M_r	relative molecular weight
MS medium	Murashige and Skoog medium
MSC	methyl sulphinyl carbanion
NMR	nuclear magnetic resonance
NS	neutral sugar
PAGE	polyacrylamide gel electrophoresis
PBS	phosphate buffered saline
PG	polygalacturonase
PGA	polygalacturonic acid (pectic acid)
PME	pectin methyl esterase
PVP	polyvinyl pyrrolidone
PVPP	polyvinyl poly pyrrolidone
RG	rhamnogalacturonan
RID	refractive index detector
SAM	S-adenosyl methionine
SDS	sodium dodecyl sulphate
SE	somatic embryo
SEM	scanning electron microscopy
TFA	trifluoroacetic acid
Tris	Tris(hydroxymethyl) aminomethane
UA	uronic acid
X-Gluc	bromochloro-S-indolyl-β-D-glucuronic tetracyclohexylammonium salt

Synopsis

Mango (*Mangifera indica* Linn.), a dicotyledonous fruit of the family *Anacardiaceae*, is the most important tropical fruit of India,

grown commercially in more than 87 countries. It is popularly known as "*The King of Fruits*". Mango currently ranks fifth in total production among major fruit crops worldwide. The world production of mango is estimated to be 23.4 x 10^6 MT per anum. India ranks first in mango production, accounting for 54.2% of the total mango produced worldwide. In spite of being the richest source of quality mango varieties in the world, the fruit economy in India is far from satisfactory. One of the limiting factors is the relative short ripening period and post-harvest life. In addition, extensive textural softening during ripening leads to adverse effects upon storage. Thus, an in-depth understanding of the biochemical and physiological events occurring during ripening is essential to identify the crucial targets contributing to textural softening. Delaying the ripening-associated changes will lead to greater 'commercial value addition'.

Textural softening during fruit ripening is of commercial importance as it directly dictates fruit shelf life, its keeping quality and post harvest physiology, which is due to *in vivo* carbohydrate hydrolysis during ripening by respective carbohydrate hydrolases. The extent of depolymerization of various carbohydrate polymers during ripening is a direct index for their contribution towards textural softening. By implication, the corresponding hydrolases would be the targets for controlling the ripening process at textural level. Control or modification of fruit texture, and shelf life extension with retention of desirable organoleptic attributes in a ripe fruit is the ultimate goal in modern 'Fruit Biotechnology'. During ripening stony hard unripe mango becomes soft spongy ripe fruit. Ripening involves a series of biochemical processes including biosynthesis and partial or complete degradation of high molecular weight cell wall carbohydrates.

Tomato is the only fruit system studied for suppressed expression of key ripening specific enzymes related to textural softening where fruit ripening was manipulated at gene level to get firmer tomatoes with extended shelf life by individually suppressing ACC synthase and EFE at ethylene level, PG and PME at cell wall level, by antisense RNA technology. Suppression of ethylene biosynthesis resulted in overall control of the ripening process, which was triggered by exogenous ethylene-boost. Genetic manipulation at the textural level resulted specifically in "improved texture" in the transformed tomatoes, where PG suppression yielded firmer fruits, while PME suppression resulted in fruits with higher solid content. Pectin regulation at the cell wall level is the only aspect that is studied thoroughly in the context of textural softening during ripening so far. But, the participation of other equally important carbohydrates and their degrading enzymes both at cellular as well as at cell wall level in fruit softening during ripening is totally un-explored.

The earlier studies on mango fruit softening mainly focused on the post harvest physiology, especially, organic acid metabolism, fruit flavors volatiles, overall composition and gross changes in total pectin during ripening. However, detailed studies on the quantitative and qualitative changes of cell wall polysaccharides and their *in vivo* hydrolysis by corresponding hydrolases in relation to textural softening have not been carried out.

The aim of the present study was to understand the factors contributing to the textural changes in relation to carbohydrate degradation by respective hydrolases during ripening of mango and also, tissue culture and transformation studies on different genotypes of mango. This study was undertaken to pinpoint the new enzyme targets (hitherto not known) responsible for fruit softening,

which was studied at both substrate (water soluble and insoluble polysaccharides) as well as enzyme (respective hydrolases) levels. Some new hydrolases other than PG/PME, hitherto unexplored, were observed in mango fruit, which could serve as important targets for carbohydrate dissolution *in vivo*. Mango fruit, apart from being untouched for studies on textural regulation, is also a tough system for *in vitro* culturing and genetic transformation. The study also involves a successful attempt towards induction of somatic embryogenesis from nucellar and cotyledonary explants of mango and expression of GUS gene in somatic embryos from different genotypes of mango via *Agrobacterium tumefaciens* mediated transformation.

The main objectives of the present research were as follows:

1. To study the changes in some important biochemical components, specifically the carbohydrate degradation pattern during ripening of mango,
2. To purify and characterize the major water soluble pectic (CWS and HWS) and alkali soluble hemicellulosic polysaccharides from unripe and ripe mango pulp,
3. Screening for the various enzyme activities during ripening process,
4. To look into *in situ* mannan hydrolysis by the related hydrolases and to purify and study the properties of α-mannosidase, the most active glycosidase in mango (and banana), and
5. To induce somatic embryo maturation from nucellar and cotyledonary explants of mango and to express GUS gene via *Agrobacterium tumefaciens* mediated transformation in mango somatic embryos.

This thesis entitled “Biochemical basis of textural softening in mango during ripening” is presented chapter wise as detailed below.

Chapter I: General Introduction

This chapter provides an overview of the current knowledge on mango, with special reference to biochemical changes occurring during ripening, *in vivo* carbohydrate hydrolysis and the related hydrolases, various aspects of pectin regulation in fruits in the context of fruit ripening, with particular emphasis on textural softening, *in vitro* somatic embryogenesis and *Agrobacterium tumefaciens* mediated transformation studies. A brief background on ripening associated changes and fruit cell wall is also presented. At the end is highlighted the aims and scope of the present investigation.

Chapter II: Materials and Methods

This Chapter includes details about the chemicals procured, instruments used, materials obtained and various methodologies employed in the study. Spectrophotometric determinations, fractionation procedures, chromatographic techniques, homogeneity criteria and structural studies carried out are all described with relevant literature references.

Chapter III: Cell wall carbohydrates in ripening mango: Implications in softening

For the purpose of clarity, this chapter is subdivided into individual sections and the results are presented following a brief introduction.

Section 1: Textural softening in ripening mango: Changes in cell wall carbohydrates

Textural softening during ripening of mango resulted in the reduction of starch from 18 to 0.2%, cold water solubles from 0.76 to 0.62%, hot water solubles from 0.55 to 0.31%, pectin from 1.9 to 0.5%, hemicellulose from 0.8 to 0.2% and cellulose from 2 to 0.9%.

The content of total alcohol insoluble solids (including starch) decreased from 22 to 3%. Physiological loss in weight (PLW) was 10% and the pH increased from 2.8 to 5.1 at ripe stage. Concomitantly, total soluble solids (TSS, Brix) increased from 7 to 20% and total soluble sugars from 1 to 15%. Loss of cell structure integrity, cell wall thinning, increased intercellular spaces, loosening of cells and almost total disappearance of starch and dissolution of pectin from middle lamella and primary cell wall were evidenced by microscopic studies. Thermal characteristics and pasting properties of unripe mango starch were also studied. Most of the gluconeogenic enzymes increased significantly during ripening exhibiting highest activity at ripe stage, except for maleic enzyme, which remained constant through out. A significantly higher yield of carbohydrates was obtained from unripe material than from the ripe fruits. The loss of galactose and mannose from water-soluble polysaccharides, galactose and arabinose from hemicelluloses, uronic acid and rhamnose from pectic fractions and glucose from cellulose pointed out to *in vivo* solubilization of the respective polymers during fruit ripening.

Section 2: Changes in the profile of cold water soluble polysaccharides

The entire range of CWS polysaccharides of mango pulp was studied both at unripe and ripe stages. Eight fractions were resolved upon ion exchange chromatography (IEC) with differential gradient elution. A significant decrease in their levels from unripe to ripe stage was evident in most of the fractions except fraction I, which showed increased levels (11.3 to 25.6%) while fraction II showed only marginal increase from 86.8 to 88.4%. There was an extensive drop in the molecular weight of all the fractions. Sugar analysis revealed arabinose and galactose, and galacturonic acid (~20%).

Section 3: Changes in the profile of hot water soluble polysaccharides

The HWS polymers were resolved into 10 distinct fractions upon IEC. Two of them were major, which got eluted out in 0.15 M $(NH_4)_2CO_3$ and 0.15 M NaOH. Considerable drop in their levels (55.6 to 28.4 and 79.2 to 14.4 mg %) and molecular weight (3548 to 125 and 1995 to 794 kDa) from unripe to ripe stage was observed. Their sugar composition revealed arabinose and galactose.

Section 4: Changes in the profile of EDTA soluble pectic polysaccharides

Pectic polymers were resolved into neutral and two acidic fractions, the latter eluting with 0.05 and 0.10 M $(NH_4)_2CO_3$. The mg % drop in their levels was 60 to 7, 89 to 13 and 74 to 2, and molecular weight drop was 250 to 70, 1333 to 21 and 473 to 298 kDa for fractions I, II and III, from unripe to ripe stage, respectively. The results indicated extensive depolymerization of pectic polymers *in vivo*. Sugar composition by GLC analysis indicated fraction I to be arabinogalactan-type polysaccharide, while fractions II and III to be heterogalacturonans containing more than 62% galacturonic acid.

Section 5: Changes in the profile of alkali soluble hemicellulose polysaccharides

The alkali soluble hemicelluloses were separated into 9 peaks upon IEC. The major fractions were found in 0.10 M NaOH eluates. The mg % drop in their levels was 57.72 to 8.9% and 45.6 to 7.7% and the molecular weight drop was 2512 to 1000 and 2818 to 1122 kDa, for the major fractions IV and V from unripe to ripe stage, respectively. High levels of glucose and xylose indicated xyloglucan-

type of polysaccharide.

Section 6: Structural characterization of the major cold water soluble polysaccharides

The major CWS fractions were further purified by GPC and structural studies employing optical rotation, FTIR, permethylation followed by GC-MS and ^{13}C-NMR were done. Results revealed an arabinogalactan-type structure having 1→5 linked arabinan side chain, linked to 1→4 linked galactan main chain through 1→3 linkages.

Section 7: Structural characterization of the major hot water soluble polysaccharides

The GPC purified major HWS fractions were also shown to be arabinogalactan-type polysaccharides. FTIR spectra showed a few absorbances characteristic of pectic polysaccharides.

Section 8: Structural characterization of the major hemicellulose polysaccharides

The low positive specific rotation of the purified major fraction indicated the anomeric configuration of the main chain to be of β-type. Permethylation analysis revealed a xyloglucan-type molecule having 1→4 and 1→3-linked glucan main chain, which was further involved in extensive branching. Both arabinose and xylose constitute the side chain branch off residues, with xylosyl units being involved in additional branching.

Chapter IV: Carbohydrate hydrolases in ripening mango

The results are presented in three sections.

Section 1: Enzymes involved in carbohydrate hydrolysis in vivo

This section describes the screening for the entire range of carbohydrate hydrolases (~10 glycanases and 9 glycosidases) at different stages of ripening. Generally, the hydrolases showed increased activity during ripening, most of them showing a peak in activity around climacteric, while PME, an esterase showed a steady decrease in activity. Among glycanases, mannanase, galactanase and arabinanase were particularly high in mango while xylanase was very low. As for pectic enzyme, there was an inverse correlation, where the PG was highest, the PME was lowest. Cellulase, hemicellulase and amylase showed a steady increase in activity, while laminarinase (β-1,3 glucanase) exhibited a activity peak around climacteric stage. Among glycosidases, α-mannosidase activity was highest followed by α and β-galactosidase, β-glucosaminidase and β-glucosidase activities. In the *in vitro* study a slight activity was observed on the respective endogenous substrates.

Section 2: In situ mannan hydrolysis and the related hydrolases: a comparison with banana

The endogenous mannan solubilization in mango was studied. Drop in mannose levels from unripe to ripe stage in differentially fractionated polysaccharides of mango in comparison with that of banana was observed. Considerable mannan hydrolysis at the ripe stage in the hemicellulose, pectic and water-soluble fractions was observed. Both mannanase and α-mannosidase, implicated in mannan solubilization, exhibited a peak in the activity around climacteric stage of ripening. While in banana fruit, mannanase activity was very less, whereas α-mannosidase was found to be the major glycosidase.

Section 3: Purification and partial characterization of α-mannosidase

The α-mannosidase of mango (and banana) was resolved into two distinct peaks (isoforms I and II) on DEAE-Sephadex as well as GPC on Sephadex G-200. Isoform I was the major enzyme (80%) in both the fruits. They were thermally stable and showed more acidic pH optima of 4.8 as compared to banana, 5.8. The km for *p*NP α-mannopyranoside was much lower for the isoform I indicating a higher substrate affinity and therefore higher specific activity. They did not catalyze the hydrolysis of *p*NP-β-mannopyranoside. Interestingly, α-mannosidase of banana fruit acted on β-D-mannan. They were inhibited only to the extent of about 40% by Hg^{2+}, Cu^{2+}, Zn^{2+} and Mg^{2+} (at 1 μM level).

Chapter V: Induction of somatic embryos from explants of mango and expression of β-glucuronidase gene via Agrobacterium tumefaciens mediated transformation

This chapter deals with induction of somatic embryos from different explants of mango and transformation using *Agrobacterium tumefaciens*. A successful attempt on repetitive and proliferative somatic embryogenesis was achieved in different genotypes of Alphonso variety where the frequency for normal somatic embryogenesis was higher in nucellar explants than in cotyledonary explants. Media composition for further organization of embryogenic callus to embryos, their development, maturation and germination leading to the formation of shoot/root was developed. Each stage of embryogenic tissue, starting from proembryogenic cell masses to fully developed somatic embryo was tested for their amenability for genetic transformation, where both stage of the culture and genotype played a crucial role. Expression of β-glucuronidase (GUS) gene from immature embryos co-cultivated with *A. tumefaciens* was achieved and also observations were made on the susceptibility of mango seedlings to different strains of *A. tumefaciens*. High frequency

transformation was observed after infecting cotyledonary and nucellar explants with *A.tumefaciens* cultured with acetosyringone.

Chapter VI: Summary and Conclusions

This chapter gives a concise resume of the salient research findings derived from the study. Carbohydrate regulation at the cell wall level during fruit ripening is important in the context of fruit texture. In mango fruit, a significant drop in molecular weight as well as abundance in all the carbohydrate fractions at the end of ripening clearly indicates controlled depolymerization *in vivo*. Appearance of various cell wall-degrading enzymes seems to be important in tissue softening. *In vitro* somatic embryogenesis as well as expression of GUS gene in mango gave new leads.

Finally, the literature cited have been numbered and listed at the end of the thesis.

Chapter 1

General Introduction

Fruit is a seed receptacle developed from an ovary. This definition encompasses a very wide range of fruit types, which are generally classified into simple, aggregate and composite fruits. Mango (*Mangifera indica*) is a simple fruit belonging to the subtype drupe fruit, and contains a single large seed surrounded by fleshy mesocarp. Being commercially valuable food crops, fresh as well as processed fruits form an important part of our diet. Fruits provide useful food reserves and are an important source of essential mineral nutrients and vitamins, but they are generally low in protein and fat contents. The quality of a fruit is influenced by variety, and nutritional status and environmental conditions during growth of the parent plant. Fruits play a very important role in human nutrition, by providing additional source of energy, necessary growth factors, carbohydrates, dietary fibers and antioxidants, essential for maintaining normal health. Fruits also contain a very high percentage of their fresh weight as water. There is an ever-increasing demand for both improved quality and extended variety of fruits available.

Fruits are classified into tropical, subtropical and temperate fruits based on their distribution in different climates. Fruits can further be classified as either climacteric or non-climacteric based on the pattern of respiration and ethylene biosynthesis during ripening. For climacteric fruits, the respiration rate and ethylene formation is minimal at maturity and raise dramatically to a climacteric peak, at the onset of ripening, after which it declines (Tucker, 1993). Unlike the non-climacteric fruits, which are incapable of continuing the ripening process after their detachment from the parent plant, the climacteric fruits when harvested at mature stage can be ripened off the parent plant. Non-climacteric fruits produce very small quantity of endogenous ethylene, and do not respond to external ethylene

treatment and show a gradual decline in their respiration pattern and ethylene production, throughout the ripening process (Gamage and Rahman, 1999).

Mango - "The King of Fruits"

Mango (*Mangifera indica* Linn.), which is a dicotyledonous fruit belonging to the order sapindales in the family *Anacardiaceae*, originated in the Indo-Burmese region (Subramanyam *et al.*, 1975; Tjiptono *et al.,* 1984). The word 'mango' originated as early as 16th century from the ancient Tamil word 'mangos'. Mango is known to be the most important tropical fruit of Asia, grown commercially in more than 87 countries (Purseglove, 1972). Mango currently ranks fifth in total production among major fruit crops world wide (FAO, 1999). India ranks first among world's mango producing countries, accounting for 54.2% of the total mango produced worldwide.

Mango is the most important fruit of India, with more than a thousand varieties known so far (Iyer, 1991). Cultivation of mango in India covers an area of 12.2×10^6 hectares. Andhra Pradesh has the highest productivity, with 0.24×10^6 hectares dedicated to mango cultivation, and producing 2.9×10^6 MT per year. Uttar Pradesh, Bihar, Karnataka, Himachal Pradesh, Maharastra, Orissa, Tamil Nadu and West Bengal are the other major mango producing states. Most of the Indian varieties possess strong aroma and more intense peel coloration, characterized by attractive fragrance, delicious taste and high nutrition value, owing to high amounts of vitamin C, β-carotene and minerals (Sagar *et al.*, 1999). In 1998–1999 India exported 45.41×10^3 MT of mango as fresh fruits valued at 791.3 million rupees, and 455.49×10^3 MT of sliced and dried mango, valued at 18.2 million rupees. India exports fresh mangoes to more than 50 countries. Mango fruits have been utilized for long time at

every stage of growth, while the raw fruits are utilized for products like pickles, chutney or mango sauce, *amchoor* (raw mango powder) and green mango beverage (*panna*), the ripe ones are used in making pulp, juice, nectar, squash, mango leather, frozen and canned slices, jam, ready-to-serve beverages, mango puree, mango cereal flakes, mango powder, mango toffee and mango fruit bars (Singh, 1990).

The most important mango varieties cultivated are Alphonso (Badami), Banganapalli (Baneshan), Bangalora (Totapuri), Bathua, Bombay Green (Bhojpuri), chousa (Khajari), Dashehari (dasheri), Fajri, Gulabkhas, Himsagar, Kesar, Krishnabhog, Langra (Langarhi), Jamadar, Mallika, Mankurad, Mundappa, Mulgoa (Mulgoba), Neelam, Pairi (Paheri), Rajapuri, Suvarnarekha (Swarnarekha) and Vanraj (Knight, 1997; Salunkhe and Desai, 1984). Alphonso is the leading commercial variety and rated best in the world. It is known by different names in different regions, viz., Badami, Gundu, Khader, Appas, Happus and Kagdi. Mature mango trees produce upto 1000 inflorescence each with 500-6000 flowers (Fig. 1.1) (Clarke and Clarke, 1987). Fruit set is usually less than 10% and only 0.1-0.25% reach the harvesting stage (Purseglove, 1974). The fruit of Alphonso variety is medium to large in size, ovate oblique in shape with a prominent ventral shoulder and orange yellow in color, and each fruit weighing 225-325 g. The fruit is attractive to the consumer by its excellent fruit quality and good keeping quality. The fruits are characterized by thin skin, soft flesh with low fibre content and sweet aroma (Knight, 1997]. The flavor is captivating and the taste is of high quality with an excellent sugar/acid blend. Maharastra, Gujarat, Madhyapradesh and Karnataka are the major producers of this variety in India.

Figure 1.1 Mango: Inflorescence and fruits

The development of the mango fruit can be divided into 4 different stages (Singh, 1960):

1. The juvenile stage (upto 21 days from the day after fruit set) is the stage of rapid cellular growth.
2. Stage of maximum growth (21-49 days) is the stage of cell enlargement and maturity.
3. Maturation and ripening stage (49-77 days) is the stage of respiration climacteric and ripening process.
4. Senescence stage (77th day onwards) is the post ripening stage, which is prone for microbial attack followed by death and decay.

Compositional changes during development

The chemical composition of mango pulp varies with the location of cultivation, variety and stage of maturity. The major constituents of the pulp are water, carbohydrates, organic acids, fats, minerals, pigments, tannins, vitamins and flavor compounds (Table 1.1). During maturation of mango, the period of rapid growth is characterized by an increase in alcohol-insoluble solids; principally

starch accumulation takes place in the pulp-tissue. The rate of starch accumulation is rapid at the beginning of fruit growth and slows down later, but it continues to increase up to maturity. There is an increase from 1 to 14% in starch content in Alphonso mango during development (Leley *et al.,* 1943; Quintana *et al.,* 1984). At initial stages of fruit development no systematic trend was observed in the sugar content, but towards the end of maturity, both reducing and non-reducing sugars were found to be increasing (Mann *et al.,* 1974).

Table 1.1
Food value per 100 gm of ripe mango pulp

Calories	62.1-63.7 Cal
Moisture	78.9-82.8 g
Protein	0.36-0.40 g
Fat	0.30-0.53 g
Carbohydrates	16.20-17.18 g
Fiber	0.85-1.06 g
Ash	0.34-0.52 g
Calcium	6.1-12.8 mg
Phosphorus	5.5-17.9 mg
Iron	0.20-0.63 mg
Vitamin A (carotene)	0.135-1.872 mg
Thiamine	0.020-0.073 mg
Riboflavin	0.025-0.068 mg
Niacin	0.025-0.707 mg
Ascorbic Acid	7.8-172.0 mg
Tryptophan	3-6 mg
Methionine	4 mg
Lysine	32-37 mg

The soluble sugars of the fruit pulp consisted mainly of glucose, fructose and sucrose (Tandon and Kalra, 1983; Pandey *et al.,* 1974). Jain (1961) reported the presence of glucose, fructose and maltose, in addition found xylose in ripening mangoes. The total sugar content of mangoes varies between 11.5 and 25% (fresh

weight). Starch increases up to 15% of the fresh pulp of green, mature fruits. In developing mango fruits, acidity increased at early growth phase, reached a peak and then declined gradually until harvest (Wardlaw and Leonard, 1936). In Alphonso mango, the acidity reached maximum (4.2-4.4%) in about 7 weeks and declined slowly to around 2.7-2.8 at the time of harvest (Lakshminarayana *et al.,* 1970). Jain (1961) states that pectin increases from the fifth week of fruit set until the stone is formed; thereafter the pectin content falls. In the case of Dashehari mango cultivar, water-soluble pectins showed a steep rise after 70 days, reaching a maximum at 101 days of fruit growth (Tandon and Kalra, 1984). The ammonium oxalate-soluble fraction showed a similar increase during fruit growth. The alkali soluble fraction (protopectin) increased upto 70 days after fruit set but decreased thereafter until harvest. During ripening of the fruit, sucrose rose from 5.8 to 14.2% of the fresh weight, while the pH rose from 3.0 to 5.2. In the post-climacteric stage, the content of non-reducing sugars fell to 0.6% 10 days after the climacteric peak. Total acidity varied from 0.13 to 0.71% (as citric acid). Jain *et al.,* (1959) reported the presence of oxalic, citric, malic, succinic, pyruvic, adipic, galacturonic, glucuronic and mucic acids, together with two unidentified acids; Stahl (1935) noted the presence of tartaric acid. Citric acid is the major organic acid present in mango fruit.

Mango fruit contains 0.5-1% protein on a fresh weight basis (Lakshminarayana, 1980). Tandon and Kalra (1983) reported a decrease in the soluble protein content upto 44 days after fruit set, which increased again until 96 days. A Peruvian variety has an exceptionally high content, 1.57-5.42% of protein (Jain, 1961). The skin of Java grown fruit contains 1-2% protein and the pulp 0.6-1%. Pandey *et al.*, (1974) detected 12 amino acids during fruit growth. At

peak stage, only alanine, arginine, glycine-serine, and leucine-isoleucine were detected, while others were present in traces. At maturity their levels were predominant, which decreased during ripening, with the exception of alanine.

Pathak and Sarada (1974) reported that lipid content in peel and pulp of five mango varieties ranged from 0.75 to 1.7% and 0.8 to 1.36%, respectively. Selvaraj *et al.* (1989) reported that total lipid in seven commercial cultivars ranged between 0.26 and 0.67% at harvest. A major component of the pulp was reported to be a triglyceride, while mono- and di-glycerides were minor components (Gholap and Bandyopadhyay, 1975). The characteristic odor that appeared in the fruits during ripening is due to components of ester and carbonyl types, which are varietal specific. The major volatile components of mango are terpenes although several other hydrocarbons, esters and alcohols were also found to be present in ripe mango fruit (Hunter *et al.*, 1974; MacLeod and Gonzalez, 1982; Pino *et al.*, 1989). Siddappa and Bhatia (1954) reported that vitamin C content was maximum (300 mg/100 g) in Pairi variety in the early stages of growth although the ripe mango is an excellent source of this vitamin. Spencer *et al.* (1956) reported its downward trend from 88 to 22 mg % within 5-10 weeks after fruit set in Mulgoa, Pico, Amini, and Turpentine varieties of mango during growth. Gosh (1960) reported 36 mg of folic acid in 100 g of green fruit and Gopalan *et al* (1977) found 0.08 mg of thiamine (Vitamin B1) and riboflavin (Vitamin B2) and 0.09 mg of niacin per 100 g of ripe mangoes.

At the initial stages, there was a steep fall in peel chlorophyll, which slowed down at later stages of development and the pulp chlorophyll became negligible as the fruit approached maturity

(Tandon and Kalra, 1983). Total carotenoids and β-carotene remained very low initially and increased gradually as the fruits approached maturity and ripening. Sixteen different carotenoids were identified, of which β-carotene was found to account for 60% (Jungalwala and Cama, 1963). Increase in carotene was accompanied by a decrease in acid and an increase in sugar content. Some of the phenolic compounds identified in mango are gallic acid, indigallic acid, gallotannin, quercetin, isoquercetin, mangiferin, and ellagic acid (El-Ansari *et al.*, 1969; Rhodes, 1980) Ash content decreased during development with some increase near maturity, while crude fiber remained more or less constant (Kalra *et al.*, 1995).

Post harvest preservation of mango

Mango fruit is vulnerable to post harvest losses due to its high perishable nature. Storage and ripening of mango are beset with number of problems. Many factors, such as cultivar, stage of maturity, size grading, method of harvesting, handling, packaging and mode of transport, affect the storability of mango fruits. Most losses are caused by preventable transportation and inappropriate storage methods. The post harvest life of mango usually does not exceed 2-3 weeks and is limited by physiological deterioration of the fruit related to over-ripening and by pathogen infection and development leading to decay. Various methods of post harvest techniques have been employed to extend the shelf life of mango fruit and reduce losses, through inhibition of respiration and ethylene production, which slows deterioration and senescence (Shewfelt, 1986). These can be classified as physical and chemical methods, which include refrigeration or cold storage, polythene film packaging, wax coating, sub-atmospheric pressure storage, controlled atmosphere storage, modified atmospheric storage, irradiation, heat

treatment and use of various chemicals. A combination of these can also be adopted to extend the shelf life of the fruit (Kader, 1980).

The current storage techniques are expensive, and also not fully satisfactory (Nwanekezi *et al.,* 1994). Further, a variety of disorders including development of off-flavor can result if fruits are exposed to O_2/CO_2 concentrations below/above certain threshold levels (Kader *et al.,* 1989). Therefore storage and ripening of mangoes continue to be a challenging problem and needs attention. In recent years, with molecular-biology studies, 'Tomato biotechnology' took a new turn of events, wherein fruit ripening was manipulated at gene level, which is considered to be a very promising approach. Control of ripening process has been very successfully shown by antisense RNA technology to be possible where firmer tomatoes were obtained with extended shelf life by individually suppressing ACC synthase, ethylene forming enzyme (EFE), polygalacturonase (PG) and pectin methyl esterase (PME). One or more genes were identified and used in the 'sense' or 'antisense' orientation to extend the shelf life of commercially important fruits (Bansal, 2000). To control the post-harvest life of any fruit by molecular approach, a basic understanding of the events occurring during fruit ripening is thus essential.

Post-harvest physiology of mango

Since mangoes are generally harvested at a mature-green stage, post-harvest changes are principally concerned with events associated with ripening and senescence and with the effects of post harvest handling techniques, and accordingly post-harvest life of mango has been divided into three phases (Pantastico *et al.*, 1984):

a) Storage life (or Transportation life), which encompasses the period from harvest during which the fruit remains unripe and in a condition resistant to physical damage during normal handling,

b) Ripening period, which designates the period from harvest until the fruit attains the stage of maximum consumer acceptability. This period encompasses the storage life plus the final stage of ripening, and
c) Shelf life, which starts when the fruit is fully ripe and is the period in which fruit remains in an edible condition.

In general, mangoes take 6-14 days to ripe under ambient conditions, depending on the variety and environmental conditions and gradually become overripe and later. As a climacteric fruit, the period of ontogeny is characterized by a series of biochemical changes initiated by the autocatalytic production of ethylene and increase in respiration (Rhodes, 1980). Ripening results in the development of characteristic color, taste and aroma with desirable softening. Much work dealing with biochemical changes during ripening was expended to study the post-harvest physiology of mango fruit (Gomez-Lim, 1997; Hulme, 1971; Kalra *et al.,* 1995; Krishnamurthy *et al.,* 1971; Padmini and Prabha, 1997), specifically the organic acid metabolism (Selvaraj *et al.,* 1989; Shashirekha and Patwardhan, 1976), overall composition and gross changes in cell wall and total pectin during ripening (Brinson *et al.,* 1988; El-Zoghbi, 1994; Muda *et al.,* 1995; Roe and Bruemmer, 1981; Subramanyam *et al.,* 1975; Tucker and Seymour, 1991). However, considerable differences do exist between cultivars of same species (Selvaraj *et al.,* 1989).

Fruit ripening

The ripening process is concerned mainly with alterations in biochemical components already existing in the organ. Fruit ripening is a genetically programmed, highly co-ordinated and irreversible phenomenon involving a series of physiological,

biochemical and organoleptic changes that lead to the development of a soft, edible, ripe fruit with desirable quality. A spectrum of biochemical changes such as, increased respiration chlorophyll degradation, biosynthesis of carotenoids, anthocyanins, essential oils and flavor components, increased activity of cell wall degrading enzymes, and a transitory increase in ethylene production are instrumental for these changes involved during fruit ripening (Brady, 1987; Rhodes, 1980).

Ripening changes involve a multiplicity of biochemical pathways that affect all the cell compartments. The ripening of fruit is accompanied by the change in color of the fruit, which is caused by the degradation of the chlorophyll leading to unmasking of previously present pigments (Tucker and Grierson, 1987) and dismantling of the photosynthetic apparatus (Piechulla *et.al.,* 1985), synthesis of different types of anthocyanins and its accumulation in vacuoles (Medlicott, *et.al.,* 1986), and accumulation of carotenoids such as β-carotene, xanthophyll esters, xanthophylls and lycopene in the plastids (Lizada, 1993; Tucker and Grierson, 1987). The increase in sweetness, as a result of gluconeogenesis, hydrolysis of polysaccharides, especially starch, decreased acidity and accumulation of sugars and organic acids with an excellent sugar/acid blend are responsible for the taste development (Selvaraj *et al.,* 1989; Tucker and Grierson, 1987). The increase in flavour and aroma during fruit ripening is owing to the production of a complex mixture of volatile compounds viz., ocimene and myrcene (Lizada, 1993) and degradation of bitter principles, flavanoids, tannins and related compounds (Tucker and Grierson, 1987). The metabolic changes during fruit ripening include increase in biosynthesis and evolution of ethylene (Yang, 1985), *de novo* synthesis of enzymes

catalyzing ripening specific changes, and increase in respiration mediated by mitochondrial enzymes (Tucker and Grierson, 1987).

The ripening phenomenon is associated with loss of firmness, hydration of cell wall, changes in cell wall thickness, decrease in the structural integrity and increase in the intracellular spaces (Tucker and Grierson, 1987). The major textural changes resulting in the softening of the fruits are due to enzyme-mediated alteration in the structure and composition of cell wall, partial or complete solubilization of cell wall polysaccharide (pectins and celluloses, Tucker and Grierson, 1987), and hydrolysis of starch and other storage polysaccharides (Selvaraj *et al.*, 1989; Fuchs *et al.*, 1980). An increase in soluble but decrease in insoluble proteins was reported during ripening of mango fruits (Sharaf *et al.*, 1989). The changes in gene expression during ripening involves the appearance of new 'ripening-specific mRNAs (Tucker and Grierson, 1987) as well as tRNA, rRNA and poly (A^+) RNA and disappearance of some mRNAs and proteins. However, some mRNAs are found to remain constant throughout ripening and these changes are known to be activated by plant hormones (Gomez-Lim, 1997). Fruit ripening is controlled by ethylene, which is autocatalytically synthesized in small concentration prior to initiation of ripening, which in turn triggers the entire array of changes during ripening. An overview of biochemical events during fruit ripening, depicted in Fig. 1.2, shows a couple of control points at ethylene (1) and post-ethylene (2) levels.

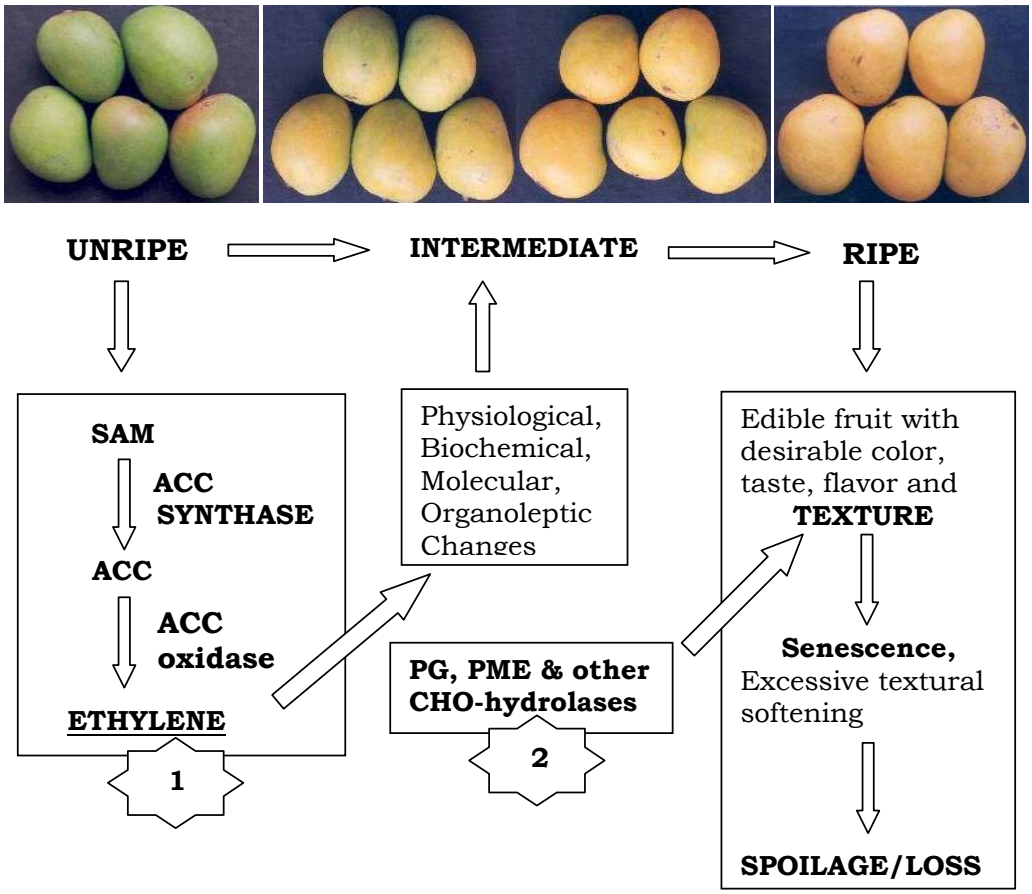

Figure 1.2
An overview of fruit ripening with particular emphasis on textural softening. (SAM = S-adenosyl methionine; ACC = 1-aminocyclopropane-1-carboxylic acid; PG = polygalacturonase; PME = pectinmethylesterase)

Textural softening during fruit ripening

The softening process is an integral part of the ripening of almost all fruits. Fruit ripening is associated with textural alterations and extensive softening of the tissue, which is dramatic in climacteric fruits. Texture is a major quality attribute that determines the acceptance of a fruit. Textural changes during ripening arise from a loss of turgor and/or enzymatic degradation of structural as well as storage polysaccharides especially starch (Tucker and Grierson, 1987). Depending upon their nature, inherent composition and organization, different fruits soften at different rates

and to varying extents (Tucker and Grierson, 1987). Fruits like mango, papaya, avocado, sapota and banana undergo drastic and extensive textural softening from stone hard stage to soft ripe stage, while fruits like apple and citrus fruit do not exhibit such drastic softening, although they undergo textural modifications during ripening.

Fruit texture

The texture of fruit can be attributed mainly to the structural integrity of the cell wall and middle lamella, as well as to the turgor pressure generated with in cells by osmosis and accumulation of storage polysaccharides (Jackman and Stanley, 1995). Change in turgor pressure, degradation of starch and cell wall polysaccharides determines the content of fruit softening. In citrus fruits, softening is mainly associated with change in turgor pressure, a process associated with the post-harvest dehydration and/or loss of dry matter. Starch is the bulk polysaccharide present in some fruits like mango and banana, and its enzymatic hydrolysis results in pronounced loosening of cell texture with development of sweetness, due to sugar accumulation. However, textural changes during ripening of most of the fruits are largely due to changes in the physicochemical properties of the cell wall (John and Dey, 1986), which is mainly due to the degradation of cell wall polysaccharides, endogenously controlled and catalysed by various carbohydrate hydrolases (Tucker and Grierson, 1987; Fischer and Bennett, 1991; Huber, 1983a). Subtle structural changes of the constituent polysaccharides may occur during fruit softening, without affecting much of the gross cell wall composition (Brady, 1987; Fischer and Bennett, 1991). Cell wall polysaccharides may undergo (partial) hydrolysis or solubilization resulting in changes in their molecular mass, solubility and degree of substitution of the individual

polysaccharides. Non-covalent changes in the cell wall are detected by the localized alteration in pH or ionic concentration, whereas covalent modification of the cell wall (polysaccharides) generally results from the enzymatic processes (Carpita and Gibeaut, 1993; Seymour and Gross, 1996; Fischer and Bennett, 1991; Fry, 1995).

The major classes of cell wall polysaccharides that undergo modifications during ripening are pectins, cellulose and hemicelluloses. In fruits, which are known for excessive softening, the cell wall is thoroughly modified by de-esterification and depolymerization, accompanied by an extensive loss of neutral sugars and galacturonic acid, followed by solubilization of the depolymerized oligo- and polysaccharides (Voragen *et al.,* 1995). Softening is normally accompanied by an increase in the concentration of soluble pectic polysaccharide. It appears that pectin polymers become less tightly bound in the cell wall during ripening, and the cell wall loosening involves hydrolysis of galactose-containing polysaccharides (Seymour *et al.,* 1989). Brinson *et al.* (1988) reported net loss of arabinose, galactose and galacturonic acid during cell wall degradation of mango.

Textural softening is of commercial importance as it directly dictates fruit shelf life and its keeping quality, which should be considered to avoid mechanical damage during harvesting and transportation. In general, the textural properties of fruits play a significant role in consumer acceptability. The increased interest in controlling the textural qualities of fruit stimulated further research on cell wall biochemistry, with particular reference to cell wall polysaccharides and their degradation (Van-Buren, 1979; Jackman and Stanley, 1995; Rizvi and Tong, 1997). The textural qualities of the fruit are attributed to its inherent composition, particularly the

cell wall composition. The 'Textural' characteristics are attributed to the mechanical properties of the final organ, which in turn depends on contributions and interactions at different levels of structure (Waldron *et al.,* 1997). Attempt to understand the molecular mechanism of fruit softening have directly led to the investigation of cell wall polymers, their compositional changes and the related cell-wall degrading enzymes during ripening (Knee, 1978).

Structural polysaccharides and textural changes

Plant polysaccharides, in general, are an extremely diverse set of biopolymers, which play a very important role as structural elements, such as celluloses, hemicelluloses, pectins; reserve polysaccharides such as, starch and galactomannan; gel formers, such as gums and mucilages; and physiological information carriers such as antigens. Fruit polysaccharides, upon their degradation *in situ*, play a crucial role in textural softening during ripening.

Plant polysaccharides play a major role in storage, mobilization of energy and in maintaining cell and tissue integrity due to their structural and water binding capacity. Polysaccharides from different sources vary in their chemical-biological, physico-chemical, and structural-functional characteristics (Tharanathan *et al.,* 1987). Cell wall polysaccharides differ widely in their physical and nutritional properties (Aman and Westerland, 1996). They regulate utilization of other dietary components in the food. Recently plant polysaccharides have emerged as important, bioactive natural products exhibiting a number of biological properties, such as regulating gene expression and host-defense mechanism, which includes release of enzymes and proteins involved in the generation of elicitor-active oligonucleotide fragments form the cell wall.

Carbohydrate hydrolysis during ripening

Fruit softening mechanism is determined by the molecular changes occurring in cell walls during ripening, which can be analyzed by either polymers released during ripening or changes in total wall material and these observed changes can then be correlated with the enzyme activities present in the tissue and with the action of these enzymes on isolated cell walls. Polysaccharides are polymers in which many monosaccharides of various types are covalently linked by glycosidic bonds. The glycosidic bond is formed between hemiacetal or hemiketal of one monosaccharide (glycosyl donor) and a hydroxyl group of the succeeding monosaccharide (glycosyl acceptor or aglycone) with the elimination of water. Polysaccharides are classified as homo- or hetero-polymers, based on the type of constituent monosaccharide units present. Homopolymers are made up of only one type of monosaccharide unit, whereas heteropolymers have more than one type of monomeric units. In addition, another group called "glycoconjugates" is also included usually under the broad definition of carbohydrates. Glycoconjugates include; a) glycolipids, b) glycoproteins, and c) proteoglycans.

Starch

Starch, the major biopolymeric constituent of plants, occurs as characteristic semicrystalline insoluble granules of various shapes and sizes (Tharanathan, 1995). Apart from its energy contribution, the other important role of starch is to contribute to the texture and as a result, to the organoleptic properties of food. Chemically, starch is composed of two main components, namely amylose (Am) and amylopectin (Ap) and a minor third component known as the intermediate fraction, which is neither Am or Ap. The proportion of these components depends upon the type of starch, its maturity,

agro-climatic conditions and the type of cultivars. The characteristics of Am and Ap, mainly their molecular weight, degree of polymerization and linearity or otherwise affect their capacity to bind iodine and to attack by enzymes. Ap is a highly branched molecule consisting of a main chain of (1→4)-linked α-D-glucose residues with short chains of (1→6)-α-D-glucose-linked branches. During plant growth the average size, shape and chemical composition of starch granules may change. Starch is degraded by a variety of enzymes such as α- and β-amylases, glucoamylase, pullulanase, etc. to oligodextrins and glucose.

Pectins and pectic substances

Pectins are the prominent structural constituents of primary cell wall and middle lamella but major polysaccharides in middle lamella, along with some cellulose microfibrils, and all together contribute to the fruit texture, while they may be virtually absent in secondary walls (Van Buren, 1979). Pectin content varies from fruit to fruit and mango has been reported to contain 0.66-1.5% pectin (Nwanekezi *et al.,* 1994; Thakur *et al.,* 1997).

Tissue softening is attributed to enzymatic degradation and solubilization of protopectin, the insoluble, high molecular weight parent pectin into soluble polyuronides (Sakai *et al.,* 1993; John and Dey, 1986). Protopectin increases before physiological maturity but decreases during mango fruit ripening (Tandon and Kalra, 1984). Native pectin plays an important role in the consistency of fruit and also in textural changes during ripening, storage, cooking or irradiation and other processing operations. Pectins are likely to be the key substances involved in the mechanical strength of the primary cell wall and are important to the physical structure of the plant (Sirisomboon *et al.*, 2000). Their degradation during ripening

seems to be responsible for tissue softening, as reported for a number of fruits including tomato, kiwi, apple and bush butter (Seymour *et al.,* 1990; Redgwell *et al.,* 1992; De Vries *et al.,* 1984; Missang *et al.,* 2001a and b). Thus, elucidation of chemical structure of pectin is essential in understanding its role in plant growth/development and during ripening of fruits (Thakur *et al.,* 1997).

The edible portion of most plant foods i.e. fruit pulp or the mesocarp is composed of parenchymatous tissue consisting of cells that are ~50-500 μm across and polyhedral or spherical in shape. Parenchymatous tissues are thought to consist principally of calcium salts of pectic substances, which are deposited in early stages of the cell growth, specifically when the area of cell wall is increasing (Voragen *et al.,* 1995). Middle lamella is heat labile and their dissolution result in separation of plant cells. Ultrastructural studies in ripening fruits have also shown that cell wall breakdown was accompanied by dissolution of middle lamella and gradual dissolution of fibrillar network of primary cell wall (Pesis *et al.,* 1978; Ben-Arie *et al.,* 1979a; Crookes and Grierson, 1983; Jackman and Stanley, 1995). Deesterified pectins in the middle lamella are associated with calcium ions, and its removal usually leads to cell separation (Aman and Westerlund, 1996). The association involves binding of two or more polymeric chains, in the form of corrugated egg-box (Fig. 1.3), with interstices in which calcium ions are packed and coordinated (Grant *et al.,* 1973).

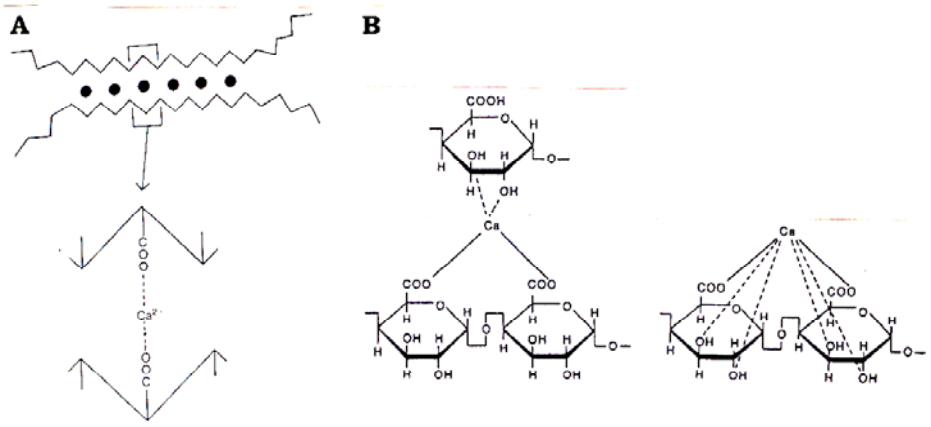

Figure 1.3
(A) The 'egg-box' model for the non-covalent linkage of adjacent acidic pectin polymers
(B) Binding of calcium to galacturonic acid (part of pectin)

Pectins are structurally diverse heteropolysaccharides containing partially methylated galacturonic acid residues; methyl esterified pectins, deesterified pectic acids and their salts; pectates and the neutral polysaccharides, which lack galacturonan backbone, i.e., arabinans, galactans and arabinogalactans, as illustrated in Fig.1.4 (Aspinall, 1980; Isherwood, 1970). The latter are usually associated with acidic pectins as side chains to the main galacturonan backbone (Aspinall, 1980; Doner, 1986). The primary pectin chain, i.e., α-D-galacturonans, consists largely of D-galacturonic acid linked by α (1→4) linkages (BeMiller, 1986), wherein the carboxyl groups are partially esterified with methanol and the hydroxyl groups are partially acetylated with acetic acid (Pilnik and Voragen, 1970). They occur mainly in chair L-form and as both C-1 and C-4 hydroxyl groups are on the axial position, the polymer formed is a *trans* 1,4-polygalacturonan (Sakai *et al.,* 1993). The degree of polymerization, degree of esterification, and the proportion of neutral sugar side chains are the principal factors contributing for heterogeneity (Rexova-Benkova and Markovic, 1976).

Arabinan

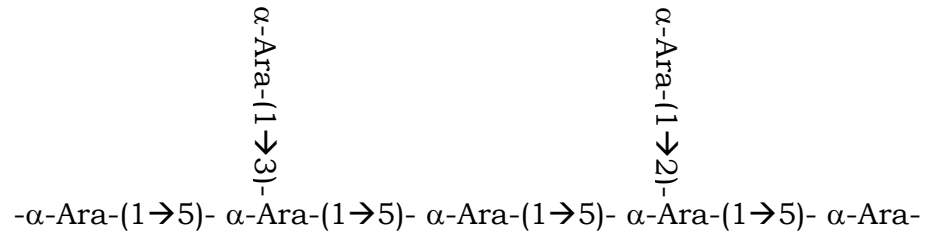

Galactan

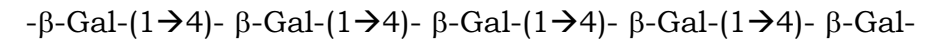

Arabinogalactan Type-I

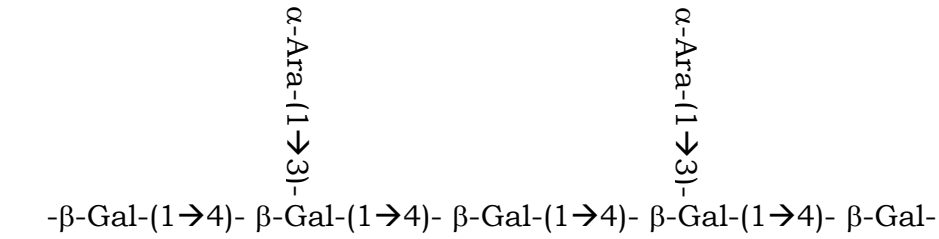

Arabinogalactan Type-II

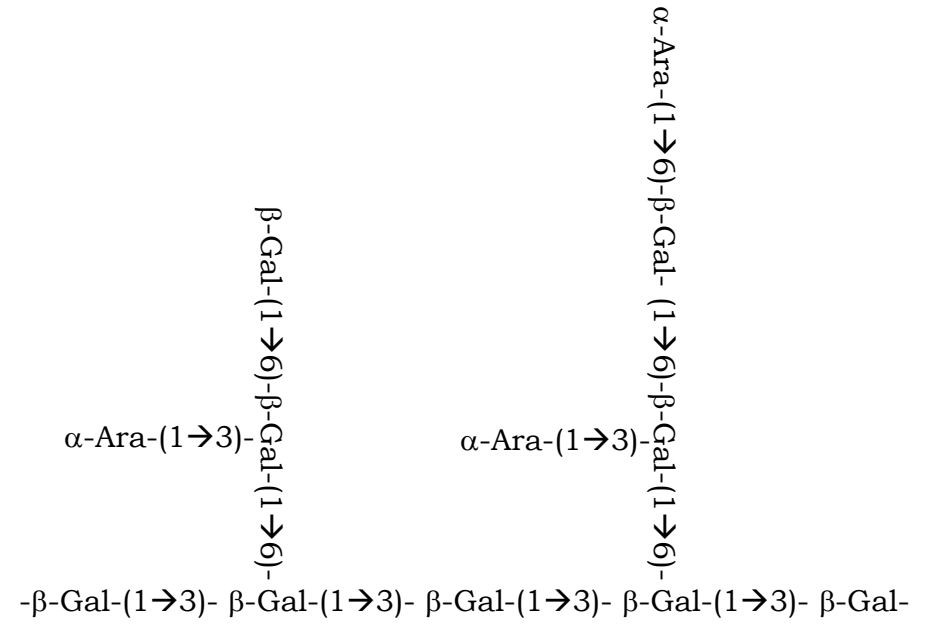

Figure 1.4
Structures of arabinans, galactans and arabinogalactans

Arabinogalactans (AG) are heteropolymers of D-galactose and L-arabinose residues (Fig. 1.4). Two structurally different forms of AGs are found in plants (Smith 1999; Whitaker, 1984). AG-I is a simple polysaccharide composed of chains of β-(1→4) linked D-galactose residues with single L-arabinose residues linked to O-3 of the galactose residues (Whitaker 1984; Smith, 1999). They have been isolated from different fruits including apple, kiwi, tomato and pineapple (De Vries *et al.,* 1983; Redgwell *et al.,* 1988; Seymour *et al.,* 1990; Smith and Harris, 1995). AG-II are complex and branched polysaccharides, consisting of chains of β-(1→3) linked D-galactose residues linked to chains of β-(1→6) linked D-galactose residues at the O-6 position of the main chain. The O-3 and O-6 positions of the side chains are in turn linked to terminal L-arabinose residues (Whitaker, 1984; Smith, 1999). Plant arabinogalactans are known for their multifaceted physiological and functional characteristics (Dey and Dixon, 1985). They possess freeze-inhibition, water holding and adhesive properties. Due to their specific carbohydrate binding properties, they may possibly affect cell-cell interaction (Dey and Dixon, 1985).

The primary cell wall pectic polysaccharides have a relatively higher proportion of neutral oligosaccharide chains on their backbone and these side chains are much longer than those of the pectins of middle lamella (Knee *et al.,* 1975; Selvendran, 1985; Sakai *et al.,* 1993). The side chains are concentrated in “hairy regions”. Highly esterified and slightly branched rhamnogalacturonan, the “smooth regions”, are present in middle lamella whereas highly branched rhamnogalacturonan, the “hairy regions” are present in primary cell wall. In plant cell wall, the side chains of the pectin molecules link to protein, hemicellulose and cellulose (Fig. 1.5).

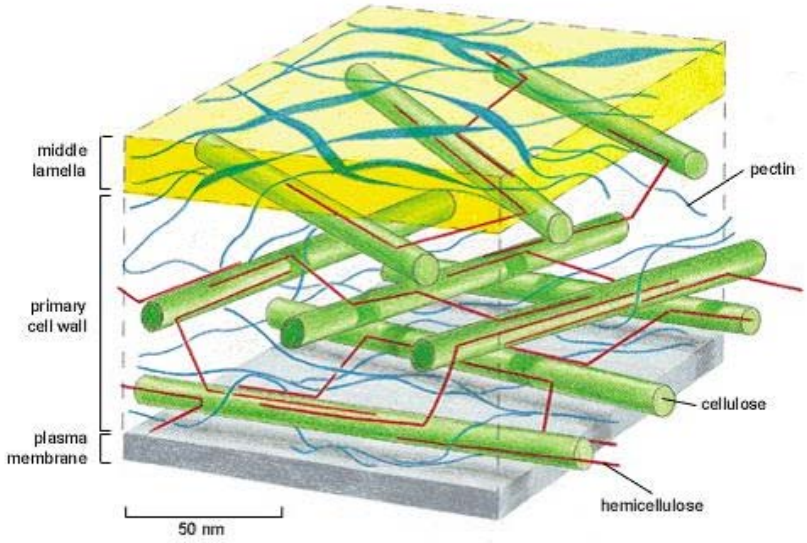

Figure 1.5
Schematic representation of structural aspects of pectins from middle lamella and primary cell wall interconnected with cellulose and hemicellulose

The non-sugar substituents of acidic and neutral pectins are essentially methanol, acetic acid, phenolic acids and amide groups, and contribute for their structural diversity (Mac Dougall *et al.,* 2001). Chelator-soluble pectins have high degree of methylation as well as high degree of acetylation than those extracted with alkali (Thomas and Thibault, 2002). Phenolic acids, especially ferulic acid and p-coumaric acid are found esterified to the non-reducing ends of the neutral arabinose/galactose residues. Ferulic acid facilitates oxidative cross-linking between pectins or with other polysaccharides in the cell walls, by the formation of diferuloyl bridges, which would limit wall extensibility (Brownleader *et al.,* 1999) and plays a significant role in growth regulation and defense mechanism (Fry, 1982).

Changes in pectic polysaccharides during ripening

During ripening fruits loose firmness, and unless the fruit is dehydrated, osmotic properties of the cell and the turgor pressure usually remain constant. While in plant tissues, it is assumed that turgor pressure alone is not contributing for the loss of firmness, instead it is the result of changes in the cell wall polysaccharides (Van Buren, 1979). Much work done related chemical changes in cell walls to fruit softening has been focused towards the characterization of changes in pectic substances (Krall and McFeeters, 1998). Being soluble in water, pectins can be deesterified and depolymerized mostly by enzymatic reactions. The retardation of textural softening by the addition of Ca^{++} ions is related to the ability of divalent cations to form calcium bridges between the pectic polysaccharide chains (Krall and McFeeters, 1998). In some, limited degradation of the pectic polymers might be due to the methylation of galacturonic acid groups (Voragen *et al.,* 1995). Loss of firmness during heat treatment of acid fruit has been attributed to hydrolysis of glycosidic bonds in cell wall polysaccharides (Doesburg, 1965). Arabinofuranosyl linkages are most labile, whereas the glycosidic linkages are most stable (Voragen *et al.,* 1995).

Changes in the proportion and characteristics of pectic substances are reported in many fruits. During ripening, the progressive loss of firmness is the result of a gradual solubilization of protopectin in the cell walls to form pectin and other products (Grierson *et al.,* 1981; Sakai *et al.,* 1993). Solubilization followed by depolymerization and deesterification of pectic polysaccharides is the most apparent change occurring during ripening of many fruits (Jimenez *et al.,* 2001; Missang *et al.,* 2001b). Pectins from ripe fruit exhibited a lower degree of esterification, a lower average molecular

weight and decreased neutral sugar content compared to pectins from unripe fruits (Huber and Lee, 1986).

The loss of neutral sugar side chains from the pectin is another important feature occurring during ripening. Out of 17 types of economically important fruits, 14 types showed a net loss of galactose and arabinose, from the cell wall during ripening, but no such loss was observed in ripening plum and cucumber fruits (Gross and Sams, 1984). A net loss of neutral sugars during ripening of pear, apple and tomato was reported (Ahmed and Labavitch, 1980a; De Vries *et al.,* 1984; Gross and Wallner, 1979). The mutant tomato fruit ('rin') containing little or no PG activity also showed substantial loss of galactose suggesting that this loss is not due to the action of PG (Gross and Wallner, 1979). These evidences suggest that other cell wall hydrolases, especially glycosidases play an important role in textural softening during ripening.

Celluloses and hemicelluloses

The cell wall is made up of cellulose fibrils imbedded in a matrix consisting largely of pectic substances, hemicelluloses, proteins, lignins, lower molecular weight solutes and water. Cellulose occurs naturally as an insoluble material, which is not easily degraded by enzymes. Celluloses are linear polymer of (1→4) β-D-glucosyl residues, which form the skeletal scaffolding of the cell wall through the formation of microfibrils, ~5-15 nm in diameter consisting of several thousand units (Jackman and Stanley, 1995). The glucan chains are assembled into a paracrystalline array, which are arranged in parallel to each other to form a microfibril (Smith, 1999). An apparent dissolution of the middle lamella and cell wall fibrillar network due to cellulolytic activity in ripening of avocado, pear and apple was demonstrated (Pesis *et al.,* 1978; Ben-Arie *et al.,*

1979). Ripening associated changes involving dramatic decrease in the content and molecular size of hemicellulose are reported in tomato (Huber, 1983a), strawberry (Huber, 1984), pepper (Gross *et al.,* 1986), muskmelon (McCollum *et al.,* 1989), kiwi (Redgwell *et al.,* 1991), melon (Rose *et al.,* 1998) and mango (Mitcham and McDonald, 1992). The amount of hemicellulose decreased steadily during ripening of many fruits including mango (Mitcham and McDonald, 1992).

Hemicelluloses are a distinct group of neutral sugar polysaccharides. They are the only cell wall polysaccharides that have the capacity to strongly bind the cellulose microfibrils through hydrogen bonding. Xyloglucans, mannans, xylans, galactan, glucans, arabinoxylans and glucuronoarabinoxylans are the major hemicelluloses found in plant cell wall.

Xyloglucans are the major hemicelluloses found (20%) in dicotyledonous primary cell wall. The basic structure consists of a backbone of β-(1→4) linked D-glucosyl residues with α-D-xylosyl side chains linked to O-6 of glucosyl residues (Fig. 1.6). Xylans are the major hemicellulosic components of monocots. They consist of a backbone of β-(1→4) linked D-xylosyl residues. Xylans are strongly associated with cellulose through the hydrogen bonding (McNeil *et al.,* 1984). Ripening associated changes involving dramatic decrease in the size of hemicelluloses are reported in tomato, pepper, strawberry and muskmelons (Huber, 1983a; Gross *et al.,* 1986; Huber, 1984; McCollum *et al.,* 1989). Degradation of arabinans by fungal arabinases and arabinofuranosidase has been reported (Voragen *et al.,* 1987).

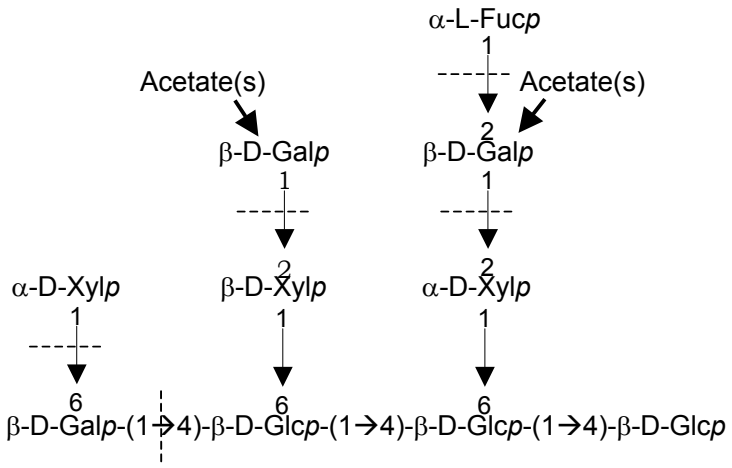

Figure 1.6 Structure of xyloglucan

Other important hemicellulosic components include mannans, which serve as food reserve polysaccharides and confer plasticity and the ability to stretch. In plant systems, mannans exist mostly in the β- configuration, either as hetero- or homopolymers. The β-D-mannan polymers (linear homoglycan of β-(1→4)-linked-D-manno pyranosyl unit) are documented in higher plant systems whereas α-D-manno-oligomers (oligosaccharides of α(1→4)-linked-D-mannose) exist as homo-or heterooligomers in oligosaccharides, glycoproteins and glycolipids. The main group of mannose containing polysaccharides from cell walls of higher plants are glucomannans, galactomannans or galactoglucomannans. A large group of galactomannans is present in seeds of leguminous plants, while gluco- and galactoglucomannas are the main hemicellulose component of coniferous woods. The main backbone of glucomannan consists of glucose and mannose linked via 1,4-β-glycosidic bonds with branches of single α-1,6 linked galactose residues. In galactoglucomannan, galactose residues are linked to mannose or glucose in backbone via 1,6-α-glucosidic bonds.

In fruits, it was noted that mannan type of substrates may undergo endogenous hydrolysis during ripening, thus contributing to textural softening either directly or indirectly. Mannose is an important component of the cell walls from the fruits such as apples and tomatoes (Knee, 1978; Wallner and Bloom, 1977). Stevens and Selvendran (1984) obtained a polysaccharide fraction from depectinated apple cell walls that contained a very high proportion 1,4-linked mannosyl residues.

Cell wall degrading enzymes in the context of fruit ripening

Plant cell wall polysaccharides are degraded by the plant's own enzymes during physiological developments such as fruit ripening, seed germination, and cell wall extension. In avocado, apple and pear, the middle lamella becomes dissoluted and the fibrillar structures sparse during softening (Pesis *et al.,* 1978; Ben-Arie *et al.,* 1979). Tomato fruit also shows loss of middle lamellar structure during ripening (Crookes and Grierson, 1983). These changes are considered to result from the action of cell wall degrading enzymes, essentially the hydrolases. Most of these enzymes, present in low levels, are constitutive through out fruit development and ripening (Tucker, 1993). But during ripening, generally all the hydrolases increase in activity, particularly cell wall hydrolases, showing maximum activity at climacteric stage.

A wide range of cell wall hydrolases are identified in fruit tissues (Huber, 1983b; Fischer and Bennet, 1991; Fry, 1995). The major carbohydrate hydrolases involved in polysaccharide dissolution *in vivo* can be broadly classified into of two types; viz, glycanases and glycosidases. Glycanases (glycanohydrolases) by definition are a class of enzymes cleaving high molecular weight polymers (polysaccharides) into shorter chains, while glycosidases

(glycohydrolases) generally act on shorter chain oligosaccharides, which may be homo- or hetero-oligomers or glycoproteins or glycolipids. The carbohydrate hydrolases may also be involved in the signal transduction by the way of deglycosylation. The entire range of these enzymes has been listed in Table 1.2.

Table 1.2
Different types of carbohydrate hydrolases in fruit systems

Glycanases	Glycosidases
Mannanase	α-mannosidase
Arabinanase	α-galactosidase
Galactanase	β-galactosidase
Polygalacturonase	α-glucosidase
Pectin methyl esterase	β-glucosidase
Cellulase	α-hexosaminidase
Hemicellulase	β-hexosaminidase
Amylase	α-xylosidase
Glucanase	β-xylosidase
Xylanase	α-arabinosidase
Rhamnogalacturonase	β-arabinosidase

Among cell wall hydrolases, pectin-degrading enzymes are mostly implicated in fruit softening. Pectic enzymes are classified, based on their mode of action on pectin and pectic substances into; PG, PME, pectate lyase and pectin lyase (Wong, 1995; Sakai *et al.,* 1993). The other enzymes such as arabinanase, galactanase and β-galactosidase act on the side chains of the galacturonide backbone, degrading the entire pectic substance. Increased solubilization of the pectic substances, progressive loss of tissue firmness and rapid rise in the PG activity accompany normal ripening in many fruits including tomato and banana (Tucker, 1993; Pressey, 1986a and b; Pathak and Sanwal, 1998).

Little is known about the enhancement of cellulase or hemicellulase activity in connection with fruit softening. Cellulase is a multienzyme system composed of several enzymes; endo-glucanase (EC 3.2.1.4), exo-glucanase (EC 3.2.1.91) and glucosidase (EC 3.2.1.21); (Sobotka and Stelzig, 1974). Endoglucanase hydrolyses the β-1,4-linked glucose residues at random positions. Exo-glucanase breaks the bonds at non-reducing end of the chain, producing glucose or cellobiose (dimers of β-1,4-linked glucose), whereas β-glucosidase splits cellobiose into glucose molecules. Cellulose levels in unripe fruit are generally low and increase dramatically during ripening (Awad and Yang, 1979). The loss of firmness, climacteric rise of respiration and ethylene evolution in ripening fruit was directly correlated with marked increase in cellulase activity (Pesis *et al.,* 1978; Roe and Bruemmer, 1981; Abu Sarra and Abu-Goukh, 1992). Cellulase has been implicated in softening process in tomato (Hobson, 1981). Cellulase activity was reported in several Indian mango cultivars (Selvaraj and Kumar, 1989), which increased during ripening especially in Alphonso. The progressive textural loss in 'keitt' mango was attributed to marked increase in cellulase activity (Roe and Bruemer, 1981).

Mannanase is a glycanase, which catalyses the hydrolysis of β-1,4-mannans, a polymer of mannose (Priya Sethu *et al.,* 1996; Prabha *et al.,* 2000). The role of an endo-β-1,4-mannanase in fruit softening is suggested by its ripening-specific accumulation. Pressy (1989) have characterized endo-β-mannanase in ripening tomato. McCleary and Matheson (1974) reported that the degradation of galactomannan involves endo-β-mannanase. It has been proposed that β-endomannanase is the rate-limiting enzyme controlling germination timing (Still and Bradford, 1997).

Xylanases (EC 3.2.1.8) catalyse the hydrolysis of β-1,4-xylan, β-1,4-D-endo-xylanase and β-1,4-D-exo-xylanase are reported as cell wall degrading enzymes in fruits such as avocado and banana (Seymour and Tucker, 1993; Prabha and Bhagyalakshmi, 1998). Xylanase, arabinanase and mannanase are localized both in soluble and bound form, which showed an increase during ripening. It was interesting to note that arabinanase, galactanase and mannanase and to some extent laminarinase were very prominent enzymes in mango fruit giving activity peaks at climacteric stage of ripening (Prabha *et al.,* 2000).

α-Amylase (EC 3.2.1.1) and β-amylase (EC 3.2.1.2) are the two amylases in plant tissues capable of metabolizing starch. α-Amylases hydrolyse the α-1,4-linkages of amylose at random to produce a mixture of glucose and maltose. β-Amylase attacks only the penultimate linkages and thus releases only maltose. Amylase activity increases to some extent during ripening (Tucker and Grierson, 1987). These enzymes are unable to degrade the α-(1→6) branch points of amylopectin, which are catalysed by amyloglucosidases. Mango and banana are the major starch containing fruits (~15 to 20%), where the starch was almost completely hydrolysed during ripening to free sugars, thus contributing to loosening of cell structure and textural softening.

Among glycosidases, the prominent enzymes found in ripening fruit were α-mannosidase, β-hexosaminidase and α- and β-galactosidases (Priya Sethu *et al.,* 1996; Suvarnalatha and Prabha, 1999). α-Mannosidase (EC 3.2.1.24), documented in very few fruit systems, acts on short chain oligomers (~8-10) of mannose units present either as glycoprotein, glycolipid or hetero-/homopolysaccharides. This enzyme partially degrades the pectic

and hemicellulosic components of the cell wall and is possibly related to breakdown of polysaccharides. Increased activity of α-mannosidase during ripening has been reported for tomato, grape, muskmelon, olive, pear and watermelon (Pharr *et al.,* 1976; Ahmed and Labavitch, 1980b; Nakagawa *et al.,* 1988; Fils Lyvaon and Buret, 1991; Heredia *et al.,* 1993; Burns and Baldwin, 1994). Interestingly, it not only showed an activity peak during ripening/softening of mango, banana, papaya, bell pepper and tomato but was also the most active enzyme amongst the glycosidases examined. The physiological role of most of the glycosidases during ripening is not known.

One novel approach to elucidate the role of enzymes in cell wall degradation and softening is to employ antisense RNA technology. This technology was one of the first molecular approaches used for delaying fruit ripening (Bansal, 2001). It has been possible to obtain firmer tomatoes with longer shelf life by specific suppression of PG gene expression with antisense RNA (Smith *et al.,* 1988). Pectin methyl esterase (PME) suppression resulted in increased solid content in tomato (Tieman *et al.,* 1992). The genes coding for PG, PME and other enzymes have been cloned in tomato (Gray *et al.,* 1992; Smith *et al.,* 1988; Tieman *et al.,* 1992) and other fruits (Bansal, 2001).

Tissue culture studies

As the traditional methods of breeding have almost reached a stagnation point in terms of productivity, obviously it needs to be supplemented by biotechnological methods. Propagation of plants through tissue culture, including sophisticated techniques of meristem culture and disease indexing is of immense use in making available healthy propagation materials. Besides this, tissue culture

techniques have direct application in large-scale production of plants in relatively smaller space, shorter time as well as rapid multiplication of valuable genotypes and improved plants. It also has added advantages such as the non-seasonal, almost round the year production of plantlets and conservation of germplasm for convenient international exchange.

One of the unsolved problems in biology is the process by which single cell (e.g. germ cells), or small populations of seemingly identical cells undergo the co-ordinated divisions and development that result in the formation of a complex, highly structured mature organism in which a great many different cell types may be present. This is the process of differentiation, and clearly involves the differential expression of genetic information. The main type differentiation seen in plant cell and tissue cultures are root formation and shoot production, collectively termed organogenesis. In few cases these processes occur simultaneously in an apparently co-ordinated manner and this phenomenon is called somatic or adventive embryogenesis. Numerous plant species have been reported to be capable of forming somatic embryo from diverse explants (Williams and Maheswaran, 1986; Kiyosue *et al.*, 1993). Somatic embryogenesis offers distinct advantages over regeneration via organogenesis (Williams and Maheswaran, 1986).

Protoplast Culture

Although protoplasts can be isolated from a range of tissues of almost any plant species, regeneration of plants from protoplasts is one of the most difficult *in vitro* techniques. Reports of success with recalcitrant woody species are limited and applications to tropical and subtropical fruit species are rare. The only exception is with citrus species. There have been reports of protoplast isolation of

non-woody tropical fruit species papaw (Litz, 1986a) and banana (Krikorian *et al.,* 1988), although sustained cell division was not achieved.

Micropropagation and somatic embryogenesis are currently being used with commercial tree species. Conventional breeding approaches with woody, perennial fruit crops have been complicated by generational cycles as long as 6 to 7 years, and by the absence of useful genetic markers. The advantages of efficient generation of tropical, perennial fruit trees from cell and tissue cultures in crop improvement programs have been reviewed by Kochba and Spiegel-Roy (1977). The propagation *in vitro* of superior, disease-indexed selections that are otherwise hard to propagate clonally would have an immediate effect on the production of many tree crops. Mutant selection, the recovery of horticulturally useful somaclonal variants from cell and protoplast cultures, and the use of recombinant DNA may alter the breeding strategies for many tropical fruit crops. Unfortunately, the application of cell culture techniques to the improvement of woody, crop plants has been limited due to the absence of methods of regeneration from tissues of mature origin. Mango is a tropical fruit tree of great economic importance. Difficulties in establishing aseptic mango cultures from mature explants associated with contamination, recalcitrance and phenolic browning, greatly hinders the micropropagation of mango. Somatic hybridization via protoplast fusion could be an alternative to overcome these problems (Sofiari *et al.,* 1998).

Agrobacterium tumefaciens **mediated mango transformation**

Genetic transformation, developed for many plant species, is usually based on the delivery of defined foreign genes into plant cells, obtaining integration of the genes into plant genomes and observing

expression of the genes in the regenerated plants. Numerous DNA delivery systems have been reported. The preferred method of gene for dicots is *Agrobacterium*-mediated transfer. Co-cultivation of callus, suspension cultures or leaf discs with *Agrobacterium* has been used to successfully transform many species (Komari *et al.*, 1989), for example efficient systems have been described for major crop species such as potato (Visser *et al.*, 1991), tomato (McCormick, 1991) and sugar beet (Lindsey *et al.*, 1991). The successful application of plant transformation techniques is dependent on plant tissue culture protocols to regenerate transformed plants. Transgenic plants of a number of fruit species have been produced, including kiwi-fruit (Uematsu *et al.*, 1991), citrus (Vardi *et al.*, 1990), strawberry (Nehra *et al.*, 1990), grape (Mullins *et al.*, 1990), peach (Hammerslag *et al.*, 1989) and plum (Mante *et al.*, 1991).

Mango tissue seems to be relatively easily amenable to regeneration *in vitro.* Litz group has reported considerable success with somatic embryogenesis from cultures of mango. For example, *Agrobacterium* transformation was successful after co-cultivation of an embryogenic mango culture (Mathews *et al.,* 1992). Although it has a very long regeneration time, the prospects for gene transfer in mango seem quite good and encouraging.

Scope and objectives of the present investigation

Textural softening during fruit ripening is of commercial importance as it directly dictates fruit shelf life, its keeping quality and post harvest physiology, which is due to *in vivo* carbohydrate hydrolysis by respective carbohydrate hydrolases. Control or retention of fruit texture is the main objective of modern 'Fruit Biotechnology'.

The aim of this study was to identify the crucial carbohydrate polymers (substrate level) undergoing depolymerization during ripening with the respective hydrolases (enzyme level) involved in fruit softening process, and induction of somatic embryogenesis from mango nucellar and cotyledonary explants and expression of GUS gene in mango. It must be noted that such a study forms the basis for any further investigation at the gene level. So far, the literature reports on mango fruit focus more on post-harvest physiology, especially to deal with overall biochemical changes during ripening. However, the precise nature of carbohydrate polymers and the corresponding enzymes; their qualitative and quantitative changes during ripening of Alphonso mango in relation to textural softening has not been studied. Identification and characterization of the major carbohydrate polymers as well as their respective hydrolases during mango fruit ripening helps in identifying the crucial enzyme-polymer targets, which are involved in the softening process. This study on events that occur during ripening is essential for investigating systems in which the post-harvest as well as pre-harvest physiology of the fruits can be controlled. Cloning of specific genes into mango fruit with their antisense constructs would lead to knowledge base in ***'mango biotechnology'*** for developing ***'transgenic mango'***. Developing transgenic mango for important ripening specific genes is clearly the future program in the area of fruit ripening. Development of somatic embryogenesis from nucellar as well as cotyledonary explants of mango (Alphonso cv.) and expression of GUS gene via *Agrobacterium tumefaciens* serves as a basis for studies on antisense RNA technology for the major glycosidase for the improvement of fruit texture, in turn delay fruit ripening.

Accordingly, the main objectives of the present investigation were as follows:

1. To study the changes in some important biochemical components, specifically the carbohydrate degradation pattern during ripening of mango,
2. To purify and characterize the major water soluble pectic (CWS and HWS) and alkali soluble hemicellulosic polysaccharides from unripe and ripe mango pulp,
3. Screening for the various enzyme activities during ripening process,
4. To look into *in situ* mannan hydrolysis by the related hydrolases and to purify and study the properties of α-mannosidase, the most active glycosidase in mango (and banana), and
5. To induce somatic embryo maturation from nucellar and cotyledonary explants of mango and to express GUS gene via *Agrobacterium tumefaciens* mediated transformation.

Studies carried out in detail showed indeed a drastic drop in the molecular weight as well as the qualitative and quantitative nature of several polysaccharide fractions, concomitantly with a higher activity of β-mannanase and α-mannosidase in ripening mango. These two enzymes are reported in mango, for the first time. Taken together, this information was very useful in understanding the phenomenon of mango fruit ripening process, which results in textural softening of the ripened fruits.

Chapter **2**

Materials and Methods

Instruments used for various experiments

1. Beckman microzone cellulose acetate membrane electrophoresis, model R-101, Beckman, USA.
2. Buchi Rotavapor, Flash evaporator, model RE 111, Switzerland.
3. Capillary electrophoresis (CE), CE-56 model, Prince Technologies, Netherlands.
4. Centrifuges: Hermle- Z 320K; Remi-RC8; Sigma-202 C, Germany; HEROLAB, Uni Cen 15 DR refrigerated centrifuge, Wiesloch.
5. Differential Scanning Calorimeter, DSC (+) Rheometric Scientific, UK, Instrument equipped with thermal software version 5.40.
6. FT-IR Pellet maker, Delta press, Tetragon Scientific, USA.
7. FT-IR Spectrometer, Perkin-Elmer Spectrum 2000 equipped with windows 2.1 version, USA.
8. GC-15A, Gas chromatograph, fitted with flame ionization detector (FID) & electron capture detector (ECD), Shimadzu, Kyoto Japan.
9. GC-MS, Shimadzu mass spectrometer QP-5000, combined with GC-17A, Kyoto, Japan.
10. HPLC 6A Shimadzu equipped with UV and RI detectors and LC10A equipped with RI, fluorescence and photodiode array detectors.
11. HPSEC unit, Shimadzu HIC-6A systems controller equipped with RID-6A RI detector, SCL-6A systems controller and CR-4A Chromatopac integrator units fitted with E-linear and E-1000 μ-Bondapack columns (30 cm x 3 mm i.d.) connected in series.
12. Homogenizer, Sorvall Omni mixer, USA.
13. Julabo USR1- Ultrasonicator

14. Laminar flow clean air work station, Type-Horizontal, Model-278, Airflow control systems (Pvt) Ltd., Bangalore.
15. Light Microscope, Ernst Lietz Labovert, 520573, Wetzlar, GMBH, Germany; Inverted Microscope, Leica, WILD M3Z, Switzerland.
16. Liquid scintillation counter, LS 6500, multipurpose scintillation counter, Beckman, USA
17. LKB, Bromma, USA, fraction collector.
18. Mettler AE-100 digital balance.
19. Millipore membrane filters, Millipore Corporation, USA.
20. NMR, Brucker 400 MHz, Germany.
21. Pharmacia mini slab gel electrophoresis, model SE 250-10A-75, Hoefer Pharmacia Biotech Inc., CA, USA.
22. pH meter, Control dynamics, MODEL APX 175 E/C, Bangalore.
23. Polarimeter, Perkin Elmer, model 243, USA.
24. Rapid Visco analyzer, model 3D, Newport Scientific Instruments, Australia.
25. Rotary/gyratory shaker, New Brunswick Scientific, Edison, N.J., USA
26. Scanning electron microscope, model SEM 435 VP, Leo Electron Microscope Ltd. Cambridge, U.K.
27. Sugar refractometer, Bellingham and Stanley Ltd., Tunbridge wells, England.
28. Texture analyzer, Llyod Universal Texture Measurement Instrument, LR5K, Fareham, Hampshire, UK.
29. UV-Vis double beam spectrophotometer, Shimadzu, UV-160 A, Kyoto, Japan.
30. Virtis Freeze Mobile, model 12SL lyophilizer, USA.
31. Water bath with temperature control, Tempo, Instruments and equipments (I) Pvt. Ltd., Bombay.

Chromatographic columns

GLC analysis

GC column: OV-225 (3% on Chromosorb W (100-120 mesh) packed column (SS column, 5' x 1/8"), Pierce Chemical C0., Rockford, Illinois, USA.

GC-MS column: SP-2330 capillary column, 30 m x 0.32 mm i.d, 0.02 μ film coating, Supelco, USA.

HPLC analysis

1. E-linear (7.8 mm x 30 cm) and E-1000 (3.9 mm x 30 cm) columns, μ-Bondagel, Waters Associates, Milford, USA.
2. Shimpak-C_{18} column (4.6 mm x 250 cm) from Shimadzu Corporation, Tokyo, Japan.

Chemicals

From Sigma Chemicals Co., St. Louis, MO, USA.

Abscisic acid, acrylamide, agar, ammonium persulphate, bis-acrylamide, 6-benzyladenine, benzylaminopurine, blue dextran (20,00,000 Da), bromophenol blue, bromothymol blue, bovine serum albumin (BSA, 66,000 Da), CMC-carbodiimide (N-cyclohexyl-N-2-morpholinoethyl carbodiimide-methyl-p-toluenesulphonate), carbazole, Coomassie Brilliant Blue (CBB) G-250, CBB R-250, cytochrome C (12,300 Da), deuterium oxide, 2,4-dichlorophenoxyacetic acid, dialysis tubing (MW cut off 12000 Da), dinitrosalicylic acid (DNS), O-dianisidine, gelrite, gibberlic acid, iodomethane (methyl iodide), kinetin, metahydroxybiphenyl, molecular weight markers (14-94 kDa), ovalbumin (45000 Da), phenyl methyl sulfonyl fluoride (PMSF), polyvinyl pyrrolidone (PVP), polyvinyl polypyrrolidone (PVPP), potassium ferricyanide, ruthenium red, sodium azide, sodium borodeuteride, sodium borohydride, starch, TEMED (N,N,N^1,N^1-tetramethylethylenediamine),

trifluoroacetic acid (TFA), triphenylmethane and Tris (hydroxymethyl) methylamine [2-amino-2-(hydroxymethyl) propane–1,3-diol], Triton X-100.

Enzymes: Glucoamylase (E.C. 3.2.1.3) and glucose oxidase (E.C. 1.1.3.4) from *Aspergillus niger.*

Substrates: Arabinogalactan, carboxymethyl cellulose (12,300 Da), pectin (Citrus), galactan, galactomannan, galacturonic acid (GalA), glucan, glucose-fructose-fructose (gf_2), mannan, *p*NP substrates, polygalacturonic acid (PGA).

Ion exchange resins and gel matrices: Amberlite IR-120-P (8% cross-linked, 16-50 mesh), CM cellulose, DEAE–cellulose (0.86 meq/mL), DEAE-Sephadex A-50, Dowex 50 H^+, Dowex 1 OH^-, Sepharose CL-4B (4%, cross-linked) (fractionation range for dextrans 30,000–50,00,000 Da).

From Pharmacia Fine Chemicals, Uppsala, Sweden

SDS-PAGE M_r markers, Sephadex G-200, T series standard dextrans (T-10, T-20, T-40, T-70, T-150, T-500 and T-2000)

Other sources

Sugar standards (rhamnose, fucose, xylose, arabinose, glucose, galactose, mannose, maltose, meso-inositol), L-glutamine and antibiotics such as bialophos, kanamycin and timetin, were from ICN Pharmaceuticals Inc., Life Sciences group, Cleveland, USA. X-Gluc (Bromochloro-S-indolyl-□-D-glucuronic tetracyclohexylammonium salt) was from Scima R, USA. L (+) cystanium chloride and potassium bromide (spectroscopic grade) were from E-Merck, Darmstadt, Germany. Cellulose acetate membranes: Beckmann Instruments International, S.A., Geneva,

Switzerland. Crimper, decapitator and vials for methylation analysis were from Pierce Chemical Co., Rockford, Illinois, USA. Sep-Pak C-18 cartridges were from Waters Associates, Millford, USA. Termamyl was obtained from NOVO, Denmark, and Sodium hydride (99%) from Aldrich Chemical Co., Milwaukee, USA. Dimethyl sulfoxide, (UV spectroscopy grade) and bovine serum albumin (BSA) were from Sisco Research laboratories, Mumbai, India.

All other chemicals, organic solvents and acids (Analytical reagent, AR grade) were procured from E-MERCK (India) Ltd., British Drug House (India) Pvt.Ltd., Ranbaxy Laboratories Ltd., Qualigens Fine Chemicals and SD Fine Chemicals, Ltd.

All the reagent preparations, determinations and experiments were done using deionised double glass distilled water. Degassed double distilled water was used for ion exchange chromatography and gel permeation chromatography. Degassed triple distilled water was filtered through millipore membrane (Type HA, 0.45 μm) and used for HPLC, capillary electrophoresis and polyacrylamide gel electrophoresis.

Materials

Matured, freshly harvested, locally available varieties of mango *(Mangifera indica* cv. Alphonso and Malgoa), banana *(Musa paradisiaca)*, and papaya *(Carica papaya)*, were procured from orchards through a local dealer, and were washed thoroughly with tap water, rinsed with distilled water, and finally wiped with alcohol and stored at ambient temperature (room temperature) for normal ripening. Mango fruit pulp at various stages of ripening was used for various experiments. Freshly harvested fruits were taken immediately to denote unripe stage, while the subsequent stages of

ripening were picked up from the fruits kept for normal ripening. The four stages of mango ripening (Fig. 2.1) were as follows (determined subjectively by firmness measurements);

Stage I: Mature, unripe – stony hard, dark green

Stage II: Pre-climacteric – intermediate, light green

Stage III: Post-climacteric – intermediate, yellowish green

Stage IV: Ripe – soft, yellow

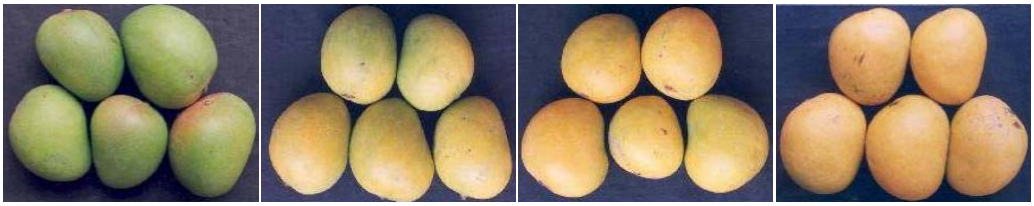

Figure 2.1
Different stages of ripening mango
(Stages I-IV from left to right, respectively)

Methods

Purification of solvents

Acetic anhydride, pyridine and phenol were purified by distillation in an all glass apparatus. Anhydrous ether was obtained by distilling over calcium chloride and the distillate was preserved in a brown bottle over metallic sodium wire. Anhydrous dimethyl sulfoxide (DMSO) was obtained by distilling over fresh calcium hydride, under vacuum (7 mm mercury) and the constant boiling fraction (B.P. 63°C) was collected and stored over molecular sieves (4 Å).

Analytical methods

Colorimetric Determinations

(1) Total carbohydrate by phenol–sulphuric acid method (Dubois *et al.*, 1956)

Total carbohydrate was determined by taking 0.5 mL of the sample in a test tube into which were added 0.3 mL of phenol (5%)

and 1.8 mL of concentrated sulphuric acid (sp.gr.1.84) and the contents were mixed thoroughly. After cooling the tubes at room temperature (~20 min), the absorbance was read at 480 nm against a reagent blank. Sugar content was determined by referring to the standard graph, prepared by using D-glucose or D-galacturonic acid (5-50 μg/0.5 mL).

(2) Uronic acid by metahydroxy biphenyl method (Blumenkrantz and Asboe-Hansen, 1973; Kintner and Van Buren, 1982)

Uronic acid was determined by taking 0.2 mL of the sample in a test tube and was allowed to cool in an ice cooled water bath for 10 min, into which was added 1.2 mL of concentrated sulphuric acid containing 0.0125 M sodium tetraborate and mixed vigorously. The above mixture was kept in a boiling water bath precisely for 5 min and cooled immediately in an ice cooled water bath. Then 20 μL of 0.15% metahydroxy biphenyl (prepared by dissolving in 0.5% NaOH) was added, vortexed vigorously and kept at room temperature for 20 min. The absorbance was read at 525 nm using a reagent blank. Uronic acid content was determined by referring to the standard graph, prepared by using D-galacturonic acid (0-15 μg/mL).

(3) Reducing sugar by dinitrosalicylic acid (DNS) method (Miller, 1959)

DNS (1 g) was dissolved in 50 mL of solution containing 30.0 g of sodium potassium tartarate and 0.4 M NaOH. The resulting solution was made upto 100 mL with water and filtered through Whatman No.1 filter paper and stored in a brown bottle. Reducing sugar was estimated by taking 1 mL standard sugar solution (100-1000 μg/mL), into which was added 1 mL of DNS reagent and tubes were kept in boiling water bath for 10 min. Tubes were cooled at room temperature and the color developed was read at 550 nm against a reagent blank.

(4) Reducing group by potassium ferricyanide method (Imoto and Yagishita, 1971)

Potassium ferricyanide (500 mg) was dissolved in 1 L of 0.5 M Na_2CO_3, filtered and stored in a brown bottle. To a test tube containing 750 µL of standard galacturonic acid (0-50 µg/mL), 1 mL reagent was added and kept in a boiling water bath for 15 min in a test tube covered by aluminium foil. After cooling to room temperature, the color was measured at 420 nm. The reducing sugar in the assay mixture was estimated by using standard slope value.

(5) Glucose by glucose oxidase method (Dahlqvist, 1964)

Glucose oxidase (125 mg, 2000 units) was dissolved in 50 mL of Tris-hydrochloric acid buffer (0.5 M, pH 7) in a 100 mL volumetric flask by gentle shaking. Aqueous peroxidase (0.5 mL, 1 mg/mL), O-dianisidine (0.5 mL, 10 mg/ mL in 95% ethanol) and Triton X–100 (1 mL, 10 mL in 40 mL of 95% ethanol) were added, mixed well and made upto the mark with Tris-HCl buffer and filtered through Whatman No. 1 filter paper. Glucose was determined by taking 0.25 mL of the standard glucose solution (0-50 µg/0.25 mL), to which was added 1.5 mL of Tris glucose oxidase reagent and incubated at 37^0C for 1 h. Absorbance was read at 420 nm against a reagent blank within 1h of color development.

(6) Protein by Bradford's method (Bradford, 1976)

Coomassie brilliant blue-250 (10 mg) was dissolved in 95% ethanol (5 mL) and to that 85% (w/v) phosphoric acid (10 mL) was added. The solution was made upto 100 mL with water and filtered through Whatman No. 1 filter paper to remove any undissolved residue. Standard BSA solution was prepared by dissolving BSA (5 mg) in 100 mL of water.

To a solution (0.2 mL) containing protein (2-10 μg) was added 0.8 mL Bradford reagent and mixed well before taking the absorbance at 595 nm of the blue color developed.

(7) Determination of starch (Hassid and Neufeld, 1964)

Sample (0.5-1.0 g) was taken in a conical flask and dispersed in 50 mL water. Termamyl (0.1 mL, heat stable α-amylase) was added and then kept in a boiling water bath for 10 min. After cooling, acetate buffer (pH 4.6) was added to 0.05 M concentration and equilibrated at 60^0C. To this glucoamylase (50 mg) was added and incubated in a shaking water bath at 60^0C for 2 h. The solution was filtered and made up to a suitable volume and the liberated glucose was determined by the TGO method. The glucose value multiplied by a factor 0.9 gave the starch content.

(8) Determination of moisture (Ranganna, 1977)

The sample (5 g) was taken in a dish, previously dried and weighed. The dish along with its lid was placed in an electric oven maintained at $105^0 \pm 1^0$C for 5 h, and later cooled in a desiccator and weighed. The process of heating and cooling was repeated, till a constant weight was obtained. The percentage moisture content was calculated using the formula,

Moisture (%) = [(Initial weight – Final weight) ÷ weight of the sample] x 100

(9) Determination of total soluble solids (TSS/Brix) (AOAC, 2000)

Homogenized mango pulp sample was applied or smeared uniformly onto the prism surface of sugar refractometer. The top lid was closed and viewed through the eyepiece. The demarcation line indicating the white and black background corresponds to the reading. The reading for both unripe and ripe mango pulp was recorded.

(10) Determination of viscosity (Rinaudo *et al.*, 1993)

Polysaccharide solutions of known concentrations (1.0% by weight) were prepared by dissolving polysaccharides in distilled water and making it up to the volume with water. The solutions were stirred for 30 min and undissolved particles were removed by centrifugation at 4000 rpm for 10 min. The viscosity of the solutions was measured by Oswald viscometer by noting the time taken to pass through the capillary tube maintained at $30^0C \pm 1^0C$.

Reduced viscosity (η_r) = $d_1/d_2 \times t_1/t_2$

Where, d_1 and d_2 = density of solution and solvent, respectively (both determined using specific gravity bottle)

t_1 and t_2 = Efflux time of solution and solvent, respectively.

Specific viscosity (η_{sp}) = $\eta_r - 1$

(11) Determination of pasting characteristics of starch by Rapid Visco analyzer (Tharanathan and Tharanathan, 2001; AACC, 2000)

Hot paste viscosity studies were carried out using Rapid Visco analyzer fitted with a thermoregulator set to 6^0C/min programming (both during heating and cooling). The sample (3 g) was suspended in water (24 mL) and placed in an aluminium can (70 mm x 38 mm) containing a plastic paddle. The viscosity values (RVU) were recorded throughout the temperature range of gelatinization followed by subsequent retrogradation. All the determinations were done in duplicate and the mean values were taken.

(12) Differential scanning calorimetry (DSC) (Russel and Juliano, 1983)

DSC analysis was carried out using DSC (+) Rheometric Scientific, UK, instrument equipped with thermal software version 5.40. Sample (5 mg) was accurately weighed into a small aluminium cup and water was added (1:3, w/w) to get approximately moisture

content of 50-80% (w/v). The cup was capped, re-weighed and heated from 30-100^{0}C for unripe mango starch. An empty pan was used as a reference. A minimum of two measurements was performed for the sample. Both gelatinization temperature and enthalpy were recorded by the use of indium as a standard.

(13) Determination of para-nitrophenol (*p*NP) (Priya Sethu *et al.,* 1996)

To 100 µL of standard *p*NP solution (0-1 µg/mL), was added 1 mL of 0.25 M Na_2CO_3 and the yellow color was measured at 420 nm against a reagent blank containing water and 0.25 M Na_2CO_3. The released *p*NP in the assay mixture was estimated by using the standard slope value.

Enzyme assays

Preparation of acetone Insoluble Powder (AIP) from mango and banana fruit pulp (Chan and Tam, 1982)

Mango and banana fruits, at four different stages of ripening (as described earlier) were peeled and grated using a grater. The pulp was diluted with 0.2 M sodium phosphate buffer (pH 7.0) containing soluble polyvinyl pyrrolidone (PVP, 0.1%) and the pH was maintained 7.0 by dropwise addition of 6 M NaOH. The pulp tissue was homogenized thoroughly for 1 min and immediately poured into a container having chilled acetone (-18^{0}C) and stirred well. The homogenate was filtered through cotton cloth and the residue was re-extracted twice in a similar way and air dried (acetone insoluble powder i.e., AIP) and stored in a freezer for further studies.

Enzyme extraction (Priya Sethu *et al.*, 1996)

AIP from mango and banana pulp, at different stages of ripening were used to extract various carbohydrate hydrolases using

different buffer systems as used for the assay (given below) in the presence of 0.25 M NaCl. The extraction of the enzyme was performed for 12 h at 4^0C with intermittent stirring. The resulting suspension was passed through four layers of nylon cloth and the filtrate centrifuged at 7000 rpm for 15 min. The clarified filtrate served as the crude enzyme extract and was dialysed against 10 mM sodium acetate buffer (pH 4.4, at 4^0C with three-four changes over a period of 24 h using fresh dialysis bags (MW cut off 12,000 Da) which were washed according to the instruction manual. The dialysed enzyme extract was used for the assay.

Glycanases (Pressy and Avants, 1976)

(1) β-Endomannanase

The activity was assayed by measuring reducing groups released from mannan. The reaction mixture contained enzyme extract (0.125 mL) and 0.1% (w/v) substrate in 1.0 mL of 100 mM sodium acetate buffer (pH 5.0) and incubated at 37^0C. One unit of enzyme activity is defined as the amount of enzyme that catalyzed the formation of 1 μM reducing group per h.

(2) Polygalacturonase

The reaction mixture consisted of 0.2 mL of 0.1 M acetate buffer (pH 3.8) and 0.125 mL of 0.25% polygalacturonic acid, and the pH was adjusted to 3.8 using 1 M NaOH. To this, 125 μL of enzyme was added and incubated at 37^0C for 2 h. The reaction was stopped by keeping the tubes in a boiling water bath for 5 min and estimated for the reducing sugar by DNS method. One unit of enzyme activity is defined as μM of galacturonic acid released in 1 h. Similarly, activities of galactanase and arabinanase were assayed using galactan and arabinogalactan substrates, respectively by following reducing group analysis by DNS method.

(3) Pectin methyl esterase (PME) (Hagerman and Austin, 1986)

PME activity was measured by the rate of citrus pectin de-methylation with decrease in pH at room temperature, as determined by a decrease in the absorbance at 620 nm. To 1mL of 0.5% citrus pectin, were added 0.15 mL of Bromothymol blue and 0.85 mL of water, mixed well and the pH was adjusted to 7.5, such that the absorbance of this reaction mixture at 620 nm was approximately equal to 0.28. To this, 0.1 mL of enzyme was added and the rate of decrease in 620 nm absorbance was recorded every minute. One unit of PME activity is defined as μM of acid released in 1 min.

(4) Cellulase (Abu-Sarra and Abu-Goukh, 1992)

The activity was assayed by measuring the reducing groups released from carboxymethyl cellulose. The reaction mixture contained 0.5 mL of 0.1% (w/v) CMC and 0.25 mL of 100 mM sodium acetate buffer (pH 5.0) into which 0.25 mL of enzyme was added and incubated at 37^0C for 2, 4, 6 and 12 h. One unit of enzyme activity is defined as the amount of enzyme that catalysed the formation of 1 μM reducing group per h. Similarly, the hemicellulase activity was assayed by using hemicellulose.

(5) Amylase (Bernfeld, 1955)

To 0.25 mL of starch solution (0.5%), 0.125 mL of enzyme was added and incubated at 37^0C for 120 min. The activity was measured by taking known volume of this solution for reducing group determination by DNS method.

Other glycanases like xylanase and glucanase (laminarinase) were assayed by using xylan and glucan substrates, respectively. The reaction mixture contained enzyme extract and 0.1% (w/v) substrate in 1.0 mL of 100 mM sodium acetate buffer (pH 5.0) and

incubated at 37^{0}C. One unit of enzyme activity is defined as the amount of enzyme that catalysed the formation of 1 μM reducing group per h.

Glycosidases (Priya Sethu *et al.*, 1996)

(1) α-Mannosidase

The reaction mixture contained 0.05 M sodium phosphate buffer (pH 6.6,100 μL), 20 mM *p*NP mannopyranoside (50 μL) and 50 μL of enzyme and incubated at 37^{0}C for 15 min. The reaction was terminated by adding 0.25 M Na_2CO_3 (1 mL) and the liberated paranitrophenol was measured at 420 nm. One enzyme unit is defined as 1 μM *p*NP released in 15 min.

(2) β-Galactosidase

The reaction mixture consisted of 0.1 M acetate buffer (pH 3.8, 100 μL), 13 mM *p*NP galactoside (50 μL) and enzyme extract (50 μL). After 15 min of incubation at 37^{0}C, the reaction was terminated by adding of 0.25 M Na_2CO_3 (1 mL) and the liberated paranitrophenol was measured at 420 nm. One enzyme unit is defined as 1 μM *p*NP released in 15 min. Similarly, assays were done for other glycosidases like galactosidase, glucosidase, xylosidase, arabinosidase, fucosidase and hexosaminidase.

Extraction and purification of α-mannosidase from mango and banana

The respective AIP at climacteric stage III of ripening were used for enzyme extraction at 4°C. AIP (10 mg) was homogenized with 0.05 M Na-Pi buffer (pH 6.6) containing 0.25 M NaCl in a Sorval mixer and kept at 4^{0}C for 12 h. The ratio of AIP to buffer was 1:10. The resulting suspension was filtered through four layers of nylon cloth and the filtrate was centrifuged at 7000 rpm for 15 min. The clarified filtrate (crude enzyme) was dialysed and used for further

purification.

Concentration of the enzyme extract (Pathak and Sanwal, 1998)

The dialysed enzyme extract was kept immersed along with the bag in saturated sucrose solution to get a concentrated enzyme extract, followed by a brief dialysis against 10 mM sodium phosphate buffer (pH 6.0) at 4^0C with three–four changes over a period of 24 h, to remove sucrose. This enzyme extract was further subjected to ion exchange purification.

Purification of the enzyme

DEAE-Sephadex A-50 chromatography

The ion exchange resin was washed with water to remove fines, and then treated successively with HCl (0.05 N) and NaOH (0.05 M). After each treatment, the pH was adjusted to neutrality by washing thoroughly with water. The regenerated material was suspended in NaCl (0.05 N), packed in a column (3.2 cm x 12.5 cm) with a bed volume of about 100 mL at a flow rate of 60 mL/h and excess NaCl was washed off with water.

The suitably concentrated enzyme extract was loaded on to the column and eluted with 20 mM sodium phosphate buffer (pH 6.0, 200 mL) followed by buffer containing stepwise (increasing) gradients of NaCl (0-1 M, 400 mL). Fractions (4 mL) were collected using a fraction collector and the protein concentration was monitored by reading absorbance at 280 nm. Enzyme activity in the fractions was assayed and active fractions were pooled separately into two different fractions, designated as Isoform I and Isoform II. The pooled fractions were dialysed extensively against buffer with three changes over a period of 12 h and concentrated using sucrose.

Gel permeation chromatography

GPC was performed on Sephadex G-200 gel matrix, swollen in 0.05 M sodium phosphate buffer (pH 6.0) and was packed into a long glass column (85 cm x 1.2 cm, 96 mL) at a flow rate of 12 mL/h. The void volume was determined by using pre-dialysed blue dextran (2,000,000 Da) and calibrated with protein MW markers; BSA (66,000 Da), Ovalbumin (45,000 Da) and cytochrome C (12,300 Da). The standard curve was obtained by plotting log molecular weight versus V_e/V_0; where, V_e=elution volume; V_0=void volume.

The partially purified Isoforms I and II were loaded separately on to the column and eluted with 0.05 M sodium phosphate buffer (pH 6.6) containing 0.05 M NaCl. 2.5 mL fractions were collected. The protein and enzyme activity of each fraction was determined as described earlier. The molecular weight of the purified enzyme was obtained from the standard curve. The active fractions were pooled, concentrated and fold purification was determined. The enzyme was stored in the freezer for further studies.

Enzyme properties

Optimal pH

The effect of pH on enzyme activity of purified enzyme isoforms was found using buffers sodium citrate buffer, pH 3.0-4.0; sodium acetate buffer, pH 4.0-5.6; sodium phosphate buffer, pH 5.7-7.2 and Tris-HCl buffer, pH 7.0-8.0, and incubating at 4^0C for 24 h. The enzyme activity was determined after knowing the optimum pH. Later the enzyme was added to the reaction mixture consisting of buffer of defined pH and substrate, and incubated at 37^0C and the absorbance was read at 420 nm.

Optimal temperature and thermal stability

The effect of temperature on the hydrolytic activity of the enzyme at optimal pH was assayed at different temperatures ranging

from 20-80^{0}C. The stability was measured by pre-incubating the enzyme with 0.1 M sodium phosphate buffer at different temperatures for 15 min. After incubation, the enzyme was immediately cooled and assayed for the remaining activity at optimal temperature. The temperature at which 50% of the activity is retained (Tm) was calculated. The activity of the untreated enzyme was used as the control (100%).

K_m and V_{max}

The Michaelis–Menton constants were determined by incubating the enzyme at optimum temperature with 0.1 M sodium phosphate buffer (optimum pH) containing different substrate concentrations. The kinetic parameters (K_m and V_{max}) were calculated by the double reciprocal Line Weaver-Burk plot.

Inhibition Study

The effect of metal ion (Ca^{++}, Mg^{++}, Fe^{++}, Mn^{++}, Zn^{++}, Cu^{++}, Cd^{++}, Hg^{++}) and EDTA on enzyme activity was studied by pre-incubating the enzyme in sodium phosphate buffer (optimum pH) in the presence of 0.1-1.0 mM of each metal ion for 30 min prior to the addition of the substrate and the remaining enzyme activity was assayed immediately.

Effect of product analogues on enzyme activity

Effect of product analogues on enzyme activity was determined by pre-incubating the enzyme with sodium phosphate buffer (optimum pH) containing 2.0 mM product analogues, such as galacturonic acid, galactose, glucose, mannose, fucose, rhamnose, arabinose and xylose for 20 min at 4^{0}C. The remaining enzyme activity was assayed immediately.

Substrate specificity

Substrate (synthetic) specificity of the enzyme was determined by incubating the enzyme with various *p*NP glycosides at 13 mM concentration. After incubation at 37°C for 15 min the *p*NP released was determined as mentioned earlier.

Activity on natural substrates

The activity on natural substrates like polygalacturonic acid (0.06%), pectin (0.06%), galactomannan (0.45%) and CMC (0.45%) was measured by incubating the substrates with the enzyme at 37°C for 7 h.

Activity on endogenous substrates

The activity on endogenous substrates (0.5-1.0 mg) was determined by incubating at optimum temperature for 7 h. Controls containing substrate without enzyme was also incubated simultaneously. The reaction was terminated by adding potassium ferricyanide reagent (1.0 mL), kept in a boiling water bath for 15 min and estimated the reducing sugar by DNS method.

Polyacrylamide gel electrophoresis

Native and SDS-PAGE was carried out using discontinuous buffer system as described by Laemmli (1970). The polyacrylamide gel (10% T) (containing 0.1% SDS for SDS-PAGE) was cast in 1.5 mm slab gel apparatus. The electrophoresis was carried out at 100 volts in 0.025 M Tris-0.3 M glycine buffer, pH 8.3 (containing 0.1% SDS as electrode buffer for SDS-PAGE). The protein was mixed with the sample buffer, pH 6.8 containing 10% (V/V) glycerol, (2% (w/v) SDS for SDS-PAGE), and 0.1% bromophenol blue. Samples were heated in a boiling water bath for 15 min and subjected to electrophoresis. The molecular weight markers were also treated similarly and

electrophoresed. The protein bands in the gel were visualized by staining with Coomassie brilliant blue G-250.

Enzymes related to gluconeogenesis

All extractions and centrifugations were done in cold (4^0C). Mango pulp (100 g) was homogenized in ~30 mL extraction medium of pH 8.5 containing sucrose (0.3 M), EDTA (10 mM), Tris (50 mM), potassium phosphate (10 mM), egg albumin (0.1%) and PVP (0.1%). The pH was maintained during homogenization with Tris/Sucrose. The homogenate after clarification was subjected to centrifugation at 10,000 x g for 20 min. The supernatant was dialyzed against buffer containing Tris HCl (20 mM) and EDTA (2 mM) and designated as supernatant fraction. To isolate mitochondrial fraction; the same blend as above was ground in a pestle and mortar into a fine suspension, clarified and centrifuged initially at 1000 x g for 10 min to remove the cell debris. The supernatant was re-centrifuged at 10,000 x g for 20 min to pellet the mitochondria. The pure mitochondrial pellet was suspended in 0.3 M sucrose (~1 mL volume), and designated as mitochondrial fraction. The post mitochondrial supernatant was centrifuged at 100,000 x g for 1 h. The pellet was washed and resuspended in ~1 mL of 0.3 M sucrose and designated as microsomal fraction.

Mitochondrial and microsomal fractions were used for succinate dehydrogenase (SDH) and glucose-6-phosphatase (G-6-pase) activity, respectively, while the supernatant fraction was used for the rest of the enzymes.

Phosphoenolpyruvate carboxykinase (PEPCK) was measured by monitoring the rate of oxaloacetic acid (OAA) formation and OD increase at 290 nm (Ting, 1968). Phosphoenolpyruvate carboxylase (PEPC) was measured by coupling the reaction with maleic

dehydrogenase and the rate of NADH oxidation followed at 340 nm (Daniel *et al.,* 1969). Fructose-1,6-biphosphatase was measured by estimating the inorganic phosphate (Taussky and Shorr, 1953) as described by Racker (1962). Maleic enzyme was measured by monitoring NADP reduction (Ochoa *et al.,* 1948). Glucokinase activity was coupled to glucose-6-phosphate dehydrogenase and the reduction of NADP was followed by OD at 340 nm (Gibbs and Turner, 1964). SDH was measured as described by Hoskins and Mackenzie (1961), where reduction of 2, 6-dichlorophenol endo phenol in the presence of phenazine methosulphate was read at 600 nm. G-6-pase was measured by following the liberated inorganic phosphate as described by Swanson (1955).

Texture measurements (Peleg, 1979; Barrett *et al.*, 1998)

Texture measurements were done using a computer interfaced texture analyzer equipped with a 100 kg load cell. Textural properties were evaluated by three parameters namely penetration, piercing and compression. The shear resistance by the intact fruit was measured using a 10 Kg load cell and a stroke speed of 10-100 mm/min. The loss in firmness as force (in Newtons) required by the probe for penetration, piercing and compression was recorded.

Penetration

Cylindrical 8 mm probe was used to penetrate one side (cheek) of the mango fruit (with or without peel) to a depth of 10 mm with a constant speed of 10 mm/min. The maximum force required by the probe to penetrate the tissue was recorded and expressed in Newtons. One measurement was made per fruit and 6 fruits were tested per treatment and the average values were taken.

Piercing

A 5 mm probe was used to pierce one side (cheek) of the

mango fruit (with peel) to a depth of 10 mm with a constant speed of 10 mm/min. The maximum force required by the probe was recorded.

Compression

Tissue blocks (15 x 15 x 15 mm) from each cheek of the mango fruit were compressed using a 50 mm circular flat plate with a stroke speed of 100 mm/min. The maximum force required by the circular plate probe to compress the block by 50% was recorded. Two measurements were made per fruit (blocks from each cheek) and 3 fruits were tested per treatment and the average values were taken.

Microscopy

Light microscopy (Johansen, 1940)

Preparation of the tissue was done by taking sections (small blocks) of fresh unripe and ripe mango fruits cut (in water) using a sharp blade and later mounted on a slide. The sections were viewed under a light microscope.

Scanning electron microscopy (El-Otmani and Coggins, 1985)

The dried samples of unripe and ripe fines (starch) and alcohol insoluble powders from mango, banana and papaya were spread uniformly on a double sided conducting adhesive tapes pasted on a metallic stub. It was coated with gold (~40 Å) in a sputter coating unit for 5 min and observed in the SEM.

Alcohol solubles: Organic acids and sugars

Isolation of free sugars (Shashirekha and Patwardhan, 1976)

The fruit tissues (10 g) from unripe and ripe mango were homogenized in 70% aqueous ethanol in a Sorvall omni mixer and centrifuged. The residues were repeatedly (x 3) extracted with 70% alcohol to extract the sugars completely. The extracts were pooled

and concentrated by flash evaporation. They were further centrifuged, and the resulting supernatants were analyzed for total carbohydrates, reducing sugar, and glucose. The extracts were then subjected to ion exchange chromatography, initially on Dowex 50 (H^+) (to remove amino acids/organic acids) followed by Dowex 1 (OH^-) (to hold cations, organic acids). The sugar fractions from the column were collected after thorough washing of the columns with water. The fractions were pooled, concentrated, clarified and separated by HPLC and quantitated (Prabha and Bhagyalakshmi, 1998). The total organic acid fraction was derivatized to methyl ester for GLC analysis.

Radioactive studies (Frenkel *et al.,* 1968; Satyan and Patwardhan, 1984)

Labeled compound (1.8 µCi in 50 µL of 0.4 M mannitol) was injected directly into the pulp portion through a syringe by vacuum infiltration. The actual amount of the label entering into each fruit was calculated by subtracting the remaining counts in the syringe wash. The fruits thus injected, were transferred to desiccators individually fitted with an inlet for air and were kept for respiration for 8 h, after which, the pulp portion was homogenized. Known aliquots were fixed in 70% alcohol for soluble sugars. Extraction and purification of sugars was as mentioned above. A known aliquot of the sugar fraction was analyzed for radioactivity. Liquid scintillation counting was done in Bray's cocktail and the counts expressed as % incorporation of radioactivity into the desired fraction.

Isolation of non-starch polysaccharides

Preparation of alcohol insoluble residue (AIR)

The unripe (I) and ripe (IV) mango fruits were selected to make alcohol insoluble residues (AIR). A known weight of fruit pulp was

separately soaked in 3 volumes of 95% ethanol. Slicing the tissue and plunging them into alcohol were done instantaneously in order to avoid endogenous metabolic activity due to cutting. They were homogenized in a sorvall omni mixer and the resulting slurry was kept at 60^0C for 40 min to arrest endogenous enzyme activities and to facilitate protein co-agulation (Rose *et al.*, 1998; Chang *et al.*, 1993; Carrington *et al.*, 1993). The slurry was cooled to room temperature and filtered through two layers of cotton cloth. The residue was repeatedly extracted in 80% ethanol (4-5 times) to remove all the free soluble sugars. The residue was washed with diethyl either followed by petroleum ether to remove pigments, and was finally washed with acetone to remove the moisture completely, air-dried and stored.

Fractionation of AIR

Based on differential solubility, AIR was fractionated sequentially into 8 different fractions. The fractionation procedure adapted here (Salimath and Tharanathan, 1982, Rose *et al.*, 1998) was slightly modified.

The AIR from unripe and ripe fruits was extracted separately with cold water with continuous stirring using a magnetic stirrer, for 2 h at room temperature. The slurry was filtered though 4 layers of nylon cloth. The residue was repeatedly extracted with water (thrice) and filtered. The pooled filtrates were dialysed against water and precipitated with alcohol (95%) and/or lyophilized (CWS). The residue was subjected to hot water extraction with continuous stirring for 2 h at 80^0C on a water bath and Termamyl was added during extraction, to solubilize the starch. The slurry was filtered and the extraction with hot water was repeated (thrice) and the filtrates were polled and dialysed and precipitated with alcohol to get hot water soluble fraction (HWS).

The residue was extracted with 0.5% disodium EDTA (pH 4.8) with continuous stirring at 4°C, overnight (8 h) and the resulting slurry was filtered through 4 layers of nylon cloth. The residue was again extracted with 0.5% disodium EDTA (pH 4.8) with continuous stirring at 80^0C for 2 h and filtered. The extraction was repeated twice and filtered. Aliquots were taken separately from both the filtrates of cold and hot EDTA extractions for estimations and later were combined together (to get EDTA soluble fraction) and dialysed extensively against running tap water followed by distilled water at 4^0C for 2 days with several changes and precipitation with alcohol to get pectic fraction (Mort *et al.,* 1991). The residue obtained was further subjected to sodium carbonate (50 mM containing $NaBH_4$, 20 mM) extraction with continuous stirring for 2 h at 4^0C to get alkali soluble pectins. The extraction was repeated thrice and filtered and the filtrates were pooled and dialysed extensively against distilled water at 4^0C for 2 days and precipitated with alcohol. The left over residue was used for hemicellulose (hemicellulose A and B) extraction. The residue was extracted twice with 10% alkali (4 N NaOH) (residue to alkali ratio 1:10, w/v) under nitrogen atmosphere for 4 h each with continuous stirring, and filtered. The filtrates were pooled and brought down to ice cold temperature and 50% acetic acid was added dropwise till the pH was 4.5 and the precipitated polysaccharides were separated by centrifugation at 7000 rpm for 15 min and designated as hemicellulose A. The supernatant was precipitated with alcohol to get hemicellulose B. Both the precipitates were separately taken in water and dialysed extensively against water at 4^0C for 2 to 3 days with several changes and precipitated with alcohol. The left over insoluble matter constituted the cellulosic fraction.

Fractionation of extracted polysaccharides on DEAE-cellulose

Regeneration of DEAE-cellulose

DEAE-cellulose was washed thoroughly with water to remove fines. It was then treated successively with HCl (0.5 N) and NaOH (0.5 M). After each treatment, the pH was adjusted to neutrality by washing thoroughly with water. The regenerated exchanger was suspended in ammonium carbonate (0.5 M, pH 9.3), packed into a column (3.2 cm x 26 cm) and excess carbonate was washed off with water.

Fractionation

CWS, HWS, pectins and hemicellulosic fractions (0.5 g each) were dissolved in water separately and loaded on to the pre-equilibrated DEAE-cellulose column and the elution was carried out with water followed by successive elution with stepwise increasing gradients of ammonium carbonate (0.05-0.45 M) and sodium hydroxide (0.05-0.45 M) solutions (Siddiqui and Wood, 1971). The flow rate was maintained at 60 mL/h and the fractions (8 mL) collected, were assayed for total sugars; the peak fractions were pooled appropriately, dialysed and lyophilized.

Homogeneity criteria (Anderson and Stoddard, 1966)

GPC was performed on Sepharose CL-4B gel matrix, which was soaked in water overnight and washed with water to remove fines. The slurry was then packed into a column (1.4 cm x 100 cm, 175 mL) and equilibrated with NaCl (0.1 M) containing sodium azide (0.05%). The major fractions of CWS, HWS, pectic and hemicellulose polysaccharides (10 mg), obtained from DEAE-cellulose were dissolved in water (1 mL) and loaded on to the column. The elution was carried out by using NaCl (0.1 M) containing sodium azide (0.05%) at a constant flow rate of 18 mL/h. Fractions (4 ml) were collected and analyzed for total sugars. Appropriate fractions were

pooled, dialysed and lyophilized. The column was calibrated with T-series dextran standards (T-10, T-20, T-40, T-70, T-150, T-500, T-2000) and glucose (to determine bed volume) and blue dextran (to determine V_o, void volume). A calibration curve was prepared by plotting Ve/Vo versus log molecular weight (where Ve=elution volume) and molecular weight of the unknown polysaccharide was determined (Rore *et al.*, 1998).

High performance size exclusion chromatography (HPSEC) (Fishman, *et al.,* 1986)

HPSEC was carried out in a Shimadzu HPLC system (HIC-6A system controller, CR-4A Chromatopac integrator and LC-6A pump), fitted with E-linear and E-1000 μ-Bondapack columns (30 cm x 3 mm i.d.) connected in series with a guard column and Shimadzu RID-6A RI detector. The purified fractions (10 mg/mL) were dissolved in water and centrifuged at 7000 rpm for 5 min to remove any undissolved / particulate materials, prior to the analysis. Samples and standards (T-10, T-20, T-40, T-70, T-150, T-500, T-2000; 10 mg/mL, 10 μL each) were individually loaded and eluted with water at a flow rate of 0.6 mL/min at 40^0C, and the elution was monitored by refractive index detector set at 8×10^{-6} RIU.

Electrophoresis

Cellulose acetate membrane electrophoresis (Kikuchi *et al.*, 1992)

Electrophoresis, on cellulose acetate membranes was carried out using Beckman microzone electrophoretic cell (model R 101) and ammonium carbonate - NaCl buffer (0.05 M, pH 9.3) at a constant voltage of 180 V and 15 mA current for 45 min. Prior to electrophoresis the membranes were wetted with running buffer and the excess buffer was removed by blotting between the blotter papers. The polysaccharides (1 mg each) were dissolved in water (0.1 mL) and loaded (10 μL each) by using an applicator. The rate of

migration was followed by using Procion red marker dye. The polysaccharides were stained with ruthenium red (0.5% in water) and the excess dye was removed by washing with water.

Capillary electrophoresis

Electrophoresis of purified polysaccharides from CWS (unripe and ripe), HWS (unripe) and hemicellulose (unripe) fraction was carried out on silica capillary columns (75 μ i.d. x 100 cm length) using Prince CE 56 capillary electrophoresis unit. The silica column was thoroughly washed with 0.1 M NaOH and equilibrated by using borate buffer (0.2 M, pH 9.3). The column pressure, voltage and current were maintained at 100 m bars, 20kV and 8mA, respectively. Samples were dissolved in water (1-2%) and elution was monitored at 253 nm.

Determination of neutral sugar composition by gas liquid chromatography (GLC)

Hydrolysis of polysaccharides by sulphuric acid (Selvendran and O'Neil, 1988)

The polysaccharide (10 mg) was suspended in water and allowed to swell for 1-2 h at room temperature in a stoppered tube and was completely hydrolysed by prior solubilization with 72% sulphuric acid at ice cold temperature followed by diluting to 8% with water and the tubes were fitted with air cooled condenser and kept in a boiling water bath (100^0C) for 10-12 h.

Neutralization and deionization

The sulphuric acid hydrolysates were neutralized with solid barium carbonate and filtered through Whatmann No. 1 filter paper. The excess barium ions in the filtrate was removed by adding regenerated Amberlite IR-120 H^+ resin and concentrated.

Regeneration of Amberlite IR-120 H^+ resin

The resin was washed with water to remove the fines. After draining out the water completely the resin was suspended in HCl (2 N) for 1 h at room temperature with intermittent shaking. The resin was then filtered through nylon cloth and washed with water till the pH was 7.

Trifluoroacetic acid (TFA) hydrolysis

To a test tube containing the samples (10 mg) was added 1 mL of TFA (2 N) and the tubes sealed. Hydrolysis was carried out at 100^0C for 6-8 h in an oven. After the hydrolysis, the acid was removed by flash evaporation at water bath temperature of 40^0C and co-distilled with water (1 mL x 5).

Preparation of alditol acetate derivatives (Sawardekar *et al.*, 1965)

To the polysaccharide hydrolysate, which is in water (0.5 mL) was added inositol (1 mg) as an internal standard, followed by sodium carbonate solution (0.02 M) to saponify any glucuronolactones. After 15 min, sodium borohydride (20 mg) or sodium borodeuteride in deuterium oxide (D_20) (in case of methylated samples) was added in order to reduce the monosaccharides and the tubes were stoppered and kept overnight at room temperature. The excess borohydride was decomposed by adding acetic acid (2 N) dropwise till the effervescence of hydrogen stops. The boric acid formed was removed by co-distillation with methanol (2 mL x 5) and evaporated to dryness. To the dry glycitols were added distilled acetic anhydride and pyridine (0.5 mL each) and the mixture was kept at 100^0C for 2 h after tightly stoppering the tubes. After acetylation excess reagents were removed by co-distillation with water and toluene (3 x 2 mL each). After thorough drying, the alditol acetates were extracted with chloroform, filtered through glass wool and dried by flushing nitrogen gas. The derivatives were taken in known amount of chloroform and injected

to GLC.

Gas liquid chromatography

Alditol acetate derivatives were analyzed by using Shimadzu GLC system (GC-15A) fitted with FID and CR4-A monitor. OV-225 (3% on Chromosorb W (100-120 mesh) packed column (8 ft. x 1/8" i.d.) was used for analysis. Column, injector and detector port temperatures were maintained at 200^0C (185^0C in case of permethylated derivatives), 250^0C and 250^0C, respectively. Nitrogen was the carrier gas (40 mL/min) used. Alditol acetates (1-2 μL) were injected into the column and the retention time of sugars was compared with that of standards.

Structural Analysis

Optical rotation (Pilnik and Voragen, 1970; Polle *et al.*, 2002)

The specific rotation of the polysaccharides (1mL, 0.5-1.0% in distilled water) was determined by using a Perkin-Elmer (model 243) polarimeter using sodium D line lamp at a wavelength of 589 nm. The optical rotation was measured by the shift in plane polarized light, and the specific rotation $[\alpha]_D$ at 20^0C (C, 0.25 in water) was calculated using the formula,

Specific rotation $[\alpha]_D = \theta \times 100 / C \times l$

Where, θ= angle of rotation of plane polarized light

C= Concentration of the sample (in %)

l= Path length (in dm)

Carboxyl-reduction of CWS and HWS fractions (Taylor and Conrad, 1972)

The purified sample (25-30 mg) was dissolved in distilled water (6 mL), and pH was adjusted to 4.75 by using 0.1 N HCl. CMC-carbodiimide (250 mg) was slowly added over a period of 4h maintaining the pH by the addition of 0.1 N HCl. The reduction was later carried out by drop wise addition of $NaBH_4$ solution (250 mg in

3 mL), over a period of 2 h, during which the pH was maintained at 7.0 using 4 N HCl. A drop of 1-octanol was added as an antifoaming agent to prevent foaming during the additions. After reduction, the pH was reduced to 4.5 by the addition of 0.1 N HCl, and dialysed extensively, and lyophilized. The reduction was repeated (x 3) to obtain a sample containing less than 2% Gal A.

Methylation analysis

Hakomori methylation (Hakomori, 1964; Jansson *et al.*, 1976)

(a) Preparation of methylsulfinyl carbanion (MSC) (dimsyl anion)

Sodium hydride (500 mg) taken in a reaction vial (3 x 7 cm) containing a small magnetic bead, was washed repeatedly with dry distilled diethyl ether (x 4). Residual ether was removed by flushing nitrogen gas. It was then treated with dry distilled dimethyl sulphoxide (4.0 mL) at 60^0C for 4 h with continuous stirring. The hydrogen liberated was removed intermittently through an injection needle and the resulting dark greenish yellow coloured viscous solution was tested for its characteristic blood red color with triphenyl methane (Rauvala, 1979).

(b) Methylation

The (reduced) polysaccharide fraction (3-5 mg) contained in a reaction vial was dissolved in dry DMSO (1 mL) by stirring for 2 h at room temperature with occasional ultrasonication for effective solubilization. To the solution was added the prepared methylsulfinyl carbanion dropwise using a syringe and kept for stirring for 4 h at room temperature. The polyalkoxide anion generated was permethylated by adding methyl iodide (1 mL) in ice-cold condition and left stirring for 7 h.

(c) Purification of the methylated polysaccharide

The resulting reaction mixture was diluted with water (1:1,

v/v) and passed through activated Sep-Pack-C18 cartridges (York *et al.*, 1985). Activation of Sep-Pack cartridge fitted into a syringe was carried out by flushing it successively with ethanol (40 mL), acetonitrile (2 mL) and water (4 mL). The reaction mixture from the activated cartridge was eluted sequentially with water (2 mL x 4) to get rid of highly polar compounds/solvents such as DMSO and NaI. Subsequent elutions (2 mL x 4) were made sequentially with acetonitrile-water (3:17, v/v), acetonitrile-water (1:4, v/v), acetonitrile (100%), methanol (100%) and finally with ethanol (100%), at a constant flow rate of 1-2 drops/sec. The eluted fractions were concentrated separately by flash evaporation and tested for the presence of methylated polysaccharides on precoated thin layer chromatography strips by charring with 5% sulphuric acid in methanol (v/v). The fractions eluted in dry acetonitrile and methanol showed positive reaction, they were pooled, flash evaporated to dryness and stored in the desiccator.

(d) Acid hydrolysis and Derivatization

To the dry permethylated polysaccharide aqueous formic acid (90%, 2 mL) was added and hydrolysed in a sealed tube at 100^0C for 2 h. The excess acid was removed by co-distilling with methanol (2 mL each x 4). It was then subjected to 2 N TFA hydrolysis, at 100^0C for 4 h in a sealed tube. The acid was removed by flash evaporation and the residual TFA was removed by co-distilling with methanol followed by deuterium oxide (0.5 mL) and flash evaporated to dryness. The sample was taken in D_2O (0.5 mL) and subjected to reduction with $NaBD_4$ (10 mg) overnight and the alditol acetates were prepared as described earlier.

(e) GC-MS (Jansson *et al.*, 1976)

The permethylated alditol (^{2}H) acetates were analyzed by GC followed by combined GC-MS (York *et al.*, 1985). GC-MS was

performed on a high performance quadrupole Shimadzu mass spectrometer QP-5000 combined with GC-17A, using SP-2330 capillary column (30 m x 0.31 mm i.d., 0.02 μ film coating) operating at an ionization potential of 70 eV with a temperature program mode of 180-200^{0}C, with 4^{0}C raise per min. The mass range was 40-400 amu (m/Z) and helium was the carrier gas.

Infrared spectroscopy (Kacurakova *et al.*, 1994; Coimbra *et al.*, 1998)

Polysaccharide (10 mg) was blended with Nujol or potassium bromide, to prepare a homogeneous smear or pellet. The pellet was mounted on the IR window and the spectra were recorded in the wave number 400-4000 cm^{-1} in a Perkin Elmer infrared spectrometer (2000 system GC-IR) operating at 4 cm^{-1} resolution.

^{13}C-NMR study (Hoffmann *et al.*, 1991; Pressy and Himmelsbach, 1984)

Purified sample (25 mg) was dissolved in deuterium oxide (1 mL). The deuterium resonance was used as a field frequency lock and the shifts were referenced to external TMS. The 100 MHz ^{13}C NMR spectra were recorded in Bruker AM x 400 MHz NMR spectrometer (5 mm multi-nucleus probe) operating at 60°C for 4 h using spectral width of 227 Hz with 6000 scans.

Tissue culture studies

Culture establishment

In order to establish somatic embryos for mango, 5 mango trees (Alphonso variety) growing in the campus with proven record of excellent fruit yield were selected and labeled as T_1, T_2, T_3, T_4 and T_5. Immature fruits of 1-2 cm (dia) inches were collected from these trees, washed in running tap water, surface-disinfected using 0.15%

(w/v) of aqueous mercuric chloride for 10 min and rinsed (x 5) with sterile distilled water. This step and all further operations were done under aseptic conditions. Fruits were cut open longitudinally; the immature seeds were collected aseptically. The seeds were bisected longitudinally, and the embryo masses were separated and discarded. The integuments and the cotyledons were separated and cut into 0.5 sq. cm pieces. They were cultured by placing separately on gelled medium termed as mango maintenance medium (MMM) containing (per L) the following: macronutrients of B-5 medium (Table 2.1) (Gamborg *et al.*, 1968), micronutrients and vitamins of MS medium (Table 2.1) (Murashige and Skoog, 1962), 100 mg of ascorbic acid, 400 mg of L-glutamine, 100 mg of inositol, 0.25-1 mg of 2,4-dichlorophenoxyacetic acid, 60 g of sucrose and 2 g of gelrite (for gelling) with pH adjusted to 5.8 before autoclaving at 121 psi for 15 min. The cultures were maintained in dark at 24 ± 1^0C. The integuments were positioned in such a way that the nucelli were in direct contact with the medium whereas cotyledonous explants were placed randomly on the medium. The cultures were transferred to fresh medium at 4-week intervals and maintained as stock cultures.

Culture maintenance

To sustain rapid growth and for routine maintenance, embryogenic cultures, consisting of proliferating nucellar and cotyledonary globular proembryonic masses as well as small cell aggregates (5.0 g), were subcultured separately onto solid maintenance medium with a subculture interval of 30 days or into liquid maintenance medium (LMM, 50 mL) of the same formulation as initial medium but without gelrite, in 125 mL Erlenmeyer flasks sealed with cotton plugs. The inoculum size was approximately 200 mg of proembryos. The flasks were maintained on a gyratory shaker at 90 rpm at 24 ± 1^0C in dark and subcultures were done at 5-7 day intervals to avoid the accumulation of phenolic compounds. The

embryogenic callus produced was recultured on a similar medium without ascorbic acid for the induction of somatic embryos.

Table 2.1
Macro-nutrients of Gamborg B5 medium and Micronutrients and vitamins of MS medium

	Concentration (mg/L)	Concentration
Macro-nutrients		
$CaCl_2$	113.23	1.02 mM
KNO_3	2500.00	24.73 mM
$MgSO_4$	121.56	1.01 mM
NaH_2PO_4	130.44	1.09 mM
$(NH_4)_2SO_4$	134.00	1.01 mM
Micro-nutrients		
$CoCl_2.6H_2O$	0.025	0.11 μM
$CuSO_4.5H_2O$	0.025	0.10 μM
FeNaEDTA	36.70	0.10 mM
H_3BO_3	6.20	0.10 mM
KI	0.83	5.00 μM
$MnSO_4.H_2O$	16.90	0.10 mM
$Na_2MoO_4.2H_2O$	0.25	1.03 μM
$ZnSO_4.7H_2O$	8.60	29.91 μM
Vitamins		
Glycine	2.00	26.64 μM
Myo-inositol	100.00	0.56 mM
Nicotinic acid	0.50	4.06 μM
Pyridoxine HCl	0.50	2.43 μM
Thiamine HCl	0.10	0.30 μM

Effect of stage proembryonic masses on maturation process of somatic embryos

To study the interaction between stages of somatic embryo growth and the nutrient, proliferating embryogenic cultures were sieved through specific spatula having perforations of 2 mm, 4 mm and 6 mm diameter and were separately cultured on different media. The larger size fractions were recultured in mango maintenance

medium and the fine fraction was subcultured in similar liquid medium. Approximately 1.0 g proembryos were inoculated into 50 mL LMM in 125 mL Erlenmeyer flasks. The cultures were maintained on a gyratory shaker at 90 rpm at 24 ± 1^0C in dark, and were subcultured at 5-day intervals and observations were recorded on individual parameters listed in Table 5.3 to 5.22 of chapter V.

Comparison of liquid and solid media for somatic embryo culture proliferation leading to large biomass

Embryogenic cultures were transferred from initiation medium to liquid or solid medium containing 4.44 μM of 2,4-dichlorophenoxyacetic acid (2, 4-D) and 4.6 μM kinetin. The effects of two solidifying agents, gelrite at 0.2 % (w/v) and Sigma agar at 0.8 % (w/v), on culture growth were compared. Suspensions were subcultured on the 4^{th} and 6^{th} weeks after inoculation to maintenance media, whereas cultures on solid medium were transferred at 3-week intervals. A completely randomized experimental design with three treatments and 10 replicates was used. The effects of different treatments on culture proliferation were measured 45 days after inoculation by weighing the globular proembryonic mass from 9 flasks and plates using the 10^{th} ones for reculturing.

Effect of mannitol and activated charcoal on somatic embryo maturation and germination

Embryogenic cultures were transferred from initiation medium into four different media formulations. The MS basal medium was prepared without 2,4-D but with sucrose (20 g/L), L-glutamine (100 mg) and kinetin (0.1 mL). This medium was divided into two equal parts. To one part mannitol (20 g/L) was added and other without mannitol. Each of these media was further divided into two equal

parts. For two media formulations activated charcoal was added and other two without charcoal. Embryogenic/proembryogenic globular masses from maintenance media were subcultured onto above said four different solidified germination media; i.e., (1) medium without mannitol and charcoal, (2) medium without mannitol and with charcoal (250 mg), (3) medium with mannitol and without charcoal, (4) medium with mannitol and charcoal and pH of the media was maintained 6.0. The effects of different media were measured after 45 days by counting the number of early heart-shaped somatic embryos. The experiment was a 2 x 4 factorial arranged in a completely randomized design with six replicates.

Effect of glutamine and abscisic acid on somatic embryos maturation and reversal of hyperhydric conditions

Hyperhydric heart-stage somatic embryos (3-5 mm) were removed from liquid embryogenic medium (LEM) after 23 weeks and were blotted dry with sterile filter paper and transferred to media with different levels (100–1000 mg) of L-glutamine. Similarly, hyperhydric heart-stage somatic embryos (3-5 mm) were subcultured from liquid maturation medium (LMM) after 9 weeks onto semi-solid mango maturation medium containing 0, 500, 750 or 1000 μM abscisic acid (ABA). There were 10 somatic embryos in each 100 x 15 mm petridish. The experiment was replicated five times, and was repeated twice. The experimental design was of complete randomization.

Effect of gibberlic acid-3 (GA_3) on somatic embryo maturation and later development

Somatic embryos from the treatments described above were subcultured on separate mango maturation medium for somatic embryo germination (Table 2.2), which differed from initial mango maturation medium, and was divided into two parts, G1 and G2. G1 contained somatic embryo germination medium with 2-4 mL of GA_3

(1 mg/mL) to obtain 3 mg/mL (this is supposed to supply 1 mg/L of GA_3 after autoclave because GA_3 is known to lose 2/3 of its activity during autoclaving) (George, 1994) and 0.05 mg/L of benzylaminopurine (BAP) and 2.5 g phytagel were also added. G2 contained somatic embryo germination medium with 200 mg activated charcoal and 40 g of mannitol (DeWald *et al.,* 1989b). The pH of all plant growth media was adjusted to 5.8 prior to autoclaving at 120^0C at 108 psi for 20 min. Ascorbic acid and coconut water were filter-sterilized and added to autoclaved media. Cultures were maintained in darkness under ambient temperature (24 ± 1^0C) in all of these experiments.

Table 2.2
Mango maturation medium for somatic embryo germination

Medium composition	Weight
B5 macro elements	As given in Table 2.1
MS micro elements	As given in Table 2.1
MS-Iron	As given in Table 2.1
MS-EDTA	As given in Table 2.1
MS-vitamins	As given in Table 2.1
Myo-inositol	100 mg
L-Glutamine	40 mg
Sucrose	20 g

Mango transformation using *Agrobacterium tumefaciens* (Lazo *et al.,* 1991)

Preparation of bacterial culture/activation of *A.tumefaciens*

To prepare the suspension culture for transformation, three strains of *Agrobacterium tumefaciens* AGL1, AGL1 and AGL0 with

plasmids pKIWI, pBSF16 and pBSF16, respectively, were transferred to medium (Table 2.3) for activation and incubated on gyratory shaker at 180 rpm at 25.5^{0}C to obtain approximately 1.0 OD checked at 660 nm against a medium blank. This broth (4 mL/100 mL of MMM/L, Table 2.4) was used to infect embryogenic cultures of T_1- T_5 lines of mango for co-cultivation at standard conditions for different periods.

Table 2.3
Mango germination liquid medium (MGM) for the growth of *Agrobacterium* strains

Medium composition	Weight
Mannitol	5.0 g
L-Glutamine	1.0 g
KH_2PO_4	0.26 g
NaCl	0.1 g
$MgSO_4.7H_2O$	0.1 g
Biotin	10 µL (0.1 mg/mL stock)
Tryptone	5.0 g
Yeast extract	2.5 g
pH	7.0

Co-cultivation of mango proembryos with *A. tumefaciens*

Three grams of somatic embryos or proembryonic masses of size 2-3 mm derived from nucellar and cotyledonary explants from T_1, T_2, T_3, T_4 and T_5 trees of mango maintained in liquid medium were lightly macerated by gently pressing with dissection needle and cultured in 50 mL of liquid maintenance medium to which log phase *A.tumefaciens* was added. Flasks containing the bacterial cultures, AT-AGL1- pBSF16 and AT-AGL0-pBSF16 carrying Bialophos

resistant gene and AT-AGL1-pKIWI carrying gene for kanamycin resistance were maintained on a gyratory shaker at 180 rpm at 26^{0}C in dark. Proembryos were transferred to fresh maintenance medium every 24 h for 2, 3 and 4 days to avoid excessive growth of bacterial cells. No additional bacterium was added at this stage.

Table 2.4
Mango maturation medium (MMM) for transformation

Medium composition	Weight
B5 macro elements	
$CaCl_2.2H_2O$	1.5 g
KNO_3	25 g
$MgSO_4.7H_2O$	2.5 g
$NaH_2PO_4.2H_2O$	1.5 g
$(NH_4)_2SO_4$	1.34 g
MS micro	As given in Table 2.1
MS-iron	As given in Table 2.1
MS-EDTA	As given in Table 2.1
MS-vitamins	As given in Table 2.1
Myo-inositol	100 mg
L-glutamine	400 mg
Sucrose	60 g
2,4-D	1 mL (1 mg/mL stock)
pH	5.8
Phytagel	2 g

Selection protocols for transformants

The main criteria used for identification of transformants were histochemical assay for GUS expression and the ability of proembryos to grow in liquid selection medium. The proembryos (200 mg) were transferred at different time intervals to respective

antibiotic (selection) medium with timentin (150 μg/L) to get rid of *A.tumefaciens*. As a control, segments of somatic embryos not treated with the bacterial suspensions were also cultured on medium with antibiotic. The overall control, i.e., using tobacco seedlings, was similarly treated using Murashige and Skoog Basal (MSB) medium.

Those embryogenic cultures, from all the T_1- T_5 mango lines, which were transformed using AT-AGL1-pKIWI were transferred to medium containing Kanamycin (20 μg/L) and those transformed with AT-AGL1/0-pBSF16, were transferred to medium containing Bialophos (200 μg), filter sterilized and added when medium was at 40^0C. All the media contained timentin (150 μg/L), which helped to get rid of *A.tumefaciens*. These steps were done for 3 to 4 days after co-cultivation. There were five petri plates, each plated with approximately 200 mg of proembryos. The suspension treatment contained 20 replicates with 50 mg proembryos per flask. These were kept on a gyratory shaker at 180 rpm and transferred at 3-day intervals. Culture conditions for the *A. tumefaciens*-treated proembryos were identical to those described above for the nontransformed mango cultures.

β-Glucuronidase assays

Samples of putatively transformed and nontransformed control proembryos/somatic embryos from every step of the selection procedure from both solid and liquid medium were washed with sterile distilled water and treated with bromochloro-S-indolyl-□-D-glucuronic tetra cyclohexylammonium salt (X-Gluc) as per the method of Jefferson (1987). The reaction product was observed after 1 to 16 h of incubation using stereomicroscope. Putatively transformed tobacco seedlings were also assayed in a similar way.

Recovery of transformed somatic embryos

Proembryos from liquid selection medium were transferred to liquid maintenance medium where 2,4-D was replaced with BAP (0.22 μM) containing timentin (100 μg/mL) for 30 to 50 days for somatic embryo development. All cultures in liquid selection medium were transferred at 3- to 5-day intervals to fresh medium, depending on the amount of *A.tumefaciens* growth.

Improving transformation efficiency using Acetosyringone

To enhance the transformation process, all the experiments similar to above were done using activated acetosyringone.

Chapter **3**

Cell wall carbohydrates in ripening mango: Implications in softening

***Section* 1**

Textural softening in ripening mango:
Changes in cell wall carbohydrates

Introduction

Fruits are in constant change during their lifecycle and a study of these changes during ripening is essential for nutrient analysis. It is well known that fruits are characterized by several physiological processes, which are interdependent (Gortner *et al.*, 1967; Salunke and Desai, 1984). When a fruit ripens, the pulp softens and the fruit acquires the desirable texture, which is an important attribute for its acceptability. Texture is one of the most important organoleptic characteristics of fruit that is altered during ripening. Fruit texture is of prime importance as it directly dictates fruit shelf life. The cell wall chemistry determines the fruit texture, which inturn influences the overall quality and consumer acceptability. Textural softening in fleshy fruits is primarily due to cell wall modification (Jackman and Stanley, 1995; Rizvi and Tong, 1997; Van Buren, 1979). The complex nature of cell wall makes it difficult to pinpoint the crucial factors specifically contributing to textural softening (Waldron *et al.,* 1997). The increased interest in controlling the textural qualities of fruit stimulated research in cell wall biochemistry, with particular reference to cell wall polysaccharides and their degradation. At cell wall, the extent of pectin and hemicellulose dissolution and solubilization is generally related to the degree of textural softening and cell wall changes during ripening (Huber, 1983a; Waldron *et al.,* 1997).

Microscopic observations of many fruit tissues revealed changes in the cell wall structure during ripening. Apparent change in the cell wall thickness, i.e. swelling of cell wall as observed by light

microscope, was detected during ripening of many fruits such as kiwi fruit (Redgwell *et al.,* 1997b). However, no such cell wall swelling was noticed in grapes (Nunan *et al.,* 1998). Textural softening is accompanied with disruption of cell wall and middle lamella, and appearing as electron translucent area in electron micrographs of ripening fruits. These wall changes were correlated with textural softening in tomato (Crookes and Grierson, 1983; Jackman and Stanley, 1995), avocado (Pesis *et al.,* 1978) and pear (Ben-Arie *et al.,* 1979). Softening of many fruits is strongly correlated with pectin solubilization (Redgwell *et al.,* 1997b). Usually an increase in pectin solubility, a decrease in pectin molecular weight and a loss of pectic neutral sugars such as arabinose and galactose are some of the cell wall changes reported, and it is likely that these wall modifications are brought about by pectolytic enzymes such as PG, PME or galactosidase (Seymour *et al.,* 1987, 1990; Gross and Sams, 1984).

Pectins or pectic polysaccharides are diverse group of acidic polysaccharides abundant in fruits and contribute in a substantial way to their texture (Brownleader *et al.,* 1999; Voragen *et al.,* 1995). Loss of pectin and increase in soluble galacturonide during ripening were shown in fruits like tomato (Seymour *et al.,* 1987), apple (De Vries *et al.,* 1984), kiwi (Redgwell *et al.,* 1992), plum (Boothby, 1983), peach (Hegde and Maness, 1996), melon (Rose *et al.,* 1998), banana (Wade *et al.,* 1992), persimmon (Cutillas-Iturralde *et al.,* 1993), muskmelon (McCollum *et al.,* 1989), bell pepper (Gross *et al.,* 1986; Priya Sethu *et al.,* 1996), apricot (Feminia *et al.,* 1998), cherry (Fils-Lycaon and Buret, 1990), olive fruit (Jimenez *et al.,* 2001), bush butter fruit (Missang *et al.,* 2001b) and mango (Brinson, 1988; El-Zoghbi, 1994; Muda *et al.,* 1995; Roe and Bruemmer, 1981). Very limited information is available on mango cell wall changes and the

softening process during ripening. There are considerable differences between cultivars (Selvaraj and Kumar, 1989).

Textural properties of fruits are evaluated by firmness measurement, which is an index of fruit ripeness. Three classes of instrumental or objective methods of texture evaluation, viz; fundamental, empirical and imitative are usually employed for firmness measurement (Barret *et al.,* 1998). Empirical tests, which are simple and rapid, include penetration, piercing, compression, puncture, extrusion, shear, and so on, which are now widely used. Textural softening and changes in cell structure during ripening were studied in a number of fruits, with the help of texture analyzer and microscopy (Abbott *et al.*, 1984; Ahmed and Dennison, 1971; El-Zoghbi, 1994; Jackman and Stanley; 1995; Jimenez *et al.*, 2001; Koh and Melton, 1994; McCann *et al.*, 1990; Muda *et al.*, 1995; Nunan *et al.,* 1998; Peleg, 1979; Redgwell *et al.,* 1997b; Rose *et al.,* 1998).

The major changes observed in mango fruits during ripening are reduction in fruit weight, firmness, acid content, starch, vitamin C with concomitant increase in total soluble solids, pH, sugar/acid ratio and carotenoids (Doreyappa Gowda and Huddar, 2001; Selvaraj *et al.,* 1989). Textural softening, sweetness development and sugar-acid turnover during ripening are interrelated, especially in a 'high starch', 'high acid' fruit like mango; and their biochemical relationship was examined as it is a crucial process in ripening mango. The objective here was to see the extent of correlation with textural softening in mango fruit in relation to cell wall structure and pectic changes during ripening.

Results and Discussion

Texture measurements

The texture analysis on mango fruit indicated progressive decrease in the force requirements at different stages during ripening (Fig. 3.1.1). The fruit ripened from the inside outward as in 'Harumanis mangoes (Lazan *et al.,* 1986). Internal softening had already begun at the mature green stage (stage I), when the fruit shoulders were well rounded and the fruit was externally judged to be hard. Undetectable internal ripening is largely responsible for non-uniformity in ripening within a harvested lot of fruit, leading to post harvest problems. The force required for the penetration of 8 mm probe into the fruit, through the peel, decreased from 370 N, at stage-I to 32 N at stage-IV, with drastic decrease occurring between stage-III to IV. Similar results were obtained with compression analysis on tissue blocks, where the force requirement decreased from 321 to 209 N (from stage I – III), which further dropped to 29 N, at stage-IV. The force requirement for 'piercing' decreased from 238 N to 24 N from stage I to IV, again a sharper drop was noticed from stage III to IV, as before. Thus, the energy requirement sharply decreased in later stages of ripening (i.e., from stage III to IV) than the earlier stages (stage I and II), showing a more pronounced degree of softening at the end of ripening. Similar trend of tissue softening was reported for fruits including melon (Rose *et al.,* 1998), banana (Bhagyalakshmi *et al.,* 2002) and pepino (O'Donoghue *et al.,* 1997). This loss of firmness is due to change in the ordered and compact arrangement of cell wall and middle lamella polysaccharides (Dick and Labavitch, 1989).

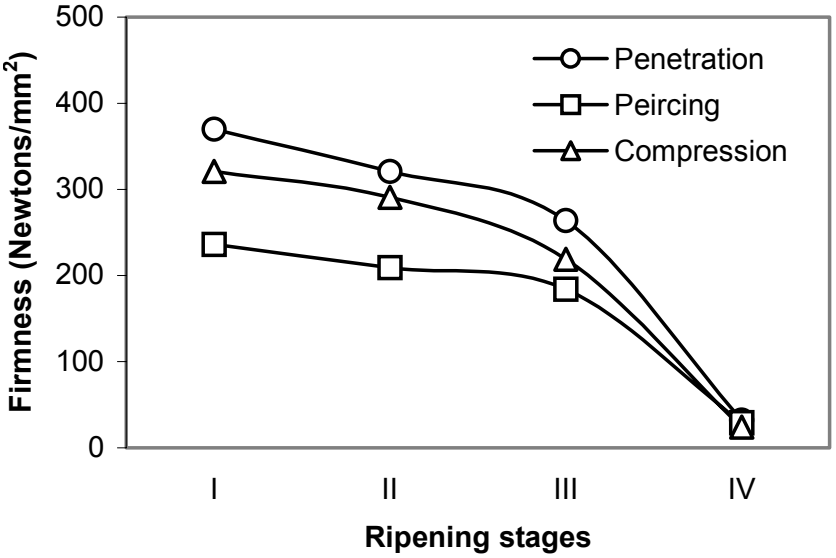

Figure 3.1.1
Changes in fruit texture at different stages of mango fruit ripening

Microscopic observations

Loss of cell structure integrity, cell wall thinning, increased intercellular spaces, loosening of cells and almost total disappearance of starch during ripening were evidenced by microscopic studies. Cell compactness was also lost during ripening. Microscopic study showed loss of middle lamella (i.e., pectin) resulting in loosening of cell wall structure (Figs 3.1.2 and 3.1.3). The more compact and rigid cell wall at the mature unripe stage (Fig. 3.1.2 A) appeared loosely structured and broader at the end of ripening (Fig 3.1.2 B). The loosening of cell wall in ripe stage makes the cell larger in size than the unripe cells. Dissolution of cell wall and middle lamella is apparent from the micrographs showing ruthenium red stained cell wall (Fig 3.1.3). The geometry and the cell wall shape also changed during ripening. Microscopic studies on mango fruit with specific staining for xylem and tannins have been

reported (Olle *et al.,* 1996). In kiwi fruit, swelling of cell wall and a three to four fold increase in cell wall thickness during ripening has been reported which strongly correlated with pectin solubilization (Redgwell *et al.,* 1997b). This swelling has resulted from the water moving to the voids left by the pectin solubilization (Newman and Redgwell, 2002). However, no such swelling was observed in grapes during ripening (Nunan *et al.,* 1998). As the physical interconnection between adjacent cells occur primarily through interlocking of pectins, the change in the degree of interconnection affects the rigidity of interaction between the polymers (McCann *et al.,* 1990), and eventually the tissue firmness. SEM studies have revealed striking changes in the structure of middle lamellae and eventual breakdown of the primary wall (Fig. 3.1.4). Under SEM of unripe tissue, the cuticle appeared as dark, thick, homogeneous layer and was not clear due its waxy nature. Thick walled cells were observed in epidermal layer. The starch granules were absent in epidermal and outer 2 or 3 layers of hypodermal cells and were sparse in inner hypodermal cells. They increased in abundance from outer to inner cortex. These changes suggested that pectin is intimately associated with the cellulose.

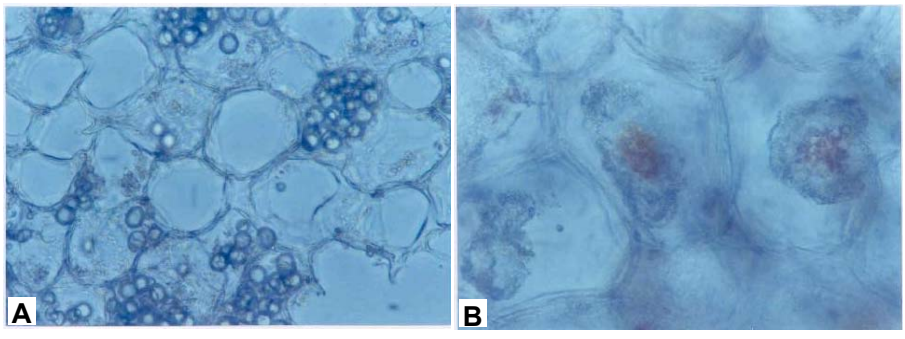

Figure 3.1.2
Light micrographs of mango fruit cell wall at unripe (A) and ripe (B) stages (magnification 100 x)

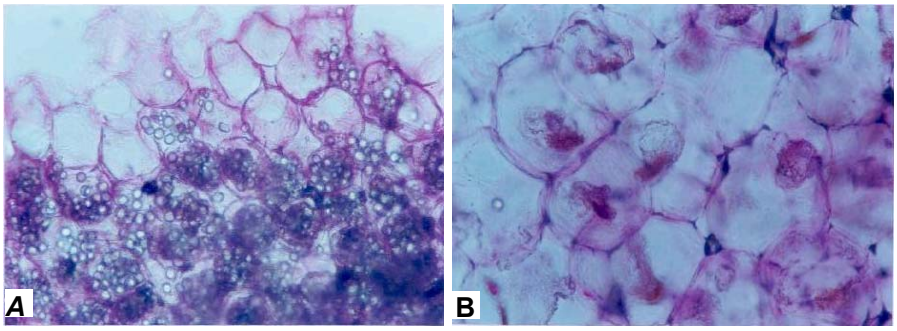

Figure 3.1.3
Light micrographs of ruthenium red stained mango fruit cell wall at unripe (A) and ripe (B) stages (magnification 100 x)

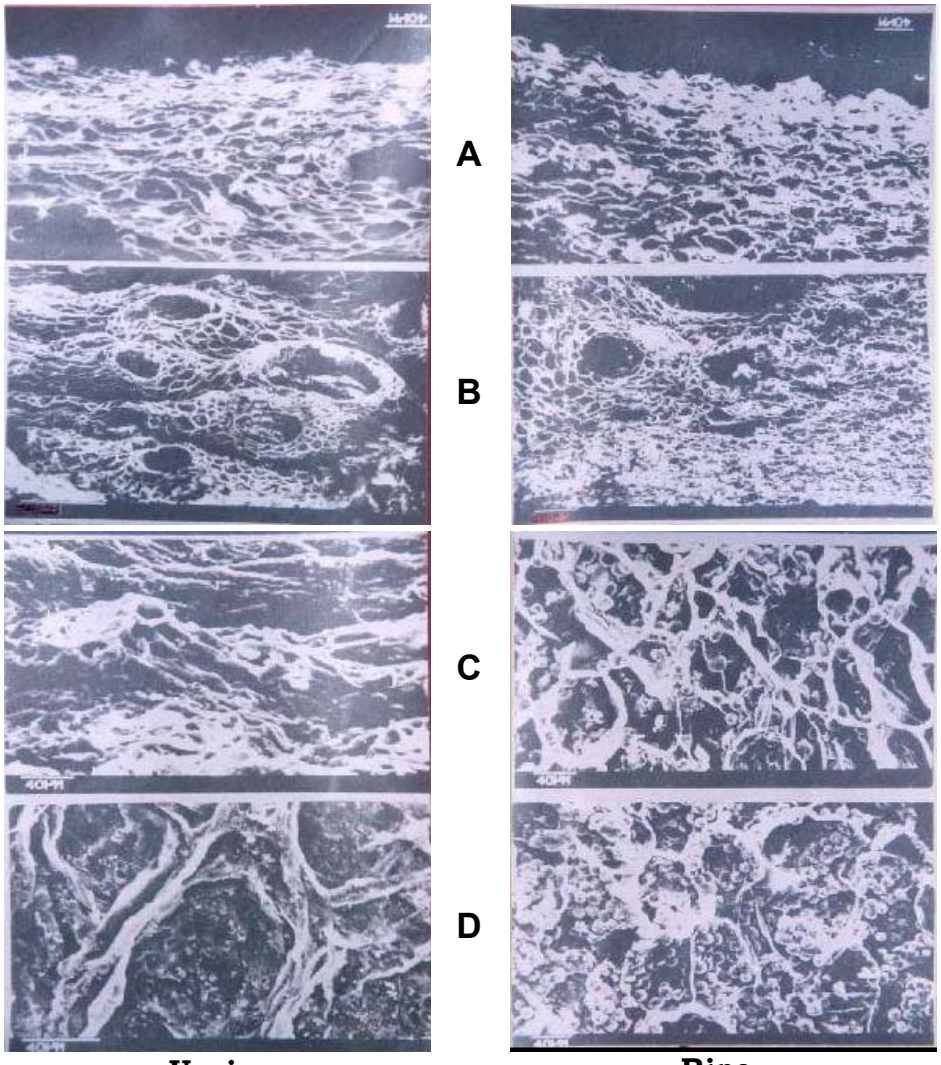

Figure 3.1.4
Scanning electron micrographs of ripening changes in mango (A to D from peel to pulp: exocarp to endocarp)

Apart from cell wall dissolution, microscopic observation also showed almost complete disappearance of starch granules at the ripe stage. Starch is one of the major polysaccharides in unripe mango. The endosperm was composed principally of starch. Loss of cell structure integrity and disappearance of starch during ripening was evident (Fig. 3.1.5). Different degrees of starch hydrolysis could be noticed, where slight distortion in the shape of starch granules was observed in 'A' of ripe mango. Disappearance of individual granules and clumped reticulate appearance was observed in B, which indicated moderate hydrolysis. Complete hydrolysis of starch granules was noticed in C. These morphological changes in mango starch granules during ripening are shown in a scanning electron micrograph (Fig 3.1.6). The starch granules at the unripe stage are spherical and of different sizes (Fig. 3.1.7). At the ripe stage, the granules get degraded by *in* vivo hydrolysis. All the granules were not equally susceptible to enzyme attack as reported by earlier researchers. The degradation pattern was found to be of exocorrosion type, degrading the entire granule in an orderly manner, big granules being more susceptible than smaller ones.

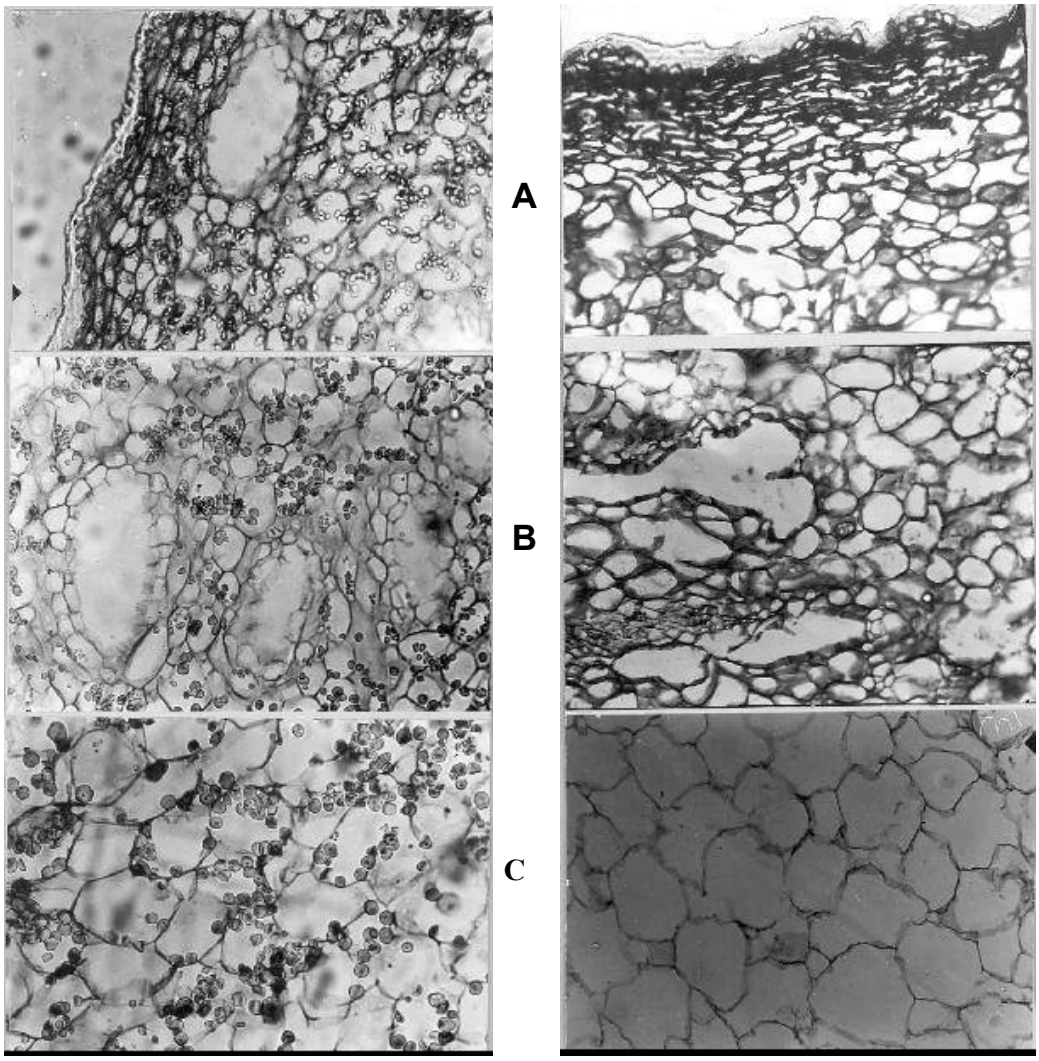

Figure 3.1.5
Light micrographs of ripening changes in mango (A to C from peel to pulp: exocarp to endocarp)

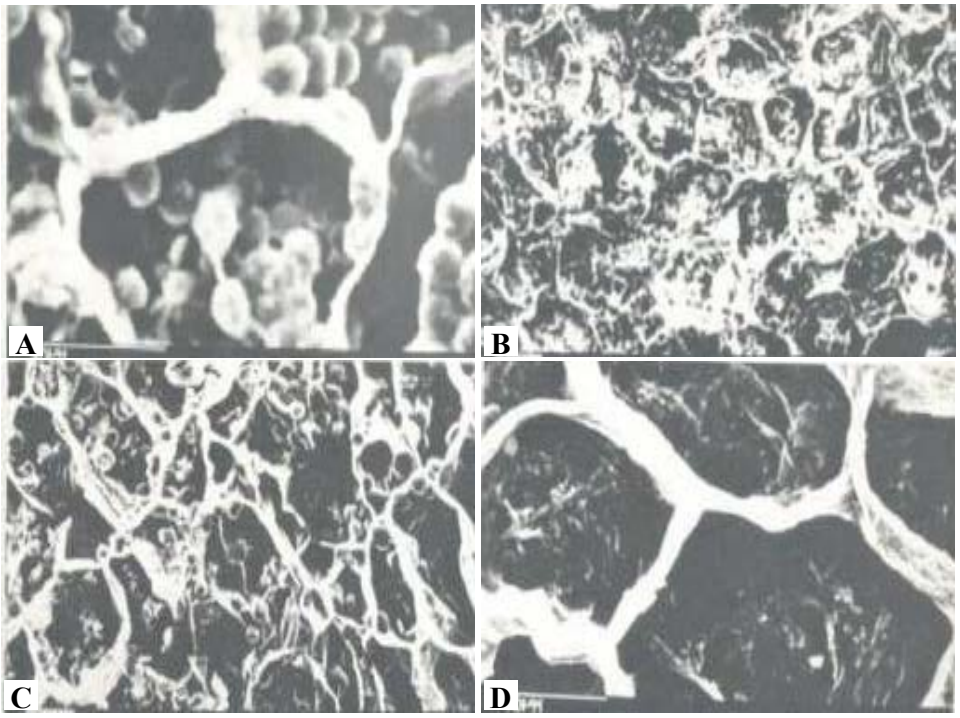

Figure 3.1.6 Scanning electron micrographs of starch hydrolysis in ripening mango (A-D ripening stages I-IV, respectively)

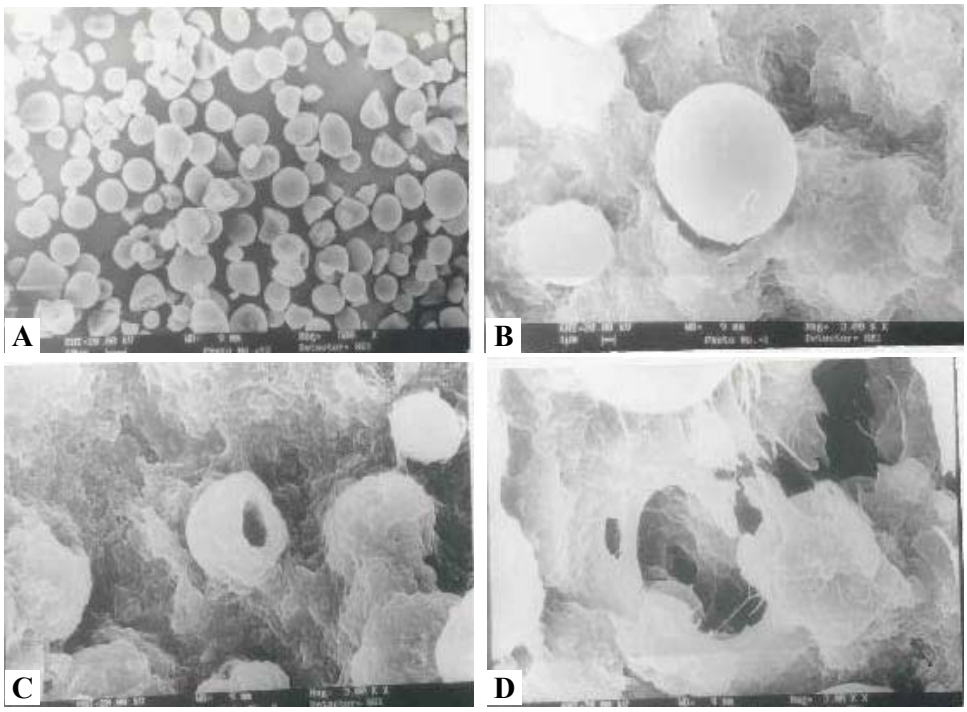

Figure 3.1.7 Scanning electron micrographs of different stages of starch hydrolysis in ripening mango (A, unripe; B/C, ripening mango; D, enlarged view of C, further degraded)

Pasting properties of unripe mango starch

Figure 3.1.8 (A) shows the pasting curve of unripe mango starch suspension derived by using rapid visco analyzer. The viscosity of the starch slurry was very minimal until its gelatinization temperature, 71.5^{0}C, then on it registered a rapid rise, reaching a peak value (P) of 317 RVU. Due to rupture of the swollen granules during continued heating-cooking, there was considerable breakdown in viscosity, and at the end of the heating period (5 min at 95^{0}C) the hot paste viscosity (H) was 105 RVU. Upon cooling the gain in viscosity (cold paste viscosity, C) at the end of cooling phase was 144 RVU. The latter is attributed to gelling on account of reassociation of starch molecules, through hydrogen bonding network, in the paste (retrogradation phenomenon). Accordingly the breakdown viscosity (BDV=P-H) was 212 RVU. The very low negative SBV value indicates extensive breakdown of starch molecules, a property referred to as shear thinning. Whether it is due to any associated–adsorbed amylase over the starch granular surface has to be looked into. Such a drastic decrease in the hot paste viscosity is reported in sweet potato starch, which is known to contain a high percentage of thermostable α-amylase adsorbed over the starch granular surface (Madhusudhan *et al.*, 1993). The severity of heat treatment plays a major role in influencing the pasting behaviour. Reduction in viscosity is particularly advantageous in the preparation of weaning and supplementary foods from starchy materials (Muyonga *et al.*, 2001). On the other hand the content of starch in ripe mango was negligible (< 0.1 %) and RVU data (Fig. 3.1.8 B) was in accordance with this inference. No hot paste viscosity was observed.

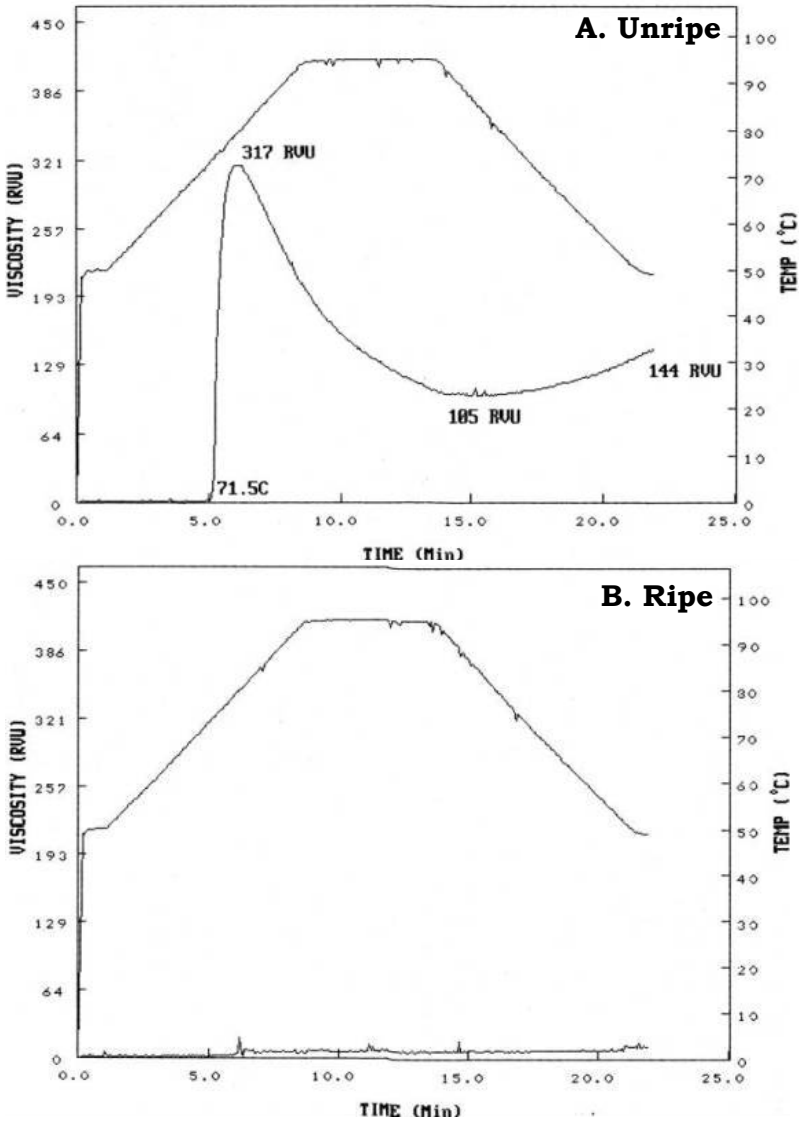

Figure 3.1.8 Pasting curves of mango starch

Thermal characteristics of mango starch

In Figure 3.1.9, is given the DSC characteristics of unripe starch. From the thermogram, it is obvious that the endothermic peak was seen at ~67^{0}C, which was slightly less than its gelatinisation temperature range. Its enthalpy value was 8.99 mcal/mg, a value much higher than observed for grain starches. The latter, however depends on the water content, for example, enthalpy increases with increase in water content.

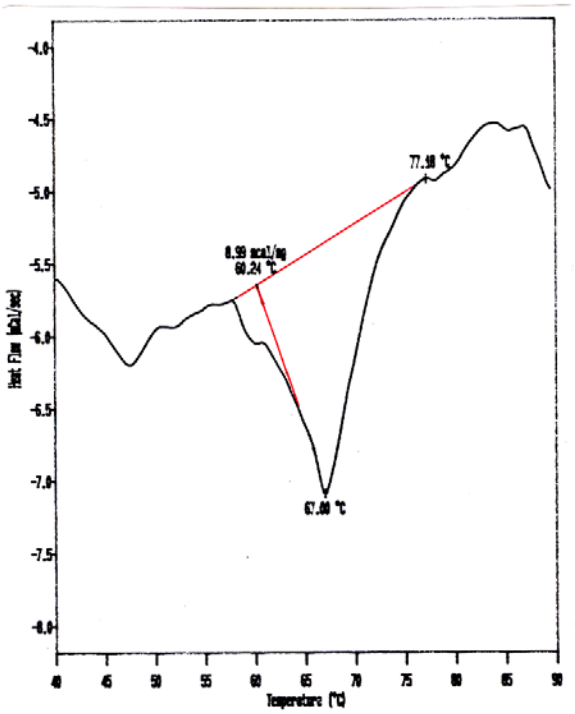

Figure 3.1.9
DSC thermogram of starch from unripe mango

Changes in the constituents of mango during ripening

Fruit softening during ripening is due to *in vivo* carbohydrate hydrolysis or depolymerization and is crucial as it directly dictates fruit shelf life and its keeping quality, while organic acid turnover during ripening which is central in intermediatery metabolism directly affects taste by its sugar/acid ratio (Shashirekha and Patwardhan, 1976).

The unripe mango weighed about 306.6g on an average, including peel, pulp and seed weight of 17.0g, 250.0g and 34.5g, respectively, whereas for ripe mango, the total weight was about 252.2g with peel, pulp and seed weight of 10.7g, 212.4g and 24.1g, respectively (Table 3.1.1). The moisture content of the pulp was almost same for both unripe and ripe mango (~78.0%).

Table 3.1.1
Changes in some biochemical components related to textural loss and taste development during ripening of mango

Mango	*Fresh weight in grams*				**Moisture (%)**	**pH**	**Brix (Total soluble solids)**	**Soluble sugars by HPLC (%)**
	Total weight	**Peel weight**	**Pulp weight**	**Seed weight**				
Unripe	306.6	17.0	249.5	34.5	77.8	2.8	7	Higher oligosaccharides (100)
Ripe	252.2	10.7	212.4	24.1	78.3	5.1	20	Glucose (54.05) and Fructose (45.95)

AIR was prepared from unripe and ripe mango pulp using aqueous alcohol (~80%) at 60^0C (Chang *et al.,* 1993). The extraction of fruit tissue in hot ethanol successfully inactivates cell wall enzymes and prevents the autocatalytic generation of reducing groups (Carrington *et al.,* 1993). Preparation of AIR induces coprecipitation of cytoplasmic proteins, polyphenols and salts in cell wall material (Selvendran, 1975). A comparison was made between unripe and ripe mango pulp in some important biochemical components related to textural loss and taste development during ripening. Fruit softening in mango was accompanied with reduction of starch from 18 to 0.2%, pectin from 1.9 to 0.5%, cellulose from 2 to 0.9% and hemicellulose from 0.8 to 0.2%, total alcohol insoluble solids (including starch) decreased from 22 to 3% (Fig. 3.1.10). Physiological loss in weight (PLW) was 10% and pH altered from 2.8 to 5.1 at ripe stage. Concomitantly, total soluble solids (TSS, Brix) increased from 7 to 20% and total soluble sugars from 1 to 15% (Fig.3.1.11). The decreased yield of AIR from 7.85 to 2.91g% fresh weight from unripe to ripe stage may indicate that large alcohol-insoluble polymers are degraded to alcohol-soluble polymers during ripening (El-Zoghbi, 1994) and starch to soluble sugars (Bhagyalakshmi *et al.,* 2002; Roe and Bruemmer, 1981; Selvaraj and Kumar, 1989). The carbohydrate and uronic acid contents of AIR

from unripe and ripe fruits were 100 and 67.8%, and 18.8 and 47.93%, respectively. Starch constitutes the bulk of the AIR of unripe fruits, while pectin constitutes the major part of AIR of ripe fruits. As fruit ripens, pectin content in AIR increases as a consequence of generation of more number of free carboxylic groups (by deesterification of pectins) (Redgwell *et al.,* 1992). Similar ripening changes were also found in other climacteric fruits (banana and papaya). Two extreme stages of ripening i.e. unripe and ripe were selected by many authors to study carbohydrate changes during ripening (Huber and Lee, 1986; Huisman *et al.,* 1996; Knee, 1978).

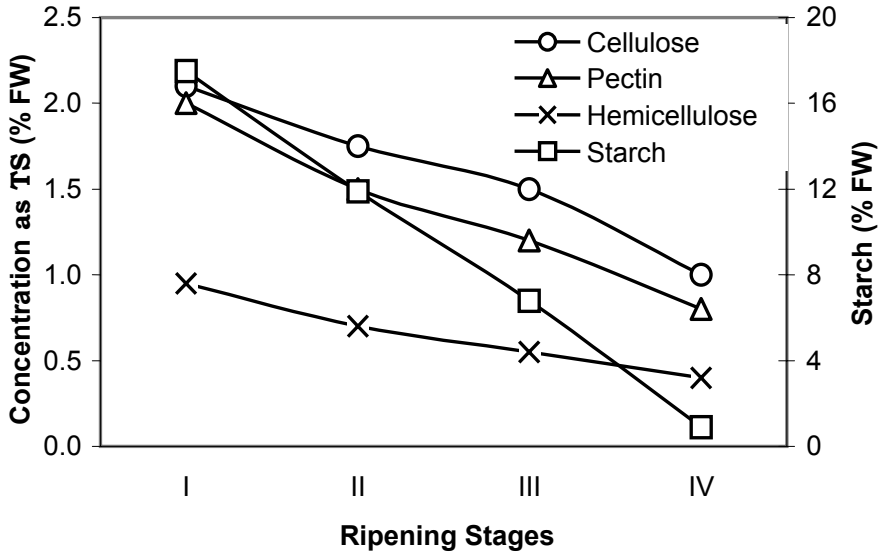

Figure 3.1.10
Changes in the carbohydrate components in ripening mango

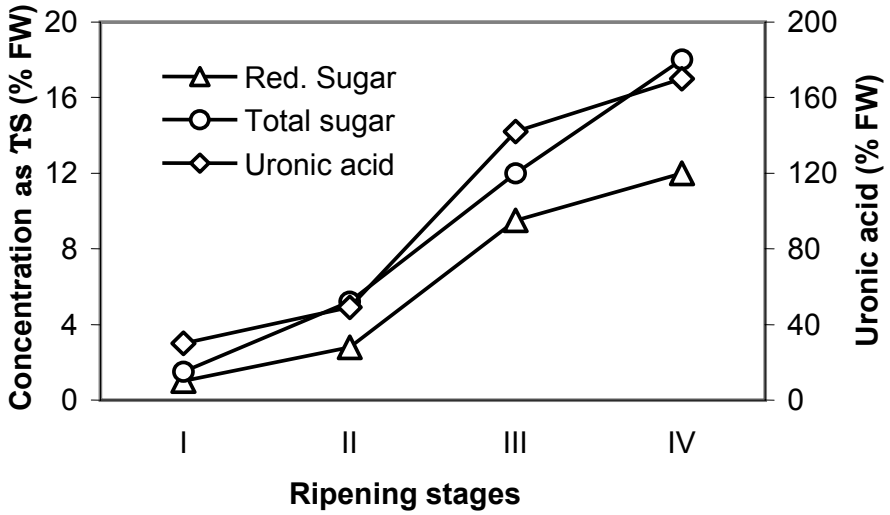

Figure 3.1.11
Changes in the carbohydrate components in ripening mango

The total carbohydrate content increased from 3.8 to 30% with a concomitant increase in 70% alcohol soluble sugars from 7 to 20% from unripe to ripe stage (Table 3.1.2). There was not much change in the carbohydrate content even after purification on Dowex 50 H^+ and Dowex 1 OH^-. The reducing sugar content in 70% alcohol soluble sugars increased from 1.06 to 9.22% (Fig.3.1.12). The difference in total carbohydrate to reducing sugar is not only due to non-reducing sugars such as sucrose but also from the non-reducing end groups of higher oligosaccharides. The glucose content increased from 0.17 to 2.89% and was almost same for further purified samples of unripe and ripe mango. These changes can be attributed to the degradation of carbohydrates, particularly starch, by various hydrolytic enzymes (carbohydrases). Increase in free sugar content during ripening was also reported in other mango variety and in banana (Lazan *et al.,* 1993).

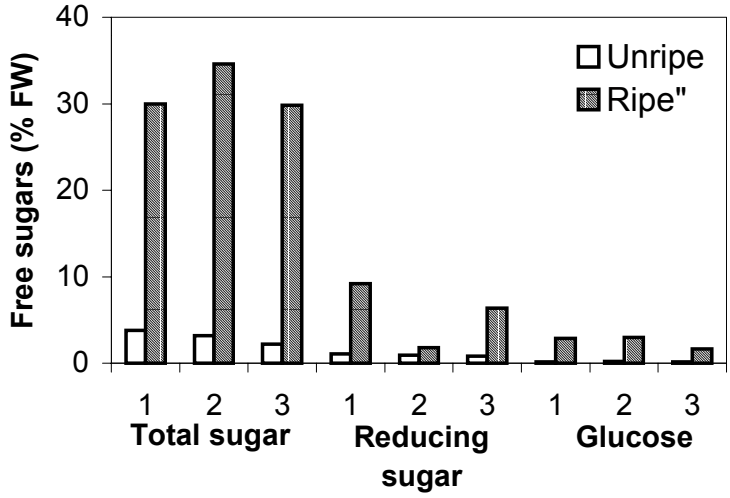

Figure 3.1.12
Percentage free sugars per 100g fresh weight of mango (1, 70 % alcohol soluble sugars; 2, Dowex 50 H^+ purified sugars; 3, Dowex 1 OH^- purified sugars)

Table 3.1.2
Changes in free sugars per 100g fresh weight of mango

Mango	Total carbohydrate (%)			Reducing sugar (%)			Glucose (%)		
	70% alcohol soluble sugar	Dowex-50 H^+	Dowex-1 OH^-	70% alcohol soluble sugar	Dowex-50 H^+	Dowex-1 OH^-	70% alcohol soluble sugar	Dowex-50 H^+	Dowex-1 OH^-
Unripe	3.8	3.2	2.2	1.1	1.0	0.8	0.2	0.2	0.2
Ripe	30.0	30.6	29.8	9.2	5.8	6.4	2.9	3.0	1.6

The composition of 70% alcohol soluble sugars of mango (as determined by HPLC) was found to be 100% higher oligosaccharides

in unripe mango, whereas in ripe mango glucose and sucrose were present in the ratio of 54.05% and 45.95%, respectively (Fig. 3.1.13). Mono- and oligosaccharides from the pulp were identified as sucrose, fructose, glucose, galactose, maltose, arabinose, rhamnose, and xylose (Table 3.1.3).

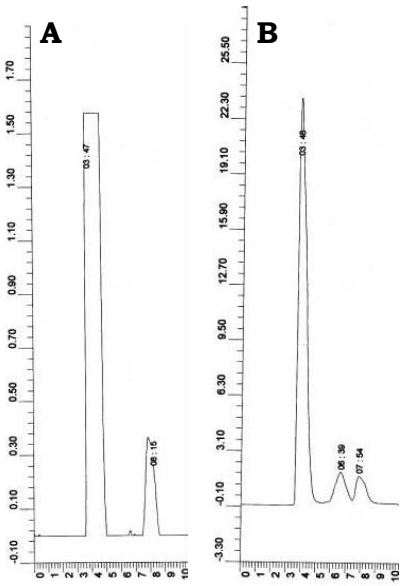

Figure 3.1.13
HPLC profiles of free sugars from unripe (A) and ripe (B) mango

Table 3.1.3
Profiles of individual sugars and organic acids in unripe and ripe mango pulp (g per 100g FW)

Sugars	Unripe	Ripe	Organic acids	Unripe	Ripe
Sucrose	0.02	5.000	**Citric acid**	2.48	0.22
Fructose	0.61	4.900	**Maleic acid**	0.03	0.16
Glucose	0.38	3.900	**Succinic acid**	0.29	0.03
Galactose	Tr	0.120	**Uronic acid**	0.01	0.03
Maltose	Tr	0.100			
Arabinose	-	0.070			
Rhamnose	-	0.030			
Xylose	-	0.002			

Note: The values are mean of 3 individual fruits, SD within 7%

Since gluconeogenesis is related to carbohydrate metabolism, which was found to be specially powerful in mango, some interesting

observations noted regarding this are also recorded here. Sucrose, glucose and fructose levels increased by 250, 10 and 6 folds, respectively, while succinate and citrate levels decreased by 8 to 10 folds. Among the organic acids, only maleic and total uronic acids increased by 5 and 3 folds, respectively (Table 3.1.3). The decrease in organic acids during ripening was accompanied by a decrease in starch and a concomitant increase in total soluble solids and sucrose level. Similar observations were made regarding organic acid content but contrasting results were noticed about the sugar levels in 'Harumanis' mango (Lazan *et al.,* 1993).

^{14}C-starch distribution into glucose, fructose and sucrose (Table 3.1.4) clearly indicated efficient sugar inter-conversions. On the other hand a significant incorporation of radioactivity both from ^{14}C-citrate and ^{14}C-aspartate into sugar fractions indicated powerful gluconeogenesis in this fruit system. Most of the gluconeogenic enzymes such as fructose-1,6-biphosphatase (FDPase), phosphoenolpyruvate carboxykinase (PEPCK), phosphoenolpyruvate carboxylase (PEPC), succinate dehydrogenase (SDH), glucose-6-phosphatase (G-6-Pase) and glucokinase, increased significantly during ripening, exhibiting highest activity at the ripe stage, except for maleic enzyme, which remained constant throughout (Fig 3.1.14 A and B).

Table 3.1.4

Incorporation of radioactivity of ^{14}C-starch and ^{14}C-organic acids into sugar fractions of mango pulp

^{14}C compounds	Mango	Total counts incorporated in total sugar fraction (μCi)	% Distribution of radioactivity		
			Glucose	Fructose	Sucrose
^{14}C-starch	Unripe	0.006	52	43	5
	Ripe	0.400	28	32	40
^{14}C-citrate	Unripe	0.002	70	23	7
	Ripe	0.085	20	25	55
^{14}C-aspartate	Unripe	0.003	50	30	10
	Ripe	0.025	25	28	47

Note: The values are mean of 3 individual fruits, SD within 7%

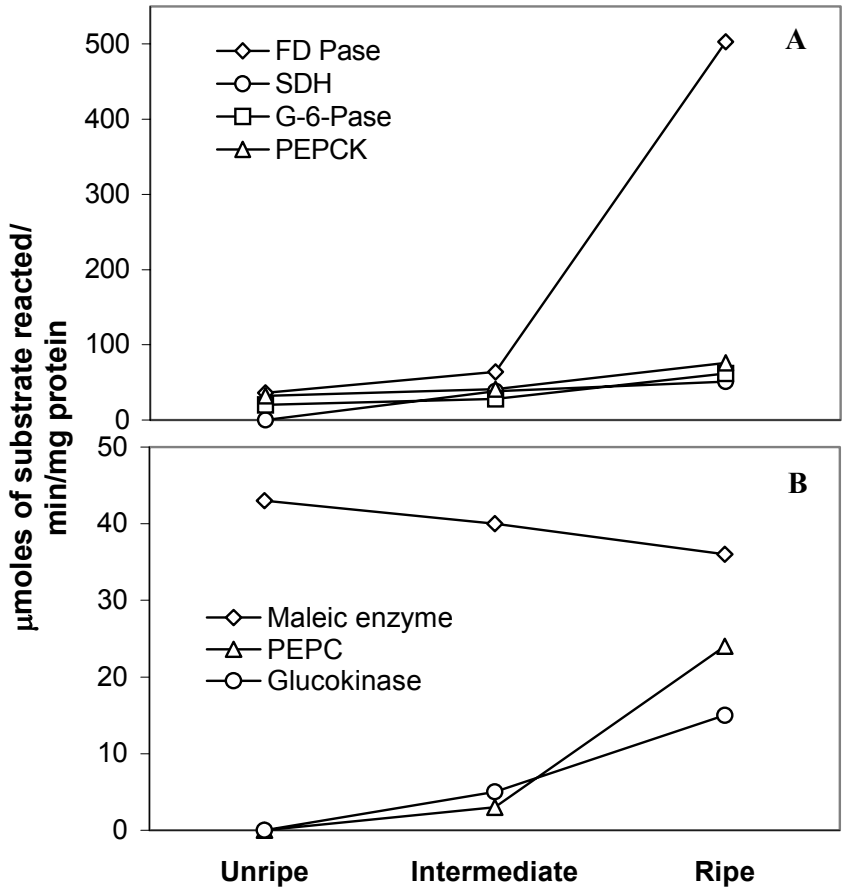

Figure 3.1.14

Changes in the profiles of gluconeogenic enzymes

During ripening, decline in AIR and concomitant increase in total soluble sugars was reported for mango (Brinson *et al.,* 1988; Roe and Bruemmer, 1981; Selvaraj and Kumar, 1989) and other fruits like papaya (Chan and Tam, 1982), guava, date (El-Zoghbi, 1994) and strawberry (Huber, 1984). Decrease in AIR as well as fruit firmness are the general physicochemical features accompanying the ripening of seven Indian mango varieties (Selvaraj and Kumar, 1989) and other fruits (Ben-Arie *et al.*, 1979). Apparent increase in AIR during development and decrease during ripening was reported in 'Dashehari' mango (Tandon and Kalra, 1984). Increase in AIR during ripening was reported for bush butter fruit, which is mainly attributed to dehydration (Missang *et al.*, 2001a).

Fractionation of AIR

The AIR from the mesocarp of mangoes at two extreme stages of ripening unripe (I) and ripe (IV) were obtained by homogenization of the tissues, after soaking in alcohol, centrifugation and residue was washed with organic solvent. It is believed, AIR content is large at the unripe stage because of involvement with starch, cellulose, hemicellulose, pectin, lignin and protein, whereas in the ripe stage it is low because of alcohol soluble sugars and pigments accompanying ripening. The AIR was fractionated sequentially based on their differential solubility into eight different fractions (Fig. 3.1.15), viz., cold water solubles (CWS), hot water solubles (HWS), EDTA soluble pectic fractions showing the highest galacturonic acid content, and the alkali extracted fractions, hemicellulose 'A' and 'B', and the insoluble residue, cellulose/lignin. Ripening resulted in a reduction in the amount of all these fractions. The cell wall material after fractionation was consistently higher in 'Alphonso' than in 'Malgoa', although it decreased during ripening in both the cultivars and also in other climacteric fruits like banana and papaya (Table 3.1.5).

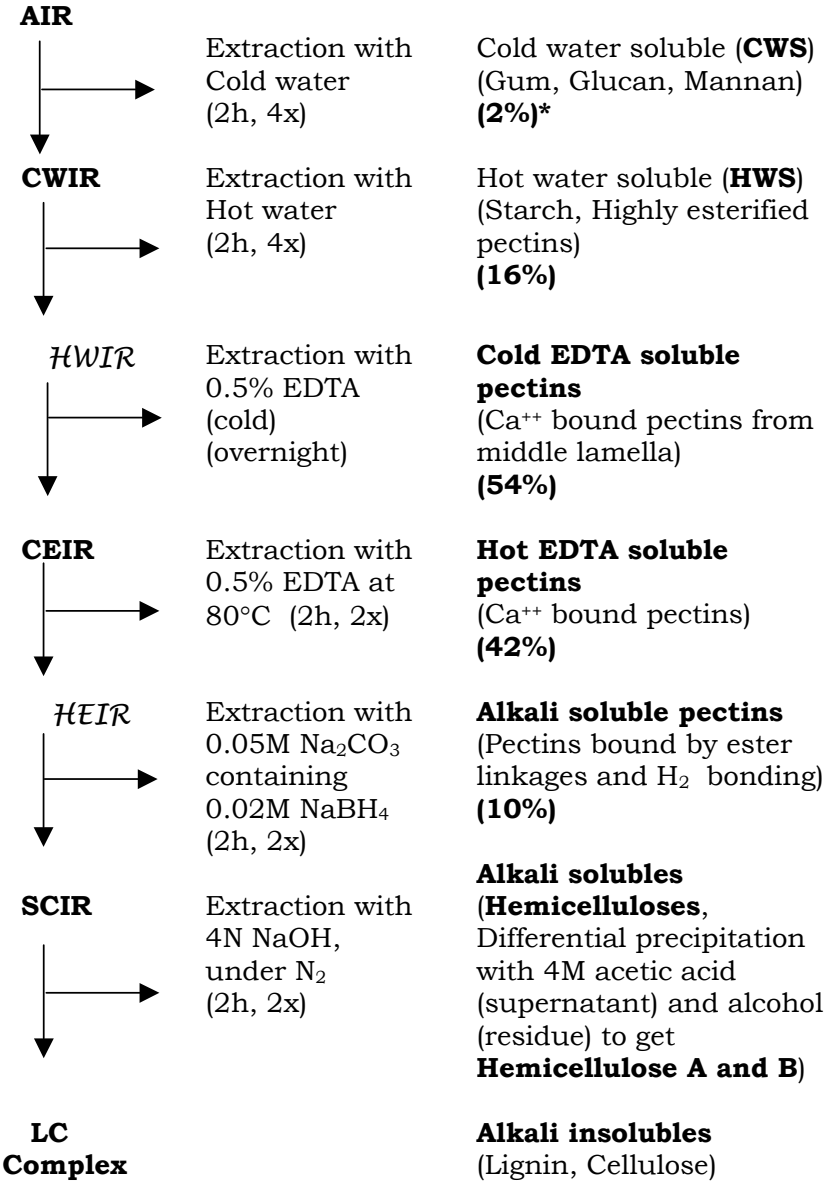

Figure 3.1.15
Flow chart for the sequential extraction of carbohydrates based on differential solubility

AIR-Alcohol insoluble residue; CWIR-Cold water insoluble residue; HWIR-Hot water insoluble residue; CEIR-Cold EDTA insoluble residue; HEIR-Hot EDTA insoluble residue; SCIR-Sodium carbonate insoluble residue; LC-Lignin/cellulose; * % GalA of Total Sugars (shown for unripe stage to indicate extractability)

Table 3.1.5
Yield in grams per 100 g FW of the tissue

Fractions	Mango				Banana		Papaya	
	Alphonso		Malgoa					
	Unripe	Ripe	Unripe	Ripe	Unripe	Ripe	Unripe	Ripe
AIR	7.85	2.92	4.79	2.67	17.34	4.09	2.84	2.32
Fines	15.50	0.03	5.30	0.10	12.24	2.76	-	-
CWS	0.76	0.62	0.01	0.92	0.81	0.38	0.15	0.78
HWS	0.55	0.31	0.13	0.04	6.65	0.19	0.03	0.14
Pectic	1.86	0.38	1.80	1.28	1.58	1.10	0.86	0.54
Hemicellulose (Total)	0.80	0.20	0.34	0.09	4.52	0.85	0.55	0.05
Hemicellulose A	0.18	0.04	0.12	0.04	0.81	0.82	0.08	0.05
Hemicellulose B	0.62	0.15	0.22	0.05	3.72	0.03	0.47	0.01
Cellulose/lignin	2.03	0.80	1.02	0.47	2.33	0.74	1.23	0.65

Changes in the mechanical properties indicated pulp softening as pulp viscosity decreased in all the fractionated polysaccharides during ripening (Table 3.1.6). CWS fraction was found to be more viscous than other polysaccharides and its viscosity was 19.67 at the unripe stage and 4.35 at the ripe stage. Viscosity results from the friction and enlargement of polymers. The decrease in viscosity should be attributed to the breakdown of polymers, such as cell wall polysaccharides and starch but not to the increase in the water content, because there was no significant change in the moisture content between unripe and ripe stages of mango (Table 3.1.1).

Table 3.1.6
Proximate composition of the fractionated polysaccharide fractions

Fractions	Solubility (%)		Total carbohydrate (%)		Uronic acid (%)		Neutral sugar (%)		UA:NS Ratio		Reduced viscosity (η_r)		Specific viscosity (η_r-1)	
	Unripe	Ripe	Unripe	Ripe	Unripe	Ripe	Unripe	Ripe	Unripe	Ripe	Unripe	Ripe	Unripe	Ripe
CWS	95.0	94.0	99.9	59.0	14.3	21.5	85.6	37.5	0.2:1	0.6:1	19.7	4.4	18.7	3.4
HWS	82.2	30.4	77.2	42.3	11.9	21.5	65.3	20.8	0.2:1	1.0:1	3.7	2.1	2.7	1.1
Pectic	30.4	97.0	48.2	10.5	12.2	18.9	36.0	8.5	0.3:1	1.2:1	3.1	2.9	2.1	1.9
Hemicellulose (Total)	38.4	49.5	36.7	63.2	6.1	9.4	30.6	53.8	0.2:1	0.2:1	2.7	2.1	1.7	1.1
Hemicellulose A	79.2	32.8	80.6	16.3	11.6	6.8	69.0	9.5	0.2:1	0.7:1	2.1	1.1	1.1	0.1
Hemicellulose B	93.1	89.8	81.4	82.2	12.8	13.7	68.6	68.5	0.2:1	0.2:1	2.5	2.1	1.5	1.1

The fractionated carbohydrates were acid hydrolyzed to see their compositional differences between unripe and ripe stages. The monosaccharides released by hydrolysis with acid are shown in Table 3.1.7. A significantly higher yield of monosaccharides was obtained from unripe material than from the ripe fruits. At the ripe stage, the loss of galactose and mannose from water soluble polysaccharide fractions, galactose and arabinose from hemicellulose fractions, uronic acid and rhamnose in pectic fraction and glucose from cellulose fraction point out *in vivo* solubilization of the respective polymers. There is a marked reduction in the arabinose, galactose and galacturonic acid contents of the mesocarp cell walls during the ripening process indicating loss of the pectin complex in CWS, HWS and EDTA soluble fractions. Some of the glucose from the cell wall preparations is likely to be derived from starch, which constitutes upto 16% of the mature unripe fruit tissue. This gives a direct index of the *in vivo* hydrolysis by loss of sugar components during ripening. The presence of high galacturonic acid along with relatively high galactose and arabinose residues indicates that these fractions are pectic in nature (Table 3.1.7). Chelator solubles are usually pectic polysaccharides, which are generally associated with Ca^{++} ions (Smith and Harris, 1995). EDTA by chelating with Ca^{++} ions favours pectin solubilization. EDTA extracts pectins from the middle lamella, while Na_2CO_3 extracts covalently bound pectins essentially from the primary cell wall (Redgwell *et al.*, 1990). The amount of galacturonic acid was much higher in EDTA-solubles indicating that the pectins in the cell wall of mango pulp are essentially ionic in nature and are concentrated in the middle lamella region. High amount of pectins in chelator-solubles were reported for other fruits (Missang *et al.*, 2001a; Redgwell *et* al., 1991). The amount of polysaccharides solubilized by Na_2CO_3 was higher than that solubilized by EDTA was reported for Kiwi fruit (Redgwell *et al.,* 1992).

Table 3.1.7
Carbohydrate composition (mg %) of the fractionated polysaccharide fractions

Fractions	Rha		Ara		Xyl		Man		Gal		Glc		Pentoses: Hexoses	
	Unripe	Ripe	Unripe	Ripe	Unripe	Ripe	Unripe	Ripe	Unripe	Ripe	Unripe	Ripe	Unripe	Ripe
AIR	0.4	0.7	2.2	8.5	0.8	2.9	0.4	0.7	0.9	4.1	76.6	13.7	1:2.3	1:1.5
CWS	0.2	0.1	1.6	0.7	0.1	0.2	1.2	0.1	1.9	0.6	55.7	2.5	1:31.1	1:3.0
HWS	0.4	1.0	2.3	4.3	0.04	2.0	0.1	0.5	1.7	2.8	15.3	21.7	1:21.0	1:2.5
Pectic	0.4	0.3	2.5	1.4	0.1	0.1	0.3	0.1	1.4	0.5	36.4	3.3	1:13.0	1:2.2
Hemicellulose (Total)	0.3	2.8	2.0	4.2	2.2	12.7	0.8	1.8	0.8	4.8	77.9	60.0	1:17.6	1:3.4
Hemicellulose 'A'	0.4	0.6	1.1	2.1	1.0	8.0	0.5	0.6	0.3	0.9	89.6	11.4	1:36.3	1:1.2
Hemicellulose 'B'	0.2	2.7	0.8	0.9	3.1	21.2	0.8	5.9	1.0	7.9	90.2	51.3	1:22.3	1:2.6
Alkali insoluble residue	2.0	0.5	10.4	2.2	3.4	2.5	3.4	1.8	7.8	1.3	55.2	76.2	1:4.2	1:15.0

Low level of galacturonic acid was reported in Na_2CO_3-solubles for olive fruits (Jimenez *et al.*, 2001), while high level was reported for nectarines (Lurie *et al.,* 1994). Generally, arabinose and rhamnose residues were higher and galacturonic acid was lower in Na_2CO_3-solubles than chelator-solubles pectins (Hegde and Maness, 1996). The EDTA-solubles decreased during ripening in contrast to chelator-soluble pectins as reported for avocado (Femenia *et al.,* 1998).

Of the AIR from both unripe and ripe mango, cold water solubilized ~18%, hot water solubilized ~11%, EDTA solubilized ~14% and alkali solubilized ~5%. The other components of AIR were alkali-solubilized pectins, celluloses, proteins and probably non-sugar cell wall constituents such as polyphenols and lignins (Selvendran, 1975; Thomas and Thibault, 2002). EDTA was used as extractant as it extracts more chelator-solubles than other chelators (Renard and Thibault, 1993). A steady decline in all the fractionated polysaccharides was observed during ripening. Low sugar content in the EDTA-soluble pectins and persistence of high amount of EDTA in spite of prolonged dialysis was reported for sugar beet pectins (Fares *et al.,* 2001). Banana chelator-soluble pectins decreased from 1.1 to 0.8% during ripening (Bhagyalakshmi *et al.,* 2002). Concomitantly, the soluble galacturonide content increased in CWS (39.17-71.9%) and EDTA soluble fractions (59.0-69.6%) whereas it decreased in HWS and hemicellulose fractions during ripening. The degradation of pectic polysaccharides resulted in the accumulation of soluble galacturonide in ethanol-soluble fraction.

The water-soluble as well as chelator-soluble pectins and also hemicelluloses decreased during ripening in Alphonso mango, unlike in other mango varieties, as reported in other fruits such as cherry

(Fils-Lycaon and Buret, 1990), peach (Hegde and Maness, 1998), strawberry (Nogata *et al.*, 1993), kiwi (Redgwell *et al.*, 1992), nectarine (Lurie *et al.,* 1994), and bell pepper (Priya Sethu *et al.,* 1996), while increase of the same was reported in pear (Ben-Arie *et al.*, 1979), spanish pear (Martin-Cabrejas *et al.*, 1994), apple (De Vries *et al.,* 1984), avocado (Huber and O'Donoghue, 1993), apricot (Femenia *et al* .,1998), banana (Prabha and Bhagyalaksmi, 1998), olive (Huisman *et al.*, 1996), 'Keitt', 'Ngowe' and 'Tommy Atkins' varieties of mango (Mitcham and McDonald, 1992; Muda *et al.,* 1995; Roe and Bruemmer, 1981). In tomato there was no change in the chelator-soluble pectin during ripening (Gross, 1984). Increase in soluble galacturonide during ripening was also reported for pear (Ben-Arie *et al.*, 1979), tomato (Huber, 1983b), muskmelon (McCollum *et al.*, 1989), and kiwi (Redgwell *et al.*, 1992). Generally, fruit softening is accompanied by a decrease in the amount of insoluble pectic substances and a concomitant increase in soluble polyuronides (Doesburg, 1965; Kertesz, 1951). The results showed that water-soluble as well as EDTA-soluble pectins are the major polysaccharides that undergo drastic degradation during ripening along with hemicelluloses, which also contribute for tissue softening phenomenon.

The decrease in cellulose (2.0 to 0.9%) content was also observed during ripening (Table 3.1.5). In ripening tomato fruit, cellulose was not considered to be significant for textural loss (Tucker and Grierson, 1987). In mango, it appears that apart from pectin, cellulose (to some extent) may also be a component contributing to the changes in cell structure at the cell wall level. The disappearance of starch may also be an important factor contributing to textural softening. Banana is another climacteric fruit, which is rich in starch (12.24%) that almost disappears during

ripening (2.75%). Prabha and Bhagyalakshmi (1998) have reported complete degradation of starch during ripening of banana.

A clear correlation between textural loss and pectin content was reported in Japanese pear, where water soluble as well as chelator-soluble pectins were found to affect the fruit texture (Sirisomboon *et al.*, 2000). The texture of sweet cherry fruit was reported to be related to equilibrium between the relative pectic fractions (Fils-Lycaon and Buret, 1990). Loss of pectic polysaccharide in relation to textural softening was reported in olive (Marsilio *et al.*, 2000) and tomato (Jackman and Stanley, 1995). A positive correlation between chelator-soluble pectins and loss of tissue firmness was reported (Chang *et al.*, 1993; Yu *et al.*, 1996). Chelator-soluble pectins exist as pectic acids that bind calcium and form cross-links, which is responsible for tissue firmness (Yu *et al.*, 1996; Neal, 1965). In apple, papaya, and capsicum, a clear correlation between textural loss and cell wall degradation, especially the breakdown of pectin, cellulose and hemicellulose was reported by many authors (Abbott *et al.*, 1984; Bhagyalaksmi *et al.*, 2002; Koh and Melton, 1994; Prabha *et* al., 2000; Priya Sethu *et al.*, 1996). As the compactness of the cell wall structure was modified, polymers and enzymes were able to come in contact with each other resulting in degradation of wall polymers during ripening. Pectic polymers, which are the hydrophillic polymers in the cell wall, are the first to be solubilized (Redgwell *et al.*, 1992). The breakdown of tightly bound insoluble protopectin to soluble polyuronides, which are loosely bound to the cell wall, appears to influence the fruit/textural softening during ripening (Doreyappa Gowda and Huddar, 2001). The pectin solubilization results in the loosening of middle lamella and primary cell wall by lowering the degree of cross-linking (Newmann and Redgwell, 2002). There exist a clear correlation

between the cell wall swelling and the degree of pectin solubilization, suggesting that the wall swelling is the consequence of the changes occurring in the viscoelastic properties of the cell wall during pectin solubilization (Redgwell *et al.*, 1997b). The highly branched pectic polysaccharides in the primary cell wall are accessible for hydration and degradation, and as a result, their solubilization leads to marked decrease in neutral sugar side chains and eventually textural softening.

Conclusions

Ripening of mango is characterized by changes such as hydrolysis of starch, a concomitant increase in total sugar, free sugars, soluble polyuronides, and a decrease in titrable acidity. Ripening is also characterized by rapid and extensive softening of fruit, which correlates positively with an increase in the activity of most of the carbohydrate hydrolases and with the solubilization of respective polysaccharides.

Section 2

Changes in the profile of cold water soluble polysaccharides

Introduction

Fruit development, involving a coordinated series of biochemical processes, results in the biosynthesis as well as degradation of cell wall components. The cell walls of fruits have received considerable attention especially with respect to changes occurring during maturation and ripening. Much work in the area of fruit ripening has been focused on ripening-associated changes with specific reference to textural softening which is mainly due to changes in cell wall structure and composition (Brady, 1987; Brownleader *et* al., 1999; Hobson, 1981; Seymour and Tucker, 1996; Sirisomboon *et al.*, 2000; Tucker and Seymour, 1991; Waldron *et al.*, 1997). Knowledge of the composition and structure of cell wall polysaccharides of fruit during ripening may provide an insight into the chemical, physical, and enzymological processes involved. Pectin and hemicelluloses are the major polysaccharides contributing to the above phenomenon (Sirisomboon *et al.*, 2000).

Pectins, the complex cell wall polysaccharides can be extracted by cold water, hot water, weak acids, weak base and chelating agents. Hemicelluloses are extracted with higher strength of alkali. After extraction, fractionation of polysaccharides was normally accomplished by a combination of various fractionation methods; precipitation with alcohol, ion exchange chromatography (IEC) and/or gel permeation chromatography (GPC). High performance size exclusion chromatography (HPSEC) is the most versatile technique used for separating molecules based on their molecular size differences as well as to determine the relative molecular weight of polysaccharides. Once the sample is fractionated, composition

analysis of monosaccharides, in qualitative and quantitative terms, was performed by GLC, after converting the sugars into volatile derivatives (Selvendran *et al.,* 1979; York *et al.,* 1985).

Changes in the cold water soluble, hot water soluble, EDTA soluble pectic and hemicellulose fractions of the cell wall, especially increased solubility, depolymerization, deesterification, and loss of neutral sugar side chains are described in many fruits, (Femenia *et al.,* 1998; Hegde and Maness, 1998; Missang *et al.*, 2001b; Rose *et al.,* 1998). However, a detailed investigation to show the entire spectrum of water soluble (cold and hot), EDTA soluble pectic polymers and also hemicelluloses present and their qualitative and quantitative changes during ripening is not well documented in fruits.

Very little is known about the cell wall structure and pectin and hemicellulose composition of mango fruit. Only gross changes in the mango cell wall pectins with a net loss of sugar residues in total pectin during ripening have been reported (Brinson *et al.,* 1988; El-Zoghbi, 1994; Mitcham *et al.*, 1992; Muda *et al.*, 1995; Roe and Bruemmer, 1981). One of the approaches to deduce the nature of the physicochemical and enzymological process involved in pectin hydrolysis *in vivo* is to characterize the changes occurring in the polyuronide structure and composition during ripening. This section specifically deals with the dissolution *in vivo* of cold water soluble polysaccharides, their qualitative and quantitative changes, and drop in the molecular weight.

Results and Discussion

Cold water soluble (CWS) polysaccharides constitute ~18% of the AIR from both unripe and ripe mango, showing a decrease from 0.755g to 0.615g % FW (w/w). The observation that the galacturonic acid to neutral sugar ratio was higher in the ripe stage than unripe stage [Table 3.1.6] was indicative of a more pronounced dissolution of neutral sugar residues upon ripening.

The CWS fractions were subjected to DEAE-cellulose ion exchange chromatography and the column fractions were assayed colorimetrically for total sugars. The elution profiles depicted in Fig. 3.2.1 gives both qualitative as well as quantitative profiles of the entire CWS polysaccharides. Fractions were eluted stepwise from the column by water and with increasing molarities of $(NH_4)_2CO_3$ and NaOH. CWS from unripe and ripe mango pulp was resolved into 10 distinct fractions (I to VIII). The major fraction was found in 0.15 M and 0.2 M $(NH_4)_2CO_3$ eluates. At higher strength gradients [0.3 to 0.45 M $(NH_4)_2CO_3$], no carbohydrate peaks were detected. 0.15, 0.30 and 0.45 M of NaOH gradients showed some minor peaks but with lower levels of uronic acid (<5%). Loss in qualitative (carbohydrate content) and quantitative levels (yield as dry weight) from unripe to ripe stage was observed in all the fractions. A slight increase in fraction I and III (neutral and 0.15 M $(NH_4)_2CO_3$) and about 40% increase in total carbohydrates of VI and VII (0.3 M NaOH) may indicate that the degradation of protopectin during ripening. Similar observation was shown in bush butter fruit (Missang *et al.*, 2001a). Changes in the IEC profiles of CWS pectins from unripe and ripe tomatoes have been reported (Huber and Lee, 1986; Gross *et al.*, 1986).

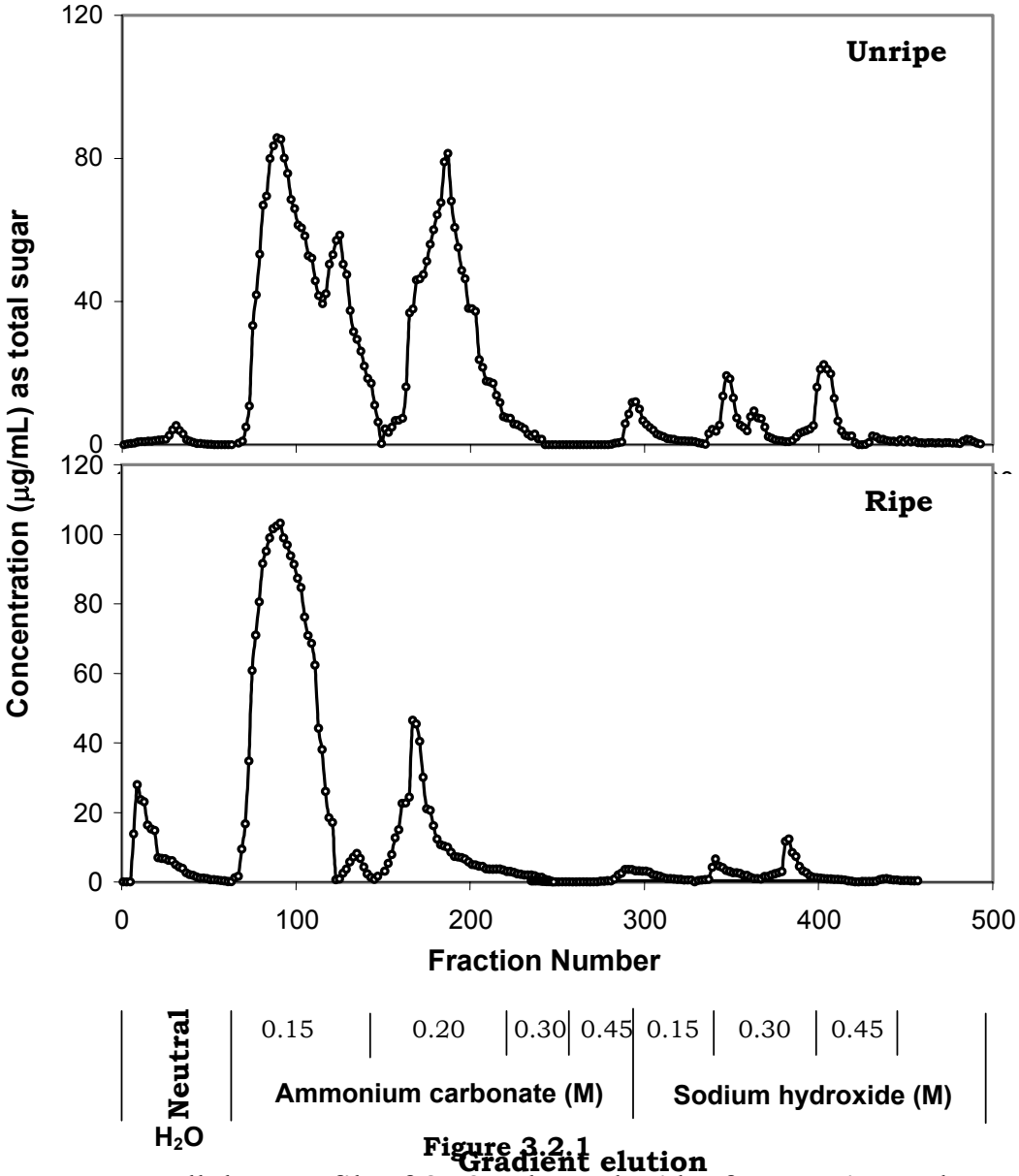

Figure 3.2.1
DEAE-cellulose profile of CWS polysaccharides from unripe and ripe mango

Ion-exchange chromatography has been successively applied by various investigators to fractionate CWS polysaccharides (Gross *et al.,* 1986, Dick and Labavitch, 1989; Fares *et al.*, 2001; Stevens and Selvendran, 1984). However, molecular weight and covalent linkages of neutral sugar also influenced elution patterns (De Vries *et al.,* 1986). Ammonium carbonate and NaOH (weak and strong alkali respectively) were used for fractionating carbohydrate polymers on DEAE-cellulose column (Siddiqui and Wood, 1971). Ammonium ions

are found useful for quantitative elution of pectic fractions from anion-exchanger.

The relative abundance and their sugar composition as well as changes from unripe to ripe stage of all the CWS pectic fractions are detailed in Tables 3.2.1 and 3.2.2. A significant decrease in the % yield from unripe to ripe stage was evident in most of the fractions except fraction I, which increased by over one fold (11.3 to 25.6%) while fraction II showed only a marginal increase from 86.8 to 88.4%. The drop in their levels for the fractions III and IV from unripe to ripe stage was 55.9 to 14.1% and 83.9 to 43.3%, respectively. Nevertheless, there was no complete disappearance of any of these fractions at the end of ripening indicating a controlled depolymerization of CWS polysaccharides.

Table 3.2.1
Abundance and composition (%) of DEAE-cellulose fractionated CWS polysaccharides

Fr. No.	Polymeric fraction	Yield		Total carbohydrate		Uronic acid		Neutral sugar		UA:NS Ratio	
		Unripe	Ripe	Unripe	Ripe	Unripe	Ripe	Unripe	Ripe	Unripe	Ripe
I	**Neutral**	11.3	25.6	63.3	68.8	13.3	18.3	50.0	50.5	0.3:1	0.4:1
II	**0.15M $(NH_4)_2CO_3$**	86.8	88.4	68.8	62.7	23.6	27.0	45.2	35.7	0.5:1	0.8:1
III		55.9	14.1	51.7	54.2	28.3	24.4	23.4	29.8	1.2:1	0.8:1
	a										
	b										
IV	**0.20M $(NH_4)_2CO_3$**	83.9	43.3	40.9	33.3	24.0	26.1	16.9	7.2	1.4:1	3.6:1
V	**0.15 M NaOH**	22.6	14.7	100.0	80.4	4.7	4.1	95.3	76.3	0.05:1	0.05:1
VI	**0.30 M NaOH**	29.4	11.7	50.2	95.3	2.7	1.8	47.5	93.5	0.06:1	0.02:1
VII		27.2	15.4	51.5	92.6	2.6	1.6	48.9	91.0	0.05:1	0.02:1
	a										
	b										
VIII	**0.45 M NaOH**	7.5	4.9	54.7	50.3	2.4	1.3	52.3	49.0	0.05:1	0.03:1

Galacturonic acid was present in all the fractions and it decreased in NaOH eluted fractions (Table 3.2.1). Fractions II, III, IV contained high galacturonic acid content (~25%) compared to other

fractions. Fractions V, VI, VII, VIII contained glucose as the major neutral sugar, and were not considered for further studies.

All the fractions showed galactose, arabinose, glucose and rhamnose, which are the characteristic neutral sugars of pectic type polymers. Based on the composition data, fraction I, appeared to be a heteropolymer, probably present as glucomannan covalently linked to pectic polymers (Mitcham and McDonald, 1992) or strongly linked to cellulose (Redgwell *et al.,* 1997a). Fractions II, III and IV were heterogalacturonans containing different ratios of arabinose, galactose, rhamnose. A substantial increase in the pentose to hexose ratio was observed in all the fractions indicating the degradation of hexosans rather than pentosans during ripening (Table 3.2.2). The presence of both galacturonic acid and neutral sugar in these fractions may suggest that they are branched pectins of rhamnogalacturonan-type.

Table 3.2.2
Neutral sugar composition (mg %) of CWS fractions

Fr. No.	Polymeric fractions	Rha		Ara		Xyl		Man		Gal		Glc		Pentoses: Hexoses	
		Unripe	Ripe	Unripe	Ripe	Unripe	Ripe	Unripe	Ripe	Unripe	Ripe	Unripe	Ripe	Unripe	Ripe
I	**Neutral**	0.5	1.6	2.5	8.1	0.3	1.7	37.9	15.6	2.6	10.6	6.7	12.5	1:16.4	1:3.4
II	**0.15 M a**	2.1	1.8	8.8	11.2	0.4	0.2	5.6	0.6	20.8	15.8	7.6	6.1	1:3.0	1:2
III	**$(NH_4)_2CO_3$ b**	2.3	2.7	9.2	10.8	0.3	0.6	0.5	0.7	6.2	8.7	5.0	6.3	1:1	1:1.1
IV	**0.20 M $(NH_4)_2CO_3$**	2.7	0.8	7.4	3.0	0.7	0.5	0.9	0.4	1.5	0.9	3.7	1.6	1:0.6	1:0.7
V	**0.15 M NaOH**	1.7	3.3	1.7	8.5	1.8	3.9	0.3	1.5	0.2	3.9	89.5	55.1	1:17.2	1:4.0
VI	**0.30 M a**	4.3	3.6	4.9	4.4	6.9	8.3	5.0	1.1	4.9	6.2	21.4		1:2.0	1:47
VII	**NaOH b**	0.8	2.5	0.8	1.5	2.8	10.0	3.7	2.6	3.1	3.9	37.7	70.4	1:10.0	1:6.0
VIII	**0.45M NaOH**	1.1	0.9	1.9	1.2	4.8	2.9	4.2	1.1	1.4	2.3	38.4	40.4	1:6.0	1:9.0

During ripening of mango, loss of galacturonic acid (20-30%) and galactose, arabinose and rhamnose (>50%) residues in all the CWS pectic fractions were observed. Similar loss of acidic and neutral sugars was observed in total pectic fraction of ripening fruits such as persimmon (Cutillas-Iturralde *et al.*, 1993) 'Ngowe' mango (Brinson *et al.*, 1988) and tomato (Gross, 1984). Gross and Sams (1984) reported a net loss of galactose/arabinose from the cell wall of 14 types of fruits. Loss of galacturonic acid was also reported in other varieties of mango (Brinson *et* al., 1988; Mitcham and McDonald, 1992). However, polyuronide synthesis during ripening was reported for plum and cherry fruits (Boothby, 1983; Fils-Lycaon and Buret, 1990). Increase in the levels of neutral sugars of chelator-soluble pectins during ripening was also reported for olive fruit (Huisman *et al.*, 1996). Thus, the cell wall neutral sugar composition varies among fruits and the metabolism of pectins in relation to textural softening differs from fruit to fruit, as mentioned by Gross and Sams (Gross and Sams, 1984). In peach, softening is associated with change in the sugar composition of pectin and hemicellulose as well as their change in molecular mass (Hegde and Maness, 1998; Hegde and Maness, 1996).

Changes occurring during ripening resulted in changes in the molecular weight distribution of the CWS polymeric fractions. The elution patterns (both GPC and HPSEC) showed a broad molecular weight distribution. During ripening a shift to lower molecular weight material was noticed in all the fractions. At unripe stage, the molecular weight distribution became broader, due to the extraction of very high molecular weight material. The pattern did not change much, but peak height and area decreased during ripening.

Only a few reports have been published concerning molecular weight changes of CWS pectic fractions during ripening (Jimenez *et* al., 2001). The average molecular weight decrease of CWS was

observed in peach (Shewfelt *et al.*, 1971; Pressey *et al.*, 1971). The conversion of protopectin to water soluble pectin in the peach was accompanied by polymer degradation but not to the extent observed in mango. Degradation of mango polysaccharides apparently proceeded to the stage that the product molecules were small enough to be soluble in ethanol and were not precipitated in the AIR. Mort *et al.*, (1991) and Fishman *et al.,* (1986) concluded that pectin-aggregation makes gel permeation chromatography a poor technique for the determination of molecular weight, and thus HPSEC was used to determine the molecular weight. Figure 3.2.2 and Table 3.2.3 gives the molecular weight changes from unripe to ripe stage of all the CWS fractions, as determined by HPSEC. Molecular weight determination by HPSEC was reported by many authors (Huisman *et al.*, 1996; Jimenez *et al.*, 2001; Missang *et al.*, 2001b; Oesterveld *et al.*, 2000; Olle *et al.*, 1996). The molecular weight difference from unripe to ripe stage was 2818 to 1995 and 1995 to 126 kDa, for the major fractions (II and IV), respectively. The profiles showed peaks for unripe at ~14-16 min and for ripe at ~16-21 min. Broad distribution of molecular weight of pectins, eluting in ~13-14 min and ~14-17 min was reported in mango (Olle *et al.*, 1996).

The presence of specific substrates in qualitative and quantitative terms and their changes during ripening give a direct evidence to speculate the corresponding enzyme targets. However, only gross information about the changes in the substrates can be obtained by compositional data and molecular weight analysis. Thus, a clear understanding of the pectin structure is necessary to determine the type of enzymes involved in the degradation of these substrates during softening of mango fruit.

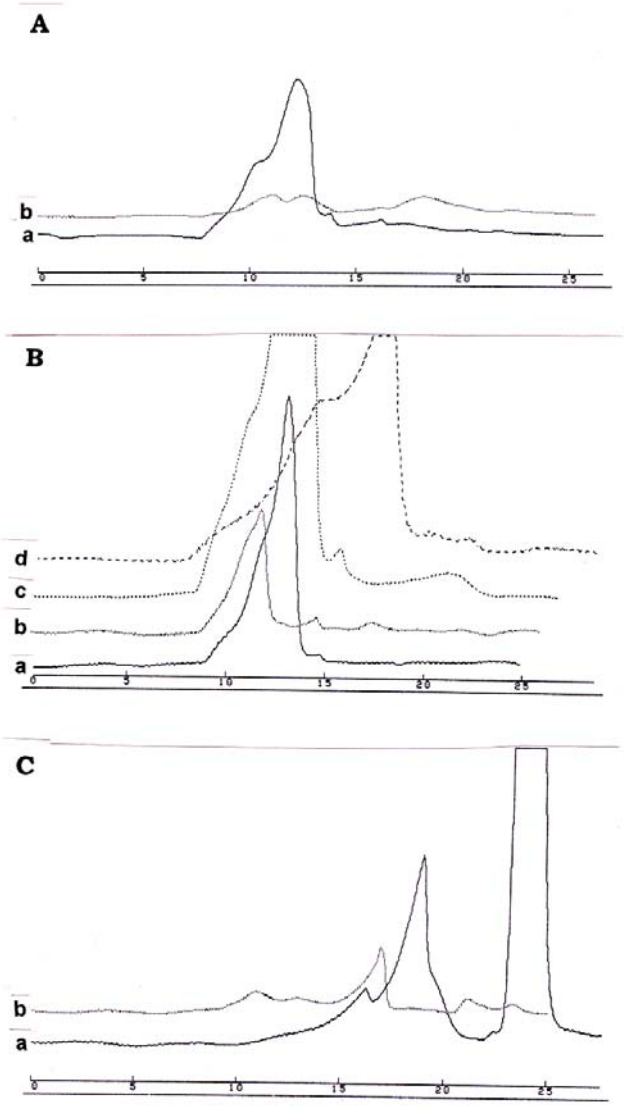

Figure 3.2.2 (a) HPSEC profiles of CWS fractions

A: a, neutral unripe; b, neutral ripe

B: a, 0.15 M $(NH_4)_2CO_3$ unripe fr.1; b, 0.15 M $(NH_4)_2CO_3$ unripe fr. 2; c, 0.15 M $(NH_4)_2CO_3$ ripe fr. 1; d, 0.15 M $(NH_4)_2CO_3$ ripe fr. 2

C: a, 0.20 M $(NH_4)_2CO_3$ unripe; b, 0.20 M $(NH_4)_2CO_3$ ripe

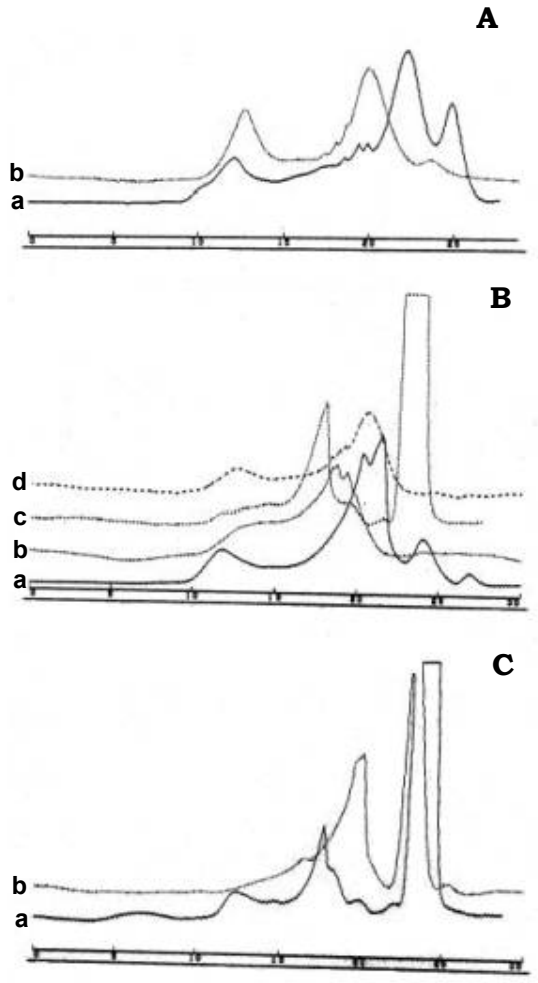

Figure 3.2.2 (b) HPSEC profiles of CWS

A: a, 0.15 M NaOH unripe; b, 0.15 M NaOH ripe
B: a, 0.30 M NaOH unripe fr. 1; b, 0.30 M NaOH unripe fr. 2; c, 0.30 M NaOH ripe fr. 1; d, 0.30 M NaOH ripe fr. 2
C: a, 0.45 M NaOH unripe; b, 0.45 M NaOH ripe

Table 3.2.3
Changes in molecular weights of CWS fractions

Fr. No.	Polymeric fraction	Molecular weight in kDa	
		Unripe	**Ripe**
I	**Neutral**	2818 355 45	631 178 63 4
II	**0.15 M $(NH_4)_2CO_3$ a**	2818 891 631 501 398 141	1995 282
III	**b**	3981 141	1995
IV	**0.20 M $NH_4)_2CO_3$**	1995 398	126 14
V	**0.15 M NaOH**	3981 40 16	1413 50 32 8
VI	**0.30 M NaOH a**	2818 2239 1995 50	1000 159 16 1
VII	**b**	2512 10	141 112 71 22
VIII	**0.45 M NaOH**	1259 80 16	112 16 1

Conclusions

The CWS polysaccharides were fractionated into neutral and acidic polysaccharides, which showed considerable variations in abundance as well as molecular weight upon fruit ripening.

Section 3

Changes in the profile of hot water soluble polysaccharides

Introduction

Much work in the area of fruit ripening has been focused on ripening-associated changes with specific reference to textural softening which is mainly due to changes in cell wall structure and composition. The cell wall turnover in the true sense (i.e. where there is continual synthesis and degradation) does occur in some plant tissues and in fruits it is probable that during maturation, there is turnover but as ripening proceeds synthesis decreases and degradation increases (Fry, 1986). The hot water soluble polysaccharides of the cell may, therefore, reflect different metabolic processes at different physiological stages.

Results and Discussion

The HWS polysaccharides extracted from unripe and ripe mango showed a two-fold decrease in their yield from 0.535 g to 0.31 g % FW. Reduction in the amount of extractable HWS polysaccharides was also observed in 'Ngowe' mango (Brinson *et al.*, 1988). The carbohydrate and galacturonic acid content of HWS was 100 and 100% and 80.15 and 67.8% at unripe and ripe stage, respectively. The galacturonic acid to neutral sugar ratio was higher in the unripe stage (Table 3.1.6), which was indicative of its more pronounced dissolution upon ripening. Further, the pectin extractability (as galacturonic acid) at ripe stage was higher (21.5%) than at unripe stage (11.9%) as in CWS fractions.

The HWS fractions, subjected to DEAE-cellulose fractionation (Figure 3.3.1), were resolved into 10 distinct peaks, designated as fractions I to X, respectively, based on their order of elution. The relative abundance and the sugar composition of these fractions are given in Tables 3.3.1 and 3.3.2. All the fractions showed a significant drop in the levels from unripe to ripe stage. 55.6 to 28.4 mg % and 79.2 to 14.4 mg % drop was observed for the major fractions III and IV from unripe to ripe stage, respectively. However, none of the fractions showed complete disappearance at the end of ripening as in the case of CWS fractions. The 0.15 M $(NH_4)_2CO_3$ eluted and neutral fractions contained higher concentrations and rest of the fractions were poor (<3%) in galacturonic acid content (Table 3.3.1).

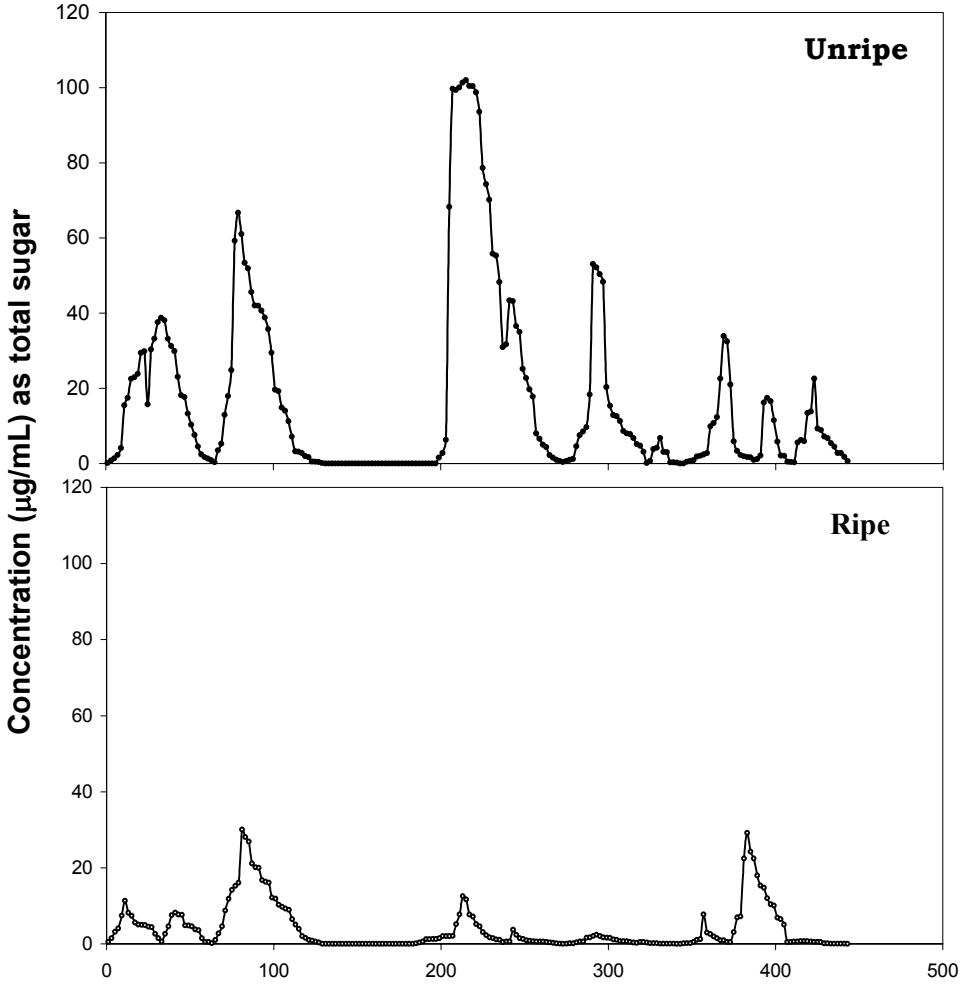

Figure 3.3.1

DEAE-cellulose profile of HWS polysaccharides from unripe and ripe mango

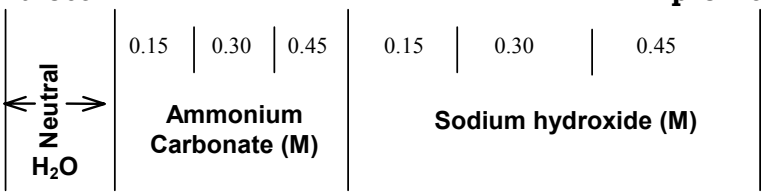

Table 3.3.1

Abundance and composition (%) of DEAE-cellulose fractionated HWS polysaccharides

Fr. No.	Polymeric fraction	Yield		Total carbohydrate		Uronic acid		Neutral sugar		UA:NS Ratio	
		Unripe	Ripe	Unripe	Ripe	Unripe	Ripe	Unripe	Ripe	Unripe	Ripe
I	Neutral a	23.5	9.3	100.0	100.0	15.0	18.2	85.0	81.8	0.2:1	0.2:1
II	b	30.2	15.4	100.0	100.0	2.0	2.6	98.0	97.4	0.02:1	0.03:1
III	0.15M$(NH_4)_2CO_3$	55.6	28.4	44.4	23.1	16.1	22.8	28.3	0.3	0.6:1	76:1
IV	0.15M NaOH a	79.2	14.4	100.0	88.0	2.9	2.4	97.1	85.6	0.03:1	0.03:1
V	b	35.3	6.2	100.0	81.7	0.8	1.2	99.2	80.6	0.01:1	0.02:1
VI	0.30 M NaOH a	43.3	5.6	100.0	93.8	0.7	1.0	99.3	92.8	0.01:1	0.01:1
VII	b	9.1	2.2	77.6	83.5	0.7	0.9	76.9	82.8	0.01:1	0.01:1
VIII	0.45 M NaOH a	29.4	7.4	100.0	87.7	0.6	0.9	99.4	86.8	0.01:1	0.01:1
IX	b	16.6	24.5	93.6	88.7	0.5	0.9	93.1	87.8	0.01:1	0.01:1
X	c	27.3	2.2	100.0	59.7	0.4	0.7	99.6	59.0	0.004:1	0.01:1

There was a total disappearance of galactose and glucose in the neutral fraction of ripe fruits, probably as a result of biodegradation of mannan, galactan and glucan or a galactomannan or glucomannan-type polysaccharide. There was also a change in the concentration of arabinose, rhamnose and xylose, which could be attributed to the degradation of associated soluble pectic polysaccharides. Similar observations were noticed in rest of the fractions, where degradation of arabinose, rhamnose, mannose and glucose were much more pronounced in NaOH eluted fractions. The increase in the pentose to hexose ratio in most of the fractions indicated the degradation of hexosans during ripening (Table 3.3.2).

Table 3.3.2
Neutral sugar composition (%) of HWS fractions

Fr. No.	Polymeric fractions	Rha		Ara		Xyl		Man		Gal		Glc		Ara : Xyl		Pentoses: Hexoses	
		Unripe	**Ripe**	**Unripe**	**Ripe**	**Unripe**	***Ripe***	**Unripe**	**Ripe**	**Unripe**	**Ripe**	**Unripe**	**Ripe**	**Unripe**	**Ripe**	**Unripe**	**Ripe**
I	**Neutral: a**	19.30	40.76	38.93	27.50	8.58	12.03	10.88	0.0	4.08	0.0	3.06	0.0	4.5:1	2.3:1	1:0.22	1:0.02
II	**b**	36.46	32.94	29.91	41.12	3.92	6.92	9.21	0.0	15.68	0.0	3.72	9.35	7.4:1	5.9:1	1:0.13	1:0.20
III	**0.15 M $(NH_4)_2CO_3$**	6.00	0.11	16.10	0.10	2.41	0.02	3.91	0.02	0.0	0.03	0.0	0.05	6.7:1	4.9:1	1:0.16	1:0.50
IV	**0.15 M NaOH: a**	0.70	0.55	4.27	9.50	9.32	5.77	1.07	1.88	1.55	7.44	80.13	60.32	1:2.2	1.6:1	1:5.8	1:4.4
V	**b**	1.39	2.07	0.99	7.87	0.36	10.56	0.37	3.22	0.32	0.0	95.71	56.67	2.7:1	0.71:1	1:35.1	1:2.9
VI	**0.30 M NaOH: a**	32.47	17.45	30.59	16.80	2.88	4.55	12.61	0.0	0.0	5.20	20.65	48.73	10.6:1	3.7:1	1:0.50	1:1.4
VII	**b**	2.79	25.85	2.40	35.10	1.78	5.28	0.62	4.29	0.69	0.0	68.20	12.06	1.9:1	6.6:1	1:8.7	1:0.24
VIII	**0.45 M NaOH: a**	9.05	20.04	12.73	25.25	2.98	9.98	0.0	0.0	1.49	0.0	73.19	31.50	4.3:1	2.5:1	1:3.0	1:0.55
IX	**b**	9.40	18.53	12.37	22.20	1.58	4.65	2.14	4.83	1.95	7.82	65.61	29.72	7.8:1	5.0:1	1:3.0	1:0.91
X	**c**	34.94	-	33.45	-	6.87	-	0.0	-	0.0	-	24.19	-	4.9:1	-	1:0.32	-

The change in the molecular mass distribution of the HWS polymeric fractions, determined by HPSEC, is presented in Figure 3.3.2 and Table 3.3.3. The high-molecular-mass material abundantly present at the ripe stage, was decreased to low and intermediate-molecular-mass material, during ripening. This was especially evident in water-soluble fraction. All the fractions were heterogeneous in molecular mass, resulting in a very low, broad peak. The molecular weight difference from unripe to ripe stage was 3548 to 50 and 1995 to 1778 kDa, for the major peaks of fractions III and IV, respectively.

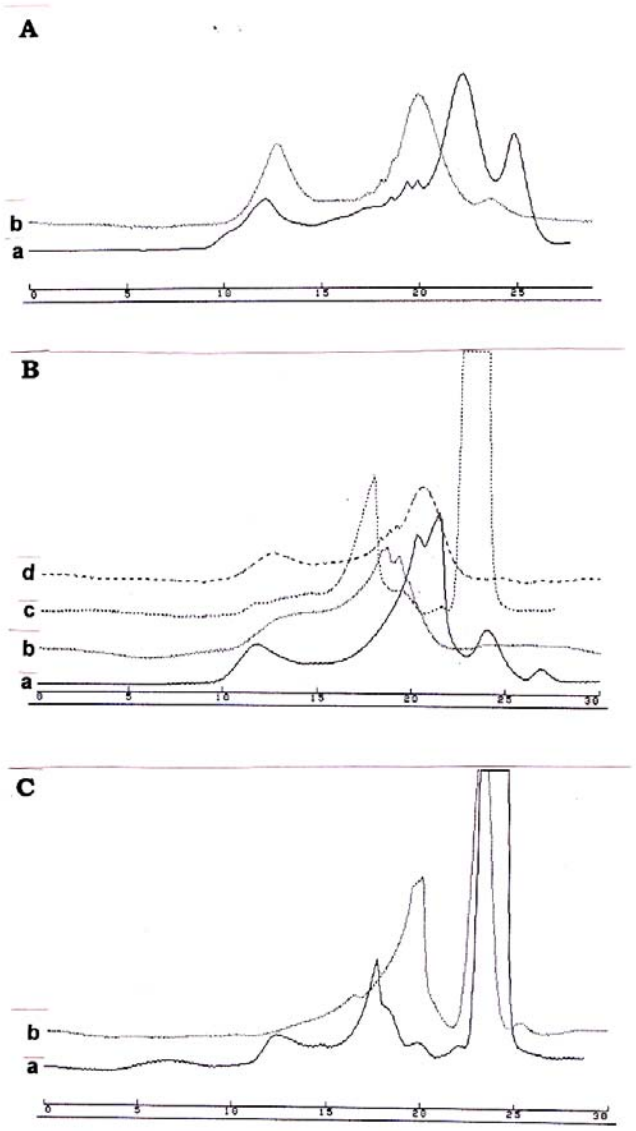

Figure 3.3.2 (a) HPSEC profiles of HWS fractions

A: a, neutral unripe fr. 1; b, neutral unripe fr. 2; c, neutral ripe fr. 1; d, neutral ripe fr. 2
B: a, 0.15 M $(NH_4)_2CO_3$ unripe; b, 0.15 M $(NH_4)_2CO_3$ ripe
C: a, 0.15 M NaOH unripe fr. 1; b, 0.15 M NaOH unripe fr. 2; c, 0.15 M NaOH ripe fr. 1; d, 0.15 M NaOH ripe fr. 2

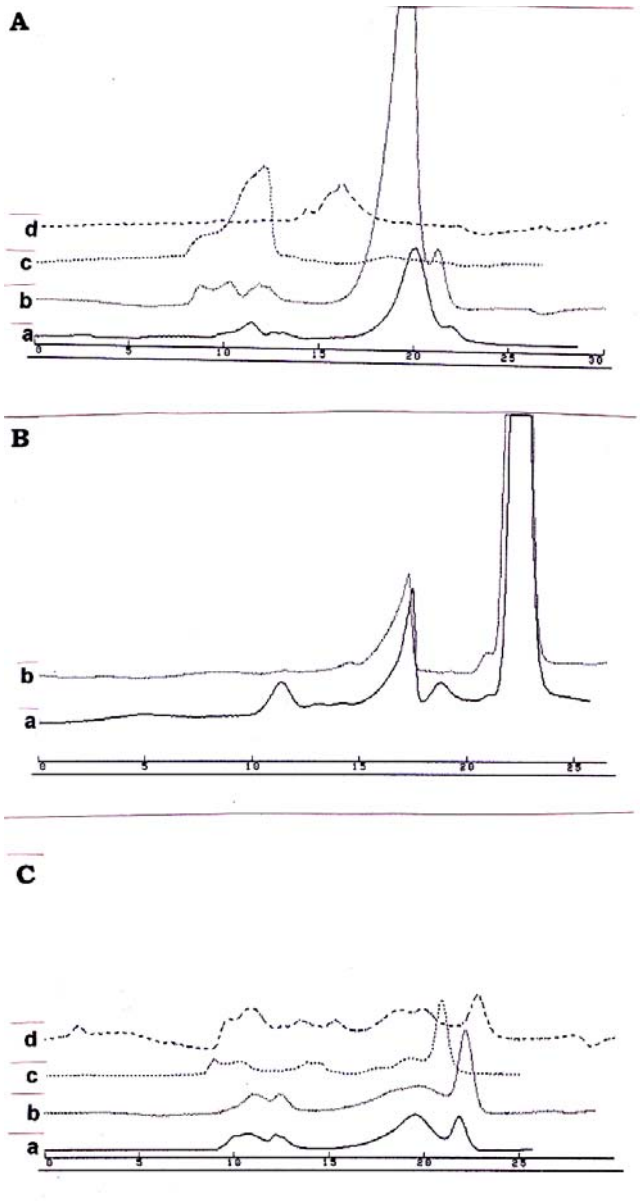

Figure 3.3.2 (b) HPSEC profiles of HWS fractions

A: a, 0.30 M NaOH unripe fr. 1; b, 0.30 M NaOH unripe fr. 2; c, 0.30 M NaOH ripe fr. 1; d, 0.30 M NaOH ripe fr. 2
B: a, 0.45 M NaOH unripe fr. 1; b, 0.45 M NaOH unripe fr. 2; c, 0.45 M NaOH ripe fr. 1; d, 0.45 M NaOH ripe fr. 2

Table 3.3.3
Changes in molecular weight of HWS fractions

Fr. No.	Polymeric fraction		Molecular weight in kDa	
			Unripe	**Ripe**
I	**Neutral**	**a**	3981	2239
II		**b**	2512 1778 13	302 126
III	**0.15 M $(NH_4)_2CO_3$**		3548 36 28	50
IV	**0.15 M NaOH**	**a**	1995	1778
V		**b**	1995 16	794
VI	**0.30 M NaOH**	**a**	1000 159	22.4 2
VII		**b**	2818 631	89
VIII	**0.45 M NaOH**	**a**	159	141
IX		**b**	631 79	36 1

Conclusions

Ripening induced changes were evident, as before, in the major fractions both in their percent abundance and molecular weight values.

Section 4

Changes in the profile of EDTA soluble pectic polysaccharides

Introduction

Pectin at the cell wall level is one of the major polysaccharides contributing to the fruit ripening phenomenon (Sirisomboon *et al.*, 2000). These complex cell wall polysaccharides can be extracted by hot water, weak acids, weak base and chelating agents such as ammonium oxalate, hexametaphosphate, EDTA, EGTA and CDTA (Renard and Thibault, 1993; Smith, 1999).

During post harvest storage, fruit can lose firmness, which has been attributed to cleavage of glycosidic bonds in cell wall polysaccharides (Doesburg, 1965). Since turgor pressure, present in living plant tissues, is not a factor in most storage processes, firmness loss is considered to be a result of changes in cell wall components, particularly cell wall polysaccharides (Van Buren, 1979). However, the complexity of cell wall composition makes it difficult to relate changes in texture to specific chemical changes in cell wall polysaccharides. Much of the work done relate chemical changes in cell walls to textural changes in pectic substances (Bartolome and Hoff, 1972; Chang *et al.*, 1993). During processing and storage operations, pectin can be demethylated and depolymerized by both enzymatic and nonenzymatic reactions. It has been demonstrated that the solubilization of pectic polymers during mango fruit ripening was even more extensive than in tomato and kiwi fruit (Redgwell, 1991). However, a detailed investigation to show the entire spectrum of pectic polymers present and their qualitative and quantitative changes during ripening is not well documented in fruits. This section specifically deals with pectin dissolution *in vivo*, giving a complete profile of pectic polymers in unripe and ripe mango, their qualitative and quantitative changes and their drop in the molecular weight *in vivo*.

Results and Discussion

The EDTA soluble pectic substances in AIR decreased from 1.86 g to 0.38 g % FW upon ripening, with loss of resistance to shearing force. They showed high galacturonic acid content and the galacturonic acid to neutral sugar ratio was higher in the ripe stage than unripe stage, indicating a more pronounced degradation of neutral sugar residues upon ripening. Since the EDTA soluble pectin is structurally bound to the cell wall, these relationships suggest that flesh softening in the ripening process may result from disintegration of the cell wall caused by degradation of the structurally bound pectin. Huber and Lee (Huber and Lee, 1986) have reported that EDTA solubilized more pectins from ripe than from unripe tomato suggesting a higher dissolution of pectin-rich middle lamella during ripening. Further, as ripening progress more of the pectic polymers get solubilized. Redgwell and coworkers (Redgwell *et al.*, 1992) reported that pectic polymers, which were solubilized in harsh conditions, were found solubilized in mild condition at the later stages of ripening.

The presence of high galacturonic acid content along with relatively high galactose and arabinose residues indicates that these fractions are truly pectic in nature. Chelator-solubles are usually pectic polysaccharides (Smith and Harris, 1995), which are generally associated with Ca^{++} ions. EDTA by chelating with Ca^{++} ions favours pectin solubilization. EDTA extracts pectins from the middle lamella, while Na_2CO_3 extracts covalently bound pectins, essentially from the primary cell wall (Redgwell *et al.*, 1990). The amount of galacturonic acid was much higher in EDTA-solubles. High amount of pectins in chelator-solubles were reported for other fruits (Missang *et al.*, 2001a; Redgwell *et al.*, 1991).

The isolated pectins were subjected to ion exchange chromatography on DEAE-cellulose. Figure 3.4.1 gives the qualitative and quantitative profile of the entire range of pectic polymers in unripe and ripe mango. Seven distinct peaks, designated as fractions I-VII, based on their order of elution, were obtained. Three of them were major fractions, which distinctly resolved in neutral, 0.05 M and 0.10 M $(NH_4)_2CO_3$ elution. At higher strength gradients (0.15 and 0.3 M $(NH_4)_2CO_3$), there were minor peaks while 0.45 M $(NH_4)_2CO_3$ and 0.15M NaOH eluates showed no carbohydrate peaks. Stronger alkali gradients (0.3 and 0.45 M NaOH) also showed some peaks but with lower levels of uronic acid (<5%). Loss in qualitative levels (carbohydrate content) from unripe to ripe stage was observed in all the fractions. A slight increase in fraction V (0.3 M $(NH_4)_2CO_3$) may indicate that the degradation of both 0.05 M and/or 0.1 M $(NH_4)_2CO_3$ generated pectic populations of lower degrees of methylation, which was retained and eluted in higher gradients (0.3 M $(NH_4)_2CO_3$). Similar observation was made in bush butter fruit (Missang, et al., 2001b).

The unbound fraction was devoid of galacturonic acid, while the retained fractions were rich in galacturonic acid and poor in alkali eluted fractions as reported for sugar beet pectins (Fares *et al.*, 2001). From IEC column, highly esterified homogalacturonans eluting earlier than highly branched heterogalacturonans were reported for kiwi, peach, pear and bush butter fruit pectins (Dick and Labavitch, 1989; Hegde and Maness, 1996; Missang *et al.*, 2001b; Redgwell *et al.*, 1991).

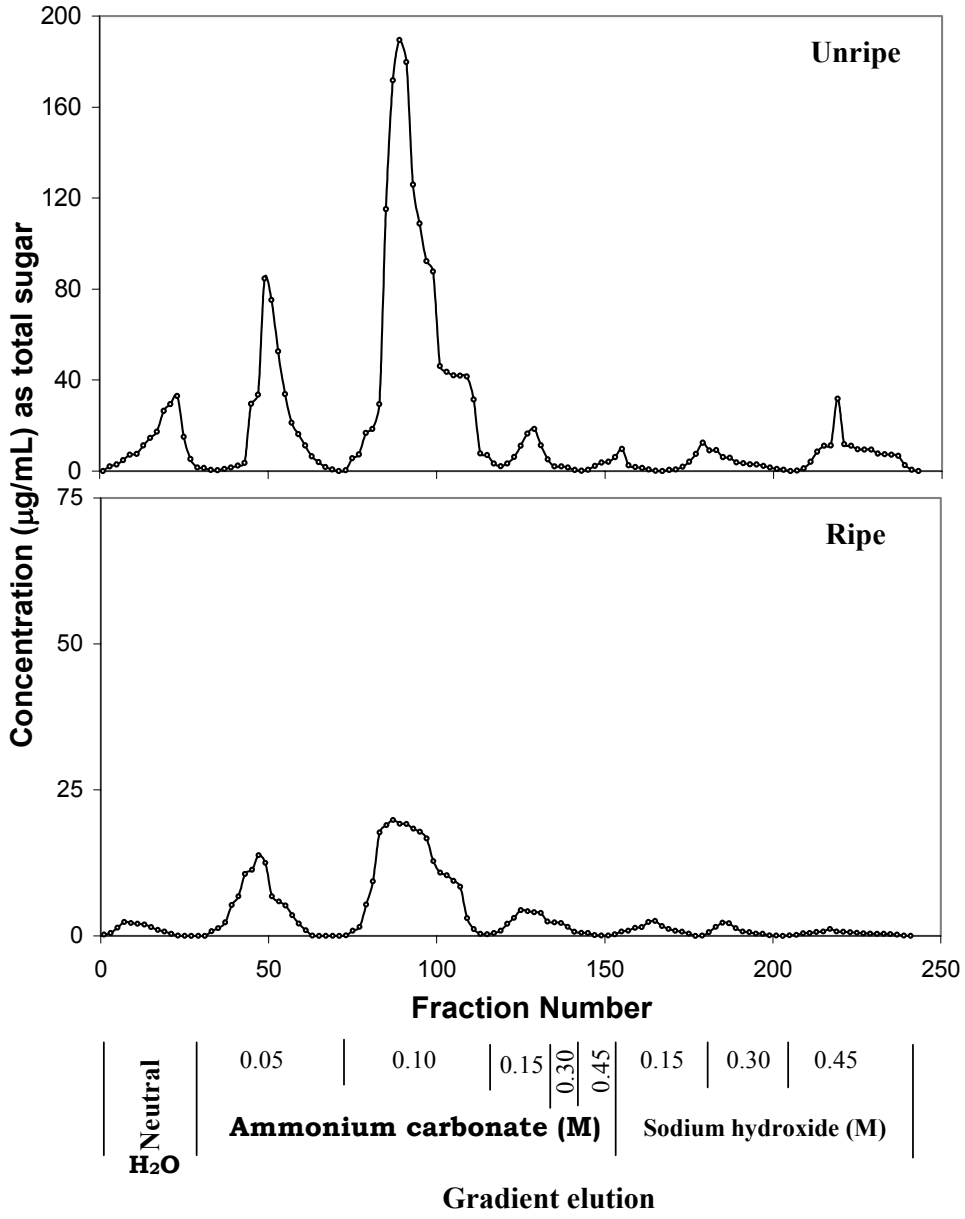

Figure 3.4.1
DEAE-cellulose profile of EDTA soluble pectic polysaccharides from unripe and ripe mango

The relative abundance and the sugar composition of these pectic fractions are detailed in Table 3.4.1. A significant decrease in their levels from unripe to ripe stage is evident in all the fractions, except fraction V. The mg % drop in their levels for the major

fractions I, II and III was 60 to 7, 89 to 13 and 74 to 2, respectively. All the other fractions showed abundance at ~20 mg % FW and declined at the ripe stage, while fraction V increased slightly. Nevertheless, there was no complete disappearance of any of these fractions at the end of ripening indicating controlled depolymerization of the pectic polymers.

Fractions I and VIII were devoid of galacturonic acid, while all other fractions showed the presence of galacturonic acid [Table 3.4.1]. Fractions II and III showed high galacturonic acid content (>60%) compared to fractions IV and V (~58%), whereas fraction VI contained low level of galacturonic acid (<6%).

All the fractions showed neutral sugars such as galactose, arabinose and rhamnose, which are characteristic of pectic-type polymers. Based on the sugar composition, fraction I appeared to be an arabinogalactan-type polymer, probably covalently linked to pectic polymers (Mitcham *et* al., 1992). Fractions II and III were heterogalacturonans with different ratios of arabinose, galactose and rhamnose. In these fractions, the *in vivo* hydrolysis of neutral sugars seemed to be more pronounced. The presence of both galacturonic acid and neutral sugar in these fractions may suggest that they contained branched pectins as reported for chelator-solubles from apple and sugar beet pectins (Renard and Thibault, 1993). Further, the presence of rhamnose indicates that these heterogalacturonans are rhamnogalacturonan-type polymer. Rhamnose is reported as a branch off sugar residue for the attachment of neutral sugar side chains (McNeil *et al.*, 1980). Dick and Labavitch (1989) also reported that 'Bartlett' pears contained heterogalacturonans having different proportions of arabinose, galactose and rhamnose.

Table 3.4.1
Abundance and composition (mg % FW) of EDTA soluble pectic polymers of mango

Fr. No.	Polymeric fractions	Total carbohydrate		Uronic acid		Neutral sugar composition					
						Rha		Ara		Gal	
		Unripe	Ripe	Unripe	Ripe	Unripe	Ripe	Unripe	Ripe	Unripe	Ripe
I	***Neutral***	60.0	7.0	-	-	2.8	0.2	14.4	2.2	38.2	0.7
II	**0.05M $(NH_4)_2CO_3$**	89.0	13.0	55.0	10.0	4.4	0.6	17.1	1.5	8.2	0.3
III	**0.10M $(NH_4)_2CO_3$**	74.0	2.0	45.0	1.3	4.4	0.1	11.9	0.2	9.2	0.1
IV	**0.15M $(NH_4)_2CO_3$**	20.0	6.0	12.0	5.0	1.2	0.1	3.4	0.9	2.0	0.1
V	**0.15M $(NH_4)_2CO_3$**	18.0	23.0	10.0	20.0	Tr	1.3	7.0	0.9	-	-
VI	**0.30M NaOH**	17.0	7.0	1.0	1.0	-	-	0.5	0.8	0.2	0.5
VII	**0.45M NaOH**	34.0	4.0	-	-	2.0	0.8	3.1	0.8	0.7	0.0

Loss of galacturonic acid, galactose, arabinose and rhamnose residues in all the pectic fractions were observed during ripening. Almost complete loss (>95%) of neutral sugar residues from ripe mango pulp was very evident from the compositional analysis, while loss of galacturonic acid was in the range 60-90%. Similar loss of acidic and neutral sugars was observed in total pectic fraction of ripening fruits such as persimmon (Cutillas-Iturralde *et al.*, 1993), 'Ngowe' mango (Brinson *et al.*, 1988) and tomato (Gross, 1984). Gross and Sams (1984) reported a net loss of galactose/arabinose from the cell wall of 14 types of fruits out of 17 tested. A dramatic loss of pectin associated monomers, rhamnose, arabinose, galactose and galacturonic acid was reported for kiwi fruit, after six days of ethylene treatment (Newman and Redgwell, 2002). Loss of galactose from the cell wall during ripening was reported in fruits like apples (De Vries *et al.*, 1984; Knee, 1973), kiwi (Redgwell *et al.*, 1992; Redgwell *et al.*, 1997a), melon (Rose *et al.*, 1998), muskmelon (McCollum *et al.*, 1989), tomato (Gross, 1984) and pineapple (Smith and Harris, 1995), while loss of arabinose was reported in pear (Ahmed and Labavitch, 1980a) and nectarines (Lurie *et al.*, 1994). Significant decrease of only galactose was reported for 'Sensation' variety of mango (Tucker and Seymour, 1991). Loss of both galactose and arabinose was observed in apples (Knee, 1978), peach (Hegde and Maness, 1996), hot pepper (Gross *et al.*, 1986), olive (Jimenez *et al.*, 2001), 'Keitt', and 'Tommy Atkins' varieties of mango (Mitcham and McDonard, 1992). Loss of arabinogalactan, the major component of the side chain of pectic polysaccharide, has been observed in a number of ripening fruits (Gross and Sams, 1984; Huber, 1983; Nunan *et al.*, 1998). Loss of galactose is mainly due to the degradation of arabinogalactan polymer, which is abundant in plant cell walls (Redgwell *et al.*, 1997a). However, in ripening plum and cucumber, no change occurred in the composition of neutral

sugars associated with pectins (Boothby, 1983; Gross and Sams, 1984).

Loss of galacturonic acid was also reported in other varieties of mango (Brinson *et* al., 1988; Mitcham and McDonald, 1992). However, polyuronide synthesis during ripening was reported for plum and cherry fruits (Boothby, 1983; Fils-Lycaon and Buret, 1990). Increase in the levels of neutral sugars of chelator-soluble pectins during ripening was also reported for olive fruit (Huisman *et al.*, 1996). Thus, the cell wall neutral sugar composition varies among fruits and the metabolism of pectins in relation to textural softening differs from fruit to fruit. In peach, softening is associated with change in the sugar composition of pectin and hemicellulose as well as their change in molecular mass (Hegde and Maness, 1998; Hegde and Maness, 1996).

Table 3.4.2 and Figure 3.4.2 give the molecular weight changes from unripe to ripe stage of all the pectic fractions, as determined by HPSEC. The molecular weight difference from unripe to ripe stage was 250 to 70, 1300 to 21 and 473 to 298 kDa, for the major fractions I, II and III, respectively. Similar profiles for unripe and ripe fruits were reported for olive (Huisman, 1996) and bush butter fruit pectins (Missang *et al.*, 2001b). Molecular weight of pectic polysaccharides ranging from ~250-40 kDa, with broadening of the peak was also shown in olive fruits during ripening (Jimenez *et al.*, 2001).

The drop in molecular weight not only reflected the quantitative loss but also reflected the dissolution of a large polymer into a number of smaller fragments at the end of ripening [Table 3.4.2]. This is especially so in the most abundant pectic polymer

(fraction II), where 1300 kDa at unripe stage resulted in very low molecular weight peaks of 21, 10, 5 and 1 kDa. Low molecular weight (1.1 kDa) homogalacturonan was reported in alcohol-insoluble polymers from soft bush butter fruit (Missang *et al.*, 2001a). Drop in molecular weight of polyuronides, from 1000 kDa to 50 kDa, was also reported for kiwi fruit (Redgwell *et al.*, 1992). A high molecular weight of 1300 kDa was reported for sugar beet pulp pectins rich in neutral sugars (Oesterveld, 2000). A possible explanation for such a high molecular weight is the presence of diferulate cross-links connecting several rhamnogalacturonans (RG) (Oesterveld, 2000). Extensive degradation of this polymer during ripening suggests that diferulate cross-linkings are probably present between these highly branched heterogalacturonans.

Table 3.4.2
Changes in molecular weights of EDTA soluble pectic fractions

Fr. No.	Polymeric fractions	Molecular weight (kDa)	
		Unripe	**Ripe**
I	***Neutral***	250	70
II	**0.05 M $(NH_4)_2CO_3$**	1,333	21 10 5 1
III	**0.10 M $(NH_4)_2CO_3$**	473 266	299 100
IV	**0.15 M $(NH_4)_2CO_3$**	266	100
V	**0.15 M $(NH_4)_2CO_3$**	299 237	53 6
VI	**0.30 M NaOH**	335 224	15 1
VII	**0.45 M NaOH**	376 237	71 34

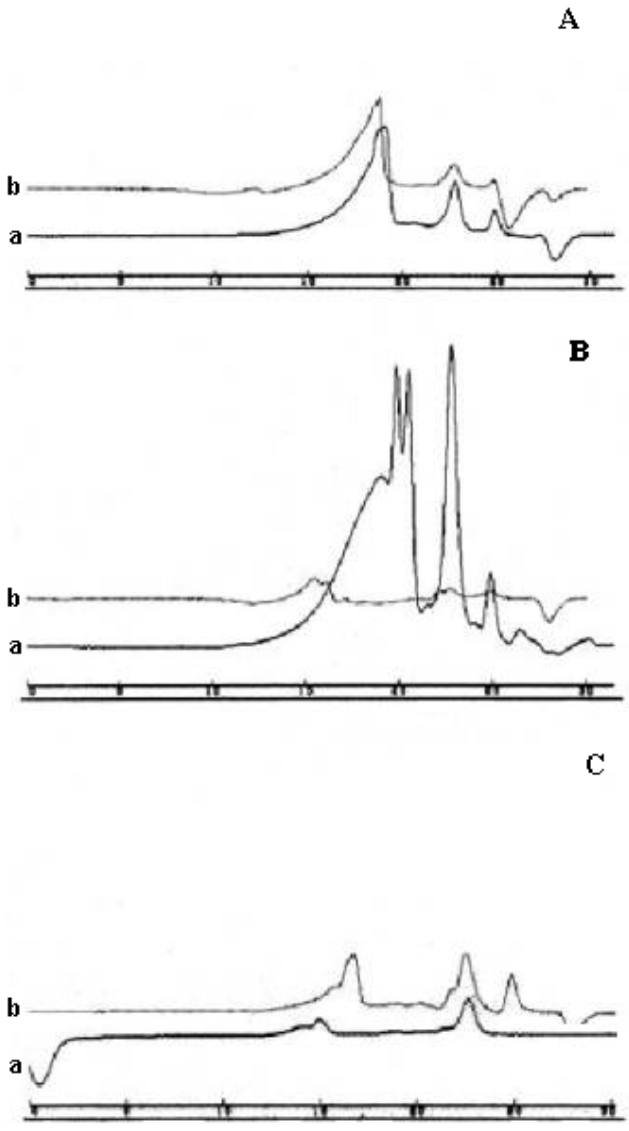

Figure 3.4.2 (a)
HPSEC profiles of EDTA soluble pectic fractions

A: a, neutral unripe; b, neutral ripe
B: a, 0.05 M $(NH_4)_2CO_3$ unripe; b, 0.05 M $(NH_4)_2CO_3$ ripe
C: a, 0.10 M $(NH_4)_2CO_3$ unripe; b, 0.10 M $(NH_4)_2CO_3$ ripe

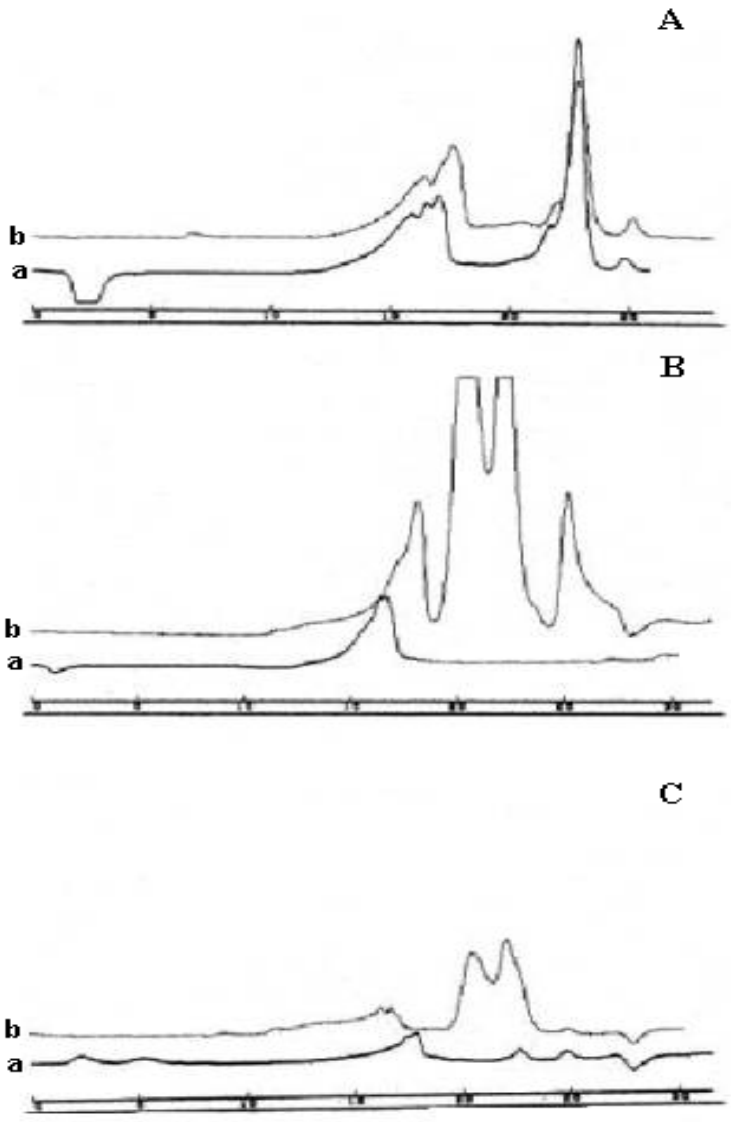

Figure 3.4.2 (b)
HPSEC profiles of EDTA soluble pectic fractions

A: a, (0.15 M $(NH_4)_2CO_3$ unripe; b, 0.15 M $(NH_4)_2CO_3$ ripe
B: a, 0.3 M NaOH unripe; b, 0.3 M NaOH ripe
C: a, 0.45 M NaOH unripe; b, 0.45 M NaOH ripe

Such a drop in molecular weight was also shown for pectic fraction of ripening tomato (Seymour *et al.*, 1987), kiwi (Redgwell *et al.*, 1992), olive (Huisman *et al.*, 1996; Jimnez *et al.*, 2001), nectarines (Lurie *et al.*, 1994) and bush butter fruit (Missang *et al.*, 2001a; Missang *et al.*, 2001b). Preliminary observation for total pectin in ripening mango fruit also indicated the change in molecular weight (Muda *et al.*, 1995; Tucker and Seymour, 1991) as well as loss of sugar residues during ripening (Brinson *et al.*, 1988). No such drop in molecular weight of chelator-soluble pectins was reported for banana (Wade *et al.*, 1992) and strawberry (Huber, 1984).

Conclusions

Extensive drop in the molecular weight (and abundance) of major pectic fraction II was observed as a result of mango ripening. Sugar composition data revealed it to be a heterogalacturonan-type polysaccharide.

Section 5

Changes in the profile of alkali soluble hemicellulose polysaccharides

Introduction

Softening of fruit is accompanied by an increase in the concentration of soluble polysaccharides. However, information about the role in fruit softening of cell wall polymers other than polyuronides is limited. Contribution of hemicelluloses towards textural softening phenomenon was observed in strawberry (Huber, 1984), Charentais melon (Rose *et al.*, 1998) and muskmelon (McCollum *et al.*, 1989). In kiwi fruit, the alkali soluble fraction contained both pectic and hemicellulosic substances contributing to textural softening (Redgwell *et al.*, 1991). In addition to the depolymerization of both pectic and hemicellulosic polymers, a characteristic feature of ripening fruit is the loss of neutral sugars (galactose and arabinose) from the cell walls (Gross and Sams, 1984). This has been associated with a decrease in neutral sugar concentration of both pectic and hemicellulosic polysaccharides (Gross and Wallner, 1979; McCollum *et al.*, 1989), although this and the relative extent of neutral sugar loss appear to vary between species.

The common structural features of hemicelluloses are a main chain with a structural resemblance to cellulose and either short side chains that forms a 'pipe-cleaner-brush shaped molecule or a different sugar interpolated in the main chain. Both these modifications prevent further aggregation with cellulose (Carpita and Gilbeaut, 1993). The extraction of hemicellulose is achieved by strong choatropic agents like 6 M urea, 6 M guanidium, 4.5 M thiocyanate guanidine or 1-6 M sodium hydroxide or potassium hydroxide. Normally, hemicelluloses are extracted by treating

holocelluloses with aqueous alkali, which may saponify any hemicellulosic ester linkages either between polysaccharides or between hemicelluloses or non-carbohydrate components (Markwalder and Neukom, 1976). The extracted hemicellulosic materials are precipitated on neutralization or mild acidification and further by subsequent addition of an excess of acetone or ethanol (Blake *et al.,* 1971). Alkaline extracted hemicelluloses have been characterized from apple and sugar beet pulp (Renard *et al.,* 1995).

Results and Discussion

The alkali soluble hemicellulosic polysaccharide decreased from 0.795 to 0.185g % FW and it was >4 fold decrease from unripe to ripe stage. The galacturonic acid to neutral sugar ratio was higher in the ripe stage than unripe stage, indicating a more pronounced dissolution of neutral sugar residues. The hemicellulosic polysaccharides upon DEAE-cellulose fractionation were resolved into 9 distinct peaks, designated as fractions I to IX, respectively, based on their order of elution (Fig. 3.5.1). The major fractions were found eluted in 0.10 M NaOH. The $(NH_4)_2CO_3$ gradients showed no carbohydrate peaks. The uronic acid content was more in 0.15M $(NH_4)_2CO_3$ (<12%) eluted fractions, while rest of the fractions showed <4% uronic acid. Loss in their qualitative and quantitative levels from unripe to ripe stage was observed in all the fractions (Table 3.5.1).

The relative abundance (Table 3.5.1) and their sugar composition (Table 3.5.2) data revealed a significant decrease in the levels from unripe to ripe stage. The mg % drop in their levels for the major fractions IV and V from unripe to ripe stage was 57.72 to 8.9% and 45.6 to 7.7%. All the other fractions

showed abundance at ~20 mg % fresh weight and declined at the ripe stage. Nevertheless, there was no complete disappearance of any of these fractions at the end of ripening indicating controlled depolymerization.

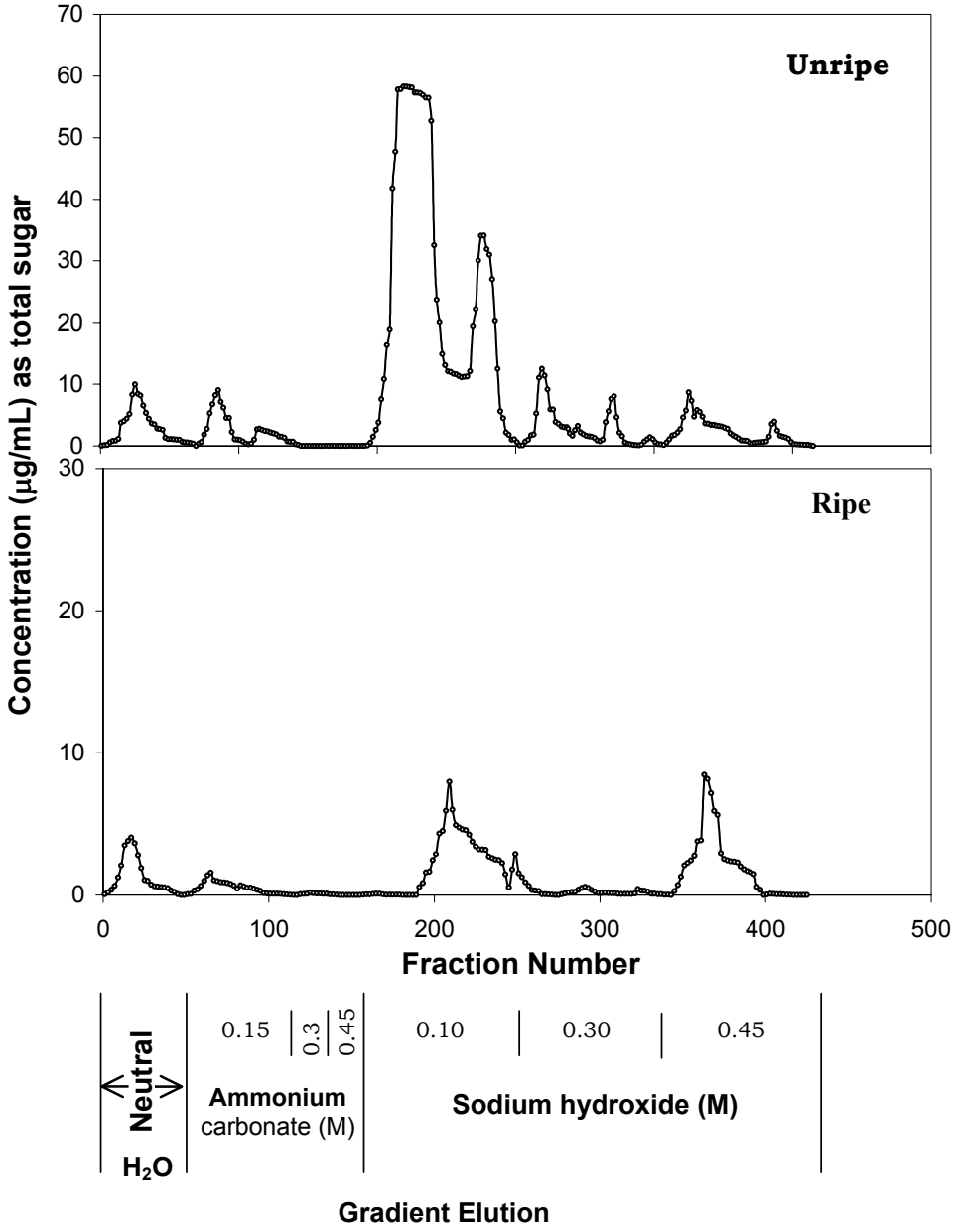

Figure 3.5.1
DEAE-cellulose profile of hemicellulose polysaccharides from unripe and ripe mango

Table 3.5.1
Abundance and composition (%) of DEAE-cellulose fractionated hemicellulose polymers of mango

Fr. No.	Polymeric fraction	Yield		Total carbohydrate		Uronic acid		Neutral sugar		UA:NS Ratio	
		Unripe	Ripe	Unripe	Ripe	Unripe	Ripe	Unripe	Ripe	Unripe	Ripe
I	Neutral	14.1	3.7	100.0	100.0	0.3	0.6	99.7	99.4	0.003:1	0.01:1
II	0.15M$(NH_4)_2CO_3$ a	10.8	2.7	100.0	84.8	10.4	11.3	89.6	73.5	0.12:1	0.15:1
III	b	9.7	1.7	100.0	97.5	6.3	8.6	93.7	88.9	0.07:1	0.09:1
IV	0.30 M $(NH_4)_2CO_3$	-	0.8	-	-	-	-	-	-	-	-
V	0.45 M $(NH_4)_2CO_3$	-	0.6	-	-	-	-	-	-	-	-
VI	0.10 M NaOH: a	57.7	8.9	100.0	100.0	2.6	3.8	97.4	96.2	0.03:1	0.04:1
VII	b	45.6	7.7	100.0	100.0	2.7	2.6	97.3	97.4	0.03:1	0.03:1
VIII	0.30 M NaOH: a	12.9	1.8	100.0	100.0	1.3	1.1	98.7	98.9	0.01:1	0.01:1
IX	b	7.5	1.0	100.0	73.7	1.5	1.2	98.5	72.5	0.02:1	0.02:1
X	c	7.9	1.2	94.2	65.4	1.7	1.7	92.5	63.7	0.02:1	0.03:1
XI	0.45 M NaOH: a	9.5	3.0	100.0	80.3	1.6	1.4	98.4	78.9	0.02:1	0.02:1
	b	7.7	0.4	100.0	-	1.2	-	98.8	-	0.01:1	-

Of the neutral sugar composition of total hemicellulose fraction, arabinose, xylose, mannose and glucose contents have decreased during ripening. Arabinose and xylose may comprise of arabinoxylan polymers that are either attached or not attached to acidic polysaccharides such as rhamno- or arabinogalacturonanas. The arabinose to xylose and pentose to hexose ratios showed the degradation of arabinoxylan type of polysaccharides as well as hexosans. Mannose is probably a component of glucomannan. The decrease in the mannose content during the ripening of mango suggests the breakdown of mannose containing polymers such as glucomannan or galactomannan. Such a breakdown of galactomannan was reported in banana cell walls (Kojima *et al.,* 1994) and in endosperm cell walls during germination of Datura seeds (Sanchez *et al.*, 1990). These results indicate that the decrease in the amount of pectin and hemicellulose constituents may also contribute to textural softening other than starch. It was also suggested that the firmness of mango was related to the presence of starch and polyuronides.

Table 3.5.2
Neutral sugar composition (mg %) of hemicellulose fractions

Fr. No.	Polymeric fractions	Rha		Ara		Xyl		Man		Gal		Glc		Ara : Xyl		Pentoses: Hexoses	
		Unripe	Ripe	Unripe	Ripe	Unripe	Ripe	Unripe	Ripe	Unripe	Ripe	Unripe	Ripe	Unripe	Ripe	Unripe	Ripe
I	Neutral	4.68	1.59	6.18	3.47	6.87	6.85	0.36	54.05	0.0	0.0	81.63	33.38	1:1.1	1:1.2	1:4.6	1:7.3
II	0.15 M $(NH_4)_2CO_3$ a	1.97	1.10	10.39	9.48	11.55	9.18	0.0	0.0	1.43	0.59	64.22	53.12	1:1.1	1.0:1	1:2.7	1:2.7
III	b	0.47	0.98	5.71	7.02	4.78	7.95	0.0	0.0	0.38	0.13	82.35	74.81	1.2:1	1.2:1	1:7.6	1:5.4
IV	0.10 M NaOH a	0.43	2.798	5.26	18.57	4.87	7.12	0.0	17.12	1.01	0.0	85.91	50.60	1.1:1	2.6:1	1:8.2	1:2.4
V	b	2.93	25.72	17.51	5.84	18.39	8.18	0.48	0.69	0.33	0.44	57.69	56.50	1:1.1	1:1.4	1:1.5	1:1.5
VI	0.30 M NaOH a	2.07	3.16	5.43	14.54	3.06	13.45	43.53	2.57	0.0	0.99	44.52	64.11	1.8:1	1.1:1	1:8.3	1:2.2
VII	b	2.46	3.04	4.92	4.99	5.61	4.99	29.83	5.65	0.0	0.0	55.54	53.09	1:1.1	1:1	1:6.6	1:4.3
VIII	c	3.97	3.19	11.93	19.82	11.18	21.35	45.40	0.76	0.0	0.19	19.97	18.42	1.1:1	1:1.1	1:2.4	2.3:1
IX	0.45 M NaOH a	6.39	2.52	21.05	10.88	20.17	13.25	33.15	8.76	0.0	4.18	17.61	39.21	1.0:1	1:1.2	1:1.1	1:2.0
	b	-	3.95	-	30.82	-	31.51	-	4.94	-	1.88	-	25.68	-	1:1.0	-	2.0:1

Table 3.5.2 shows the changes in the composition of the alkali soluble hemicellulose fractions. High levels of glucose and xylose were detected in the fractions from both unripe and ripe fruits. The other monosaccharide constituents (apart from xylose and glucose) were also present in smaller proportions, in all the fractions from both physiological stages. Significant decrease in the levels of glucose and arabinose was noticed in the neutral fractions, whereas glucose, xylose and arabinose levels decreased in 0.15 M $(NH_4)_2CO_3$ and 0.1 M NaOH eluted fractions. Mannose level decreased drastically in 0.3 and 0.45 M NaOH eluates. Hemicelluloses appear to undergo drastic change during the ripening process in comparison with the water-soluble pectins.

The decrease in cell wall hemicellulose with ripening was accompanied by a considerable decrease in the molecular weight as determined by HPSEC, which may contribute to fruit softening. The molecular weight profiles for all the fractions decreased during ripening, with more of low molecular weight polymeric fractions observed in some of the fractions. A decrease in molecular size of hemicellulosic polymers has been reported in ripening strawberries (Huber, 1984), muskmelons (McCollum *et al*., 1989) and tomatoes (Huber, 1983a). Modification of cell wall hemicellulose may, in part, be due to cellulase and hemicellulase activity, which were identified to show climacteric peak in activity during ripening (Chapter IV, section I).

Figure 3.5.2 and Table 3.5.3 gives the molecular weight changes from unripe to ripe stage of all the hemicellulose fractions. The molecular weight drop from unripe to ripe stage was 2512 to 1000 and 2818 to 1122 kDa, for the major peaks of fractions IV and V, respectively and this drop in molecular weight was obvious in all the fractions. The profiles showed a peak in the molecular weight range for unripe (~14-16 min) and ripe stages (~16-21 min).

Table 3.5.3
Molecular weight changes in hemicellulose fractions during ripening of mango

Fr. No	Polymeric fraction	Molecular weight in kDa	
		Unripe	**Ripe**
I	**Neutral**	708 251 50	355 20
II	**0.15 M $(NH_4)_2CO_3$ a**	2512	2239 200 20 9 6
III	**b**	3981	891
IV	**0.10 M NaOH a**	2512 631 251	1000 56 6
V	**b**	2818 13	1122 40 9
VI	**0.30 M NaOH a**	5623	2512 4 3 2
VII	**b**	2512	891 251 56
VIII	**c**	1259 501	355
IX	**0.45 M NaOH**	2818 45	891 282 2

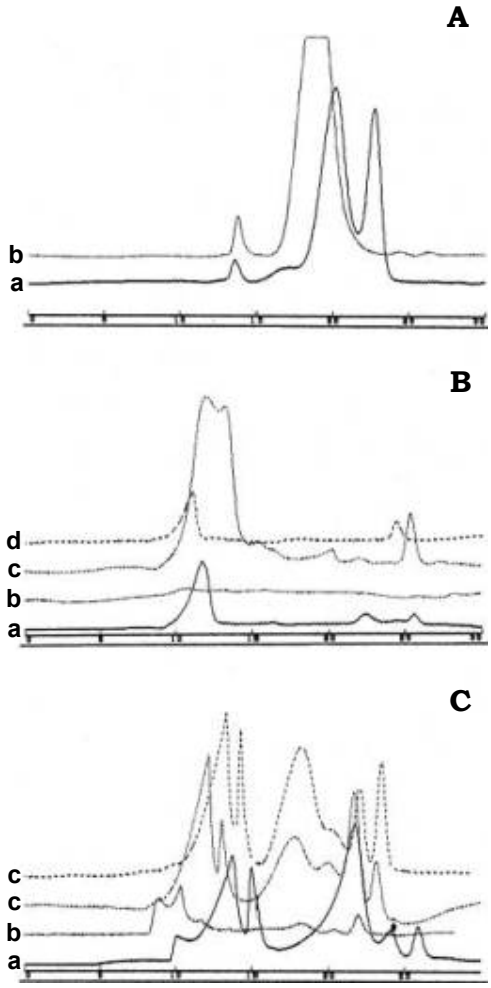

Figure 3.5.2 (a)
HPSEC profiles of hemicellulose fractions

A: a, neutral unripe; b, neutral ripe
B: a, 0.15 M $(NH_4)_2CO_3$ unripe fr. 1; b, 0.15 M $(NH_4)_2CO_3$ unripe fr. 2; c, 0.15 M $(NH_4)_2CO_3$ ripe fr. 1; d, 0.15 M $(NH_4)_2CO_3$ ripe fr. 2
C: a, 0.10 M NaOH unripe fr. 1; b, 0.10 M NaOH unripe fr. 2; c, 0.10 M NaOH ripe fr. 1; d, 0.10 M NaOH ripe fr. 2

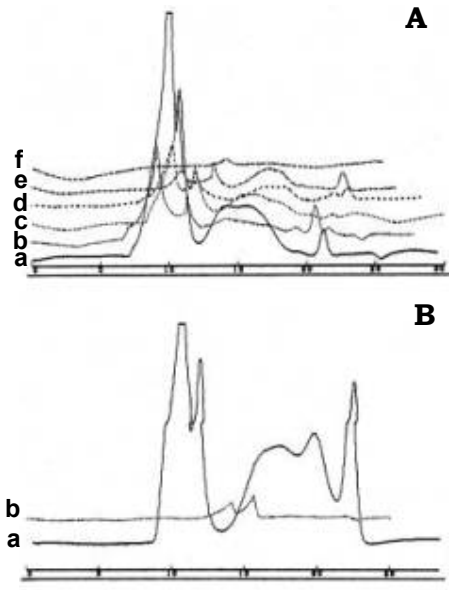

Figure 3.5.2 (b)
HPSEC profiles of hemicellulose fractions

A: a, 0.30 M NaOH unripe fr. 1; b, 0.30 M NaOH unripe fr. 2; c, 0.30 M NaOH unripe fr. 3; d, 0.30 M NaOH ripe fr. 1; e, 0.30 M NaOH ripe fr. 2; f, 0.30 M NaOH ripe fr. 3

B: a, 0.45 M NaOH unripe; b, 0.45 M NaOH ripe

Conclusions

Considerable compositional (both molecular weight and sugar composition) variations were discernible in some of the major hemicellulosic fractions, as a result of fruit ripening.

***Section* 6**

Structural characterization of the major cold water soluble polysaccharides

Introduction

The texture of fruits is determined by the properties of the cell wall and the middle lamella (Stolle-Smits *et al.*, 1997). The cell wall composition and structure change continuously during fruit development. For deducing the nature of the physico-chemical and enzymological processes involved in polysaccharide solubilization is to characterize the *in vivo* chemical changes in polysaccharide structure that accompany ripening. Changes to individual polymer fractions isolated by chemical methods can be related to the *in vivo* situation, provided precautions are taken to minimize any inadvertent degradation of the cell wall during its preparation and fractionation. It is important that changes to a specific fraction are not assessed in isolation but in relation to the changes in all other fractions. Otherwise, it is possible to attribute a physiological basis to a change that is in part an artifact of the methodology. To study the transition in the fruit from insoluble cell wall to partially solubilized cell wall, it is necessary that methods make a distinction between the insoluble cell wall and the polymers solubilized by water or EDTA extraction from the dry preparations, which are representative of the polymers solubilized *in vivo*. Pectic substances are abundant in fruit cell walls and are considered to be important in determining the texture of fruit. Pectins from various plant species have some common structural trends (Albersheim, 1975), although differences exist in their composition and structure especially during the maturation (Pilnik and Voragen, 1970).

The structure of mango fruit cell wall is of great interest because information regarding the precise substrates (carbohydrates) involved in textural regulation is scanty. Though gross changes in the water soluble pectin content during ripening were reported for a number of fruits, the structural aspects on pectic polymers have been reported

only for a few fruits like apple (Colquhoun *et al.,* 1990; Schols *et al.*, 1990), grapes (Nunan *et al.,* 1998; Saulnier *et al.,* 1988; Vidal *et al.*, 2001), kiwi (Redgwell *et al.*, 1991), raspberry (Stewart *et al.*, 2001) and tomato (Pressey and Himmelsbach, 1984; Seymour *et al.*, 1990). Most of these studies on pectins are based on methylation followed by GCMS, FT-IR and ^{13}C-NMR (Doner, 1986). Structural investigations of pectins are difficult due to their high molecular weight, the lack of homogeneity, and the absence of repeating units (Voragen *et al.*, 1995).

A convenient and complete methylation of all the accessible functional groups can be accomplished in one step using a methylation method developed by Hakomori (1964). Subsequent acid hydrolysis, reduction and acetylation yields partially methylated alditol acetates, which separate on GC-MS based on ions having difference in mass:charge (m/Z) ratio. This gives glycosidic linkage data of the polysaccharides. Methylation analysis was employed for determination of linkage analysis of most of the fruit pectins (Colquhoun *et al.*, 1990; Nunan *et al.*, 1998; Redgwell *et al.*, 1991; Saulnier *et al.*, 1988; Seymour *et al.*, 1990; Vidal *et al.*, 2001).

Mango is almost untouched for structural studies on CWS, HWS and Hemicellulose polymers. In the previous sections, the entire spectrum of CWS, HWS and hemicellulose polymers, their qualitative and quantitative changes and their extent of contribution towards textural softening were well documented. This section specifically deals with the structural aspects of the major post IEC CWS polymers of unripe mango.

Results and Discussion

The major CWS fractions (II) of unripe and ripe mango, eluted in 0.15 M $(NH_4)_2CO_3$ eluates, were chosen for structural studies.

Due to very low recovery, minor fractions were not taken for structural studies. The drop in their abundance and molecular weight at the end of ripening is depicted in Figure 3.6.1 A and B, which also denoted *in vivo* depolymerization of CWS fractions.

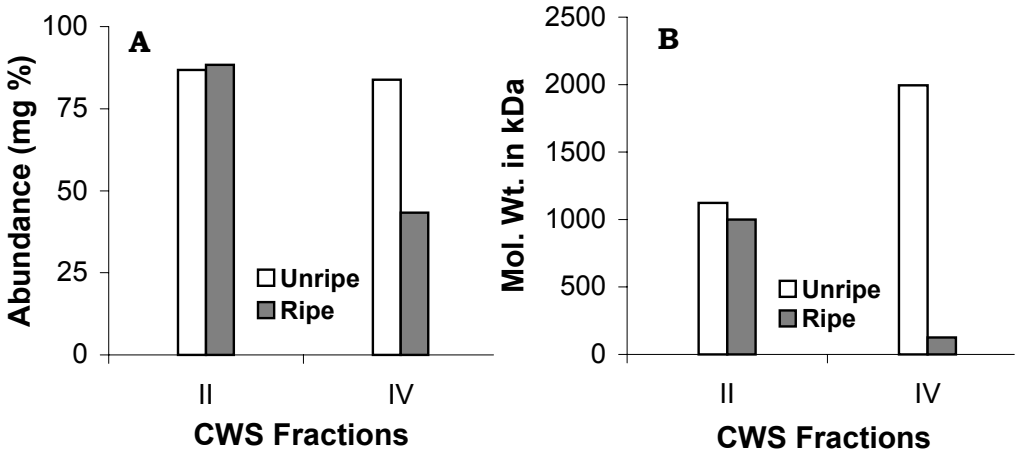

Figure 3.6.1
Abundance (A) and molecular weight (B) changes of the major CWS fractions from unripe and ripe mango

GPC on Sepharose CL-4B (Fig. 3.6.2) of fraction II showed a single broad peak, due to their high polydispersity. Their recovery (as total sugar) and galacturonic acid content were in the range 82.7-98.2% and 24–27%, respectively and the material from the column was successfully eluted with 0.10 M NaCl. This purification led to an appreciable increase in the total sugar content of the major CWS polysaccharides (Table 3.6.1). Both fractions II and IV showed a relatively constant galacturonic acid/neutral sugar ratio (~0.4%), which means that similar polysaccharide populations are eluted. Both the fractions were highly polydisperse in nature and were of high molecular weight, in the range between 1000-2000, 500-1000 kDa for unripe and ripe fractions, respectively. Similar results were observed for CWS pectic polymers from other fruits like tomato (Seymour *et al.*, 1987), kiwi (Redgwell *et al.*, 1992), melon (Rose *et al.*, 1998), nectarine (Lurie *et al.*, 1994) and bush butter (Missang *et*

al., 2001b). However, in pear, the IEC fraction resolved into 2-3 peaks upon GPC, suggesting the presence of different pectic molecular species (Dick and Labavitch, 1989).

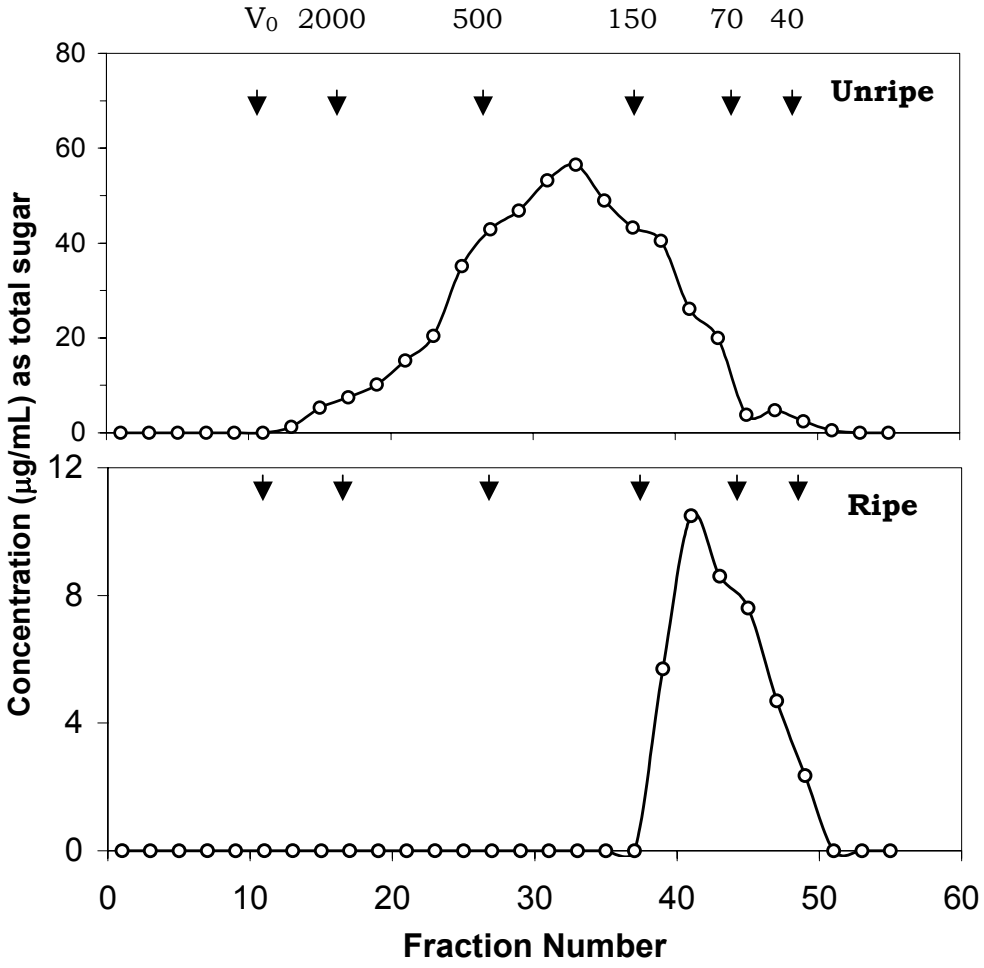

Figure 3.6.2
GPC profiles of CWS fraction II on Sepharose CL-4B column

Table 3.6.1
Physico-chemical characteristics of CWS fraction II of mango pulp

Fr. No.	Total carbohydrate %	Uronic acid %	Reduced viscosity (η_r)	Specific viscosity ($\eta_r - 1$)	Specific rotation (degrees)	Mol. wt. (kDa)
Unripe	82.7	23.6	11.2	10.2	+ 247.4	1122
Ripe	98.2	24.4	4.2	3.2	+ 272.0	1000

The molecular weights of the fraction II of CWS from unripe and ripe mango, as determined by HPSEC (Fig. 3.6.3) were 1122 and 1000 kDa, respectively. High molecular weight arabinogalactan, reported in sugar beet pulp also had a molecular weight of 1300 kDa (Oesterveld *et al.*, 2000), which is similar to that of fraction II from CWS in ripening mango. Molecular weights ranging from 1000 to 50 kDa were reported for pectins from 'Kiett' mango (Muda *et al.*, 1995; Olle *et al.*, 1996) and other fruits (Redgwell *et al.*, 1992; Rose *et al.*, 1998; Sakai *et al.*, 1993). Kokini and Chou (1993) reported that tomato pectins also exhibit high polydispersity, with the majority having the molecular weight in the range of 3 to 5.5 x 10^6 Da.

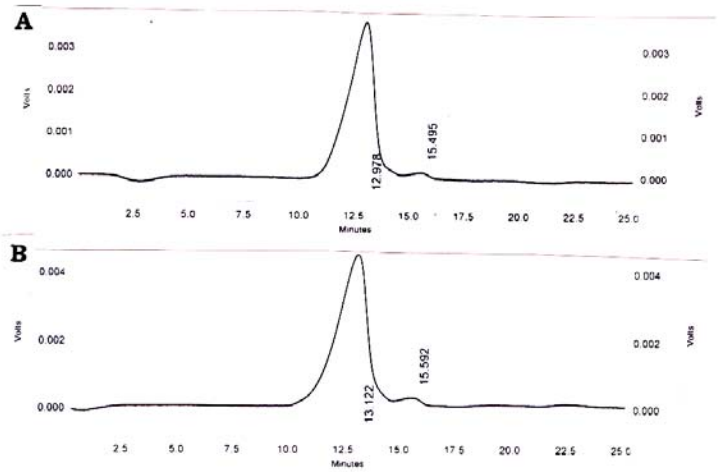

Figure 3.6.3
HPSEC profiles of the major CWS fraction II of unripe (A) and ripe (B) mango

High molecular weight (1300 kDa) was reported for sugar beet pulp pectins rich in neutral sugars, which may be due to the presence of diferulate cross-links connecting several rhamnogalacturonans (Oesterveld *et al.*, 2000). The degradation of this polymer during ripening [Chapter 3; Section 2] possibly suggests a probable diferulate cross-linking between rhamnogalacturonan molecules. Covalent linkages between rhamnogalacturonan and homogalacturonan through borate ester cross-links in sugar beet pulp pectins, as reported recently (Ishii and Matsunaga, 2001; O'Neill *et al.*, 1996; Zhan *et al.*, 1998) may also contribute to such high molecular weights.

The chemical composition of the purified fractions showed (Fig.3.6.4 A and B; Table 3.6.2) mainly galactose and arabinose, with minor amounts of glucose, rhamnose and xylose. Fraction II of ripe mango has a higher neutral sugar content (73.8%) than unripe fraction (59.1%). The content of galactose was slightly more than that of arabinose. The decrease from unripe to ripe stage in arabinose to galactose ratio (1.0:1.4 to 1.0:1.2) and pentose to hexose ratio (1.0:1.3 to 1.0:1.2) indicated the degradation of arabinogalctan-type polysaccharide during ripening.

Table 3.6.2
Neutral sugar composition (%) of major CWS fraction II

Polymeric fractions	Rha	Ara	Xyl	Gal	Glc	Gal:Ara	Pentoses: Hexoses
Unripe	3.4	20.9	1.5	28.9	4.6	1.4:1	1:1.3
Ripe	6.3	25.8	1.7	31.7	8.3	1.2:1	1:1.2

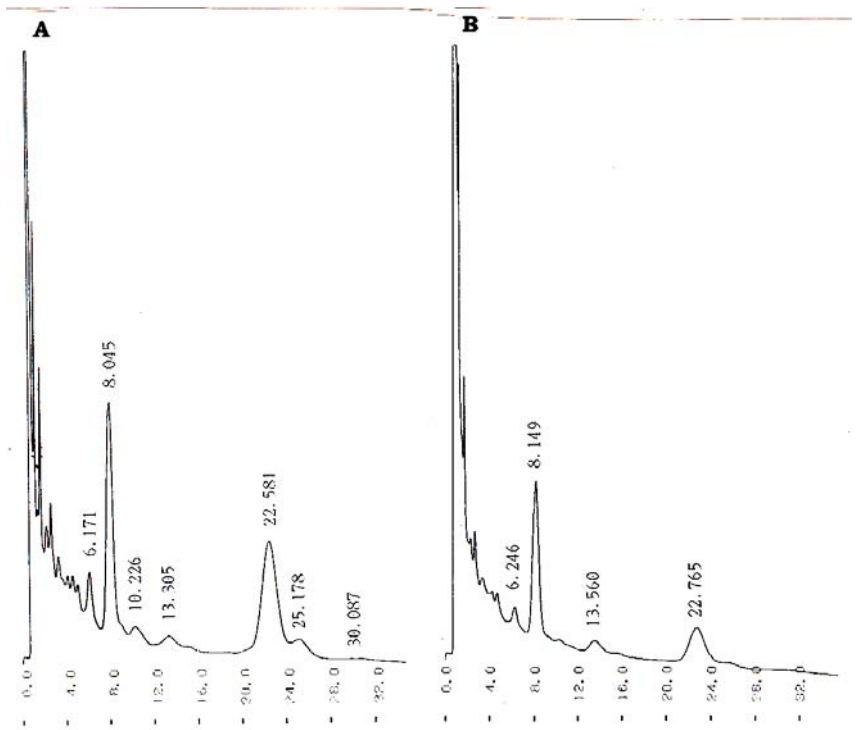

Figure 3.6.4
GC profile of sugars (as alditol acetates) derived from CWS fraction II of unripe (A) and ripe (B) mango

Homogeneity of fraction II

The cellulose acetate membrane electrophoretic profile (Fig. 3.6.5) showed a single (wide) band for both the fractions. Based on their charges, they clearly separated on cellulose acetate membrane, as reported for plant pectic substances (Kikuchi *et al.,* 1992). In capillary electrophoresis, a single migration peak at 3.77 and 4.04 min, respectively for unripe and ripe fraction II was observed, standard pectic acid (PGA) migrated at ~4.89 min, with a shoulder peak moving at 4.5 min (Fig. 3.6.6). All these results indicated fraction II to be fairly homogeneous.

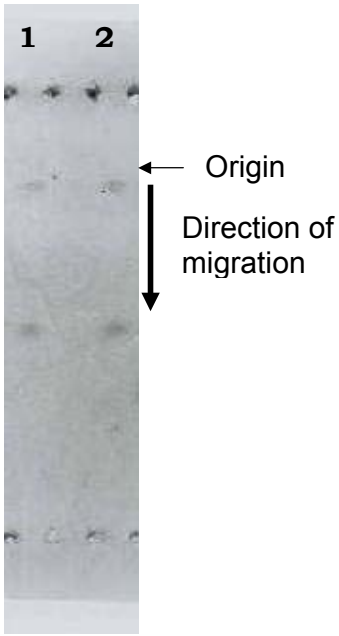

Figure 3.6.5
Cellulose-acetate membrane electrophoresis of the major CWS fraction II. 1, unripe; 2, ripe

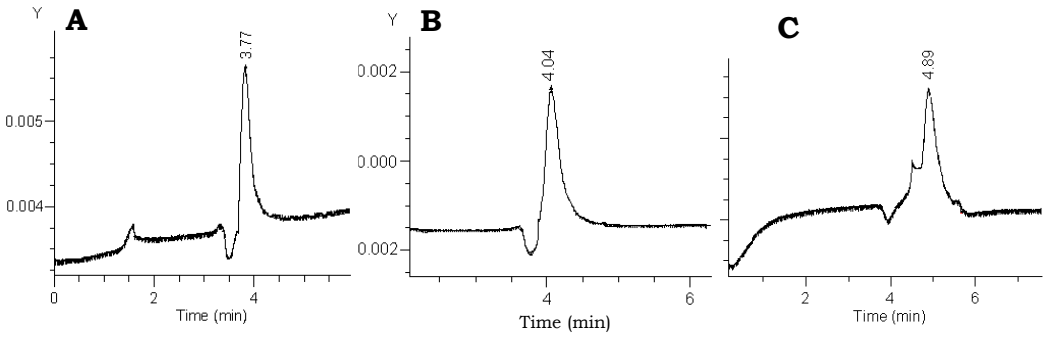

Figure 3.6.6
Capillary electropherogram of major CWS fraction II
A, unripe; B, ripe; C, standard PGA

Structural studies

From the sugar compositional data, it is likely that fraction II, from both unripe and ripe mango, is an arabinogalactan-type polysaccharide, with a relative ratio of galactose and arabinose, 1.4:1 and 1.2:1, respectively, and containing ~24% galacturonic acid. The presence of rhamnose in these fractions may possibly indicate that these arabinogalactans may be linked to galacturonic acid main chain through rhamnose residues, as reported for arabinogalactan from sugar beet (Oesterveld et al., 2000). Rhamnogalacturonans branched with several neutral polymers such as arabinans, galactans and arabinogalactans were reported for plant pectins (Nunan et al., 1998; Oesterveld et al., 2000; Saulnier et al., 1988; Schols et al., 1990; Starsser and Amado, 2002).

Molecules containing asymmetric carbon atoms have the ability to rotate the plane polarized light, which gives information regarding the configuration of the sugar residues of polymers. The high positive specific rotation for these fractions [Table 3.6.1] indicated that the anomeric configuration of the main chain is probably of α-type. A high positive specific rotation was also reported for purified citrus (+277°), apple (+300°), and sunflower (+308°) pectins (Kertesz, 1951; Pilnik and Voragen, 1970). Recently, a high positive specific rotation (+175°) for pectic polysaccharides from tansy (which is related to sugar beet pectins) and its enzyme treated fractions (+185.8° and +228.4°) was reported (Polle et al., 2002).

The pattern of glycosidic linkages between the various monosaccharide residues was established by permethylation followed by GC-MS analysis (Fig. 3.6.7). Peak identification was done by comparison with retention time data and the substitution pattern of the various permethylated alditol (^{2}H) acetates was confirmed by their diagnostic mass fragment (m/Z) values (Fig. 3.6.8). To facilitate knowing the structural involvement of galacturonic acid moieties, the fractions were carboxyl-reduced and the resulting neutral polysaccharides were found easily soluble in DMSO, which facilitated complete methylation. Carboxyl-reduction was done using carbodiimide and sodium borohydride at acidic followed by neutral pH (Taylor and Conrad, 1972). After two successive treatments, the galacturonic acid content was reduced from 24 to <2%, thus resulting in >90% reduction of galacturonic acid residues. From the results presented in Table 3.6.3, it may be deduced that both these fractions are pectic-type polysaccharides having arabinogalactan side chain appendages. Identification of 2,3,6-Me_3-galactose shows a 1,4-linkage in the backbone, which may be derived from D-galacturonic

acid residues. Nevertheless, the main chain is further involved in extensive branching, as shown by the presence of 2,3-Me_2- and 2-Me- galactoses, which are derived from 0-6 and 0-3/0-6 disubstituted galactose residues. Possibly both galactose and arabinose are involved as oligomeric side chains to the galacturonic acid backbone. All the rhamnose (2,3,4-Me_3-Rha) and a portion of arabinose (2,3,5-Me_3-Ara) and galactose (2,3,4,6-Me_4-Gal) were found to be at the non-reducing terminal units. The arabinan side chain was essentially 1,5-linked and having 0-3 and 0-2/0-3 disubstituted branch-off residues of arabinose (identification of 2-Me-Ara and free Ara). Arabinose was found to exist in the labile furanoside form, whereas galactose and galacturonic acid were probably in pyranoside form. Arabinogalactan having these types of linkages has been reported (Smith, 1999).

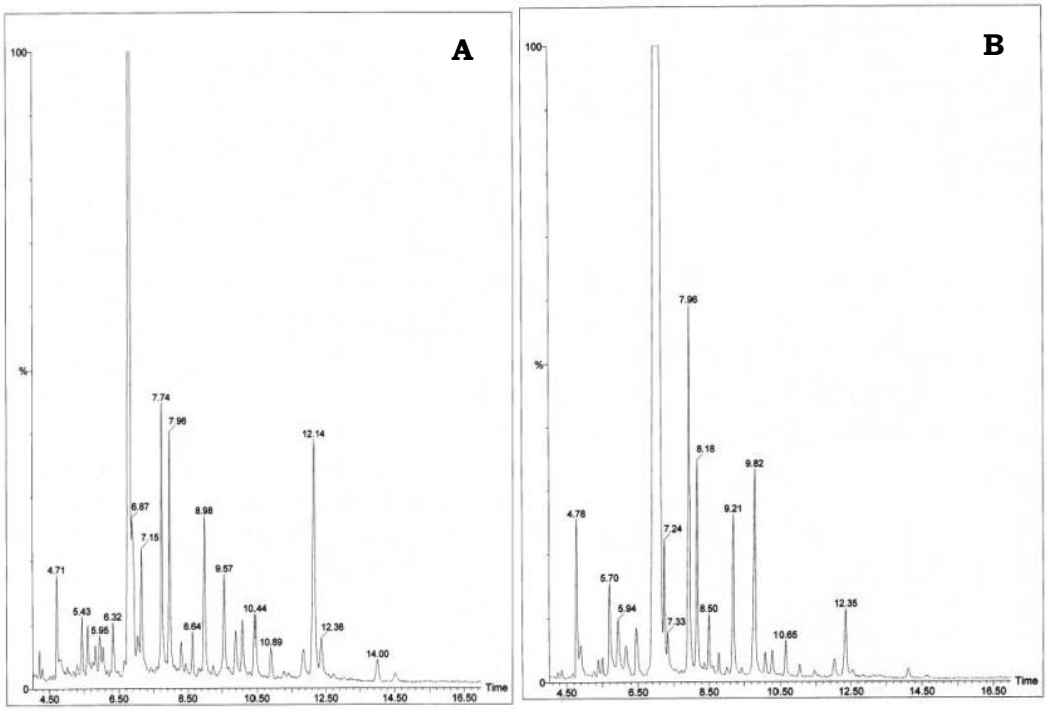

Figure 3.6.7
GC profile of carboxyl-reduced permethylated CWS fraction II of unripe (A) and ripe (B) mango

Small amounts of glucose found in the sugar analysis revealed itself upon methylation in the form of 2,3,6-Me_3- and 2,3-Me_2-derivatives, which signifies its presence as a linear 1,4-linked glucan molecule. Probably, the presence of this glucan could be attributed to the possible existence of associated polysaccharides through polymer-polymer interactions. Identification of 3,4-Me_2-glucose derivative in here is, nevertheless surprising as it indicates rather a different type of main chain linkage. These glucopyranosyl structural units belong more likely to glucan oligomers.

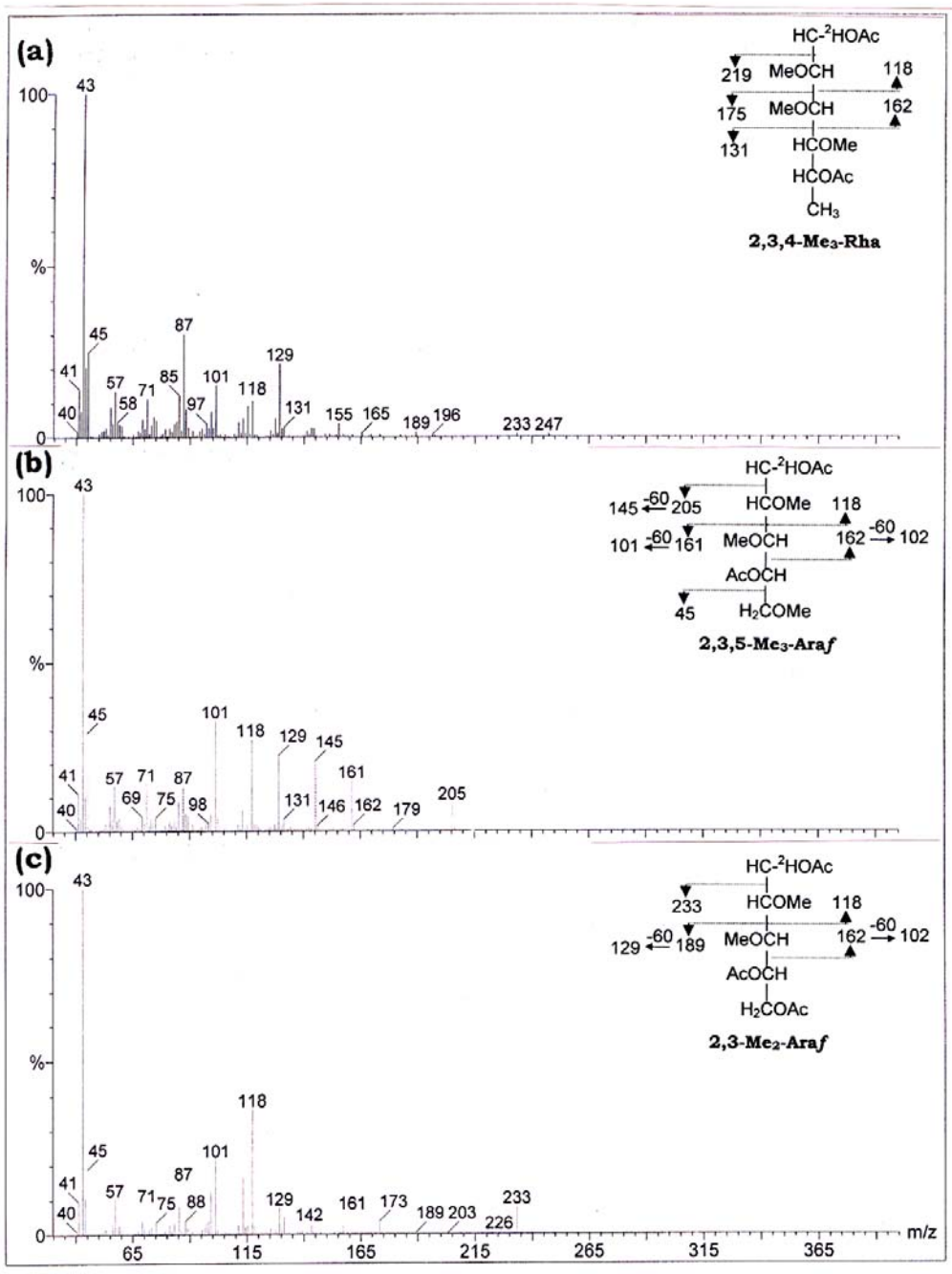

Figure 3.6.8
Mass spectra and fragmentation pattern of alditol acetates
(a) 2,3,4-Rha; (b) 2,3,5-Ara*f*; (c) 2,3-Ara*f*

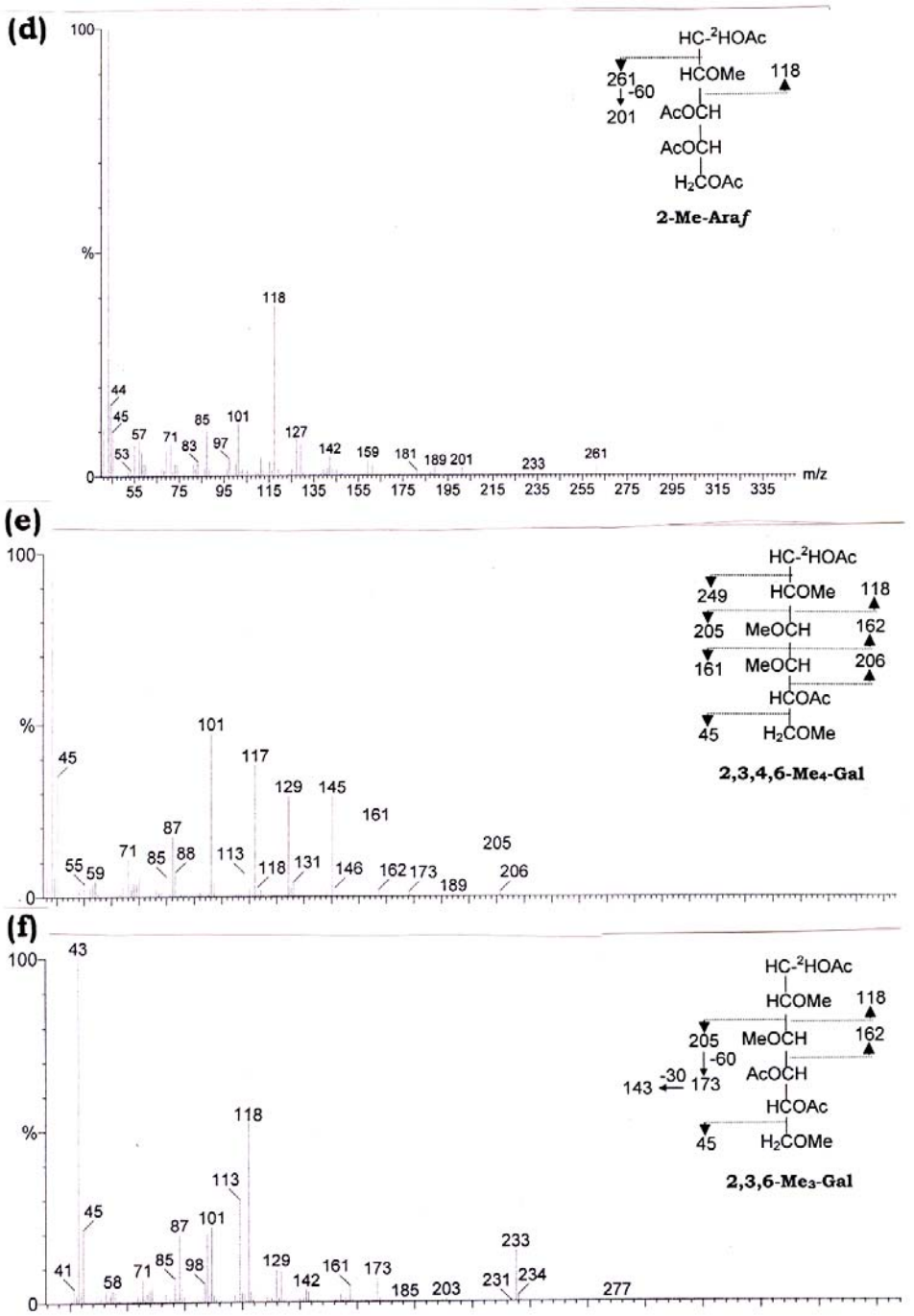

Figure 3.6.8 (Contd.)
Mass spectra and fragmentation pattern of alditol acetates
(d) 2-Ara*f* (e) 2,3,4,6-Gal (f) 2,3,6-Gal

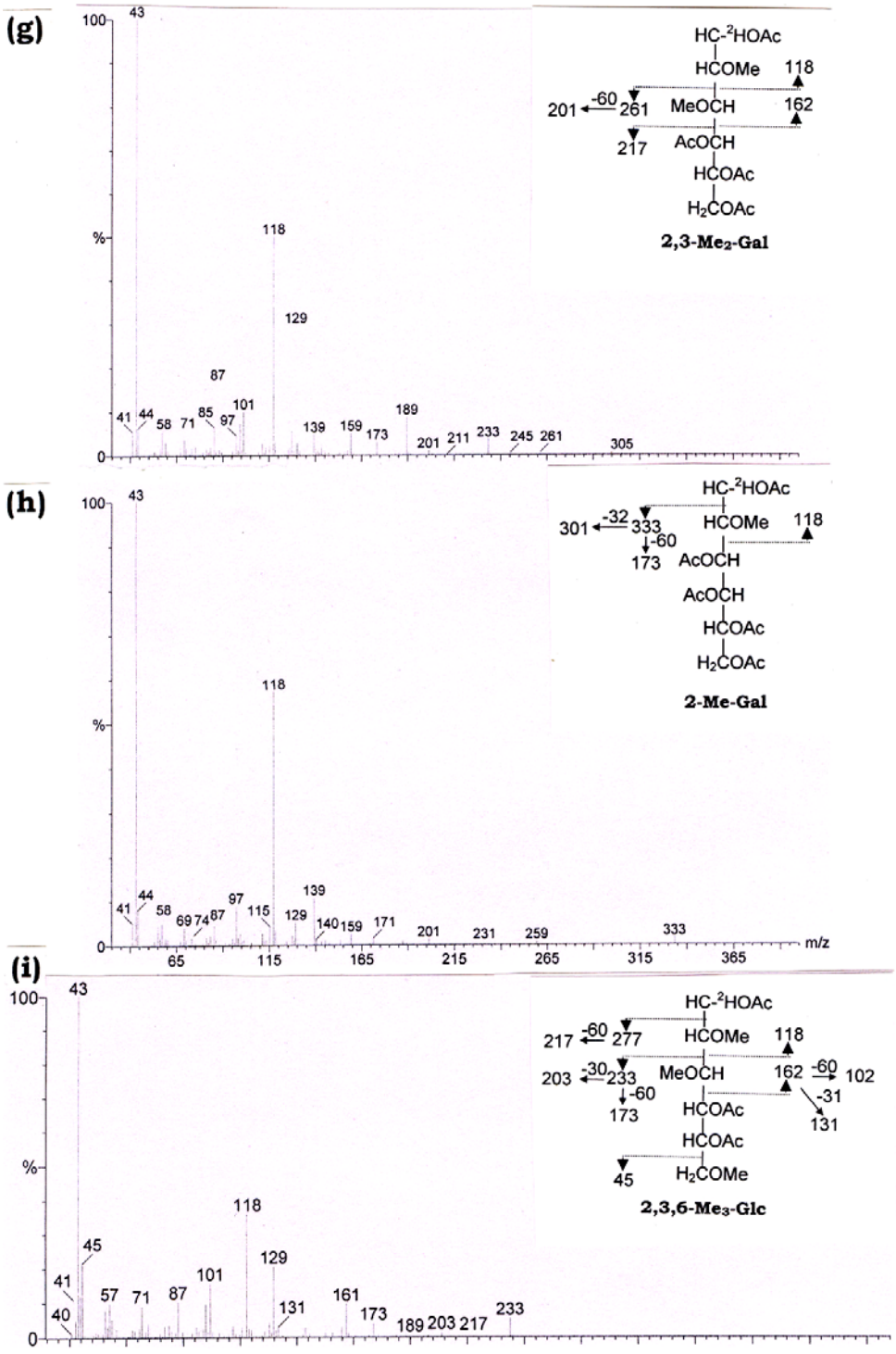

Figure 3.6.8 (Contd.)
Mass spectra and fragmentation pattern of alditol acetates
(g) 2,3-Gal; (h) 2-Gal; (i) 2,3,6-Glc

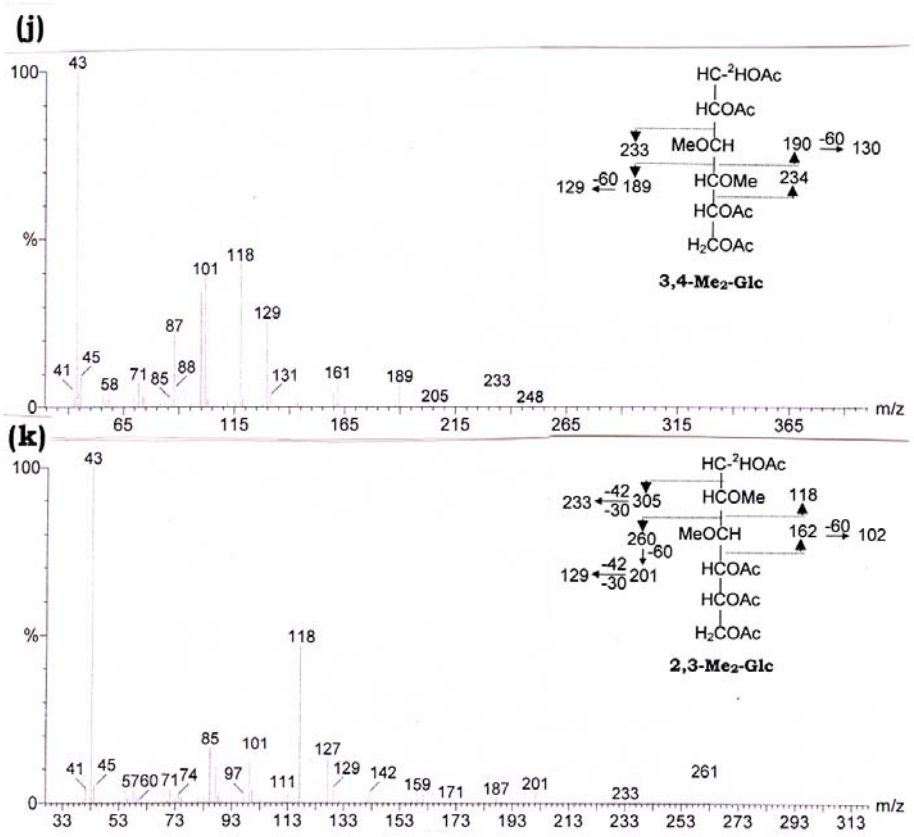

Figure 3.6.8 (Contd.)
Mass spectra and fragmentation pattern of alditol acetates
(j) 3,4-Glc; (k) 2,3-Glc

Table 3.6.3
O-Methyl ethers derived from permethylated CWS fraction II from unripe and ripe mango

Monosaccharide	O-methyl ether	Mode of linkage	Relative mole %		Diagnostic mass fragments (m/Z)
			Fr. II (Unripe)	Fr. II (Ripe)	
Rha	2,3,4-Me_3	Rha (1→	0.44	1.0	43, 102, 118, 131, 162, 175, 206, 219
Ara	2,3,5-Me_3 2,3-Me_2 2-Me	Ara_f (1→ →5) Ara_f (1→ →3,5) Ara_f (1→	0.5 0.5 1.3	0.22 0.4 0.14	43, 45, 118, 161, 162, 205 43, 118, 129, 162, 189, 233 43, 118, 201, 261
Gal	2,3,4,6-Me_4 2,3,6-Me_3 2,3-Me_2 2-Me	Gal (1→ →4) Gal (1→ →4,6) Gal (1→ →3,4,6) Gal(1→	- 10.0 1.0 0.32	0.4 14.0 1.1 0.2	43, 45, 101, 118, 129, 161, 162, 205, 249 43, 45, 118, 131, 162, 173, 203, 233, 277 43, 118, 129, 162, 189, 201, 261, 305 43, 118, 173, 261, 301, 333
Glc	2,3,6-Me_3 3,4-Me_2 2,3-Me_2	→4) Glc (1→ →2,6) Glc (1→ →4,6) Glc (1→	0.2 2.0 1.0	0.4 2.0 1.0	43, 45, 118, 131, 162, 173, 203, 233, 277 43, 129, 130, 189, 190, 233 43, 118, 129, 162, 233, 261, 305

Thus, the two acidic polysaccharide fractions were essentially of pectic-type and consisted probably a main chain of 1,4-linked D-galacturonic acid residues having side chain appendages, at several locations, of arabinose and galactose mono- and oligomers. These structural features were reminiscent of those found in other pectic polymers. Similar type of linkages has been reported for fruit pectins (Colquhoun *et al.*, 1990; Nunan *et al.*, 1998; Redgwell *et al.*, 1991).

Carbohydrates contain functional groups that absorb infrared radiation due to vibration or rotation. Analytical instruments (FT-IR) based on infrared absorbance are thus suitable for structural analysis. FT-IR was used to detect functional groups, configuration and substitution patterns of pectic polysaccharides of plant origin. The FT-IR spectra of the purified polysaccharide fractions from mango CWS, before and after carboxyl reduction (Fig. 3.6.8 and 3.6.9) in the frequency range of 400-4000cm^{-1} showed absorbances characteristic of pectic polysaccharides and comparable with those of published data (Coimbra *et al.*, 1999; Coimbra *et al.*, 1998; Filippov, 1992; Kacurakova *et al.*, 2000; Mathlouthi and Koenig, 1986; Stewart *et al.*, 2001). The spectrum showed absorption at 3401cm^{-1} (indicative of free OH groups), 1739 cm^{-1} (ester bonds), and 1606 cm^{-1} (due to carboxylate functional group). The region between 1200-850 cm^{-1} showed several absorption peaks, characteristic of carbohydrates (Coimbra *et al.*, 1999; Coimbra *et al.*, 1998; Kacurakova *et al.*, 2000). The intense peaks at 1100 and 1015 cm^{-1}, corresponded to galacturonic acid residues. The absorption at 1736 cm^{-1} for both the fractions is indicative of the presence of ester bond (C=O). Further, the absorbance at ~1402 cm^{-1}, indicative of the presence of pectin methyl ester group ($O\text{-}CH_3$), probably suggests that these fractions are esterified. The absorbance at ~1238 cm^{-1} for both the fractions is an indication of the presence of acetyl group, as

reported by Mathlouthi and Koenig (1986). The weak absorbance at ~835 cm^{-1} was indicative of α-configuration, which also correlated the specific rotation values. A minor absorption peak at 893 cm^{-1} for both the fractions may be due to β-glycosidic linkages (Kacurakova *et al.*, 2000) between the sugar residues in the side chain galactan. The absorbance at ~953 cm^{-1} in fractions is also indicative of a high content of galactose (Coimbra *et al.*, 1998). Further, carboxyl reduced fraction II showed intense peak at 1081 cm^{-1}, which is an indication of galactose residue, as well as β-(1→6) and β-(1→3) linked galactan (Kacurakova *et al.*, 2000). Intense peak at 1015 cm^{-1} may correspond to arabinan side chain as reported by Kacurakova and coworkers (Kacurakova *et al.*, 2000).

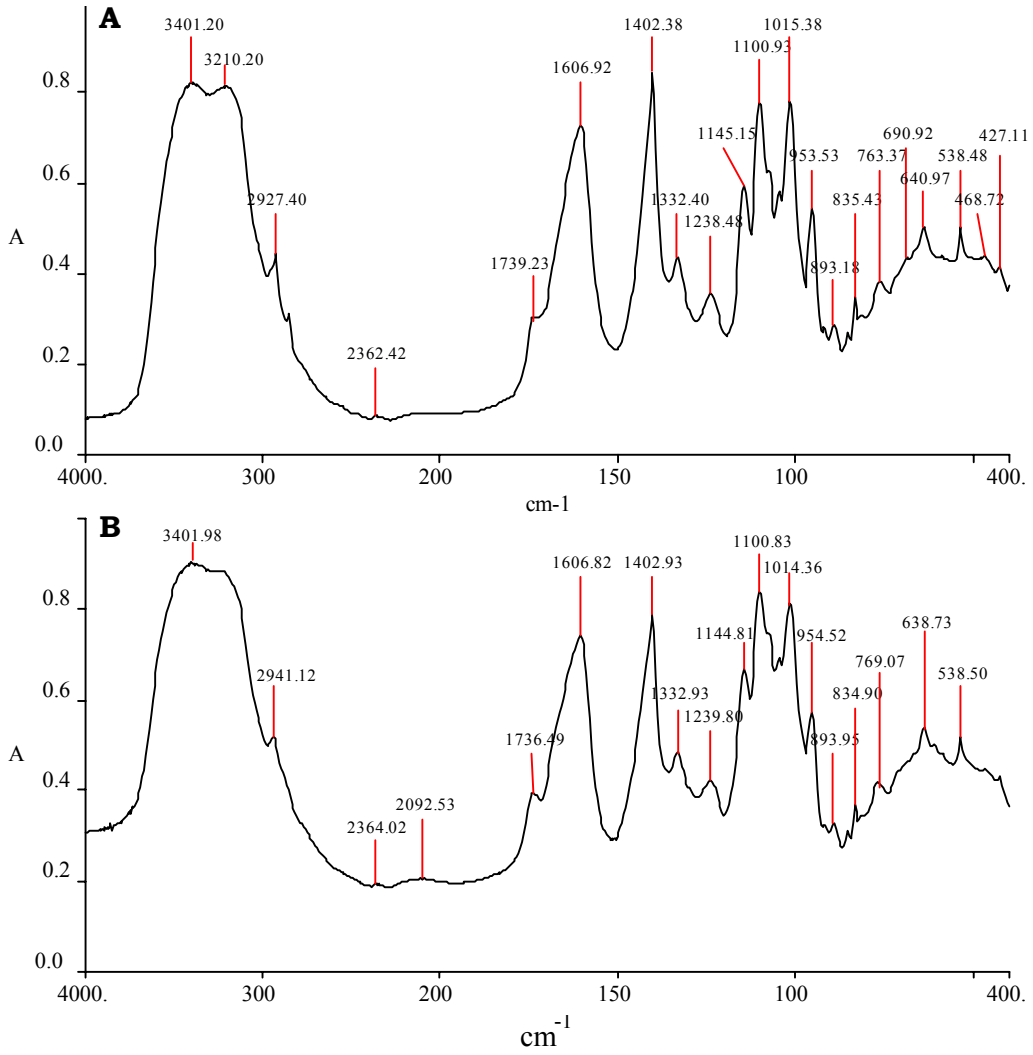

Figure 3.6.8
FTIR spectra of CWS fraction II from unripe (A) and ripe (B) mango- before carboxyl reduction

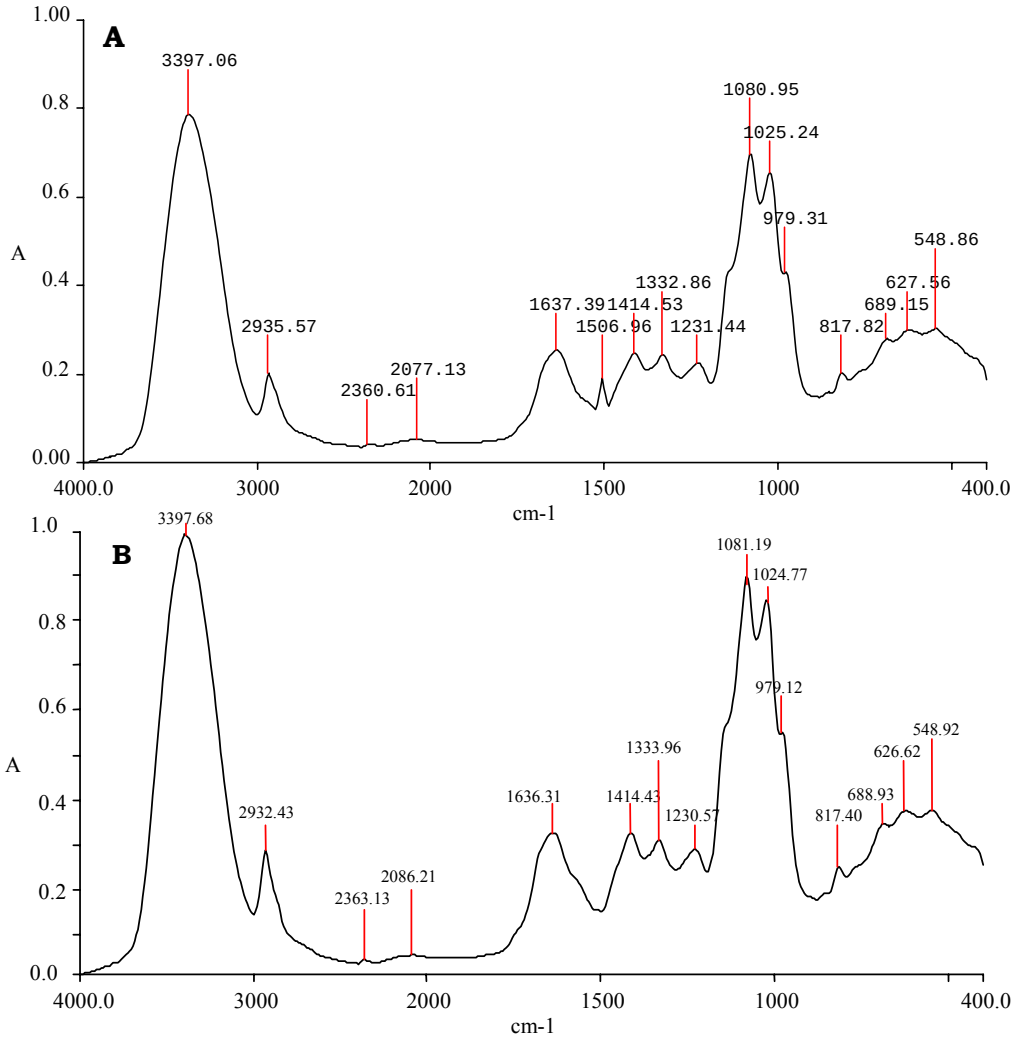

Figure 3.6.9
FTIR spectra of the major CWS fraction II from unripe (A) and ripe (B) mango-after carboxyl reduction

^{13}C NMR is a valuable technique in the structural elucidation of polysaccharides, which allows spectra of the polysaccharides to be obtained using their naturally abundant ^{13}C atoms. It gives detailed information on composition, sequence and conformation of polysaccharides, the better signal separation is mainly due to the wide range of chemical shifts involved. This technique is widely used for elucidating the structure of pectic polysaccharides from fruits (Colquhoun *et al.*, 1990; Pressey and Himmelsbach, 1984; Redgwell

et al., 1992; Saulnier *et al.*, 1988; Seymour *et al.*, 1990). The fine structural details as well as the nature of the anomeric ring carbons in the fraction II were further unequivocally established by ^{13}C NMR spectral analysis, which showed signals characteristic of pectic-type polysaccharides (Fig. 3.6.10 A and B). The spectral quality was poor, probably due to viscous nature of the samples, at the concentration required for NMR analysis. Furthermore, the galacturonic acid main chain occurring as backbone of the polysaccharide is too large and rigid to yield detectable signals, as strong signals are the result of highly flexible chains (Pressey and Himmelsbach, 1984).

Signal assignments were based on comparison with published spectra of several plant pectins (Colquhoun *et al.*, 1990; Davis *et al.*, 1990; Keenan *et al.*, 1985; Seymour *et al.*, 1990). The spectral signals in the range 100.8, 71-79 and 60-62 ppm were assigned to carbon nuclei C_1 to C_6. The signal in the region 100.8 corresponds to C_1, 71-76 ppm to C_4, C_2, C_3 and C_5, whereas those at 60-62 ppm are assigned to C_6. All the spectral frequencies were identified by making use of their chemical shift values. The two carbon nuclei C_1 and C_4, both involved in glycosidic linkages, usually are most sensitive for changes in polymer conformation. Almost comparable spectral frequencies at more or less similar chemical shift values were seen in the spectrum of fraction II from ripe mango. The assigned signals showed a close similarity with those of α-galacturonan isolated from mung bean hypocotyls and flax (Davis *et al.*, 1990), sugar beet (Keenan *et al.*, 1985), tomato fruit (Seymour *et al.*, 1990) and kiwi fruit pectins (Newman and Redgwell, 2002).

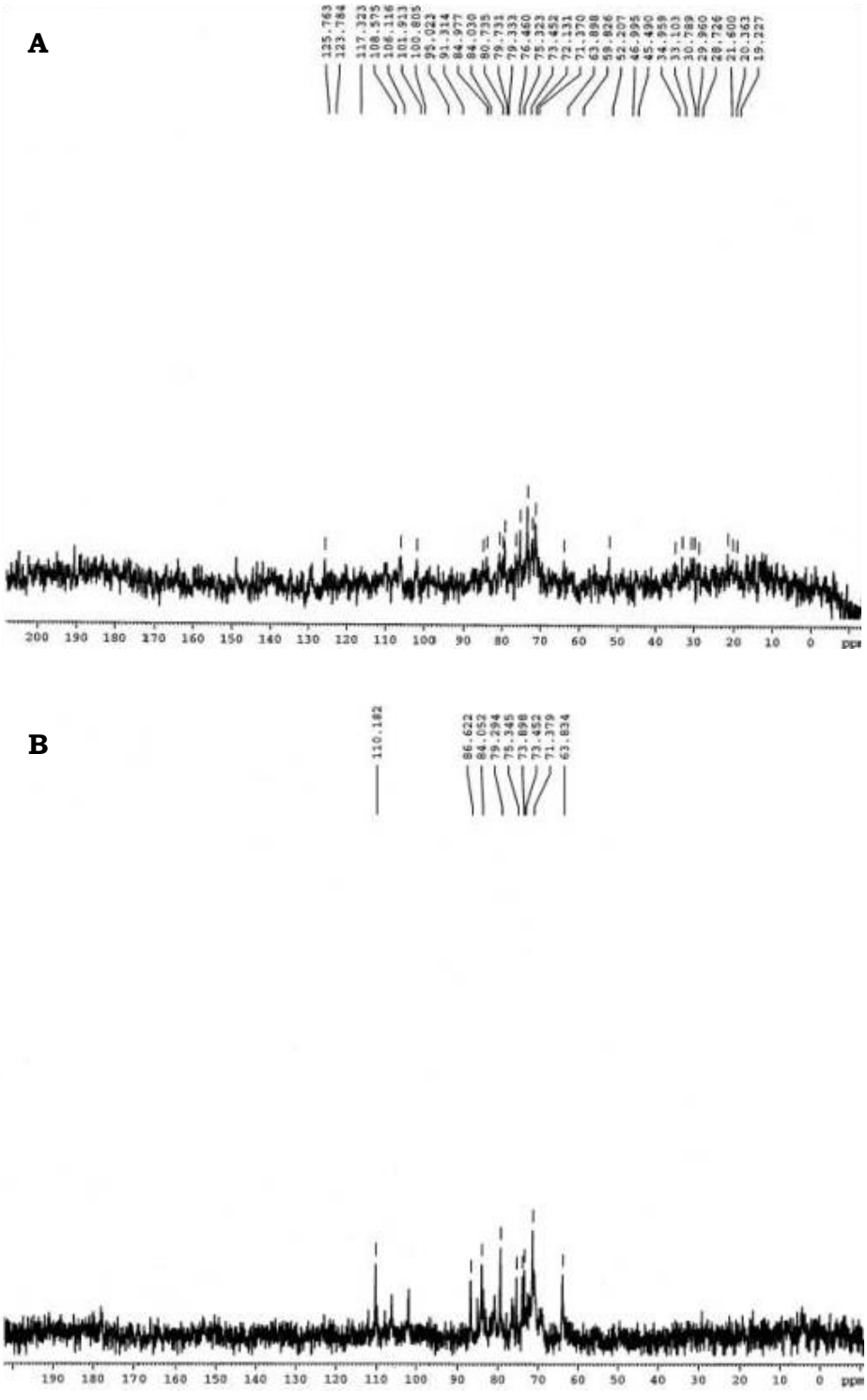

Figure 3.6.10
^{13}C NMR spectra of the major CWS fraction II of unripe (A) and ripe (B) mango

The six signals assigned to the six carbons of α-galacturonan from apple (Colquohoun *et al.*, 1990), grape (Saulnier *et al.*, 1988) and tansy pectins (Polle *et al.*, 2002) slightly vary from those of mango pectins. The variation in the signals may be attributed to the differences in the molecular organization of pectins from different origins. A signal at 19.22 is attributed to C-6 of α-rhamnose units, whereas the one at 63.89 is assigned to C-6 of β-galactose residue linked to α-rhamnose unit by 1→4 linkage. Relatively small intensity of signal at 19.22 indicates the presence of low levels of rhamnose. The signal at 21.60 is possibly due to the presence of methyl groups. The signal observed at 52.20 ppm is indicative of pectin methyl ester (-OCH_3) (Colquhoun *et al.*, 1990).

Conclusions

Put together, all these results establish that the major CWS fraction (Fr. II) of unripe and ripe mango is a branched α-1,4-linked D-galacturonan having side chain branches consisting of single residues of galactose and/or arabinose or oligomeric 1→5 linked arabinofuranose residues, linked through 1→3 linkages. The α-linkage is in good agreement with the spectral data.

***Section* 7**

Characterization of the major hot water soluble polysaccharides

Introduction

Fruit softening during ripening is an important process in most fruits, which is due to changes in cell walls. Gross changes in wall composition may not always occur, and indeed more subtle structural modifications of constituent polysaccharides are often observed during softening (Brady, 1987; Fischer and Bennett, 1991). For example, molecular mass, solubility, and the degradation/substitution (or branching) of an individual wall polysaccharide may be altered without any large change in the total amount of that polysaccharide.

Results and Discussion

Pectins from various plant species have some common structural trends (Albersheim, 1975), although differences exist in their composition and primary structure especially during maturation (Pilnik and Voragen, 1970). The major HWS fractions (III and IV) of unripe mango, eluting in 0.15 M $(NH_4)_2CO_3$ and 0.15 M NaOH, were chosen for structural studies. The significant drop in their abundance and molecular weight as well as modification of their component sugars at the end of ripening is depicted in Figure 3.7.1 (A and B), which indicated their *in vivo* depolymerization.

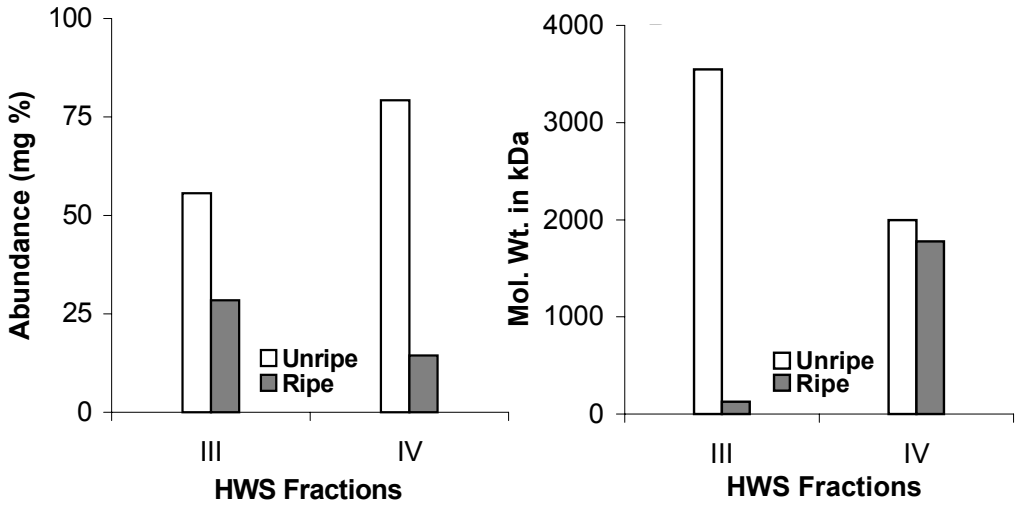

Figure 3.7.1
Abundance (A) and molecular weight (B) changes of the major HWS fractions from unripe and ripe mango

Fractions III and IV from unripe mango were individually subjected to GPC on Sepharose CL-4B (Fig. 3.7.2). They were eluted as a single broad peak, due to its high polydispersity, although some contamination was observed in fraction IV. Their yield (as total sugar) and other physico-chemical characteristics are given in Table 3.7.1. Both the fractions showed galacturonic acid/neutral sugar ratio of 0.1 and 0.03%, respectively. Their molecular weights were in the range between 1000-3000 and 1000-2000 kDa for the two fractions respectively. The molecular weights of the major HWS fractions from unripe mango, as determined by HPSEC (Fig. 3.7.3) were 3548 and 1995 kDa, respectively. The most significant change in the abundance and molecular weight of the major HWS fractions was observed during ripening.

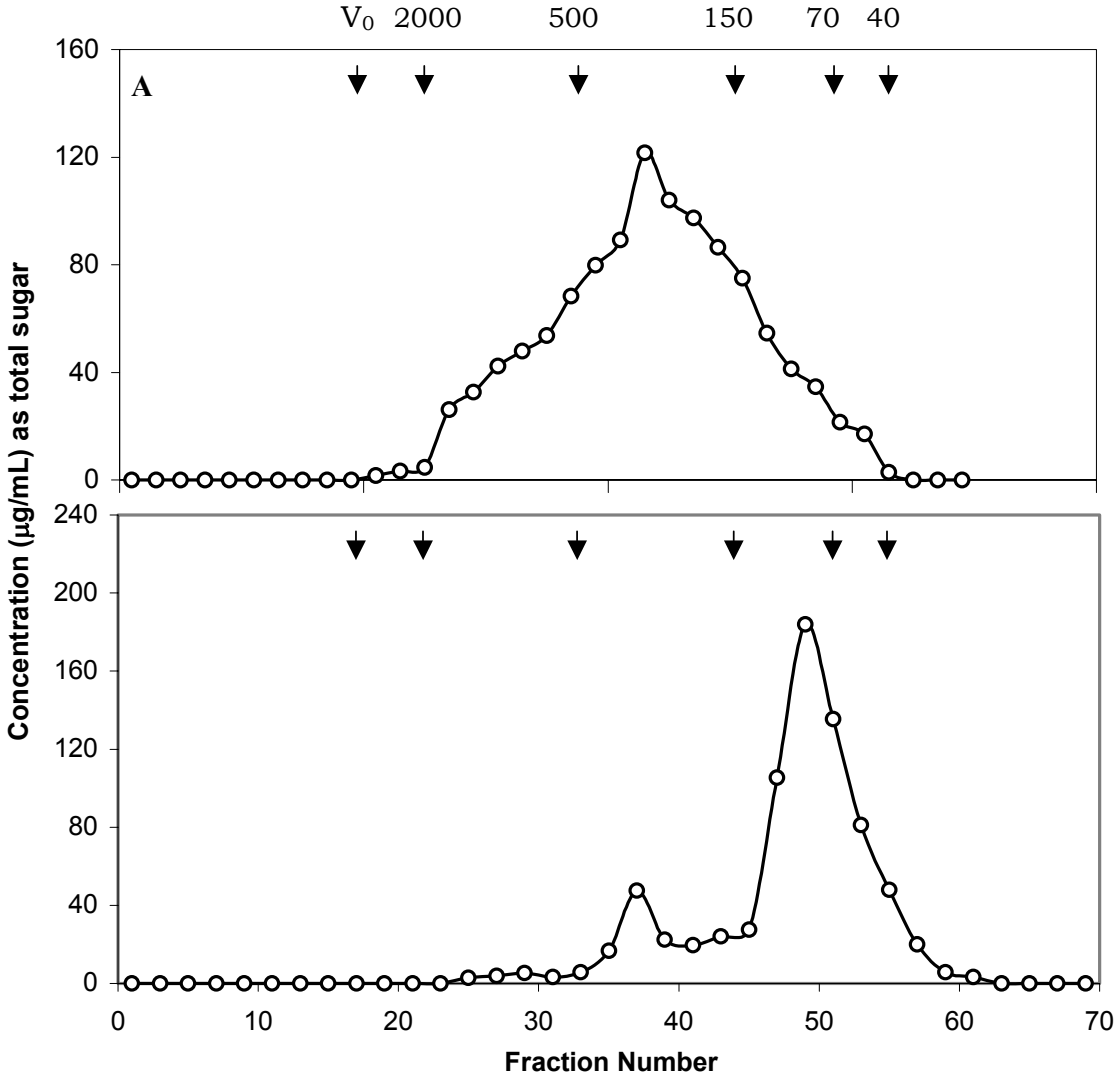

Figure 3.7.2
GPC profile of major HWS fraction III (A) and IV (B) from unripe mango on Sepharose CL-4B

Table 3.7.1
Physico-chemical characteristics of major HWS fractions III and IV of unripe mango

Fr. No.	Polymeric fractions	Total Carbohydrate %	Uronic acid %	Reduced viscosity (η_r)	Specific viscosity ($\eta_r - 1$)	Specific rotation (degrees)	Mol. Wt. (kDa)
III	**0.15M $(NH_4)_2CO_3$**	86.9	7.7	2.7	1.7	+42.0	3548
IV	**0.15M NaOH**	100.0	2.9	2.8	1.8	+64.0	1995

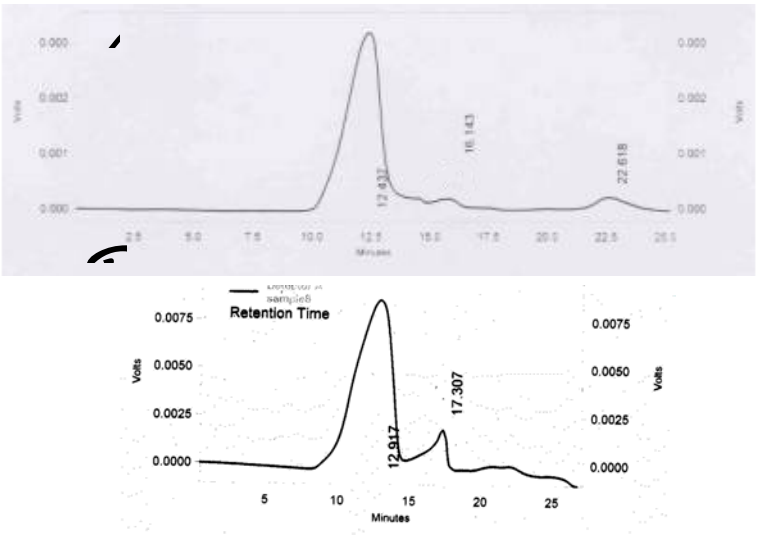

Figure 3.7.3
HPSEC profiles of the major HWS fractions III (A) and IV (B) of unripe mango

The chemical composition of the purified major HWS fractions from unripe mango is shown in the Table 3.7.2. The fractions contained mainly galactose and arabinose in almost comparable amounts, with minor amounts of glucose, rhamnose and xylose in fraction IV and small amount of rhamnose is present in fraction III. Fraction V has a higher neutral sugar content (97.1 %) than fraction IV (79.2 %). Arabinose and galactose are found in almost equivalent amounts in both the fractions.

Table 3.7.2
Neutral sugar composition (mg %) of major HWS fractions

Fr. No.	Polymeric fractions	Rha	Ara	Xyl	Gal	Glc	Ara:Gal	Pentoses: Hexoses
III	**0.15 M $(NH_4)_2CO_3$**	5.1	43.4	-	30.6	-	1:1.41	1:0.63
IV	**0.15 M NaOH**	10.1	40.2	2.6	30.1	14.0	1:1.33	1:0.83

Homogeneity of the major HWS fractions

Cellulose-acetate membrane electrophoresis profile (Fig. 3.7.4) showed a single band for both the fractions. In capillary electrophoresis, a single migration peak at ~3.8 min, was observed for these fractions (Fig. 3.7.5). Based on these results, both the fractions appeared homogeneous.

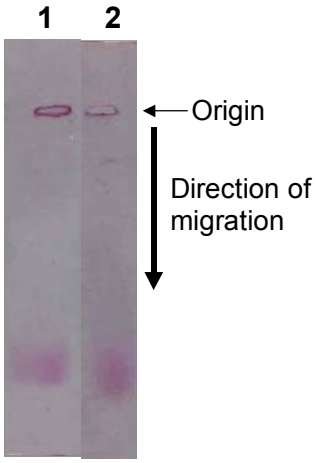

Figure 3.7.4
Cellulose-acetate membrane electrophoresis of the major HWS unripe fractions III (1) and IV (2)

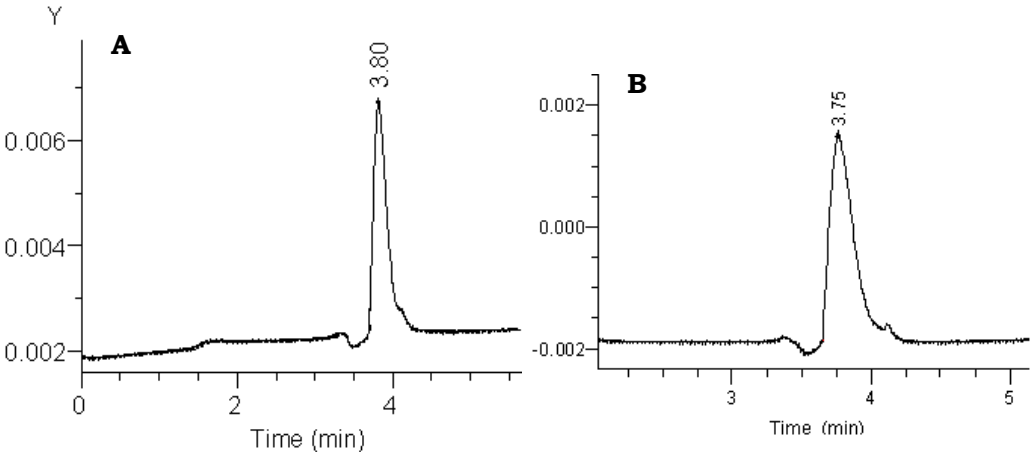

Figure 3.7.5
Capillary electropherogram of major HWS unripe fractions III (A) and IV (B)

Characterization of major HWS fractions

From the compositional data, fraction III was having galacturonic acid ~7.7%, and fraction IV ~2.9% (Table 3.7.1). Both the fractions contained neutral sugars, such as galactose, arabinose and small amounts of rhamnose and glucose in various proportions (Fig.3.7.6; Table 3.7.2). They may be of arabinogalactan-type polysaccharide, with a relative ratio of galactose and arabinose, 1.0:1.41 and 1:1.33, respectively. Substantial decrease in the hexose levels was observed in both the fractions, indicating degradation of hexosans during ripening. The low positive specific rotation for these fractions [Table 3.7.1] may be indicative of a β-type configuration.

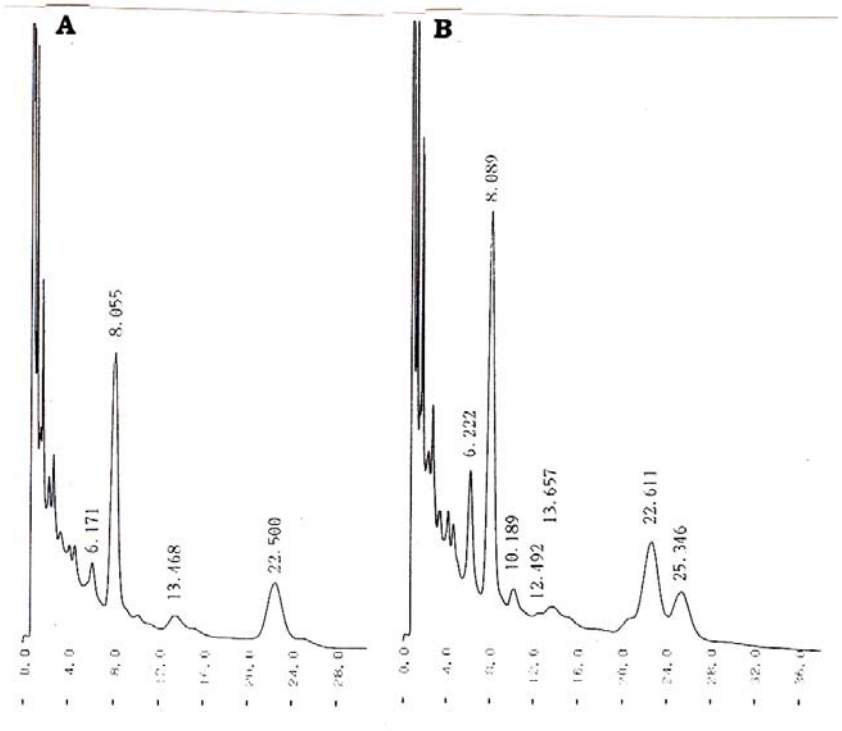

Figure 3.7.6
GC profile of sugars (as alditol acetates) derived from HWS fraction III (A) and IV (B) of unripe mango

The FT-IR spectra of the purified fractions (Fig. 3.7.7 A and B) in the frequency range of 400-4000 cm^{-1} showed a few absorbances characteristic of pectic polysaccharides. Intense peaks at 1079 and 1023 cm^{-1} may correspond to galacturonic acid residues. The weak absorption at 1736 cm^{-1} is indicative of the presence of ester bond (C=O), absorbance at ~1416 cm^{-1} suggests the presence of pectin methyl ester group (O-CH_3). A minor absorption peak at 894 cm^{-1} may be due to β-glycosidic linkages (Kacurakova *et al.*, 2000) between the sugar residues. The absorbance at ~955 cm^{-1} in fractions is also indicative of a high content of galactose (Coimbra *et al.*, 1998).

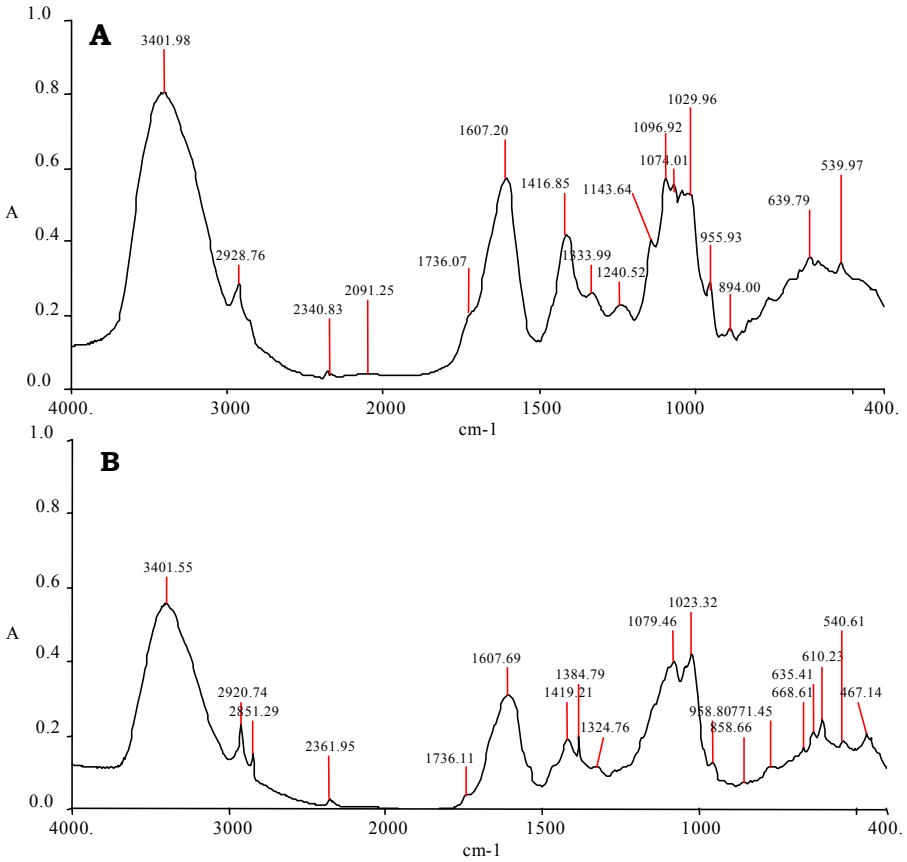

Figure 3.7.7
FTIR spectra of major HWS fractions III (A) and IV (B) from unripe mango

Conclusions

The results confirm that the major HWS fractions (III and IV) were found to be of arabinogalactan-type with a relative ratio of galactose and arabinose, 1.0:1.41 and 1:1.33, respectively.

***Section* 8**

Structural characterization of the major hemicellulose polysaccharides

Introduction

Extensive research outcome has addressed the cell wall changes that occur in ripening tomato fruit, and many reports have focused on the considerable pectin degradation that coincides with softening and expression of the pectin hydrolase PG (Huber, 1983a; Hobson and Grierson, 1993). Early models implied that PG-catalyzed pectin degradation represented the fundamental process underlying fruit softening (Crookes and Grierson, 1983); molecular genetic approaches subsequently revealed that PG-dependent pectin degradation is not essential for fruit softening (Smith *et al.*, 1988; Giovannoni *et al.*, 1989), but may play a role in other aspects of fruit quality (Kramer *et al.*, 1990; Schuch *et al.*, 1991). This suggests that other wall polymers contribute significantly to fruit firmness, and a few recent studies have examined the extent of hemicellulose degradation during fruit ripening. The principal hemicellulose in dicotyledons is xyloglucan, and it has been demonstrated that xyloglucan undergoes substantial depolymerization in many ripening fruits, including tomato (Sakurai and Nevins, 1993; Maclachlan and Brady, 1994).

Plant cell walls consist of cellulose microfibrils coated and cross-linked by xyloglucans (Hayashi and Maclachlan, 1984; McCann *et al.*, 1990), and disruption of the cellulose/xyloglucan matrix may be a key element in regulating wall integrity. Additional hemicellulosic polymers, including xylans, arabinoxylans, mannans, and galactoglucomannans, have been detected in different fruit species; however, these are typically minor components and turnover of these polysaccharides during ripening remains relatively

unexplored. Hemicelluloses also show substantial changes in the molecular mass profiles and their degree of depolymerization during ripening. The decrease in the molecular mass of xyloglucan fraction during ripening was evident. This component of cell wall is presumed to coat and cross-link the cellulose microfibrils, and thus may play an important structural role. Disruption of this close association by cleavage of xyloglucan by glycanases and glycosidases could allow cell wall loosening.

Results and Discussion

The major hemicellulose fractions (IV and V) of unripe mango were chosen for structural studies. It is possible that these fractions are extensively depolymerized during fruit ripening, with the result that they were obtained in very low yield from ripe mango. The striking drop in their abundance and molecular weight at the end of ripening is depicted in Figure 3.8.1 (A and B).

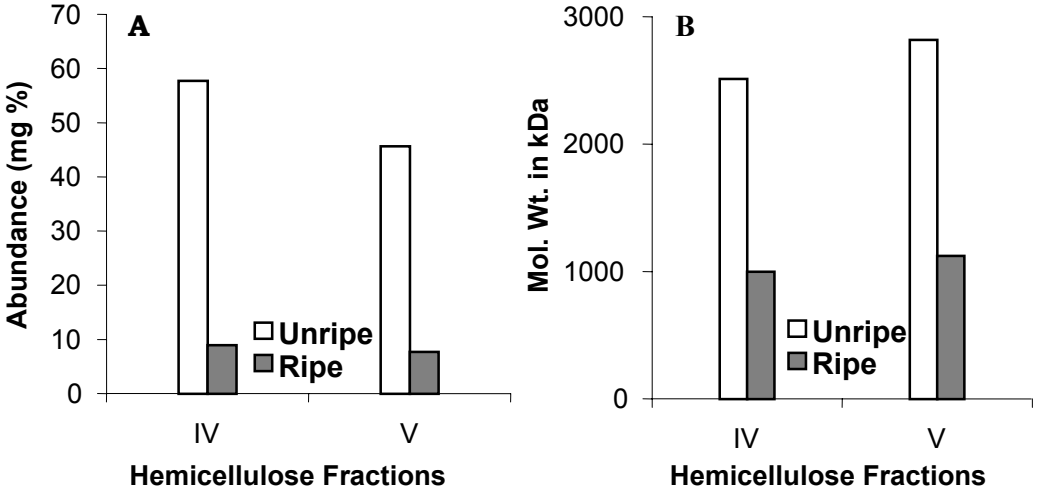

Figure 3.8.1
Abundance (A) and molecular weight (B) changes of the major hemicellulose fractions from unripe mango

Fractions IV and V, size fractionated on Sepharose CL-4B, were eluted in void volume (Fig. 3.8.2) indicating them to be of very high molecular weight. The sugar composition and other physico-chemical characteristics of these fractions are

presented in Table 3.8.1. The fractions were highly polydisperse in nature as shown by their elution profiles. The molecular weights were in the range between 2000-3000 and 1000-2000 kDa for fractions IV and V, respectively.

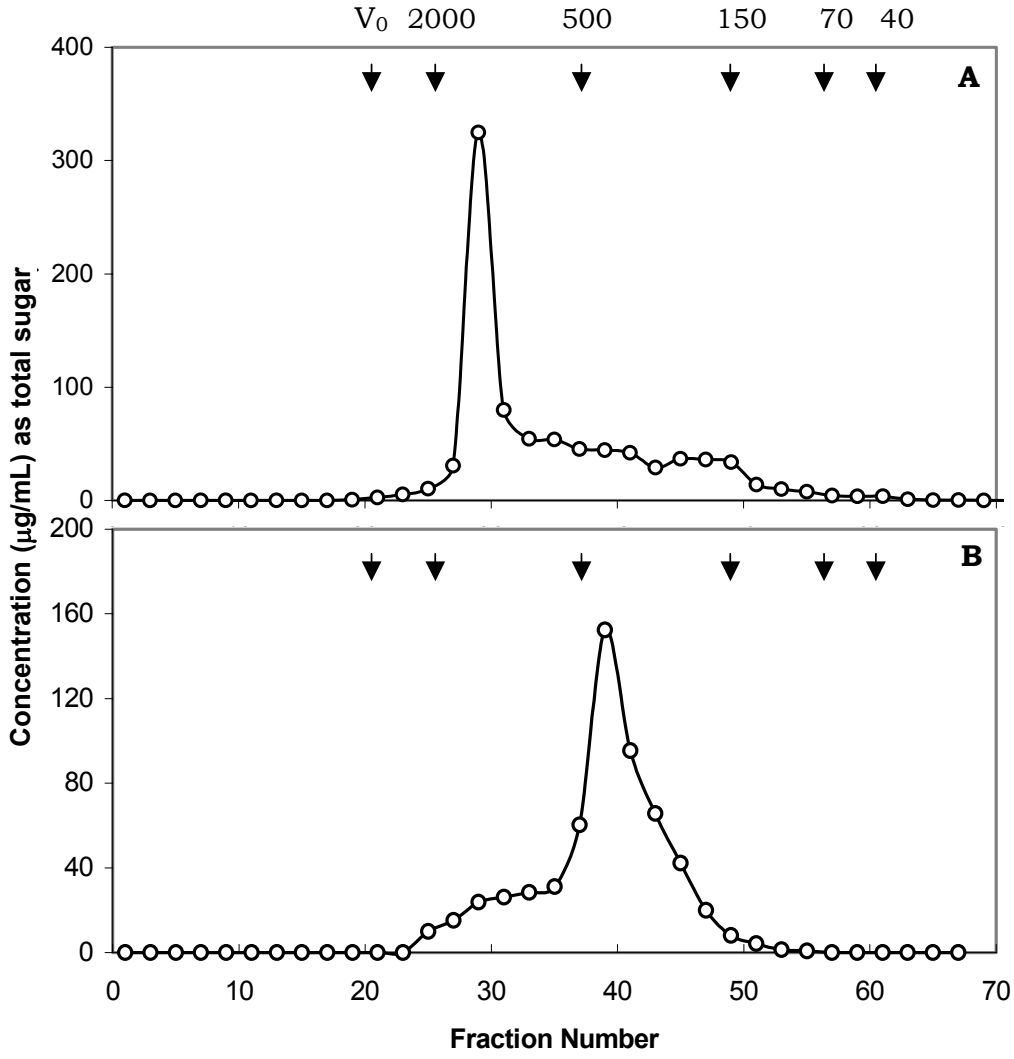

Figure 3.8.2
GPC profile for major hemicellulose fractions IV (A) and V (B) from unripe mango on Sepharose CL-4B column

Table 3.8.1
Physico-chemical properties of major hemicellulose fractions of unripe mango

Fr. No.	Total Carbohydrate (%)	Uronic acid (%)	Neutral sugar (%)	UA:NS Ratio	Reduced Viscosity (η_r)	Specific Viscosity ($\eta_r - 1$)	Specific rotation (degrees)	Mol. Wt. (kD)
IV	100.0	2.6	97.4	0.03:1	4.2	3.2	+ 64.0	2512
V	100.0	1.0	97.3	0.03:1	4.0	3.0	+ 32.0	2818

The molecular weights of the fraction IV and V of hemicellulose from unripe mango, as determined by HPSEC (Fig. 3.8.3) were 2512 and 2818 kDa, respectively. High molecular mass hemicellulosic polymers (> 1000 kDa) have been reported (Rose *et al.*, 1998; Talbott and Ray, 1992). Relatively very few reports exist of similarly fractionated hemicellulosic polymers from fruit. Hemicellulose isolated from melon and persimmon fruit tissues with low concentrations of alkali and size fractionated has been reported to exhibit a similar pattern (Rose et al, 1998; Cuttilias-Iturralde et al, 1994). A similar size distribution of xyloglucan was seen in hemicellulosic extracts from tomato tissue, and depolymerization was evident during ripening (Maclachlan and Brady, 1994).

The compositional analysis indicated that both the fractions were rich in glucose and xylose, with smaller amounts of arabinose and mannose (Fig. 3.8.4, Table 3.8.2), suggesting a xyloglucan type fraction. The presence of substantial amounts of glucose and xylose has been reported (Rose *et al.*, 1998; Talbott and Ray, 1992). This was attributed to the presence of large xyloglucan molecules existing either as free macromolecules and/or crosslinks to cellulose microfibrils (Rose *et al.*, 1998). In the present study, the ratios of xylose to glucose (1.0:3.8 and 1.0:13.2) and pentose to hexose

(1.0:3.2 and 1.0:6.2) in the both the fractions indicated the degradation of hexosans rather than pentosans (Table 3.8.2).

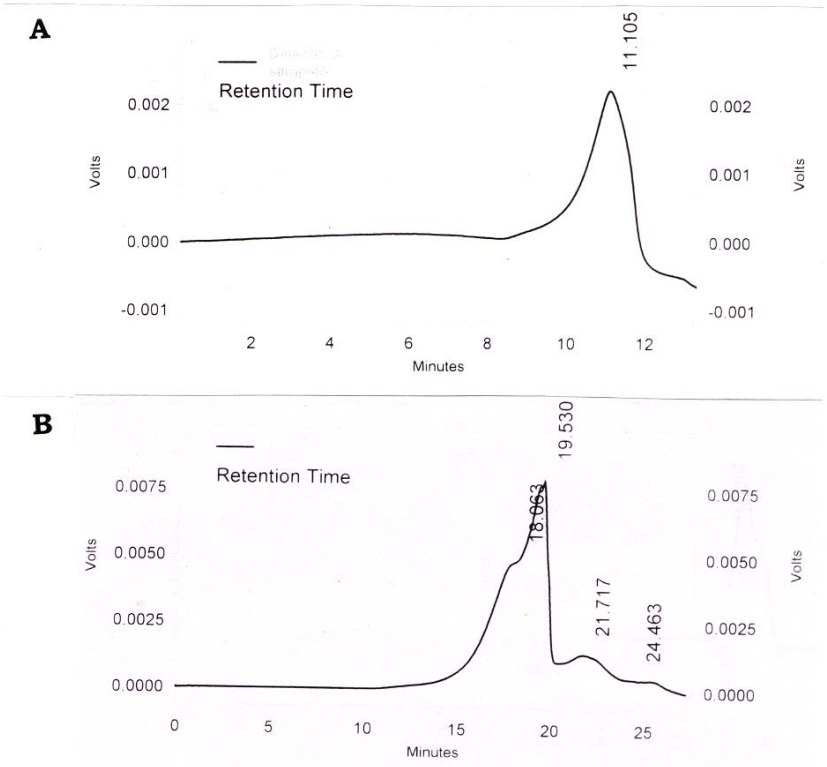

Figure 3.8.3
HPSEC profiles of the major hemicellulose fraction IV (A) and V (B) of unripe mango

Table 3.8.2
Neutral sugar composition (%) of major hemicellulose polymers of unripe mango pulp

Fr. No.	Rha	Ara	Xyl	Man	Gal	Glc	Ara:Xyl	Pentoses: Hexoses
IV	2.0	3.6	17.7	5.3	1.2	67.5	0.2:1	1:3.2
V	0.43	5.26	4.87	-	1.43	64.22	1.08:1	1:6.22

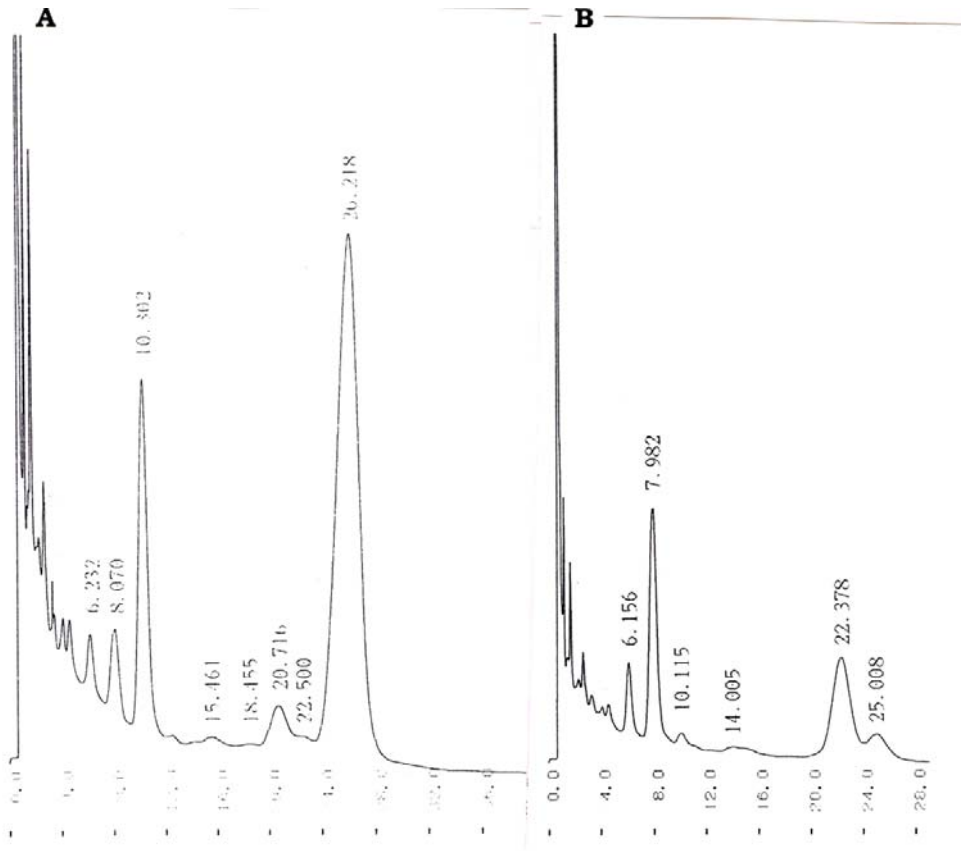

Figure 3.8.4
GC profile of sugars (as alditol acetates) derived from hemicellulose fractions IV and V of unripe mango

Homogeneity of the major hemicellulose fractions

Cellulose acetate electrophoresis (Fig. 3.8.5) showed single band, which remained in the origin for both the fractions. In capillary electrophoresis, a single migration peak at ~4.1 min, was observed (Fig. 3.8.6). It appears likely that these fractions are homogeneous.

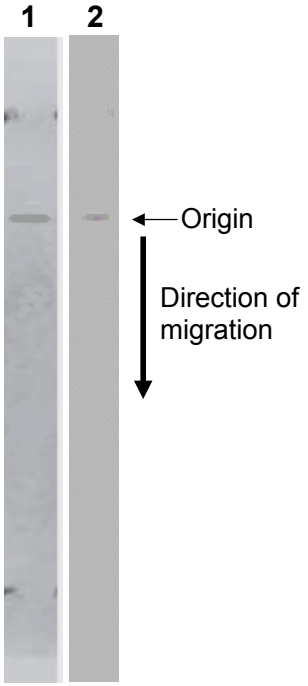

Figure 3.8.5
Cellulose-acetate membrane electrophoresis of the major hemicellulose unripe fractions IV (1) and V (2)

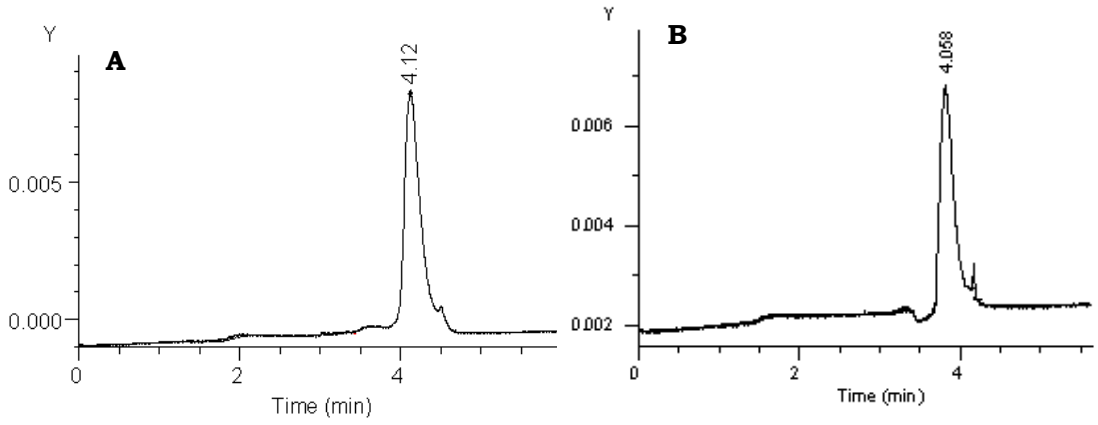

Figure 3.8.6
Capillary electropherogram of major hemicellulose fraction IV (A) and V (B) of unripe mango

Structural studies

The low positive specific rotation for these fractions [Table 3.8.1] indicated the anomeric configuration of the main chain to be of β-type.

Permethylation analysis of hemicellulosic fractions IV and V (Fig. 3.8.7 and 3.8.8) revealed a xyloglucan-type polysaccharide in them. Identification in fraction IV of structural elements [→4)-Glcp-(1→ and →4,6)-Glcp-(1→] indicated a branched 1,4-linked glucan backbone (Table 3.8.3). A few of these residues were further involved in multiple branching at 0-3 and 0-3/0-6 as shown by the presence of 2,6-Me_2-glucose and glucitol derivatives, respectively. More than one third of the main chain glucosyl moieties are involved in additional branching as indicated by their relative mole % concentration. Both arabinose and xylose constitute the side chain branch off residues, with xylosyl units being involved in additional branching (identification of 2-Me-xylose). Majority of arabinose and part of xylose were found located at the non-reducing terminal ends

(presence of 2,3,5-Me_3-Araf and 2,3,4-Me_3-Xylp). Arabinose was present in its labile furanoside form whereas xylose and glucose moieties were present in pyranoside ring form. Thus, this fraction was shown to be a highly branched xyloglucan, and its structural characteristics were similar to those of several other xyloglucans of plant sources.

On the other hand, fraction V showed slight variations in its overall structural makeup. In here the main chain was found to be composed of 1,4-linked (presence of 2,3,6-Me_3-glucose) and 1,3-linked (presence of 2,4,6-Me_3-glucose) glucosyl residues, which were further involved in extensive branching. The latter was contributed by multiply branched glucose (0-3/0-6 disubstitution as indicated by 2-methyl glucose and 0-2, 0-4/0-6 trisubstitution as shown by free glucose) residues. All the arabinofuranosyl moieties were located at the non-reducing terminal ends along with a portion of xylose (presence of 2,3,4-Me_3-Xylp) and glucose (2,3,4,6-Me_4-Glcp) residues. Unlike in the hemicellulosic fraction IV, the degree of branching in here was much more extensive. The latter due to any undermethylation was ruled out by the fact that the polysaccharide was completely soluble in dimsyl anion and the resulting permethylated sample did not show any $^{-}$OH absorption at around 3300 cm^{-1} in the IR spectrum (data not shown). Further, the lack of molar equivalence of non-reducing terminals with the branch off residues suggests considerable loss of the former during the sample preparation steps.

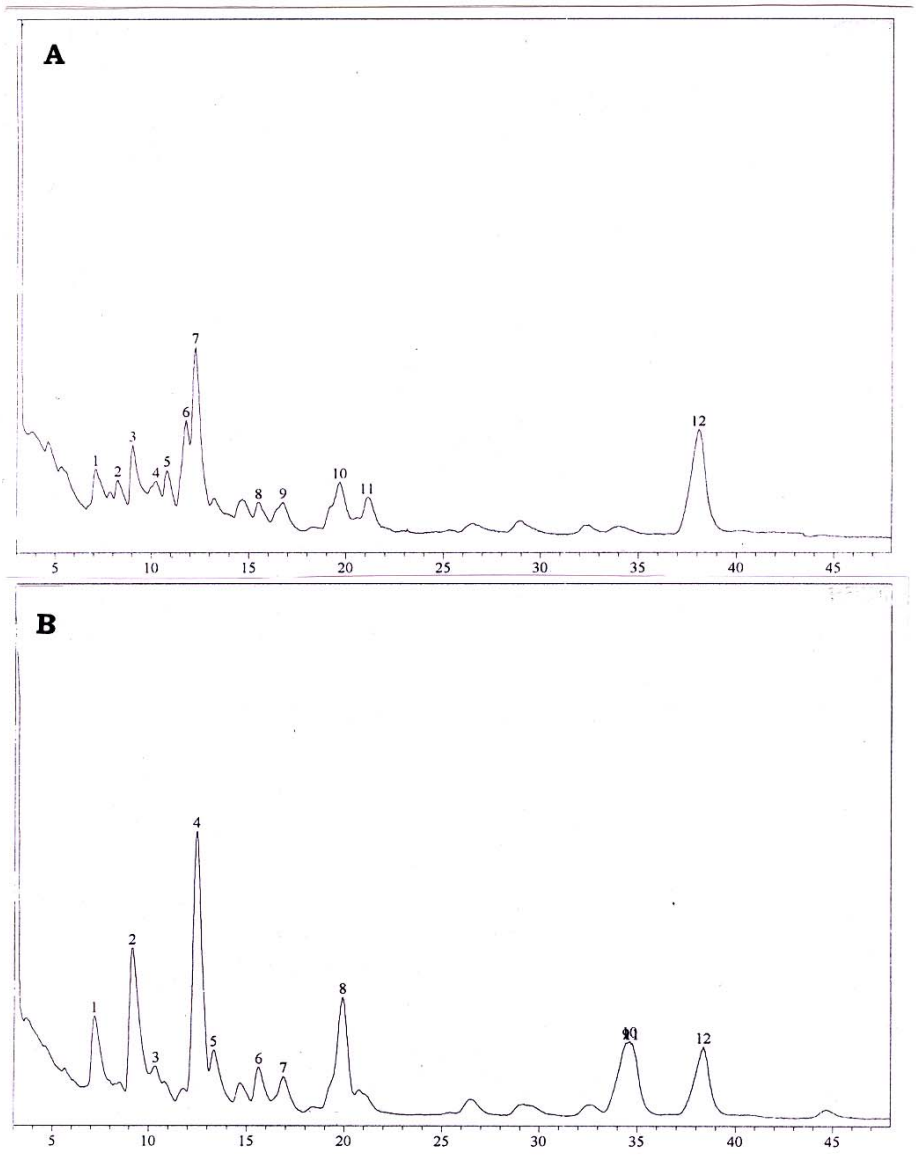

Figure 3.8.7
GC profile of permethylated hemicellulose fractions IV (A) and V (B) of unripe mango

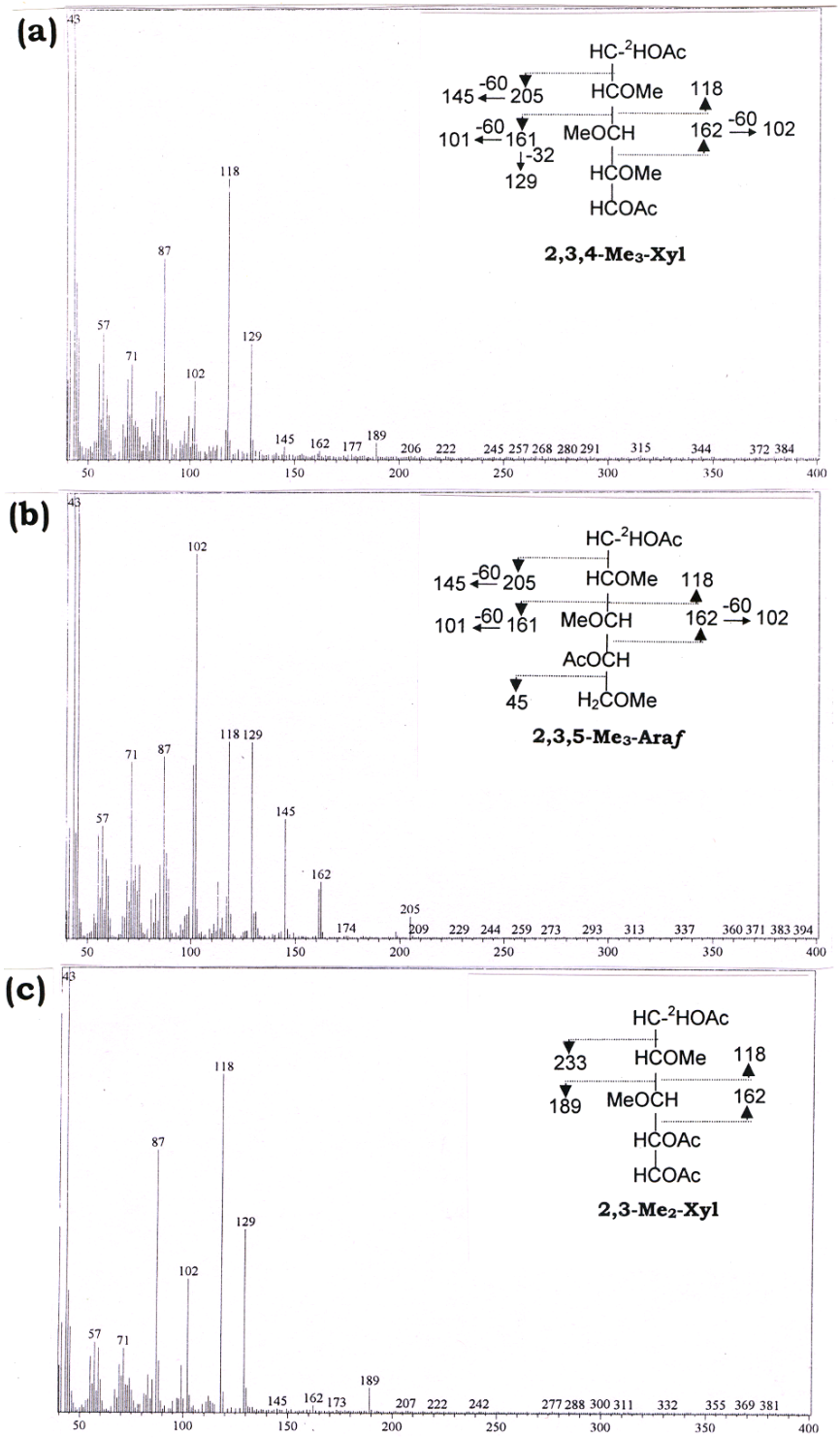

Figure 3.8.8
Mass spectra and fragmentation pattern of permethylated alditol acetates (a) 2,3,4-Xyl; (b) 2,3,5-Ara*f*; (c) 2,3-Xyl

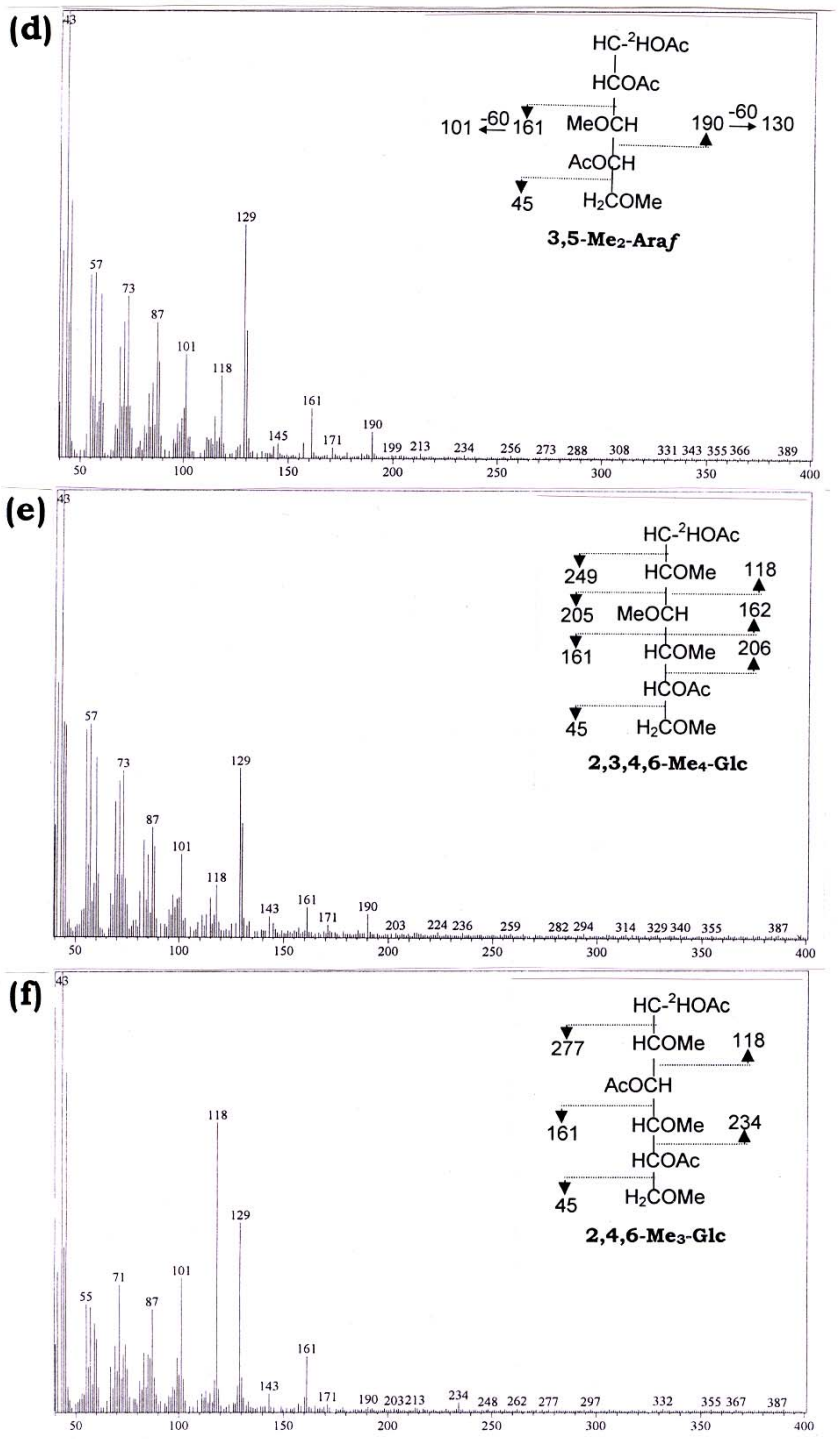

Figure 3.8.8 (Contd.)
Mass spectra and fragmentation pattern of permethylated alditol acetates (d) 3,5-Ara*f*; (e) 2,3,4,6,-Glc (f) 2,4,6-Glc

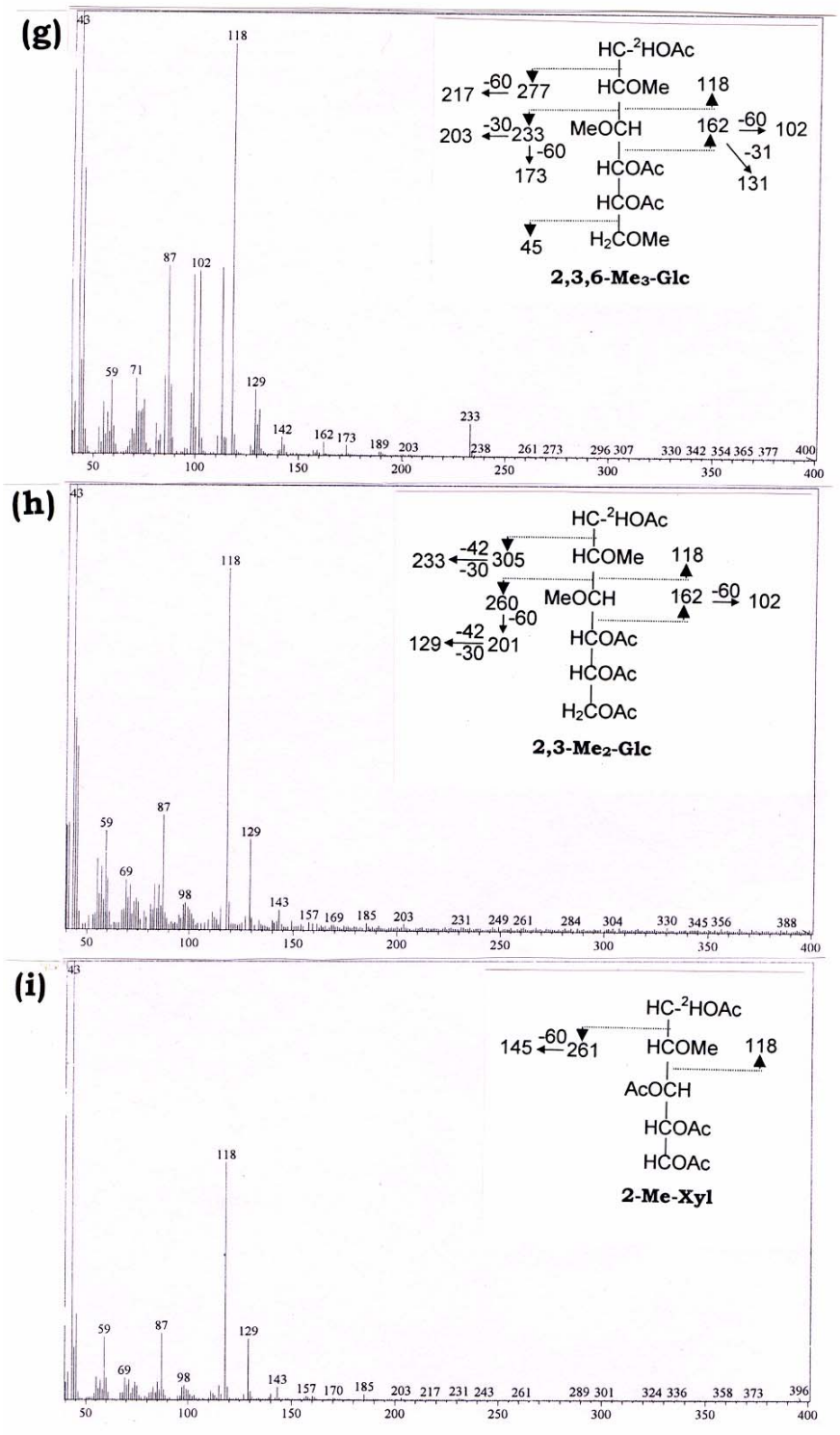

Figure 3.8.8 (Contd.)
Mass spectra and fragmentation pattern of permethylated alditol acetates (g) 2,3,6-Glc; (h) 2,3-Glc; (i) 2-Xyl

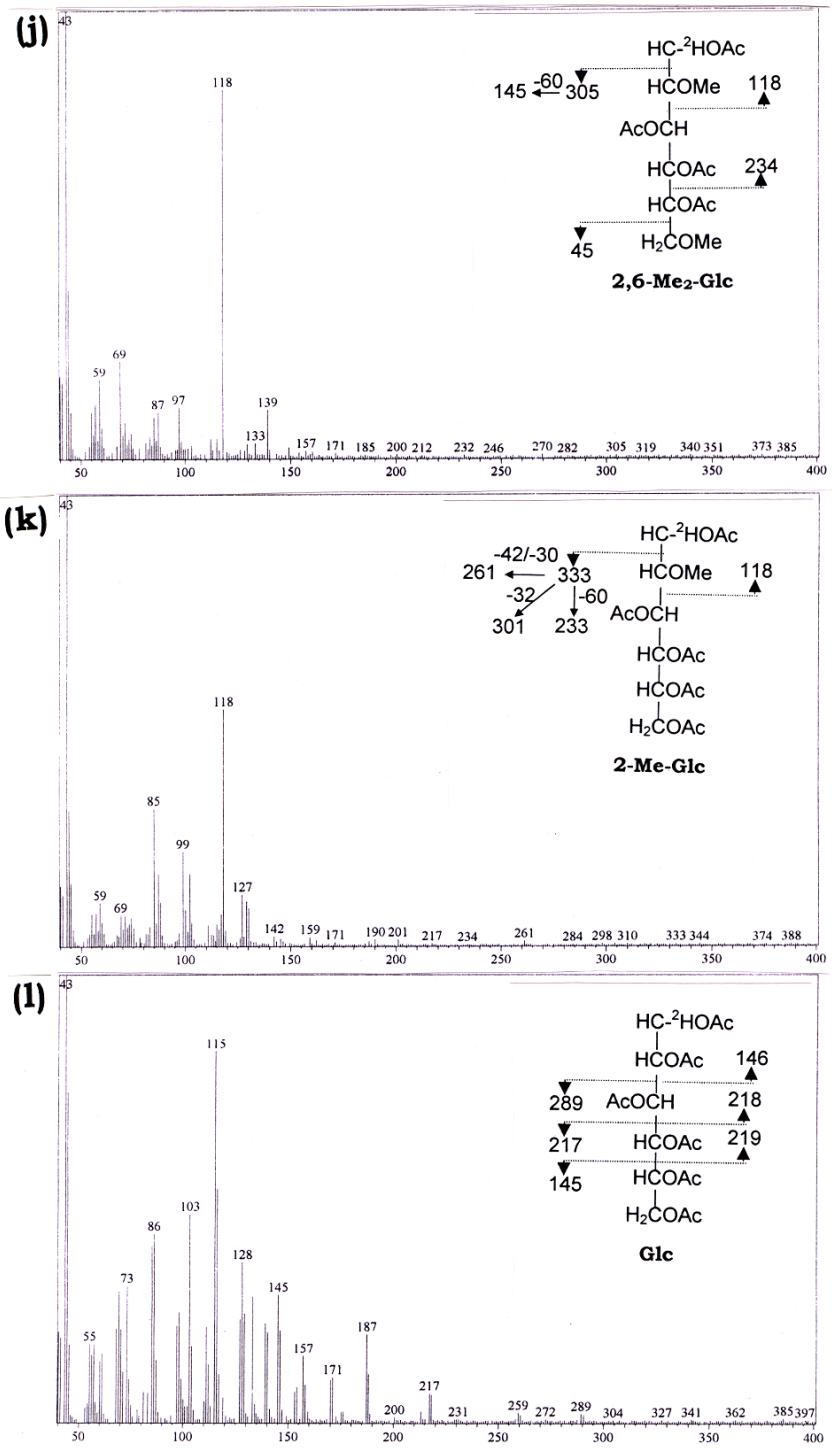

Figure 3.8.8 (Contd.)
Mass spectra and fragmentation pattern of permethylated alditol acetates (j) 2,6-Glc; (k) 2-Glc & (l) Glucitol

Table 3.8.3
O-Methyl ethers derived from permethylated major hemicellulose fractions IV and V from unripe mango

Monosaccharide	O-methyl ether	Mode of linkage	Relative mole %		Diagnostic mass fragments (m/Z)
			Fr. IV	Fr. V	
Ara	2,3,5-Me_3	Ara*f* (1→	2.3	2.0	43, 45, 118, 161, 162, 205
	3,5-Me_2	→2) Ara*f* (1→	1.0	-	43, 45, 101, 130, 129, 161, 190
Xyl	2,3,4-Me_3	Xyl*p* (1→	2.3	1.23	101, 102, 118, 129, 145, 161, 162, 205
	2,3-Me_2	→4) Xyl*p*(1→	5.0	3.0	118, 162, 189, 233
	2-Me	→3,4) Xyl*p*(1→	4.3	-	118, 201, 261
Glc	2,3,4,6-Me_4	Glc*p* (1→	-	1.0	43, 45, 101, 118, 129, 161, 162, 205, 249
	2,4,6-Me_3	→3) Glc*p*(1→	-	1.3	43, 45, 101, 118, 129, 143, 161, 203, 234
	2,3,6-Me_3	→4) Glc*p*(1→	10.0	6.0	43, 45, 118, 131, 162, 173, 203, 233, 277
	2,6-Me_2	→3,4) Glc*p*(1→	3.0	-	43, 45, 118, 139, 145, 234, 305
	2,3-Me_2	→4,6) Glc*p*(1→	10.0	0.5	43, 118, 129, 162, 233, 261, 305
	2-Me	→3,4,6) Glc*p*(1→	-	2.0	43, 118, 173, 261, 301, 333
	-	→2,3,4,6) Glc*p*(1→	2.41	6.1	145, 146, 217, 218, 289, 290

The FT-IR spectra of the purified polysaccharide fractions (Fig. 3.8.9 A and B) in the frequency range of 400-4000 cm^{-1} showed absorbances characteristic of neutral polysaccharides. The spectra showed absorption at 3401 cm^{-1} (indicative of free OH groups), and 1641 cm^{-1} (due to carboxylate functional group). The absorbance at ~1240 cm^{-1} is an indication of the presence of acetyl group, as reported by Mathlouthi and Koenig (1986). The absorbance at ~890 cm^{-1} was indicative of β-configuration. Intense peak at 1047 cm^{-1} may correspond to arabinan side chain as reported (Kacurakova *et al.*, 2000).

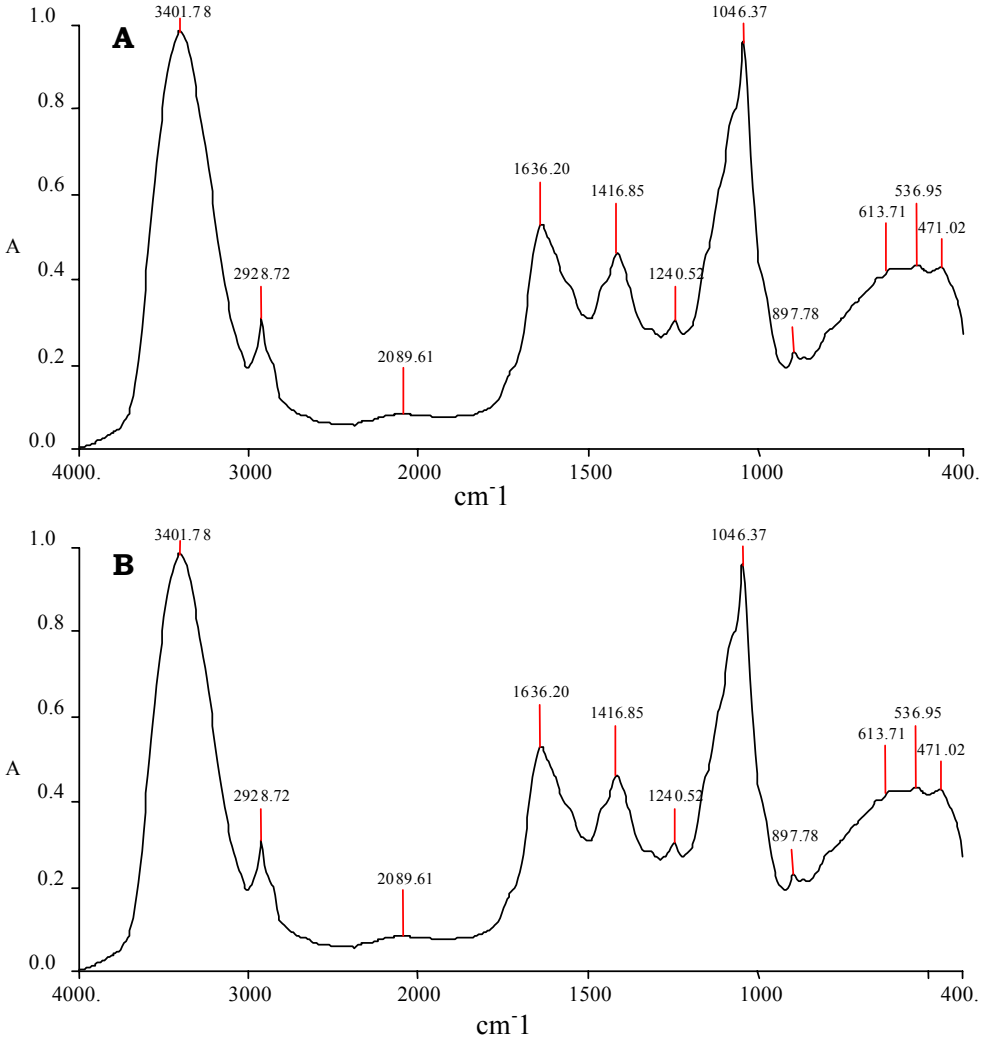

Figure 3.8.9
FTIR spectra of the hemicellulose fractions IV (A) and V (B)

Conclusions

Mango fruit shows evidence of modification of both pectic and hemicellulosic polymers during ripening, as do many other species. However the exceptionally rapid softening allowed a clear delineation of cell wall disassembly events associated with unripe and ripe stages of softening that had not been apparent in fruit that undergo more gradual and subtle textural changes. This investigation has suggested that modification of tightly bound hemicelluloses, specifically, xyloglucan may represent one of the major cell wall polysaccharides contributing for softening phenomenon.

Chapter **4**

Carbohydrate hydrolases in ripening mango

Section 1

Enzymes involved in carbohydrate hydrolysis *in vivo*

Introduction

Fruit softening/ripening is a complex process involving major transitions in fruit development and metabolism. The apparent changes in molecular size of cell wall polymers that accompany fruit ripening implicate the action of enzymes degrading specific cell wall components (Hulme, 1970). The polysaccharide network contains bonds that are susceptible to a variety of hydrolytic enzymes. Carbohydrate hydrolases can be broadly classified into glycanases and glycosidases. By definition, glycanases act on large polymers while glycosidases act on small oligomers consisting of upto 10-12 residues or monomeric glycosides (Fry, 1995). These oligomers may be present as side chains attached to glycoproteins or to other macromolecules. A wide range of cell wall hydrolases has been identified in fruit tissues (Huber, 1983b; Brady, 1987; Tucker and Grierson, 1987; Fischer and Bennet, 1991; Fry, 1995). Most of these enzymes increase in activity during ripening, showing an activity peak at climacteric stage. They are known to catalyze cell wall disassembly by acting on pectins, cellulose, and hemicelluloses. Among these enzymes, pectic enzymes are the one most implicated in fruit softening. The best-characterized pectin degrading enzymes are polygalacturonase (PG), pectate lyase, pectin methyl esterase (PME) and β-galactosidase. PME acts on the carboxyl ester bonds of methylated pectin and demethylates them to pectic acids, which is the substrate for other glycanases. PG hydrolyses the glycosidic bonds between the D-galacturonic acid residues in pectic acids. β-Galactosidase also contributes to loss in molecular weight of pectic polymers by cleaving neutral side chain residues (De Veau, 1993). PME activity has been reported for a number of fruits like banana, papaya, orange, apple, tomato, avocado, guava, strawberry and mango (Hultin and Levine, 1964; El-Zoghbi, 1994; Roe and Bruemmer, 1981; Selvaraj and Kumar, 1989; Aina and Oladonjoye, 1993). Activity of mango PME was shown to decrease (Roe and Bruemmer, 1981; El-Zoghbi, 1994; Prabha *et al.,* 2000) or

increase (Selvaraj and Kumar, 1989; Aina and Oladonjoye, 1993) or remain constant (Ashraf *et al.,* 1981) during ripening.

PG and β-galactosidase are more frequently reported in ripening fruits like tomato, banana, strawberry, pears, peach, avocado and other fruits (Pressy and Avants, 1973; Pathak and Sanwal, 1998; Lang and Dornenburg, 2000; De Veau, 1993; Ross *et al.,* 1993; Ranwala *et al.,* 1992; Dick *et al.,* 1990; Pressy, 1983). Galactosidase/galactanase enzymes were found to be associated with a number of ripening fruits like kiwi, apple and tomato (Ross *et al.,* 1993; Ross *et al.,* 1994; Carey *et al.,* 1995). However, glycanases like galactanase and arabinanase have not been well documented, especially in fruits. Interestingly, these two enzymes were found to be very prominent in mango fruit, which also correlated with the loss of galactose and arabinose from the pectin fraction at the ripe stage. But little is known about the enhancement of cellulase activity with reference to fruit softening except for reports in tomato (Hobson, 1968), avocado (Pesis *et al.,* 1978) and pears (Yamaki and Matsuda, 1977), or about the relationship between fruit ripening and hemicellulose degrading enzymes. Pharr *et al.* (1976) showed that glycosidase activities either declined or remained constant during development and ripening in tomato fruit. PG and cellulase activities in Japanese pear were mainly related to softening and β-galactosidase, partially degrading the hemicellulose component was related to tissue breakdown at over-ripening. Moreover some pear varieties showed physiological disorders such as water core (Yamaki *et al.,* 1977), mealy breakdown or pithiness with ripening. These phenomena suggested the importance of not only pectic enzymes but also hemicellulases as fruit ripens. Yamaki and Kakiuchi (1979) in Japanese pears fruit showed increased activities of xylanase, arabinanase, mannanase at the climacteric stage of

ripening which were localized both in soluble (the former) and bound (the latter) forms. They also showed increased activities of β-xylosidase and β-glucosidase during ripening.

Downward shift in the molecular weights of pectins during ripening of many fruits occur due to the action of PG and other cell-wall degrading enzymes. In *in vitro* condition, PG was found to degrade the cell-wall polymers from tomato and many other fruits, thus decreasing the molecular weight considerably (Themmen *et al.,* 1982; Wallner and Bloom, 1977). Water soluble polyuronides of strawberry released galacturonic acid and small oligomers, when treated with exoPG (Nogata *et al.,* 1993).

Roe and Brummer (1981) reported increased activity of cellulase as the flesh softened in the ripening mango. Similar trend was observed by Selvaraj and kumar (1989) and Abu-Sarra and Abu-Goukh (1992) for different varieties of mango and also in avocado fruit (Awad and Yang, 1978). Activities of mannanase, galactanase and arabinanase were high in mango whereas xylanase activity was hardly detectable. Among glycosidases α-mannosidase followed by β-galactosidase were most prominent enzymes in ripening mango (Prabha *et al.*, 2000), tomato (Watkins *et al.*, 1988) and in papaya seeds (Ohtani and Misaki, 1983). Increased activity of β-(1,3)-glucanase and β-endo mannanase was observed in ripening tomato (Wallner and Walker, 1974; Pressey, 1989) and α-mannosidase in bell pepper (Priya Sethu and Prabha, 1997) and tomato (Suvarnalatha and Prabha, 1999).

In the present investigation enzymes involved in the cell wall degradation of mango fruit pulp were assayed at different stages of ripening. Attention was focused on hydrolases that attack the

structural carbohydrates of the wall. The entire range of carbohydrate hydrolases were screened for their activities during ripening. Among glycanases β-endo mannanase was found to be the most active enzyme in mango during ripening. The choice glycosidase was α-mannosidase as it was involved in mannan hydrolysis *in vivo*. In addition, an attempt was made to mimic the *in vivo* hydrolysis of carbohydrate polymers with endogenous substrates and enzymes.

Results and Discussion

Activity profiles of carbohydrate hydrolases in mango during ripening

The climacteric peak of mango fruit was seen around 8 days after harvest and ready-to-eat ripe stage by 12th day, which is in accordance with published report (Krishnamurthy *et al.,* 1971). The entire range of carbohydrate hydrolases was monitored (Fig. 4.1.1) at different stages of mango ripening. Generally, all the hydrolases showed increased activity during ripening, most of them showing a peak in activity around climacteric, while PME, an esterase showed a steady decrease in activity. In general, during ripening the rise in enzyme activity results in increased charge density by diminishing the degree of esterification and/or decreasing the molecular weight (Jimenez *et al.,* 2001). In mango, the increase in pH (3.4 to 6.0) during ripening (Lazan *et al.,* 1986) may be a factor influencing the enzyme activities.

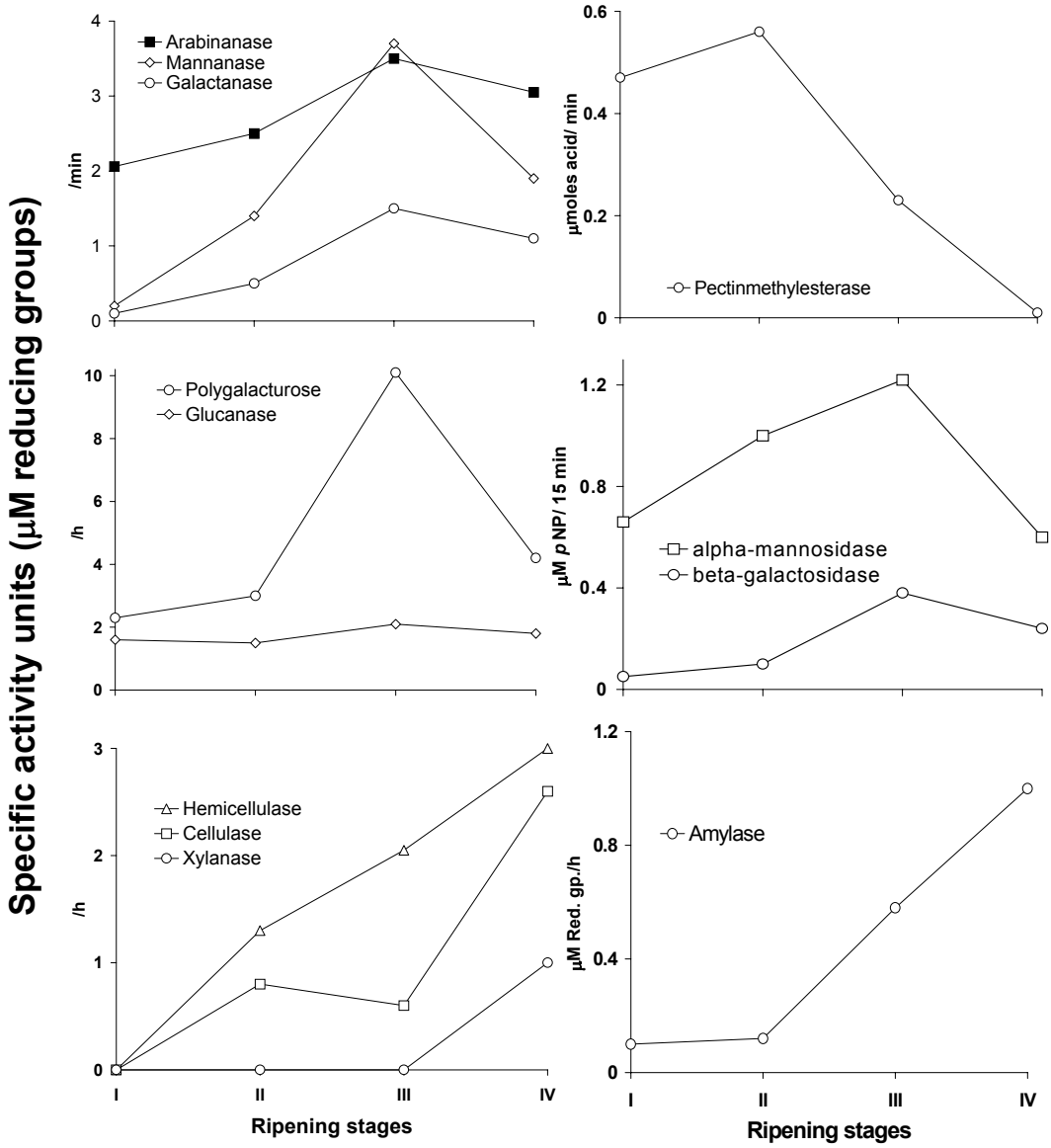

Figure 4.1.1

Activity profiles of carbohydrate hydrolases in ripening mango

Among glycanases, mannanase (with highest activity), galactanase and arabinan degrading enzymes were particularly high in mango while xylanase was very low (Table 4.1.1). High activities of galactanase and arabinanase, which is known to degrade galactan- and arabinan-type polysaccharides, correlated with a

significant loss of the corresponding sugar residues (galactose and arabinose) from the polymeric fractions. Enhanced β-endomannanase activity during ripening was shown in tomato fruit, tomato seeds and in Japanese pear fruit (Pressy, 1989; Nonogaki and Morohashi, 1996; Yamaki and Kakiuchi, 1979).

Table 4.1.1

Enzyme activity units of some glycanases and glycosidases in mango pulp at climacteric stage

Glycanases	Sp. Activity (μM reducing group/h/mg protein	Glycosidases	μM *p*NP released per 15 min/g AIP
β-Endomannnase	228	α-Mannosidase	130
Arabinanase	216	α-Galactosidase	37
Galactanase	96	β-Galactosidase	28
Glucanase	3	β-Glucosaminisidase	26
Hemicellulase	3	β-Glucosidase	16
Cellulase	2.6	β-Galactoseaminisidase	10
Amylase	1	α-Glucosidase	9
Polygalacturonase (μM GalA eq/h)	2.2	α-Fucosidase	5
Pectin methyl esterase (μM *p*NP/min)	0.55	β-Xylosidase	4
Xylanase	0.25		

As for pectic enzyme, there was an inverse correlation between PG and PME activity, as the PG activity increased the PME activity

decreased. PME makes the pectin substrate amenable for PG action. The enhanced activity of PME in the initial stage of ripening is perhaps required for preparing the substrates (i.e. demethylating pectins to pectic acid) for subsequent action by PG. Decreased activity of PME during ripening was shown in banana, apple, tomato, guava, date and strawberry (Hultin and Levine, 1964; El-zoghbi, 1994). A similar observation was reported for mango cv (Roe and Bruemmer, 1981; El-zoghbi, 1994). Total PG showed an increased activity reaching a maximum at the post climacteric stage of ripening. PG in 'Alphonso' mango increased upto half-ripe stage and declined thereafter (Selvaraj and Kumar, 1989). PG activity was barely detected in unripe fruits (Hobson, 1981), but slight activity was observed here. Similar trend of increase in PG activity was reported in fruits like tomato, banana, papaya, pear, peach, kiwi, nectarine, mango and African mango (Crookes and Grierson, 1983; Brownleader, *et al.*, 1999; Pathak and Sanwal, 1998; Selvaraj and Kumar, 1989). In climacteric fruits, the rapid synthesis of PG activity coincides with considerable textural alteration (loss of firmness) during ripeing (Pressy, 1986a; Roe and Bruemmer, 1981). Part of this increase may probably be due to the *de novo* synthesis of PG (Lazan *et al.,* 1986). The rise in the PG activity coincides with the conversion of pectic polysaccharides to water-soluble galacturonides, observed earlier (Chapter 3, Section 1 and 2).

Cellulase, hemicellulase and amylase showed a steady increase in activity, while laminarinase (β-1,3 glucanase) exhibited a activity peak around climacteric stage. A similar trend of increased activities of these enzymes was reported in banana (Prabha and Bhagyalakshmi, 1998). Laminarinase activity increased in tomato during ripening (Wallner and Walker, 1975; Selvaraj and Kumar, 1989), whereas increased cellulase activity was reported in different mango cultivars (Abu-Sarra and Abu-Goukh, 1992) and other fruits (Awad and Yang, 1979).

Among glycosidases screened, α-mannosidase activity was highest followed by α and β-galactosidase, β-glucosaminidase and β-glucosidase activities (Table 4.1.1). Increased activity of α-mannosidase has also been reported in other fruits like tomato, bell pepper, pineapple and papaya seeds (Suvarnalatha and Prabha, 1999; Priya Sethu and Prabha, 1997; Nakagawa and Takahashi, 1977; Ohtani and Misaki, 1983). β-Galactosidase activity also increased during ripening and showed an activity peak at the post-climacteric stage, as also reported in fruits like apple, apricot, plum, peach and muskmelon (Wallner, 1978; Bouranis and Niavis, 1992; De Veau, 1993). β-Galactosidase was the second major glycosidase at the climacteric stage of ripening mango fruit. In avocado mesocarp, despite low PG activity, the high *in vivo* pectin degradation was attributed to β-galactosidase activity (De Veau, 1993). In persimmon fruit PG activity was almost absent, while the pectin solubilization was high which was attributed to certain other enzymes (Cutillas-Iturralde *et al.,* 1993). Loss of galactosyl residues during ripening could occur independently of PG activity, which might involve other classes of enzymes like β-galactosidase and galactanase (Ali *et al.,* 1995; Carrington *et al.,* 1993; Carey *et al.,* 1995). In capsicum and tomato, the major glycosidase was β-hexoseaminidase followed by α-galactosidase and α-mannosidase (Table 4.1.2). But the total enzyme units for some of these glycosidases were much higher in tomato and capsicum, when compared to mango, banana and papaya. These observations clearly showed fruit tissue specificity in some of these enzymes.

Table 4.1.2

Activities of some major glycosidases in various ripening fruit systems

Enzymes	Mango	Banana	Papaya	Capsicum	Tomato
α-Mannosidase	130	450	224	451	604
α-Galactosidase	37	41	312	611	708
β-Galactosidase	28	320	518	263	389
β-Glucosaminidase	26	93	450	950	1047
β-Glucosidase	16	45	141	59	146
α-Glucosidase	9	21	13	6	13

In mango, it was found that all these carbohydrases are related to softening of fruit pulp during ripening. Since rhamnogalacturonans are the major EDTA soluble pectic polysaccharides of mango, the enzyme rhamnogalacturonase (RGase), which degrades these polymers (Schols *et al.,* 1990), may also be present in mango. The presence of RGase has been also shown in fruits such as bush butter (Missang *et al.,* 2001b). The PG may solubilize the backbone of rhamnogalacturonan-1 (RG-1), while the RGase depolymerizes into oligogalacturonides (Missang *et al.,* 2001b). It may be concluded that no single enzyme is responsible for the complete degradation of carbohydrate polysaccharides, instead a variety of cell-wall degrading enzymes are involved in the ultimate modification and dissolution of cell wall (Hobson, 1981).

In vivo and *in vitro* studies on carbohydrate polymers and their degradation

The cell wall polymers apparently undergo extensive ripening-related alterations. The apparent changes in molecular size of cell wall polymers that accompany fruit ripening implicate the action of

enzymes capable of degrading specific cell wall components. Depolymerization of various carbohydrate polymers during fruit ripening phenomenon is a natural process, which precisely dictates fruit texture, sweetness and succulence, thus contributing to its desirable mouth fell and taste. This is different in different fruits due to their inherent biochemical make up. *In vivo* carbohydrate hydrolysis in fruit ripening is a highly controlled process both in terms of quality and quantity, which is affected by a range of glycanases and glycosidases. In this context, it is of importance to know which of the carbohydrate polymers participate and contribute to textural softening in a given fruit and to what extent.

In the earlier experiment (Chapter 3, Section 2-5), a detailed IEC profile for the entire range of carbohydrate polymers of mango was obtained for both unripe and ripe fruit, which represented the *in vivo* hydrolysis. Attempts were made (*in vitro*) to mimic the *in vivo* degradation pattern, by subjecting the individual polymeric fractions to the action of (ripening related) enzymes and comparing the changes taking place. The purified major cold water soluble (CWS) (0.15 M $(NH_4)_2CO_3$ eluted fractions from unripe and ripe mango), hot water soluble (HWS) (0.15 M $(NH_4)_2CO_3$ and 0.15 M NaOH eluted fractions from unripe mango) and hemicellulose (0.10 M NaOH eluted fractions from unripe mango) polysaccharides were chosen and studied for their *in vitro* digestion by the purified enzyme. Interestingly the loss of neutral sugar from the fractions was significantly more prominent than the loss of galacturonic acid, which may be due to the presence of less amount of galacturonic acid in CWS (~25%) and HWS (~7%), and was very low in hemicellulose fractions (~3%). Further, a clear downward shift in the molecular weight of the water soluble as well as alkali soluble fractions was also observed (Chapter 3). The water-soluble

polysaccharides from unripe mango fruit are polydisperse in nature and so are not expected to give distinct separations on GPC. However, GPC revealed extensive depolymerization of carbohydrate polymers, as also reported for tomato pectins (Huber and Lee, 1986). Polyuronides from tomato and avocado were eluted through out the fractionation range of the gel, owing to extensive depolymerization and polydispersity (Huber and O'Donoghue, 1993). A similar observation was reported for total chelator soluble pectins during ripening of kiwi, melon and bush butter fruits (Missang *et al.,* 2001b; Redgwell *et al.,* 1997b; Rose *et al.,* 1998). Downward shift in molecular weights of polyuronides during ripening of tomato and avocado (Huber and O'Donoghue, 1993), and muskmelon fruit (Ranwala *et al.,* 1992) was also reported. However, tomato polyuronides showed less rapid and less extensive downward shift than those of avocado indicating that though this shift is a general phenomenon during fruit ripening, it varies between species. Decrease in the proportion of large molecular weight polymers has also been reported for persimmon and peach fruit chelator-soluble pectins (Cutillas-Iturralde *et al.,* 1993; Hegde and Maness, 1998). Thus, the *in vivo* results could be mimicked to some extent in the *in vitro* experiments. The *in vitro* study on carbohydrate hydrolysis was followed by incubating the purified substrate with the enzyme α-mannosidase (enzyme preparation from the stage III). *In vitro* degradation was performed using phosphate buffer (pH 6.0). The activity on endogenous substrates was almost negligible for water-soluble fractions (CWS and HWS) whereas slight activity was observed in hemicellulose fraction and also was more active on mannose rich fractions (neutral polysaccharides) (Chapter 4, Section 3). This indicates that the enzyme is substrate specific.

Section 2

In situ mannan hydrolysis and the related hydrolases: a comparison with banana

Introduction

Fruit softening during ripening is thoroughly understood in tomato fruit where it was possible to obtain extended shelf life and firmer tomatoes by suppressing polygalacturonase expression, its target enzyme. In avocado, cellulase is implicated in softening. While looking into the textural softening during ripening of mango, it was noted that cellulose and pectin (among cell wall polymers) and glucan and mannan (among cellular polymers) underwent significant solubilization *in vivo*. This study pertains specifically to *in vivo* mannan solubilization in mango and the related enzymes.

In plant systems, mannans exist mainly in the β-configuration, either as hetero- or homo-polymers and are hydrolysed by glycanase like β-endo mannanase, which contributes to textural softening. The hydrolysis pattern was monitored by studying the nature of hydrolysis products obtained from various carbohydrate polymeric fractions, which were later fractionated, based on differential solubility followed by ion exchange and gel permeation chromatography.

If β-mannans form natural substrates for β-endomannanase, what are the natural substrates for the α-mannosidase in the plant system? Does α-mannosidase, being a major glycosidase in ripening fruits, has any ripening specific role? There are no reports of these enzymes and their possible functions in ripening fruits. Extensive studies carried out in our laboratory on α-mannosidase of several fruits revealed the existence of distinct isoforms. Some interesting

observations on β-endo mannanase and α-mannosidase in mango and banana are studied here. The results are discussed in the light of endogenous substrates in textural softening during ripening. These two enzymes have been reported in a few fruit systems (Priya Sethu *et al.*, 1996; Prabha *et al.,* 2000; Prabha and Bhagyalakshmi, 1998), but they are not studied in the context of fruit ripening. Surprisingly, they showed climacteric peak in activity during ripening (Priya Sethu and Prabha, 1997; Suvarnalatha and Prabha, 1999).

While studying the enzymes involved in textural softening in ripening mango, it was noted that mannanase, galactanase and arabinanase and α-mannosidase were particularly high in this fruit. Based on these observations, it was decided to focus our attention on *in situ* mannan hydrolysis by both endo-mannanase and mannosidase. No reports are available on mannan hydrolyzing enzymes in fruits except for a detailed study of mannanase in germinating tomato seeds (Still and Bradford, 1997) and α-mannosidase of capsicum and tomato fruits (Priya Sethu and Prabha, 1997; Suvarnalatha and Prabha, 1999).

Results and Discussion

The entire range of carbohydrate hydrolases (~20 of them) were screened for their activity profile during ripening, where generally there was a climacteric peak in their activity. There was a striking difference in the enzyme profiles between mango and banana. Glycanases like mannanase, arabinanase and galactanase were abundant in mango fruit, while these enzymes could hardly be detected in banana fruit. On the contrary, xylanase activity which was almost nil in mango fruit was the most active of all glycanases in

banana fruit. Among glycosidases, α-mannosidase was the most active enzyme in both the fruit systems followed by β-galactosidase.

To study the endogenous mannan solubilization, the insoluble carbohydrates of unripe and ripe mango and banana were fractionated and their carbohydrate composition was studied (Fig. 4.2.1 A and B). Considerable endogenous mannan hydrolysis at the ripe stage in hemicellulose, pectic and water-soluble fractions was observed. In general, the endogenous mannan hydrolysis was noted in all the three fractions of mango fruit (CWS, HWS and hemicellulose), while in banana, mannose was present only in the hemicellulosic fraction. Both mannanase and α-mannosidase, implicated in mannan solubilization, exhibited a peak in the activity around climacteric stage of ripening. It is interesting to note that mannanase and α-mannosidase showed significantly high activity (Chapter 4, Table 4.1.1).

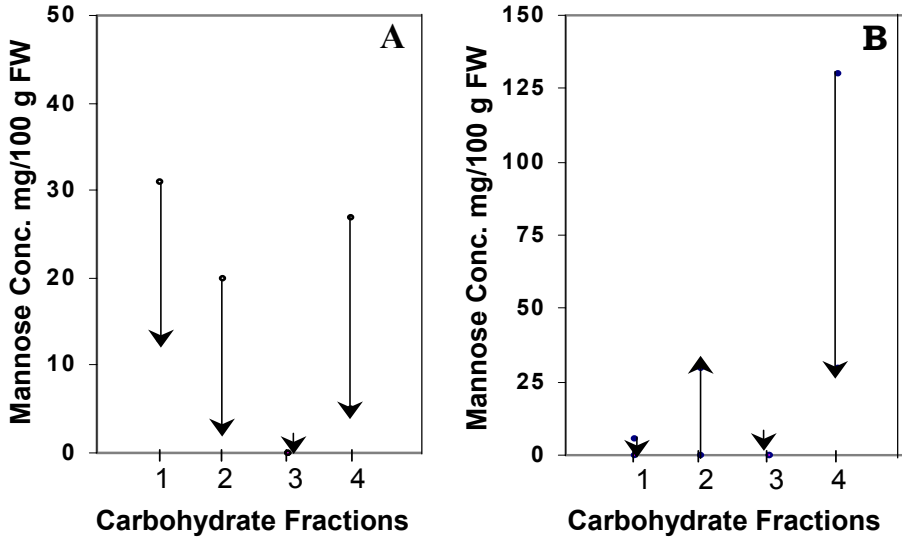

Figure 4.2.1
***In vivo* mannan hydrolysis in ripening mango (A) and banana (B)**

Arrows indicate change in mannose levels from Unripe to Ripe stage, in different carbohydrate polymeric fractions after hydrolysis.
1, CWS; 2, HWS; 3, pectic; 4, hemicellulose.

β-Endomannanase activity, abundant in mango fruit, showed a distinct climacteric peak in activity during ripening, whereas in banana fruit, its activity was very less and could only be detected in trace amounts at the climacteric stage (Fig. 4.2.2 A and B). As for α-mannosidase, it is the most major glycosidase in both mango and banana, showing a climacteric peak in activity during ripening (Fig. 4.2.2 A and B). But the total enzyme activity per unit tissue was three times higher in banana than in mango fruit.

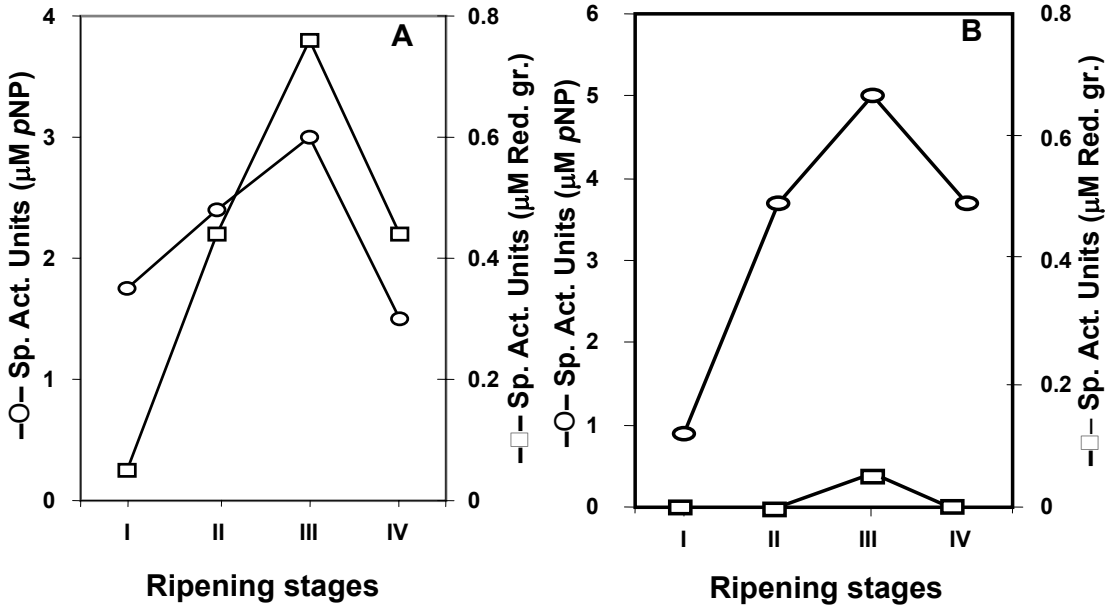

Figure 4.2.2
Activity profiles of mannan degrading enzymes in ripening mango (A); banana(B)
(--□-- β-endomannanase; --o-- α-mannosidase)

Both mannosidase as well as mannanase may be involved in mannan degradation (Pharr *et al.*, 1976). α-Mannosidase has a major role in hydrolyzing small molecular weight oligomers: viz., mannan, glucomannan and galactomannan oligosaccharides, with α-D-(1,2), α-D-(1,3), α-D-(1,4) and α-D-(1,6) linkages and also glycoproteins containing these residues, while β-endomannanase

acts internally on high molecular weight β-D-endomannans present either as homo or heteropolymers. The *in vivo* mannan could be due to the combined action of both these enzymes. It needs further examination to elucidate their individual contribution, particularly since these enzymes have been implicated in fruit softening during ripening in tomato (Pharr *et al.*, 1976; Watkins *et al.*, 1988).

Section 3

Purification and partial characterization of α-mannosidase

Introduction

α-Mannosidase is not well studied in fruit systems, except in capsicum, tomato and papaya. β-D-mannan type of polymers, though not well characterized and documented from fruit systems, are known to be widely present in other higher plant systems. But α-D-manno-oligomers, the substrates for α-mannosidase are not reported in higher plants. Whether such endogenous substrates for α-mannosidase exist in fruits is not known. If not, does α-mannosidase play a role in signal transduction (by way of de-gycosylation) or in membrane function since membranes are rich in mannose residues? These questions need to be addressed. It is possible that β-D-mannan type of polymers exist as endogenous substrates for β-endomannanase. Hence, the carbohydrate polymeric substrates undergoing major qualitative/quantitative changes from unripe to ripe stage of mango were isolated, purified and structurally characterized. Since both β-endomannanase and α-mannosidase are strongly expressed in mango, and show a climacteric peak in activity, it was felt desirable to look into their role in fruit ripening/textural softening.

Textural softening during ripening and storage is a central phenomenon directly affecting fruit shelf life and quality, which need to be controlled for effective preservation (Seymour *et al.*, 1993). Since fruits are highly perishable commodities, minimizing the loss due to excessive softening, spoilage and decay is the major aim, where the key target is manipulation of 'texture'. The aim of this study is to identify and elucidate the crucial targets in mango fruit

and explore the new targets involved in textural softening during ripening, at both substrate (carbohydrate) and enzyme levels (carbohydrate hydrolase).

Tissue softening during ripening of many fruits is the end result of enzymatic degradation of cell wall and cellular polysaccharides. Excessive textural softening is undesirable as the fruit is prone to infection, loss of fruit quality and decay. Unlike tomato fruit, which has been extensively studied for molecular biological aspects of fruit ripening and textural softening, mango and banana are gaining importance of late (Prabha and Bhagyalakshmi, 1998). Recently, PG enzyme was characterized from banana fruit where three isoforms of the enzyme were identified (Pathak and Sanwal, 1998). More recently, genes were isolated from banana fruit by Japanese researchers (Liu *et al.,* 1999). Three isoforms of pectin methyl esterase in banana fruit has been reported (Hultin and Levine, 1965). The carbohydrate metabolism related to textural softening in ripening banana fruit, has been reported recently from our laboratory (Prabha and Bhagyalakshmi, 1998).

α-Mannosidase has been used as a probe in the structural elucidation and functionality studies of biologically important glycoproteins and glycolipids containing α-linked D-mannose residues (Li and Li, 1997; Kobata, 1979). This enzyme has been reported from different sources, e.g. plants (Agrawal and Bahl, 1968; Li and Li, 1968), fungi (Bahl and Agrawal, 1969; Matta and Bahl, 1972), yeast (Yoshihisa *et al.,* 1988) and animal tissues (Okumura and Yamashina, 1988). The activity of α-mannosidase was reported to increase with ripeness in tomato (Pharr *et al.,* 1976; Watkins *et al.,* 1988; Suvarnalatha and Prabha, 1999), grape (Burns and Baldwin, 1994), muskmelon (Fils Lycaon and Buret, 1991), olive

(Heredia *et al.,* 1993), pear fruit (Ahmed and Labavitch, 1980), pineapple fruit (Nakagawa and Takahashi, 1977), watermelon (Nakagawa *et al.,* 1988) and capsicum (Priya Sethu and Prabha, 1997). This enzyme cleaves the short chains of oligomeric mannose residues (~8-10) present in oligosaccharides and glycoproteins. However, this enzyme has not been purified and characterized from ripening fruits. Mannans from plant sources contain linear chains of (1-4)-linked β-D-mannose residues (Aspinall, 1959) but the relationship between α-mannosidase activity and the consequent physiological function in fruits is not known. There is no natural substrate for this enzyme *in vivo*. The presence of high activity in ripening fruits prompted us to look into its properties in mango.

Results and Discussion

Among the entire range of carbohydrate hydrolases screened, α-mannosidase was found to be the major glycosidase and its activity increased during ripening with an activity peak at stage-III of ripening, and decreased thereafter as softening progressed (Chapter 4, Section 2). This increased activity of α-mannosidase was well correlated with loss of mannose during ripening (Chapter 3, Section 1-5). A similar observation was reported for tomato and capsicum, which accompanied fruit softening (Suvarnalatha and Prabha, 1999; Priya Sethu and Prabha, 1997). β-Endomannanase, the most abundant glycanase in ripening mango, was highly labile, and hence was very difficult to obtain in pure form for further characterization. Purification of α-mannosidase was performed with the enzyme collected at stage-III of ripening.

Purification of α-mannosidase from mango pulp: a comparison with banana α-mannosidase

α-Mannosidase, in both mango and banana showed a climacteric peak in activity during ripening. The total enzyme activity per unit tissue was three times higher in banana than in mango fruit, viz., 450 and 130 units per gram acetone dried powder of banana and mango, respectively. When subjected to IEC purification on DEAE-Sephadex A-50 two distinct peaks of activity, each designated as Isoform I and Isoform II, based on their order of elution from the column were observed. They were resolved by NaCl gradients, at 0.15 and 0.2 M for mango (Fig. 4.3.1), and 0.2 and 0.25 M for banana (Fig. 4.3.2). Isoforms having differences in their elution profile on DEAE-Sephadex A50 have been reported for many fruits including muskmelon (Ranwala *et al.,* 1992). Their relative ratio of activity being 80% and 20% for mango and 84% and 16% for banana isoforms.

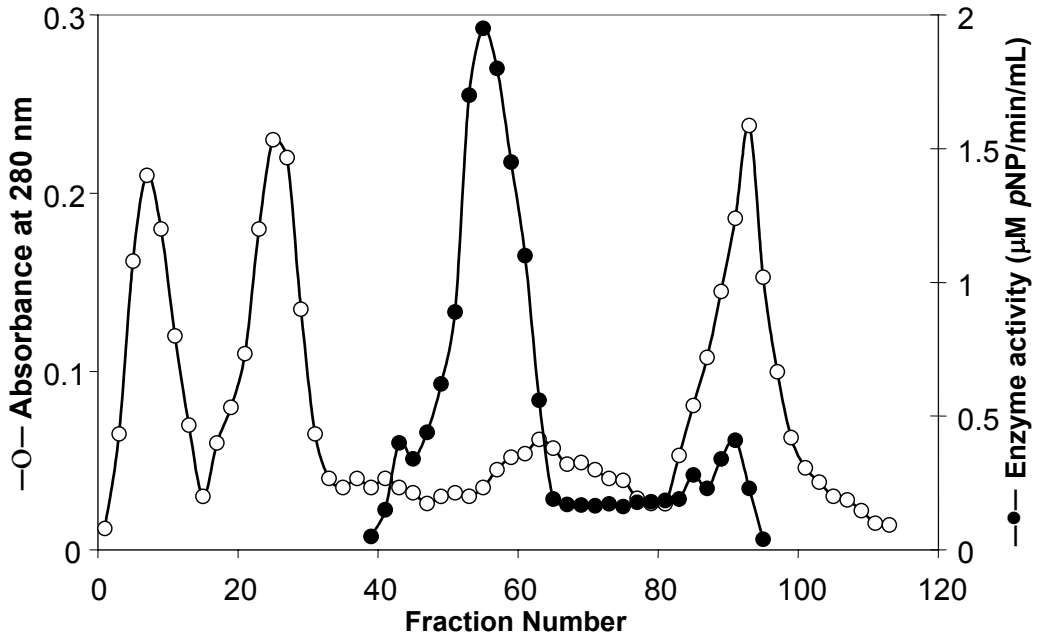

Figure 4.3.1
IEC profile of α-mannosidase on DEAE-Sephadex A-50 from mango

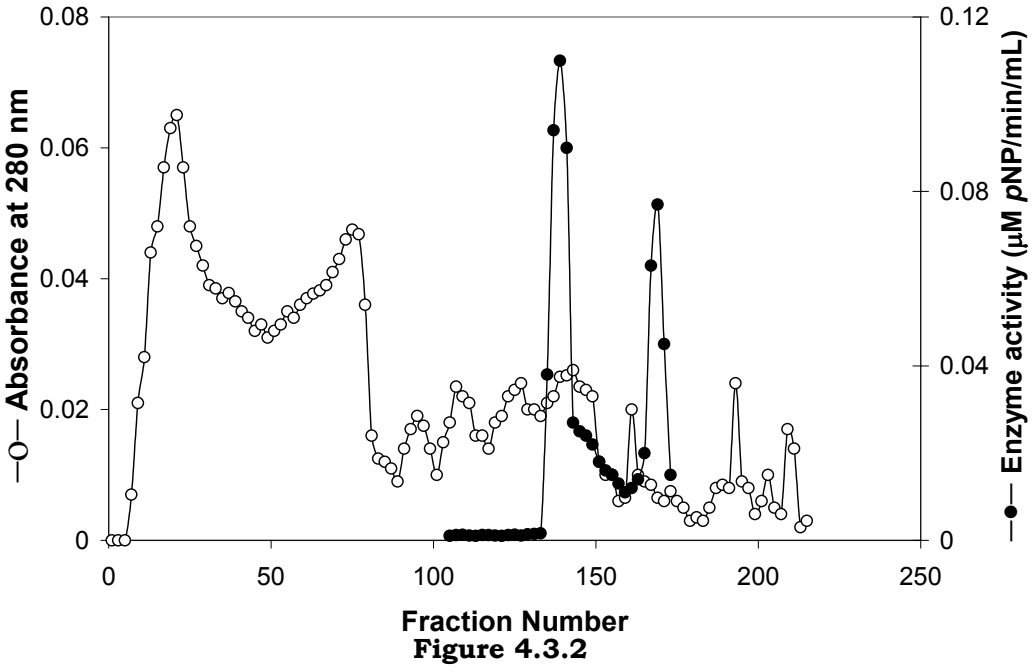

Figure 4.3.2
IEC profile of α-mannosidase on DEAE-Sephadex A-50 from banana

The two isoforms were again distinctly separable on GPC with Sephadex G-200 (Fig. 4.3.3 and 4.3.4). Based on the elution volume, their molecular weights were found to be 75 and 43 kDa, respectively for Isoforms I and II. Multiple forms of α-mannosidase reported in some ripening fruits (Suvarnalatha and Prabha, 1999; Priya Sethu and Prabha, 1997), is attributed to the complex nature of side chains of mannans and their breakdown during ripening. The molecular weight for the two isoforms of mango α-mannosidase was almost similar to those of banana and tomato isoforms, and differed from that of capsicum. Electrophoretic profiles for α-mannosidase before and after purification are shown in Fig.4.3.5 (A to E). Mango pulp in general had a very week protein profile, whereas it was strong in banana. Post GPC fraction of isoforms I and II revealed a single band around molecular weights of ~75 and 43 kDa, respectively, when subjected to PAGE with SDS alone. The lack of other bands suggests that the purified α-mannosidase is almost homogeneous.

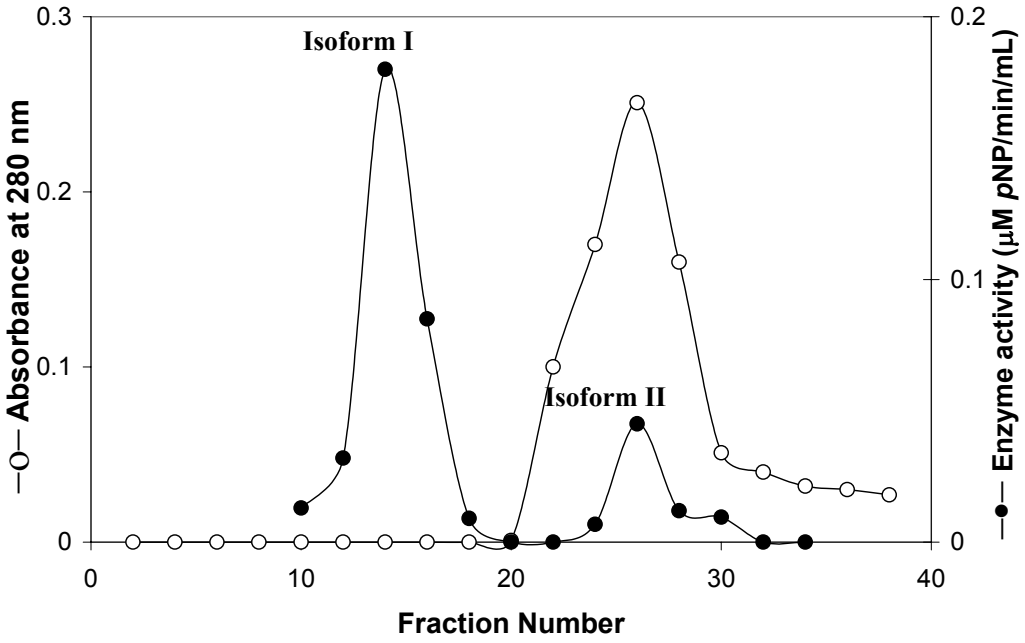

Figure 4.3.3
GPC profile of α-mannosidase isoforms from mango on Sephadex G-200

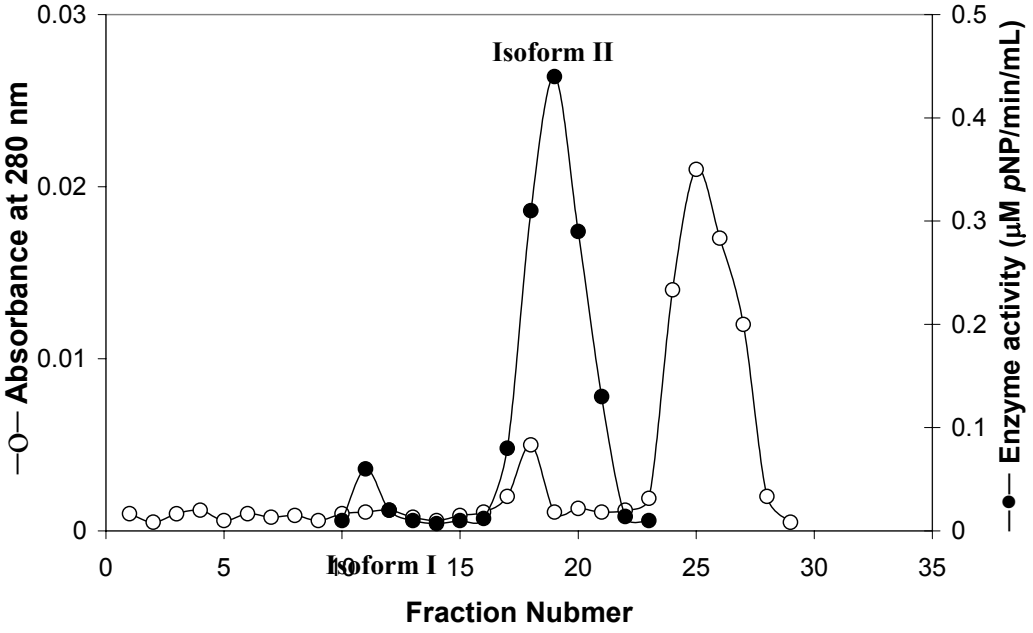

Figure 4.3.4
GPC profile of α-mannosidase isoforms from banana on Sephadex G-200

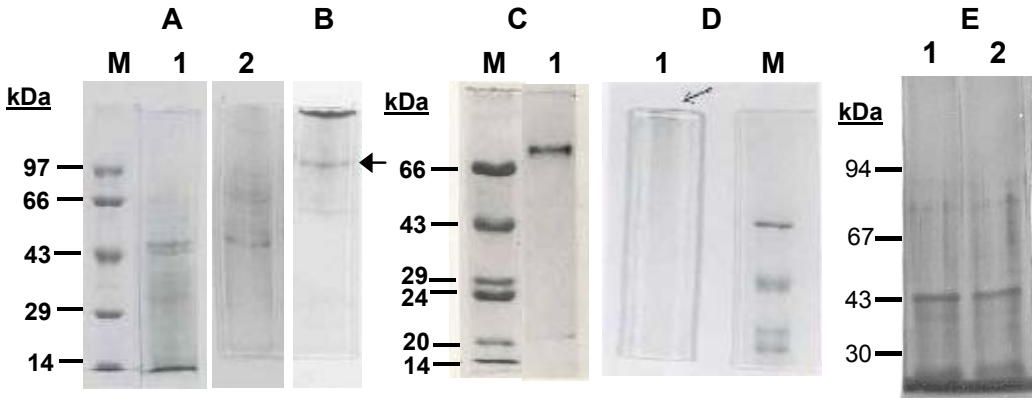

Figure 4.3.5
Gelelectrophoretic analysis α-mannosidase isoforms from mango

(A) SDS-PAGE (12% gel): M, Mol. wt. markers; *Lane 1 & 2*, mango crude extract under reducing (with β-mercaptoethanol) and non-reducing (without β-mercaptoethanol) conditions, respectively.
(B) SDS-PAGE (12% gel) of post-IEC fraction of isoform I.
(C) SDS-PAGE (12% gel): M, Mol. wt. markers; *Lane 1,* post-GPC fraction of isoform I.
(D) Native-PAGE (8% gel): M, Mol. wt. markers; *Lane 1,* GPC purified fraction (isoform I).
(E) SDS-PAGE (8% gel): *Lane 1*, post-IEC fraction of isoform II; *Lane 2,* post GPC fraction of isoform 2.

The entire purification profile of α-mannosidase of mango and banana is summarized in Tables 4.3.1 and 4.3.2. The specific activity of 1.03 for the crude extract increased to 10.06 and 1.81 upon IEC, which further increased to 36.43 and 66.0 upon GPC for isoforms I and II, respectively. The fold purification was 9.8/1.8 and 35.4/64.0 with recovery of 7 and 15%, respectively for isoforms I and II.

Table 4.3.1

Summary of purification of α-mannosidase from mango

Fractions	Total activity (U)	Total protein (mg)	Sp. Activity (U/mg protein)	Fold purification
Crude Enzyme	151.8	147.50	1.03	1.00
DEAE-Sephadex A-50				
Isoform I	15.7	1.56	10.06	9.76
Isoform II	5.0	2.76	1.81	1.75
Sephadex G-200				
Isoform I	10.2	0.28	36.43	35.37
Isoform II	2.0	0.03	66.0	64.0

1unit (U) = μM *p*-nitrophenol released/min

Table 4.3.2

Summary of purification of α-mannosidase from banana

Fractions	Total activity units	Specific activity (U/mg Protein)	Recovery (%)	Fold purification
Crude Extract	63.0	1.2	100	1.0
80% Amm. Sulphate ppt.	58.7	13.0	93	11.0
DEAE-Sephadex A-50	57.0	16.9	90	20.0
Sephadex G-200				
Mannosidase I	12.0	7.5	19	6.4
Mannosidase II	44.6	27.5	71	23.3

Enzymic properties of α-mannosidase isoforms

A comparison of the properties of α-mannosidase isoforms from mango and banana pulp is consolidated in Table 4.3.3. The pH optimum, 4.8 was same for both the isoforms, their temperature optimum being 65^0C and 75^0C, respectively for isoforms I and II. Their Km values for *p*NP-α-D-mannopyranoside were 0.7 and 1.4 mM, indicating a higher enzyme-substrate affinity for isoform II (the minor form).

Table 4.3.3

Properties of isoforms of α-mannosidase from mango in comparison with banana

Properties	Mango		Banana	
	Isoform I	**Isoform II**	**Isoform I**	**Isoform II**
Elution on IEC	0.15 M NaCl	0.2 M NaCl	0.2 M NaCl	0.25 M NaCl
Abundance	Major	Minor	Major	Minor
Km with *p*NP (mM)	1.40	0.70	2.7	0.3
pH optimum	4.8	4.8	5.8	5.8
Temperature optimum	75^0C	65^0C	65^0C	55^0C
Thermal stability for 15 min	75^0C	65^0C	65^0C.	55^0C
Native mol. weight (as per GPC)	~75,000 Da	~43,000 Da	~70,000 Da	~40,000 Da
Ability to degrade β-endomannan	No	No	Yes	Yes
Inhibition by				
Metal ions	Weak	Weak	Strong	Strong
Structural analogues	No	No	No	No

Among the metal ions tested for inhibitory action on the enzyme (Table 4.3.4), Mg^{2+}, Zn^{2+} and Hg^{2+} at 1 mM concentration exhibited about 40% inhibition of isoform II and the % inhibition was considerably lower for isoform I. There was approximately 20%

inhibition of isoform I by Cu^{2+}, while isoform II was not inhibited. Among the sugar epimers tested, mannose did not inhibit the enzyme indicating no feed back inhibition. Glucose and galactose also did not inhibit the isoforms. Both the isoforms lacked endomannanase activity. Various glycosides as *p*NP-substrates were tested to see the activity of isoforms I and II. Both the isoforms showed high substrate specificity with *p*NP-α-D-mannopyranoside, on other substrates tested showed no activity.

Table 4.3.4

Effect of various inhibitors on mango α-mannosidases I and II*

Type of Inhibitor	**% Inhibition over control**	
	Mannosidase I	**Mannosidase II**
Metal ions (1 mM conc.)		
Mn^{2+}	11.2	9.5
Mg^{2+}	19.4	36.1
Zn^{2+}	23.0	40.0
Hg^{2+}	20.6	43.0
Cu^{2+}	23.0	0.0
Fe^{2+}	20.0	7.8
EDTA (10 mM conc.)	54.0	53.0
Activity on structural analogues		
***p*NP-α-mannopyranoside**	+	+
***p*NP-β-mannopyranoside**	-	-
***p*NP-α and β-glucopyranoside**	-	-
***p*NP-α and β-galactopyranoside**	-	-

*Glucose, galactose and mannose (upto 50 mM) did not bring about any inhibition

α-Mannosidase in mango showed highest activity towards synthetic substrates but no natural substrate is available for this enzyme. The hydrolytic capabilities of this enzyme on α-D-mannose residues of some polysaccharides, such as D-galacto-D-mannan were also examined. The results showed that this enzyme could not hydrolyze the terminal α-D-mannose residues of these polysaccharides, probably because of their high molecular weights. Similar observations were reported for enzymes derived from tomato, papaya seeds, capsicum and pineapple (Suvarnalatha and Prabha, 1999; Othani and Misaki, 1983; Priya Sethu and Prabha, 1997; Nakagawa and Takahashi, 1977). As for the endogenous substrates for α-mannosidase of mango, only hemicelluloses were slightly hydrolyzed by both the isoforms (Table 4.3.5).

Table 4.3.5
Activity of α-mannosidase isoforms of mango on natural and endogenous substrates

Substrates	Activity (μM/h)	
	Isoform I	Isoform II
Natural substrates		
Galactomannan	+	+
Endogenous substrates		
CWS unripe [0.15 M $(NH_4)_2CO_3$]	21.04	21.04
CWS ripe [0.15 M $(NH_4)_2CO_3$]	16.10	21.04
CWS unripe [0.15 M $(NH_4)_2CO_3$] reduced	26.00	17.33
CWS ripe [0.15 M $(NH_4)_2CO_3$] reduced	17.33	16.10
HWS unripe [0.15 M $(NH_4)_2CO_3$]	8.66	14.85
HWS unripe (0.15 M NaOH)	33.41	49.50
Hemicellulose unripe (0.1 M NaOH)	32.20	42.10

In banana, the isoforms I and II had an optimum pH of 5.8, and optimum temperatures of 65^0C and 55^0C, respectively. They differed with respect to their km values with *p*NP-α-D-mannopyranoside as substrate. Isoform I and II had km

values of 2.7 and 0.3 mM, respectively. Isoform II, was found to be more active in degrading mannan and galactomannan. The effect of various inhibitors on the activity of the isozymes is presented in Table 4.3.6. Cu^{2+}, Fe^{2+} and Hg^{2+} inhibited both the isoforms to a large extent when compared to other divalent ions used. There was no inhibitory action by glucose and galactose, while mannose inhibited isoform I (20%) and isoform II (10%) indicating weak end product inhibition.

Table 4.3.6

Effect of various inhibitors on the α-mannosidase isoforms of banana

Inhibitors	% Inhibition over control					
	Isoform I			Isoform II		
	Inhibitor concentration			Inhibitor concentration		
	2 mM	1 mM	0.5 mM	2 mM	1 mM	0.5 mM
Ca^{2+}	54	44	-	2	2	-
Mn^{2+}	85	35	-	21	21	-
Mg^{2+}	51	31	-	21	21	-
Zn^{2+}	29	10	-	10	10	-
Hg^{2+}	100	3	39	92	92	51
Cu^{2+}	100	99	10	89	89	59
Fe^{2+}	7	3	-	9	9	-
EDTA (10mM)	28			32		
Structural analogues	50 mM	25 mM		50 mM	25 mM	
Glucose	5	0		2	-	
Galactose	2	2		8	6	
Mannose	12	11		23	22	
Mannan degradation	+			+*		

* more active hydrolysis of galactomannan in addition to mannan was observed in Isoform II

α-Mannosidase was found to be highly active at climacteric stage of mango, as also in capsicum (Priya Sethu and Prabha, 1997), banana (Prabha and Bhagyalakshmi, 1998), tomato (Suvarnalatha and Prabha, 1999) and papaya (unpublished). In mango, compared to other fruits tested, α-mannosidase activity was minimal, while β-endomannanase activity was highest (see Table 4.1.3). The α-mannosidase isoforms from capsicum and tomato (Priya Sethu and Prabha, 1997; Suvarnalatha and Prabha, 1999) showed differences in some of the properties, viz., α-mannosidase from capsicum was powerfully inhibited by Fe^{2+} and Cu^{2+}, while the isoforms from tomato and banana were inhibited strongly by Hg^{2+} and Cu^{2+}. In mango, none of the metal ions showed any significant inhibition. Further, the enzyme from banana degraded mannan and galactomannan and showed end product inhibition by mannose unlike the mannosidase of mango.

Mannosidase, an exo enzyme, has a major role in hydrolyzing small molecular weight oligomers containing mannose residues, while endomannanase acts internally on high molecular weight mannans, cutting them randomly (Snaith and Levvy, 1975). The *in vivo* mannan degradation found in ripening mango and banana could be due to the combined action of both these enzymes.

Chapter **5**

Induction of somatic embryos from explants of mango and expression of β-glucuronidase gene via *Agrobacterium tumefaciens* mediated transformation

Introduction

Mango, *Mangifera indica* L., is one of the most important fruit crops of the world. Its varietal improvement by conventional breeding is difficult because of its long life cycle, cross-pollination and heterozygosity. Plant cell and tissue culture as well as genetic engineering are important techniques for the crop improvement. However, development of an efficient protocol is the first step in utilizing the power and potential of this new technology. Micro-propagation of this crop, which leads to clones, is hindered by the rapid activation of oxidative enzymes during the excision of explants leading to the eventual death of excised tissues. Tree fruit breeding is very tedious, time consuming and also the probability of acquiring a desirable plant type is a matter of chance. Certain level of progress has been made in obtaining transgenic plants for variety 'Amrapali' from protoplast, nucellus, and young leaf explants with drawbacks such as very low frequency (Ara *et al.,* 2000; De Wald *et al.,* 1989a; Raghuvanshi and Srivastava, 1995).

Mango somatic embryogenesis *in vitro* was first reported by Litz *et al.*, (1982). The efficient regeneration of whole mango plant from somatic embryos (SEs) has not been possible due to some developmental abnormalities like rampant contamination and recalcitrance. Raghuvanshi and Srivastava (1995) reported the micro-propagation method for 'Amrapali' mango from leaf explants in which phenolics are leached into liquid medium in culture vessels on a shaker leading to extremely slow growth of shoots.

In mango, certain polyembryonic varieties were naturally endowed with *in vivo* multiple embryo formation, which means that the nucellar tissue from which natural embryos are formed is the most competent explant tissue for embryo

induction *in vitro*. Accordingly, the polyembryonic varieties would easily form SEs when nucellar tissues are cultured. In support of this, Litz *et al.,* (1982) have shown the potential of ovule culture to produce a large number of SEs from the nucellus. Later, they were able to stimulate callus, globular adventitious nucellar embryos on a medium containing 1-2 mg/L of 2,4-dichlorophenoxyacetic acid (2,4-D), where high frequency of SEs formed, particularly in a liquid medium (Litz *et al.,* 1984). Since most of the important mango cultivars in India and the United States are naturally monoembryonic, it is difficult to induce SEs from such lines. Nevertheless, this has also been achieved, where monoembryonic mango cultivars collected mainly from Florida were efficiently induced to produce SEs from nucellar explants (Litz, 1984). A major observation being that the modified MS basal medium (Murashige and Skoog, 1962), consisting of half-strength major salts, 2,4-D and glutamine was more effective than full-strength MS medium for culture initiation and maintenance in certain cultivars. Whereas, several other cultivars required cytokinin for vigorous growth and further organization (De Wald, 1987).

Though, high-frequency SE production could be obtained in suspension cultures (Litz *et al.,* 1984), the embryos failed to develop further to maturity in a normal manner. Numerous developmental anomalies, including polycotyledony, fasciation, absence of bipolarity, and formation of secondary somatic embryos from the hypocotyls were common. Precocious germination (Litz *et al.,* 1982) and progressive necrosis (Litz *et al.,* 1984) prevented the efficient recovery of mango plantlets. DeWald *et al.* (1989a) investigated the various parameters that influence the maintenance of embryogenic mango nucellar cultures, and listed the conditions that influenced SE production from the embryogenic cultures.

However, there is yet another prevalent problem in the maintenance of embryogenic cultures of mango, i.e., hyperhydricity occurring progressively. Hyperhydricity has been associated with water that is freely available in the plant growth medium (Aitken *et al.,* 1981) and the excessive uptake of water often resulting in erratic organogenesis (Pierik, 1988). Plant genotype, concentration of cytokinin and nitrogen content of the plant growth medium, culture vessel type and solidifying agent are all recognized to be important factors that influence

hyperhydricity in plant tissue cultures (Teasdale, 1987). According to Ziv (1991), the requirements for optimizing *in vitro* cultures, i.e., high relative humidity, high levels of nutrients, high concentrations of plant growth regulators and low light intensity, are the major causes of hyperhydricity. Hyperhydricity is particularly severe with mango SEs of cultivars that are highly embryogenic and that produce cotyledonary stage embryos rapidly and predictably following subculture from 2,4-D containing medium. Debergh *et al.* (1992) referred to hyperhydricity as an *in vitro* condition whereby changes in physiology are expressed in abnormal anatomy and morphology. Reversion of hyperhydricity was achieved by Monsalud *et al.* (1995) in two ways: 1) heart stage SEs (2-3 mm length) were partially dehydrated under controlled conditions at high relative humidity, and 2) by increasing the gelling agent (Gel-Gro) concentration of the plant growth medium.

Apart from growth regulators and water activity of the medium, nutrients are also known to contribute towards hyperhydricity in several species. Sucrose, one of the major nutrients, plays two possible roles in somatic embryogenesis: as an osmoticum that can stimulate and regulate morphogenesis (Litz, 1986b; Wetherell, 1984) and as a carbon source. Induction of somatic embryogenesis and the early stages of SE development often required moderate to high concentrations of sucrose (Ammirato, 1983). A requirement of 5 to 6% sucrose to maximize production of completely differentiated SEs is typical. Steward *et al.* (1975) also showed that high osmoticum levels prevented the formation of secondary SEs in carrot cultures, and Ammirato and Steward (1971) demonstrated that precocious germination of immature SEs could be inhibited by high osmotic levels.

The presence of germination inhibitors has been suggested as an important factor influencing SE development in certain species such as *Theobroma cacao* (Wang and Janick, 1984). Cytokinins have been demonstrated to stimulate normal SE maturation (Fujimura and Komamine, 1975), but particularly cotyledon development. Cytokinin (Kinetin) and auxin are important for proliferation and maintenance of mango embryogenic/proembryonic globular masses. Gross developmental abnormalities of mango SEs can be prevented to some degree by

careful manipulation of these growth regulators and other culture conditions during maintenance of putative embryogenic cultures.

Nucellus-derived plants are generally free of viruses and other disease-causing-microorganisms due to the absence of vascular connections between the surrounding maternal tissue and the nucellus (Button and Kochba, 1977). Some of the most devastating mango diseases, e.g., "de-cline" and "dieback", are caused by systemic fungal pathogens. Efficient recovery of monoembryonic mango plants from SEs therefore would eliminate the systemic diseases and facilitate storage and international exchange of germplasm. Most important, however, is the potential for using *in vitro* procedures, such as mutant selection and somaclonal variation for genetic improvement of perennial, tropical fruit trees such as mango. Because of the constant disease and the environmental stresses of the tropical environments, catastrophic losses occur frequently in clonally propagated crops. Due to the long generational cycles of mangos, conventional plant breeding has not been responsive to crop-threatening situations. Infact, little is known about mango genetics. Somaclonal variation has been derived from tissue cultures of other important crop species (Larkin and Scowcroft, 1981). Thus, the ability to regenerate the polyembryonic and monoembryonic mango cultivars from callus may result in an increased frequency of horticulturally useful somatic mutations within the most important cultivars.

Tissue culture protocols are most needed for any genetic improvement of a selected crop variety. In the present context of suppressing excessive post harvest softening, it is necessary to impart genetic characteristics that suppress rapid enzymatic *in vivo* fruit degradation as the ripening of most fruits involves cell wall degradation. Gene transfer offers the ability to introduce single new characteristics into a plant cultivar without altering any of its existing traits. The advantage is significant if the generation time of the crop is long. Mango tissue is relatively amenable to regeneration *in vitro* with several levels of success in somatic embryogenesis. *Agrobacterium*-mediated transformation was successful after co-cultivation of embryogenic mango culture (Mathews *et al.,* 1993). A prolonged

selection protocol was required to eliminate chimeral clumps, but the authors were able to obtain embryos that were resistant to kanamycin, and expressed the GUS gene that contained integrated copies of the T-DNA by Southern hybridization. Although it has a very long generation time, the prospects for gene transfer in mango seem quite good. There are a number of potential targets for gene transfers for mango, including improving fruit storage life, and resistance to pests and diseases. Certain earlier studies have shown a full-length c-DNA clone from mango fruit has homology to the rab1/YPT 3 classes of small GTPases. The corresponding mRNA is expressed in fruit, only during ripening. The likely involvement of this rab X protein in trafficking cell wall modifying enzymes through the trans-golgi network has been reported by Zainal *et al.* (1996). Similarly, the transformation of tomato with PG gene in antisense resulted in greatly reduced levels of PG mRNA and corresponding enzyme activity where a significant change in softening was detected (Smith *et al.,* 1988).

In most of the crops, a phenolic, which drives the *Agrobacterium* for infection and insertion of T-DNA, determines the amenability of a species for *Agrobacterium*-mediated transformation. Those species, which do not produce this phenolic compound, now recognized as acetosyringone, are seldom transformed. Thus, monocots are very difficult materials for genetic transformation, as they do not synthesize acetosyringone (Potrykus *et al*., 1990]. A detailed study indicated that acetosyringone and α-hydroxy acetosyringone, the two naturally occurring wound response phenolics, have been identified as signal molecules that induce the activation of 'vir' genes in *A. tumefaciens* (Bolten *et al.,* 1986; Machida *et al.,* 1986). Therefore, external application of this compound can increase *Agrobacterium*-mediated transformation frequencies. Accordingly, in *Arabidopsis,* 2 to 3% transformation was recorded without and 55 to 63% with the use of acetosyringone (Sheikholeslam and Weeks, 1987). Under these prior art, it is clear that an efficient tissue culture protocol for mango transformation is still lacking. Above all, the entire approach so far has been on nucellar explants where the cells have an inherent embryogenic potential. The purpose of the present study was to standardize SE formation and maturation from cotyledonary explants, not tried

hitherto, as well as from nucellar explants. The study is also extended to standardize simple transformation and regeneration protocols for mango cv. Alphonso.

Results and Discussion

Initially upto 4 weeks, no callus initiation was observed from any of the organs of mango (viz. young leaf, stem, root, stalk, young fruit, flower, anther and ovule) in any of the media tried. There was a rampant production of black exudate in all the cultures seeping into the medium. Several phenolic adsorbants were tried in subsequent cultures, which included soluble PVP (1 g/L), insoluble PVP (1 g/L), ascorbic acid (100–200 mg/L) and silver nitrate (5–100 mg/L). Silver nitrate to some extent helped to combat this problem. Finally, with cotyledon and nucellar tissue explant (nourishing tissue outside embryo), callus formation, and regeneration upto SEs and their further germination on different combinations of MS medium could be observed.

Difficulties in establishing aseptic mango cultures from mature explants associated with phenolic browning greatly hinder the micropropagation of mango. The exudation of phenolics from the cut ends of mango explants greatly hindered their regenerative ability *in vitro*. However, pretreatment of explants using liquid shake culture helped in overcoming this problem, which has also been reported by other workers (Raghuvanshi and Srivastava, 1995).

Initial response

Explants, placed in such a way that the nucellus was in contact with the medium, responded to produce the dark proliferative masses in 60 days (Fig. 5.1). Whereas, the cotyledonary explants extensively leached phenolics into the medium, thus requiring repeated subcultures. Cotyledonary explants started developing large protuberances from the upper surface (Fig 5.2 A and B), which later developed into roots whereas the cut ends produced dark cells which both, resulted in embryogenic masses.

The explants both nucellar and cotyledonary, which produced cell mass from the surface (Fig. 5.3 A and B) were repeatedly subcultured using the same medium but with an additional step of liquid culture maintained on gyratory shaker.

Figure 5.1
Nucellar explants of mango producing embryogenic callus (dark) on MS medium with benzylaminopurine (BAP), 2,4-dichlorophenoxyacetic acid (2,4-D) and kinetin + $AgNO_3$

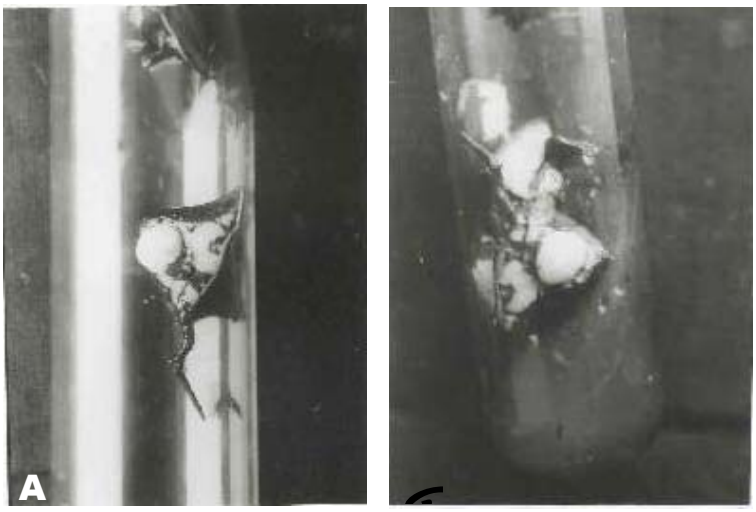

Figure 5.2 Cotyledonary explants of mango

(A) Induction of nodular outgrowth and roots on MS medium with NAA and kinetin + $AgNO_3$

(B) Formation of nodular outgrowths and roots, which later developed into embryogenic culture

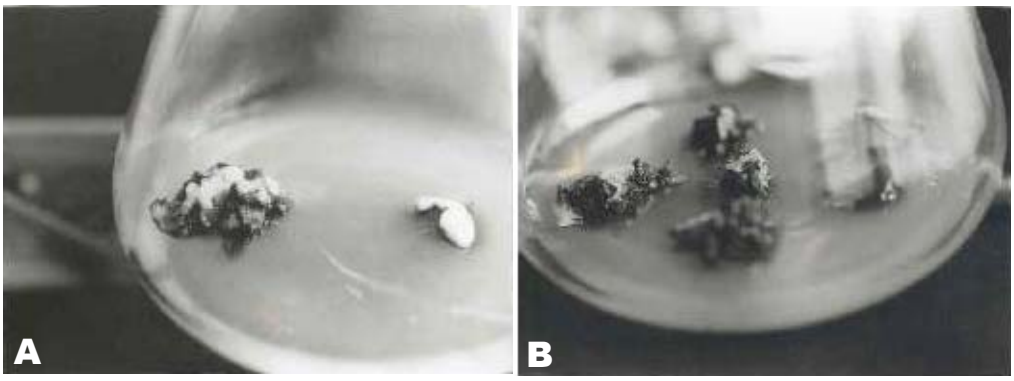

Figure 5.3
(A) Embryogenic calli with dark proliferative masses from nucellar explant
(B) Embryogenic calli from cotyledonary explant regenerating into roots and shoots

Nucellar explants

The cultured nucellar explants showed callus formation after 3 weeks. The initial callus was dark brown or black from with pale-yellow proembryogenic callus initiated within 2-3 weeks, which further proliferated in liquid medium and appeared as irregular-shaped light-yellow compact masses (Fig. 5.4 A). In liquid maintenance medium small multicellular aggregates were observed. The cellular aggregates generally formed large (0.1 to 0.5 cm) embryogenic/proembryogenic globular masses in long-term cultures (Fig. 5.4 B) that proliferated by direct budding in medium containing 2,4-D. Development of SEs appeared to progress through typical globular, heart-shaped, torpedo-shaped and cotyledonary stages of embryo development. The globular and torpedo shaped stages (Fig. 5.5 A, B and C) were seen more frequently than heart-shaped stage. The morphology of SEs was apparently similar to the zygotic embryos.

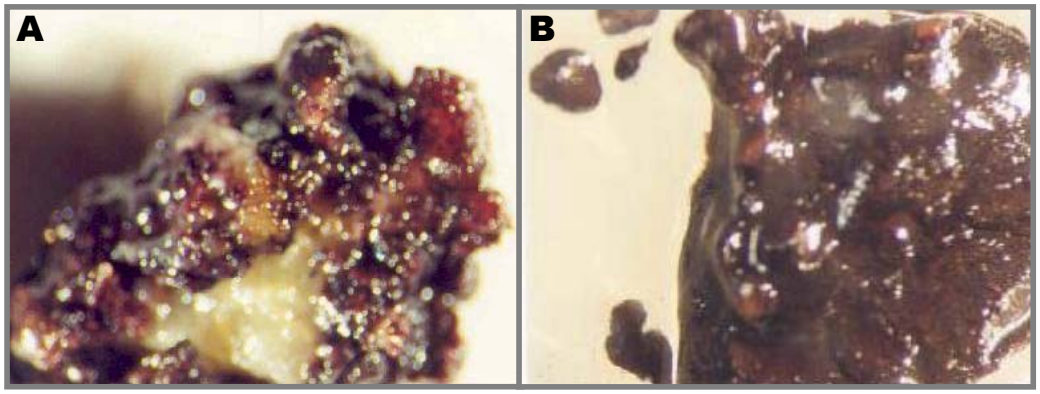

Figure 5.4

(a) Pale-yellow proembryogenic callus further proliferated in liquid medium

(b) Embryogenic/proembryogenic globular masses in long-term cultures

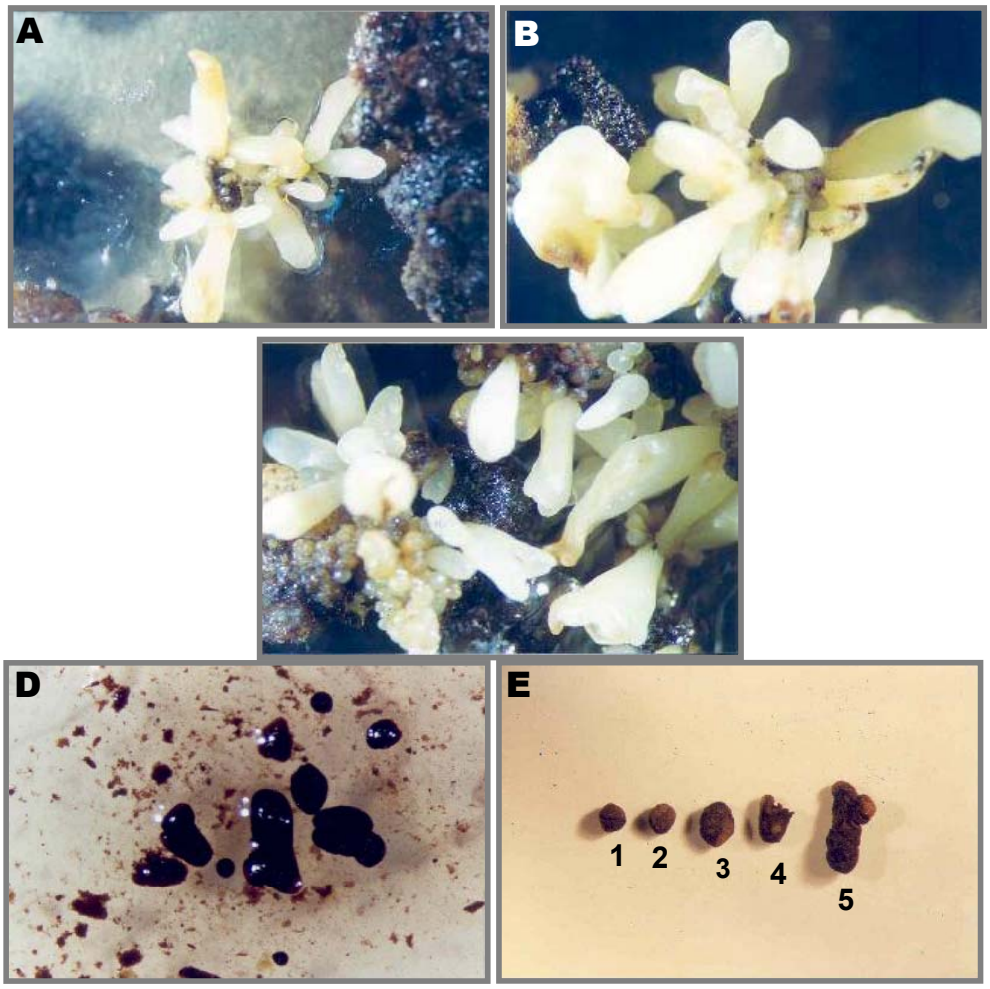

Figure 5.5

(A, B, C) Somatic embryos arising from nucellar callus

(D) Suspension culture of nucellar tissue showing somatic embryos of different stages

(E) Different stages of somatic embryos (1-3, globular; 4, heart shaped; 5, torpedo shaped) obtained from suspension cultures

Cotyledonary explants

The cotyledon tissue was fleshy and cream colored and in one week after inoculation it turned dark brown. The tissue development was obvious in two weeks and the growth was better in cultures maintained in the dark than in light. The callus was dark, compact and irregular masses were formed in one-month-old cultures (Fig. 5.6 A, B and C). Further growth of neogenic callus mass lead to death of the main explant. The callus thus formed was separated from the dead tissue and transferred to fresh similar medium but without agar and the latter was maintained on gyratory shaker. Initial blackening and slow growth has been a common feature for mango as observed by other workers (Mathews *et al.,* 1992). However, no report deals with callus formation from cotyledonary explants.

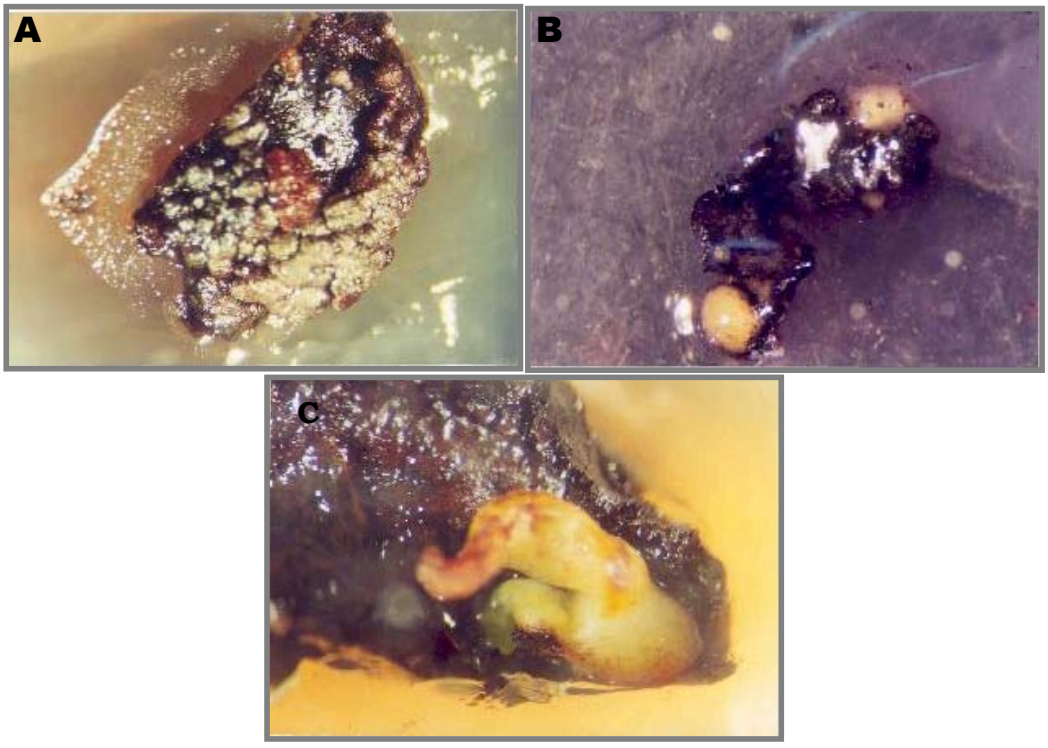

Figure 5.6

(A) Callus initiation from the surface of cotyledonary explant

(B) Cultured tissue producing nodular outgrowths

(C) Somatic embryo formation from nodular outgrowth

Nucellar explants from the monoembryonic mango cultivar produced callus, although the efficiency of callus induction was dependent on medium composition. Conditions for induction of somatic embryogenesis from nucellar explant of polyembryonic and monoembryonic have been demonstrated (Litz *et al.,* 1982; 1984). Although *in vitro* somatic embryogenesis of monoembryonic citrus occurred directly from the nucellus, without an intermediate callus stage (Rangan *et al.,* 1968), monoembryonic mango cultivars responded initially through nucellar callus formation. Nevertheless, the efficiency of somatic embryo regeneration differed with respect to cultivar. Similar observations have been made with citrus cultivars (Rangan *et al.,* 1968). Nucellar callus was slow growing, white or light green in color, and loose and friable in texture. Callus became dark brown after a few days.

Factors influencing somatic embryo induction

There are various factors involved in embryo induction in tree species. In mango, somatic embryogenesis from nucellar tissue cultures has been documented for a few cultivars (DeWald *et al.,* 1989b; Litz 1984; Litz *et al.,* 1982; 1984; 1993). Proembryonic masses have been developed from explanted nucellus in the presence of 2,4-D. In the present study, high level of glutamine (400 mg/L) was essential in addition to low levels of 2,4-D (0.1 mg) whereas in other studies a very high level of 2,4-D (1.0 to 2.0 mg) was required (DeWald *et al.,* 1989) which, in the present case, was shown to be totally inhibitory for somatic embryogenesis.

It is well known for most of the embryo cultures that high osmotic potential is a requisite for starch accumulation involved in embryogenesis. In the present study, in addition to glutamine, a high level of sucrose (60 g/L) was essential for somatic embryogenesis. A lower level of sucrose led to the formation of highly vacuolated cell hyperhydric masses. Further, higher levels (>60 g/L) did not impart any change in the frequency of somatic embryogenesis.

Comparison of liquid and solid media for SE culture proliferation

Once the embryogenic cultures were established, their further performance was checked on both liquid and solid media. After 45 days in liquid maintenance

media, significantly larger embryogenic cell aggregates and proembryonic globular masses were produced. In contrast, smaller embryogenic cell aggregates and proembryonic masses were produced on medium solidified with Gelrite. Cultures darkened more slowly in liquid medium than on solidified medium.

To check whether the overall response was common to all the genotypes (T_1 to T_5), the fresh and dry weight increase of callus were recorded in liquid and solid media using standard maintenance medium. The results have been compiled in the Table 5.1 (A and B). In both the cases the increase in fresh weight (from 100 g inoculum tissue grown for 4 weeks) was recorded. In the case of solid medium a maximum of 211 g i.e., more than 2 fold increase in T_2 followed by 189 g in T_3 was observed. Both T_1 and T_4 showed similar growth responses yielding about 172 g of fresh embryogenic biomass. T_5, though showed very low biomass increase (160 g), showed highest dry weight of 0.173 g. T_2 and T_4 showed similar dry weight accumulation whereas T_1 showed the least.

Table 5.1 (A)

Growth rate of mango cultures on solid maintenance medium

Cultures from different trees	Average fresh weight /100g	Dry weight in g	Dry weight %
T_1	171.1	0.059	8.1
T_2	211.7	0.091	11.67
T_3	189.2	0.11	11.22
T_4	173.43	0.097	8.36
T_5	159.5	0.173	10.95

Table 5.1 (B)
Growth rate of mango cultures in liquid maintenance medium

Cultures from different trees	Average fresh weight / 100g	Dry weight in g	Dry weight%
T_1	451.13	0.063	7.97
T_2	286.5	0.097	7.34
T_3	346.2	0.13	8.6
T_4	304.17	0.028	1.61
T_5	309.0	0.075	7.65

The same genotypes when grown in liquid medium of same chemical composition showed an array of response. The highest fresh weight of 451 g was observed in the case of T_1 followed by 346 g in T_3. Both T_4 and T_5 showed similar growth responses yielding about 306 g of fresh embryogenic biomass whereas T_2 showed lowest (286 g) biomass yield. Both T_2 and T_3 showed similar dry weight accumulation whereas T_4 (0.03 g) and T_1 (0.06 g) showed least. Thus the % dry weight of embryogenic calli varied drastically among the genotypes, which was also true for fresh weight increase. These observations clearly indicate high variations in cellular metabolic activities though exposed to similar physico-chemical conditions. Such interactions between genotypes and media have also been observed before (DeWald *et al.,* 1989b). Between solid and liquid media, the latter appears ideal for the rapid proliferation of embryogenic callus.

Patterns of responses of different genotypes of mango on somatic embryogenesis medium

In this experiment, the callus cultures of five tree genotypes (T_1-T_5) were tested for their capacity towards embryogenic cluster formation by plating the callus on MS medium with 2,4-D (0.1–0.5 mg/L), and glutamine (100 mg) but without ascorbic acid (Chapter II, Table 2.2). The responses were recorded after 8 weeks of incubation by which time the cultures had been once transferred to a fresh medium to reduce the carryover effect from the earlier medium. The results recorded in terms of total number of clusters forming embryos, overall appearance of the culture and the type of SE formation were recorded (Table 5.2). The genotypes T_2, T_3 and T_4 showed almost similar responses forming nearly 30% embryogenic clusters and T_1 and T_5 showed about 25% cluster forming SEs of the total clusters cultured. The overall appearance was greenish to blackish green for all the cultures except in T_1, which showed green to greenish white SEs. T_4 produced excellent SEs, which was followed by T_2. However, in most of the cultures the SEs were associated with rapidly growing callus, which immediately turned black. The genotype T_4 showed highest level of SEs (4) per callus cluster, followed by T_3 (2) and T_2 (1.9). T_1 showed less (1) fully formed SE per callus cluster, which was also associated with least abnormal SE formation compared to T_3 and T_5, which showed highest

abnormal SE formation. Thus, there was a significant variation from one genotype to another in terms of callus formation, further growth, embryogenic frequency and normal SE formation. Therefore it was necessary to check different genotypes for efficient development of regeneration protocol for further application.

Table 5.2
Patterns of responses of different genotypes of mango on somatic embryogenesis medium

Cultures from different trees	Total number of clusters	Overall appearance	Quality of SEs	Fully formed normal SEs per cluster	Abnormal SEs per cluster
T_1	23	Dark callus with GW SEs	Good callussy & embryogenic	1.0	0.21
T_2	30	Greenish white embryos with black callus	Good	1.86	0.4
T_3	28	Blackish green	Good often callussy	2	1.7
T_4	30	Dark with greenish SEs	Callussy with excellent SEs	4.03	0.3
T_5	25	Dark with greenish white SEs	Good SEs, Callussy and early SEs	1.36	1.7

SE maturation occurs following the subculture of proembryonic masses to plant growth medium without 2,4-D, where they are generally able to germinate after a 3- to 5-month maturation period (DeWald *et al*., 1989). The proliferation rate of proembryos is greatly enhanced in suspension culture containing 2,4-D in comparison with semisolid medium. In practice, however, the establishment of

rapidly proliferating suspension cultures of mango is highly cultivar dependent (Litz *et al.,* 1993).

Effect of stage of proembryonic masses on maturation, germination and development process of SEs

(a) Interaction between stage of SEs of different genotypes with mannitol and activated charcoal

For T_1 genotype, charcoal alone influenced the total number of SEs during germination where, when compared to control medium, the addition of charcoal resulted in suppression of SEs of all stages with more significant effect on torpedo stage (Tables 5.3 and 5.4). Though mannitol also imparted similar effects, it was less significant on SE germination, leading to hyperhydric condition (Table 5.5). Though mannitol is expected to reduce the water activity of the medium leading to much normal embryo formation, in the present study mannitol showed a reverse effect compared to control cultures. When both mannitol and charcoal were present in the medium (Table 5.6), results were almost similar to those of control medium. The significant effect being the suppression of overall length of SEs, especially of shoot length. However, mannitol effect was reflected in terms of hyperhydric conditions of somatic embryos.

Table 5.3
Effect of medium 1 on T_1 SE germination

Different stages of SEs	Overall response	Total no. of SEs germinating	Root length (cm)	Shoot length (cm)	Shoot color	Other responses
Fully grown SE of 2.0 mm long	Fair germination	4	0.40	0.50	GW	Abnormal enlargement of shoots
SEs of 1.0–1.5 mm long	Good germination	5	0.60	0.60	G + GW	Abnormal enlargement of shoots
SEs of Torpedo stage	Good germination	8	0.10	0.62	GW	Some multiplication of SEs
Early globular SEs	Abnormal germination	5	0.00	0.50	GW	Hyperhydric
Very minute undifferentiated proembryonic masses	Fair germination	5	0.00	0.62	GW	Multiplication of SEs

Note: SEs, Somatic Embryos; G, Green; W, White; GW, Greenish White

Table 5.4
Effect of medium 2 on T_1 SE germination

Different stages of SEs	Overall response	Total no. of SEs germinating	Root length (cm)	Shoot length (cm)	Shoot color	Other responses
Fully grown SE of 2 mm long	Fair germination	3	0.00	0.50	GW	Abnormal expansion of SEs + hyperhydric
SEs of 1.0–1.5 mm long	Fair germination	5	0.00	0.62	GW	Hyperhydric
SEs of Torpedo stage	Fair germination	3	0.00	0.63	G + GW	Multiplication of SEs
Early globular SEs	Fair germination	2	0.00	0.55	GW	Highly enlarged thalloid growth
Very minute undifferentiated proembryonic masses	Fair germination	3	0.00	0.70	GW	Multiplication of SEs

Table 5.5

Effect of medium 3 on T_1 SE germination

Different stages of SEs	Overall response	Total no. of SEs germinating	Root length (cm)	Shoot length (cm)	Shoot color	Other responses
Fully grown SE of 2 mm long	Fair germination	4	0.00	0.55	W	Hyperhydric
SEs of 1.0–1.5 mm long	Good germination	5	0.00	0.42	GW	Hyperhydric
SEs of Torpedo stage	Good germination	6	0.10	0.75	GW	Hyperhydric
Early globular SEs	Fair germination	4	0.40	0.43	GW	Hyperhydric
Very minute undifferentiated proembryonic masses	Fair germination	2	0.00	0.45	G + GW	Hyperhydric + Multiplication of SEs

Table 5.6
Effect of medium 4 on T_1 SE germination

Different stages of SEs	Overall response	Total no. of SEs germinating	Root length (cm)	Shoot length (cm)	Shoot color	Other responses
Fully grown SE of 2 mm long	Good germination	4	0.40	0.48	G + GW	Abnormal expansion
SEs of 1.0–1.5 mm long	Good germination	5	0.52	0.40	GW	Hyperhydric
SEs of Torpedo stage	Fair germination	5	0.00	0.40	GW	Hyperhydric highly abnormal shoot
Early globular SEs	Fair germination	6	0.00	0.70	White + Pink	Hyperhydric highly abnormal shoot
Very minute undifferentiated proembryonic masses	No germination	0	0.00	0.00	GW	Multiplication of proembryonic masses

On the contrary, in T_2, the proembryonic masses failed to produce germinating SEs on control medium where root length was suppressed in fully-grown and a lesser stage of SEs i.e., 1.2–1.5 mm (Table 5.7). This genotype did not

express any hyperhydric state at any level of organization in control medium. For this genotype charcoal did not impart SE suppressing effect. Infact, the proembryonic masses of T_2 were able to germinate and proceed further to form SEs with significant improvement in root and shoot lengths (Table 5.8). Whereas, the higher stages of SEs were suppressed from further growth. The fully-grown SEs and its lower stage ended up with hyperhydric conditions. The torpedo shaped SEs of T_2 genotype was completely suppressed from further growth in medium containing mannitol (Table 5.9). Rest of the effects of mannitol on different stages was grossly comparable to that on control medium as well as of T_1 genotype. When both mannitol and charcoal were present in the medium, a drastic inhibitory effect on stages of SEs from torpedo to fully-grown was observed. However, early stages such as proembryonic masses and early globular SEs underwent fair amount of germination resulting in greenish white somatic embryos, which were hard and starchy (Table 5.10). Thus, this genotype showed significantly different responses and followed germination pattern quite common to most of the somatic embryos of dicotyledonous species.

Table 5.7
Effect of medium 1 on T_2 SE germination

Different stages of SEs	Overall response	Total no. of SEs germinating	Root length (cm)	Shoot length (cm)	Shoot color	Other responses
Fully grown SE of 2 mm long	Enlarged SEs	3	0.33	0.50	G, GW	-
SEs of 1.0–1.5 mm long	Enlarged SEs	4	0.03	0.70	GW	Abnormal thalloid shoot
SEs of Torpedo stage	Enlarged SEs	5	0.35	0.63	GW	Greenish white SEs of early stage
Early globular SEs	Abnormal enlargement of SEs	5	0.00	0.48	W	Greenish early stages of SEs
Very minute undifferentiated proembryonic masses	Green embryogenic callus formation	0	0.00	0.00	-	Greenish white proembryonic masses

Table 5.8
Effect of medium 2 on T_2 SE germination

Different stages of SEs	Overall response	Total no. of SEs germinating	Root length (cm)	Shoot length (cm)	Shoot color	Other responses
Fully grown SE of 2 mm long	Enlarged SEs	5	0.00	0.66	GW	Hyperhydric
SEs of 1.0–1.5 mm long	Enlarged SEs	5	0.00	0.68	GW	Hyperhydric and multiplication of early stage SEs
SEs of Torpedo stage	Enlargement and multiplication of SEs	6	0.00	0.60	GW	Good multiplication of early stage SEs from the base of germinating SEs
Early globular SEs	Not much change	3	0.00	0.30	GW	Appears drying
Very minute undifferentiated proembryonic masses	Enlarged and good germinating SEs	2	0.30	0.65	GW	Multiplication of other SEs

Table 5.9
Effect of medium 3 on T_2 SE germination

Different stages of SEs	Overall response	Total no. of SEs germinating	Root length (cm)	Shoot length (cm)	Shoot color	Other responses
Fully grown SE of 2 mm long	Good germination	2	1.20	0.70	G, GW	Abnormal enlargement of other SEs
SEs of 1.0 – 1.5 mm long	Good germination	4	0.05	0.53	GW	Enlargement and multiplication of SEs
SEs of Torpedo stage	-	-	-	-	-	-
Early globular SEs	Fair germination	5	0.14	0.32	G and GW	Enlargement of SEs
Very minute undifferentiated proembryonic masses	Fair germination	2	0.00	0.40	G and GW	Multiplication of other SEs

Table 5.10
Effect of medium 4 on T_2 SE germination

Different stages of SEs	Overall response	Total no. of SEs germinating	Root length (cm)	Shoot length (cm)	Shoot color	Other responses
Fully grown SE of 2 mm long	-	-	-	-	-	-
SEs of 1.0–1.5 mm long	-	-	-	-	-	-
SEs of Torpedo stage	-	-	-	-	-	-
Early globular SEs	Fair germination	9	0.06	0.41	GW	Appear dry and hard + starchy
Very minute undifferentiated proembryonic masses	Fair germination	4	0.13	0.33	W	Appear dry and starchy

In T_3 genotype, the response on control medium was almost similar to T_1 and T_2 except for the early stages such as early globular SEs and proembryonic masses, which were less suppressed (Table 5.11). In other words, these early stages were also able to germinate with abnormal enlargement of greenish white SEs with fair amount of shoot formation and root primordia formation. For T_3, charcoal imparted suppressive effect only for the early stage i.e., stage 5 (Table 5.12). Rest of the stages continued further growth to form larger and more number of SEs with partial germination where root formation was suppressed in stages 3 to 5 i.e., torpedo stage to proembryonic mass. However, with most of the germinated embryos in the presence of mannitol showed abnormal enlargement (Table 5.13). For this genotype, mannitol imparted suppressive effect for globular stage alone. Similar type of effect for T_2 occurred at torpedo stage. Thus, a strong morphological stage-specific effect of mannitol is apparent. When both mannitol and charcoal were present together in the medium, the responses were grossly similar to control medium with improvement of germination in early globular somatic embryos and proembryonic masses where shoot length was much better

than in control. However, this genotype was somewhat similar to T_1 in terms of hyperhydric embryo formation when both mannitol and charcoal were present in the medium. The major difference being less suppressive effect of mannitol and charcoal in T_3 when compared to T_1 (Table 5.14).

Table 5.11
Effect of medium 1 on T_3 SE germination

Different stages of SEs	Overall response	Total no. of SEs germinating	Root length (cm)	Shoot length (cm)	Shoot color	Other responses
Fully grown SE of 2 mm long	Enlargement	6	0.17	0.62	G, GW	Nil
SEs of 1.0–1.5 mm long	Enlargement	6	0.00	0.43	G, GW	Multiplication of SEs in one
SEs of Torpedo stage	Fair Germination	4	0.00	0.50	GW	Multiplication of SEs
Early globular SEs	Fair Germination	2	0.20	0.55	GW	Abnormal enlargement in other SEs
Very minute undifferentiated proembryonic masses	Fair germination	2	0.00	0.55	GW	Slow abnormal growth in rest

Table 5.12
Effect of medium 2 on T_3 SE germination

Different stages of SEs	Overall response	Total no. of SEs germinating	Root length (cm)	Shoot length (cm)	Shoot color	Other responses
Fully grown SE of 2 mm long	Good germination	6	0.58	0.80	G	Abnormal enlargement
SEs of 1.0–1.5 mm long	Good germination	8	0.06	0.61	GW	Some multiplication of SEs
SEs of Torpedo stage	Good germination	6	0.00	0.65	GW	Abnormal enlargement
Early globular SEs	Fair Germination	2	0.00	0.70	GW	Abnormal enlargement
Very minute undifferentiated proembryonic masses	No germination	-	-	-	-	Enlargement and further multiplication of proembryonic masses

Table 5.13
Effect of medium 3 on T_3 SE germination

Different stages of SEs	Overall response	Total no. of SEs germinating	Root length (cm)	Shoot length (cm)	Shoot color	Other responses
Fully grown SE of 2 mm long	Good germination	4	1.63	0.65	G, GW	Abnormal enlargement of shoots
SEs of 1.0–1.5 mm long	Fair Germination	6	0.00	0.42	G, GW	Starchy SEs multiplication
SEs of Torpedo stage	Fair Germination	6	0.08	0.56	G, GW	Some multiplication of SEs
Early globular SEs	-	-	-	-	-	-
Very minute undifferentiated proembryonic masses	Fair germination		0.00	0.55	GW	Multiplication of SEs

Table 5.14
Effect of medium 4 on T_3 SE germination

Different stages of SEs	Overall response	Total no. of SEs germinating	Root length (cm)	Shoot length (cm)	Shoot color	Other responses
Fully grown SE of 2 mm long	Fair Germination	5	0.30	0.56	GW	Hyperhydric
SEs of 1.0–1.5 mm long	Fair Germination	8	0.24	0.64	GW	Hyperhydric
SEs of Torpedo stage	Fair Germination	6	0.00	0.63	GW	Hyperhydric
Early globular SEs	Highly abnormal	7	0.00	0.71	GW	Hyperhydric
Very minute undifferentiated proembryonic masses	Fair germination	3	0.17	0.43	GW	Hyperhydric

In T_4, most of the responses were comparable to T_1 with a major difference being that the charcoal did not impart any suppressive effect, instead SEs of 1.0–1.5 mm length, torpedo stage and early globular SEs were promoted to form starchy dry SEs, similar to that of T_2 (Tables 5.15 and 5.16). However, root primordia were suppressed by charcoal. Mannitol on the other hand showed inhibitory effect on early stages of SEs where germination was totally suppressed with multiplication of greenish proembryonic masses (Table 5.17). When both mannitol and charcoal were present in the medium, the inhibitory effect was on torpedo stage (Table 5.18). The significant difference being dry and starchy SE formation from fully-grown SEs, whereas the other stages resulted in hyperhydric SEs. There was a significant level of root formation from early globular SEs.

Table 5.15
Effect of medium 1 on T_4 SE germination

Different stages of SEs	Overall response	Total no. of SEs germinating	Root length (cm)	Shoot length (cm)	Shoot color	Other responses
Fully grown SE of 2 mm long	Fair germination	4	0.25	0.70	GW	Abnormal
SEs of 1.0–1.5 mm long	Fair Germination	4	0.30	0.43	GW	Abnormal
SEs of Torpedo stage	High abnormal enlargement	4	0.00	0.80	Pinkish white	Highly abnormal and hyperhydric
Early globular SEs	Fair Germination	3	0.47	0.47	G, GW	Other SEs slowly germinating
Very minute undifferentiated proembryonic masses	Fair Germination	3	0.00	0.53	GW	Slow but more organized germination

Table 5.16
Effect of medium 2 on T_4 SE germination

Different stages of SEs	Overall response	Total no. of SEs germinating	Root length (cm)	Shoot length (cm)	Shoot color	Other responses
Fully grown SE of 2 mm long	Fair germination	3	0.83	1.13	G, GW	Abnormal shoot growth
SEs of 1.0–1.5 mm long	Fair germination	5	0.12	0.78	GW	Multiplication of SEs
SEs of Torpedo stage	Fair germination	5	0.00	0.42	GW	Starchy dry SEs
Early globular SEs	Fair Germination	6	0.00	0.60	GW	Abnormal expansion
Very minute undifferentiated proembryonic masses	Fair germination	3	0.00	0.37	GW	Hyperhydric multiplication of SEs

Table 5.17
Effect of medium 3 on T_4 SE germination

Different stages of SEs	Overall response	Total no. of SEs germinating	Root length (cm)	Shoot length (cm)	Shoot color	Other responses
Fully grown SE of 2 mm long	Fair Germination	5	0.24	0.32	GW	Multiplication of SEs
SEs of 1.0–1.5 mm long	Good germination	5	0.76	0.52	GW, G	Some multiplication of SEs
SEs of Torpedo stage	Highly enlarged SEs	6	0.12	0.77	GW pinkish	Abnormal enlargement
Early globular SEs	Highly enlarged SEs	6	0.00	0.75	GW pinkish	Abnormal enlargement
Very minute undifferentiated proembryonic masses	No Germination	-	-	-	GW	Slow multiplication of proembryonic masses

Table 5.18
Effect of medium 4 on T_4 SE germination

Different stages of SEs	Overall response	Total no. of SEs germinating	Root length (cm)	Shoot length (cm)	Shoot color	Other responses
Fully grown SE of 2 mm long	Fair Germination	5	0.18	0.50	G, W	Dry, starchy
SEs of 1.0–1.5 mm long	Fair Germination	2	0.00	1.05	W	Hyperhydric
SEs of Torpedo stage	Fair germination	-	-	-	-	-
Early globular SEs	Good germination	3	1.07	0.70	GW	Hyperhydric
Very minute undifferentiated proembryonic masses	Fair Germination	6	0.00	0.45	GW	Normal and abnormal SEs + SE multiplication

In T_5, the early stages were profoundly suppressed from growing further to form/germination of SEs by both mannitol and charcoal, and the inhibitory effect was complementary to each other (Tables 5.19–5.22).

Table 5.19
Effect of medium 1 on T_5 SE germination

Different stages of SEs	Overall response	Total no. of SEs germinating	Root length (cm)	Shoot length (cm)	Shoot color	Other responses
Fully grown SE of 2 mm long	Fair Germination	2	0.50	0.60	G, W	Abnormal expansion
SEs of 1.0–1.5 mm long	Fair Germination	3	0.47	0.56	G, GW	-
SEs of Torpedo stage	Fair germination	3	0.23	0.50	W, GW	Abnormal expansion
Early globular SEs	Poor germination	2	0.00	0.55	W	Multiplication of SEs
Very minute undifferentiated proembryonic masses	-	-	-	-	GW	Early SE stages

Table 5.20
Effect of medium 2 on T_5 SE germination

Different stages of SEs	Overall response	Total no. of SEs germinating	Root length (cm)	Shoot length (cm)	Shoot color	Other responses
Fully grown SE of 2 mm long	Fair Germination	2	0.30	0.60	GW	Some abnormal expansion hypohydric
SEs of 1.0–1.5 mm long	Fair Germination	4	0.00	0.80	GW	Normal
SEs of Torpedo stage	Poor germination	-	-	-	GW	Multiplication of SEs
Early globular SEs	Poor germination	-	-	-	GW	Multiplication of SEs
Very minute undifferentiated proembryonic masses	Fair germination	2	-	0.40	GW	Multiplication of SEs

Table 5.21
Effect of medium 3 on T_5 SE germination

Different stages of SEs	Overall response	Total no. of SEs germinating	Root length (cm)	Shoot length (cm)	Shoot color	Other responses
Fully grown SE of 2 mm long	Good Germination	4	1.20	0.50	White	Abnormal roots and shoots
SEs of 1.0–1.5 mm long	Fair Germination	5	0.00	0.40	GW, W	Multiplication of SEs
SEs of Torpedo stage	Fair germination	2	0.30	0.35	G, W	Very early stages of SEs
Early globular SEs	Poor germination	2	0.00	0.45	W	Early stages of SEs and abnormal germination
Very minute undifferentiated proembryonic masses	-	-	-	-	-	Multiplication of SEs

Table 5.22
Effect of medium 4 on T_5 SE germination

Different stages of SEs	Overall response	Total no. of SEs germinating	Root length (cm)	Shoot length (cm)	Shoot color	Other responses
Fully grown SE of 2 mm long	Fair Germination	3	0.50	0.40	G, W	Abnormal hyperhydric SEs
SEs of 1.0–1.5 mm long	Fair Germination	3	0.00	0.90	G, Pinkish	Abnormal hyperhydric SEs
SEs of Torpedo stage	Fair germination	2	0.00	0.50	GW	Abnormal hyperhydric SEs
Early globular SEs	Poor germination	-	-	-	-	Multiplication of SEs
Very minute undifferentiated proembryonic masses	Poor germination	-	-	-	-	Multiplication of SEs

The present study clearly indicates the significant differences upon similar treatments in SE germination. In general, the earliest stage of SE, i.e., the proembryonic masses are not suitable as starting material for inducing germinating embryos as is done for embryo germination in most of the other dicots (Vasil, 1990). Even the other higher stages, from globular to torpedo stage, underwent growth suppressive effects in the presence of mannitol and charcoal except for T_2, which was amenable for low water activity (mannitol) and charcoal treatments. The present study also indicates that the effect of mannitol and charcoal on the status of other nutrients in the medium may also be genotype-specific. Therefore, due to very high recalcitrant behavior of mango genotypes, it is necessary to screen a large number of trees and establish a protocol for SE formation/germination, which may subsequently be used for transformation purposes.

Mango embryogenic cultures grown in different SE maturation and germination media formulations containing mannitol and activated charcoal produced significantly good SE germination and shoot and root initiation (Tables 5.3 to 5.22) (Fig. 5.7 A and B). Ammirato (1983) noted that somatic embryogenesis

and the subsequent stages of SE development and germination often require a particular sequence of changes of plant growth media and growing conditions. Mango embryos (*in vivo*) are very large at the time of physiological maturity *in vivo*, generally 3 to 4 cm long, and require several months of period in ovule to attain this size (Fig. 5.8). The *in vitro* development of SEs of tropical trees having large seeds has been difficult to realize due to the complexity of events between SE initiation and germination (Wang and Janick, 1984). Because of the long maturation period for mango SEs, manipulations of the culture media were necessary to inhibit precocious germination and other patterns of abnormal development.

Figure 5.7 (A)
Germination of SEs showing elongated shoots and root primordia
(2A and 3A: different clones of Alphonso)

Figure 5.7 (B)

Sequence of germinating SEs

(b) Effect of abscisic acid on SE maturation and reversal of hyperhydric conditions

During embryo maturation, plants produce abscisic acid (ABA), which is known to antagonize the gibberlic acid effect and induce dormancy. To know whether ABA can also reverse the precocious germination and hyperhydricity of SEs, ABA was used for different stages of normal as well as hyperhydric SEs.

This experiment mainly involved hyperhydric SEs derived from control liquid medium or secondary embryos mainly from T_3 as this clone showed maximum hyperhydric SEs. It was observed that on control medium, the primary hyperhydric SEs were unable to survive when transferred to ABA-containing medium, and all of the SEs died during the first month. However, exposure of primary SEs to ABA only for about two weeks resulted in the formation of normal SEs in 10% of the cultures. Though the reversion from hyperhydric to normal SE

was similar in treatments with and without ABA, the control SEs germinated precociously indicating that ABA imparted senescing effect. Suppression of precocious germination of the SEs was similar at all concentrations of ABA.

The secondary hyperhydric SEs, in contrast to the primary SEs, responded very well towards reversal of hyperhydricity to normal where more than half of the hyperhydric SEs underwent reversion during first two weeks after subculture. With 400 μM ABA in the medium, there was 67% reversion of hyperhydricity by the end of first month of incubation, which increased to over 90% by the end of second month on the same medium (Chapter 2, Table 2.2). The higher levels significantly affected the SE growth where most of them turned dark. The medium with 400 μM ABA was the optimum level required for reversion of hyperhydricity as well as suppression of precocious germination of SEs. Similar observations have been made by earlier workers where even 1000 μM ABA imparted similar effect as that of control (Monsalud *et al.,* 1995).

The present study indicates that the efficient production of embryogenic mango cultures and many morphologically normal somatic embryos from these cultures depends on physical and chemical factors. A correlation existed between high frequency production of normal SEs and medium composition. Kamada and Harada (1979) have shown that glutamine and glycine promote somatic embryogenesis in carrot, even in the presence of inorganic reduced nitrogen (Litz and Conover, 1982). Gelrite has been reported to be more effective in controlling vitrification in apple shoots (Pasqualetto *et al.,* 1986), and has been used effectively in media for induction and development of SEs of Longan (Litz, 1988). It was always the liquid medium that imparted hyperhydric condition and formation of normal SEs.

(c) Effect of gibberlic acid-3 on SE maturation and later development

Recent results indicate that modifications in culture media compositions coupled to maturation enhancing treatments can significantly improve the quality, frequency and uniformity of SEs (Emons *et al.,* 1993; Shetty and Mc Kersie, 1993).

Manupilation of balance of abscisic acid, gibberilic acid, L-proline, mannitol and sucrose has proven especially effective in some species (Emons *et al.,* 1993).

Some attempts for protoplast culture from 'Alphonso' variety were also made for obtaining protoplasts in very good yield, from young mango fruit pulp of early developmental stage. There were plenty of fast dividing protoplasts but we could not succeed in culturing them for regeneration (Fig. 5.9). Ara *et al.* (2000) have reported the regeneration of plants from protoplasts isolated from proembryogenic masses originating from nucellar callus of the monoembryonic cultivar 'Amrapali' of mango.

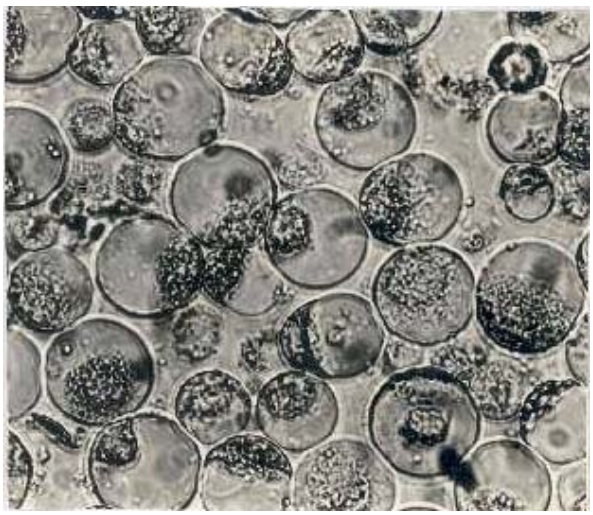

Figure 5.9

Protoplasts from mango pulp (young developing fruit)

Mango transformation using *Agrobacterium tumefaciens*

To transfer any target gene into plants like mango and banana, where genetic transformation is only recently established, it is mandatory to develop tissue culture/gene transfer protocols in respective crop. It was possible to induce direct plant regeneration from nucellus explants and embryonic cultures from cotyledonary explants of mango. These tissue culture protocols are intended to be

used for developing respective transgenic plants which are expected to produce normally ripening fruits with delayed texture degradation.

Timentin tolerance of putatively transformed proembryos on solid selection medium

The growth rate of putatively transformed proembryos on solid selection medium with 150 μg/L timentin showed a steady increase over a period of 60 days. At higher concentrations of timentin, an initial decline in growth rate was observed, possibly due to loss of non-transformed ones.

Test for transformation using β-glucuronidase assay

Expression of β-glucuronidase (GUS) from immature embryos co-cultivated with *A. tumefaciens* was achieved and also observations were made on the susceptibility of mango seedlings to different strains of *A. tumefaciens.* Wounding and co-cultivation with *Agrobacterium* caused an excessive oxidation response in mango cultures. In both control and *A. tumefaciens* co-cultivated cultures, proembryos turned black within 5 to 7 days of plating on selection medium containing 150 μg/L timentin. However, *Agrobacterium*-treated cultures showed distinct fresh growth in a period of 150 days whereas untreated control tissues did not show signs of cell proliferation even after 2 year of subculture. These fresh growth areas, after subculture on selection medium, started proliferating and produced secondary proembryos. A total of 14 fresh-growth areas were isolated from five petriplates, and these were considered as 14 independently transformed proembryos.

Samples of all 14 transformed clones showed mixtures of blue and white/yellow cells when assayed for GUS expression. 40 to 50% of the proembryos in each sample were chimeric for blue and white/yellow cells while the rest were completely white/greenish-yellow. Control non-transformed proembryos did not exhibit GUS activity after 16 h of incubation with bromo chloro-S-indolyl-B-D-glucuronic tetra cyclohexylammonium salt (X-Gluc) whereas transformed clones showed the characteristic blue color within 4 to 6 h of incubation.

The co-cultivated proembryos on transfer to liquid selection medium turned completely black with heavy exudation of phenols in a period of 24 to 40 h, irrespective of whether the exposure to timentin was immediately after co-cultivation or after 3 days of growth in nonselection medium. Histochemical reaction for GUS activity was masked because the tissue was dark. The control tissue not exposed to *A. tumefaciens* also turned black in liquid selection medium and failed to grow further.

Recovery of transformed somatic embryos

Proembryos in liquid maintenance medium with 150 μg/L timentin developed normally after transfer to liquid embryogenesis medium with the same level of timentin. Heart and torpedo-stage embryos were present in liquid selection medium after 40 to 60 days, and stained intensely blue, showing stable expression of the GUS gene.

Test for contaminating *A. tumefaciens* in mango cultures

Proembryos suspension as well as SE segments grown in LB broth did not show any visible bacterial contamination. Furthermore, when the liquid aliquots were plated on LB agar, no colonies were formed except on those plates streaked with *A. tumefaciens* suspension.

Effect of acetosyringone on the frequency of transformation

High frequency transformation was observed after infecting cotyledonary and nucellar explants with *A.tumefaciens* cultured with acetosyringone (Table 5.24 and Table 5.25). The transformation process was delayed in explants infected with bacteria cultured without acetosyringone (Table 5.23).

Influence of different plasmid clones during *Agrobacterium*-mediated transformation of mango SEs and tobacco clones using GUS marker

The control tobacco co-cultivated with pBSF16/0 for 2 days showed excellent GUS activity whereas non-transformed tissues did not show any GUS activity. Among the mango clones, T_1 co-cultivated with *A. tumefaciens* carrying

pBSF16/0 as well as that with pKIWI exhibited good transformation (GUS-positive) (Table 5.23).

Table 5.23

Influence of different plasmid clones during *Agrobacterium*-mediated transformation of mango SEs and tobacco clones using GUS marker

Material	Period of co-cultivation (days)	Results	Remarks
Tobacco GUS 'smiley' of 16/8		+ve	60 % of tissue
Tobacco non-infected		-	-
Tobacco non-infected		-	-
Mango T_1/pKIWI	2	-	-
Mango T_1/ pBSF16/0	2	-	-
Mango T_1/ pBSF16/1	2	-	-
Tobacco pBSF16/0	4	+	Excellent bh stain in patches
Tobacco pBSF16/1	4	-	-
Tobacco pKIWI	4	+	Excellent bh patches along the edges
Tobacco pKIWI	2	-	-

Table 5.24

***Agrobacterium*-mediated transformation in different clones of mango SEs under the influence of acetosyringone in infection medium using GUS test as the marker**

Material	Plasmid treated with ACS	Infection medium (solid / liquid)	Period of co-cultivation (days)	Results on X-Gluc
Tobacco 'smiley' W_{38}	pKIWI	S	2	+
T_1	pKIWI	S	3	-
T_1	pKIWI	L	3	+ (Best)
T_2	pBSF16/1	S	3	-
T_3	PKIWI	S	3	+
T_4	pBSF16/1	S	3	-
T_1	pKIWI	S	4	-
T_1	pKIWI	L	4	+
T_2	pKIWI	S	4	-
T_2	pKIWI	L	4	-
T_3	pKIWI	L	4	-
T_3	pBSF16/1	L	4	?
T_4	pKIWI	S	4	+ (Good)
T_4	pBSF16/1	L	4	+
T_5	PKIWI	L	4	-
T_5	pBSF16/0	L	4	-
T_5	pBSF16/1	L	4	-

Table 5.25

***Agrobacterium*-mediated transformation in different clones of mango SEs under the influence of acetosyringone in *A.tumefaciens*-activation medium using GUS test as the marker**

Material	Plasmid treated with ACS	Period of co-cultivation (days)	Results on X-Gluc
T_1	pKIWI	2	+
T_1	pKIWI	3	+
T_1	pKIWI	4	+
T_1	pBSF16/0	2	+
T_1	pBSF16/0	3	+
T_1	pBSF16/0	4	+
T_1	pBSF16/1	4	-
T_2	pBSF16/1	2	-

T_2	pBSF16/1	3	-
T_2	pBSF16/1	4	-
T_3	pKIWI	2	-
T_3	pKIWI	3	-
T_3	pKIWI	4	-
T_3	pBSF16/0	4	-
T_3	pBSF16/1	4	-

Agrobacterium-mediated transformation in different clones of mango SEs **under the influence of acetosyringone in infection medium using GUS test as the marker**

In the presence of acetosyringone, the different genotypes of mango responded differently to the clones of plasmid present in *A.tumefaciens.* The transformation was carried out both in liquid and solid medium. Of the five mango clones, SEs of T_1 showed good transformation where infection with pKIWI alone had been accomplished in liquid medium in the presence of acetosyringone. *A.tumefaciens* clone pKIWI was also effective for T_4, and further after 4 days co-cultivation, pBS16/1 also showed good transformation (evident from GUS test). Other mango clones were not amenable for transformation (Table 5.24).

***Agrobacterium*-mediated transformation in different clones of mango SEs under the influence of acetosyringone in *A. tumefaciens*-activation medium using GUS test as the marker**

The use of acetosyringone in the *Agrobacterium*-activation medium resulted in rapid transformation of T_1 clones of mango. The *A.tumefaciens* harboring plasmid pKIWI efficiently transformed T_1 SEs in 2 days, which expressed GUS activity. Even the strain pBSF16/0, which was not so efficient in earlier trials, showed good GUS activity in clones co-cultivated for 2–4 days. The other mango clones, even after 4 days, did not show any signs of transformation (Table 5.25).

The role of acetosyringone in the activation of the 'vir' gene responsible for T-strands that are transferred and integrated into plant chromosomes is well

established in recent literature (Mathews *et al.,* 1990; Albright *et al*., 1987; Stachel *et al.,* 1987, Wang *et al.,* 1987). Enhancement of the transformation frequency by acetosyringone has, however, been shown only in *Arabidopsis* (Scheikholeslam and Weeks, 1987) and in *Atropa belladona* (Mathews *et al.,* 1990). The present study establishes that even for mango, the external application of acetosyringone leads to enhancement of transformation frequency. Gene transfers mediated by *A.tumefaciens* provide stable integration of foreign genes in plants (Schell, 1987 a and b). Acetosyringone-induced promotion of *Agrobacterium*-mediated transformation in *Arabidopsis* (Scheikholeslam and Weeks, 1987), *Atropa* (Mathews *et al.,* 1990) and mango suggests the possible use of this chemical to improve the effectiveness of genetic transformation in experiments with other species.

Conclusions

Mango is currently the world's fifth most important fruit crop and has resisted conventional plant breeding efforts due to its long generation cycle and low frequency of fruit set. The application of biotechnology to mango improvement should be influenced by the efficient recovery of plants from SEs. Mathews *et al.* (1992) have successfully transformed mango by co-cultivation of embryogenic cultures with *A. tumefaciens*, and has been extended further by the present study using cv 'Alphonso'. Kanamycin-resistant mango embryos, which also express the GUS gene, have been obtained. Copies of the T-DNA integrated into the mango genome were confirmed by southern hybridization. A prolonged selection protocol was required to eliminate chimeric clumps. Recently, Cruz-Hernandez *et al.* (1999) reported transient and stable transformation in mango by particle bombardment of proembryogenic masses. Although, mango has a very long regeneration time, prospects for genetic transformation of mango seem quite good. Engineering resistance to pests, diseases, mango malformation, regulation of flowering, cold-tolerance and storage life as well as manipulating canopy shape and size by incorporation of *rol* genes, can be addressed when a technology for routine production of transgenic plants is developed. Moreover, the medium-term storage and exchange of mango germplasm between producing countries could also be facilitated.

Chapter **6**

Summary and Conclusions

Ripening of mango is accompanied by changes such as almost complete hydrolysis of starch, a concomitant increase in total as well as free soluble sugars, soluble polyuronides, and a decrease in titrable acidity. Ripening is also characterized by a rapid and extensive softening of fruit, which correlates positively with an increase in the activity of most of the carbohydrate hydrolases, loss of cellular intactness, extensive hydrolysis and solubilization of the respective polysaccharides. Textural softening was thus the outcome of pectin hydrolysis, degradation of CWS, HWS and hemicellulose fractions to some extent, with significant loss of galactose, arabinose and mannose residues at the ripe stage. Much of the soluble glucose accumulated in ripe fruit was probably due to starch hydrolysis, as also corroborated by the concomitant disappearance of starch in the ripe fruit and by the [^{14}C] incorporation into the sugar fractions. Majority of the carbohydrate polymeric fractions showed drastic reduction in abundance and molecular weight from unripe to ripe stage, indicating extensive *in situ* depolymerization during ripening.

Structural characterization revealed (a) the major CWS fractions to be a 1→4 linked galactan, which was occasionally involved in side chain branches consisting of single residues of galactose and/or arabinose or oligomeric 1→5 linked arabinofuranose residues, linked through 1→3 linkages, (b) the major HWS fractions were of arabinogalactan-type, and (c) the major hemicellulosic fractions to be of xyloglucan-type having 1→4 and 1→3-linked glucan main chain, which were further involved in extensive branching. Both arabinose and xylose constitute the side chain branch off residues, with xylosyl units being involved in additional branching.

Except for PME, all other carbohydrate hydrolases registered a peak in activity at the climacteric stage, while gluconeogenic enzymes showed a steady increase in activity throughout the ripening phase. Apart from amylase and pectinase, glycanases like mannanase, galactanase and arabinanase appeared crucial for mango ripening. Among glycosidases, α-mannosidase was the most active enzyme, which is reported for the first time in mango fruit.

Endogenous mannan solubilization was more pronounced in ripening mango. Considerable endogenous mannan hydrolysis at the ripe stage in hemicellulose, pectic and water-soluble fractions was observed. Both mannanase and α-mannosidase, implicated in mannan solubilization, exhibited a peak in the activity around climacteric stage of ripening.

Total α-mannosidase activity of mango (and banana) was resolved into two distinct peaks (I and II) upon ion exchange as well as gel permeation chromatography. Isoform I was the major enzyme (80%) in both the fruits. Both the isoforms were thermally stable and showed more acidic pH optima of 4.8 as compared to banana, 5.8. The km for pNP α-mannopyranoside was much lower for isoform I in both the fruits indicating its higher substrate affinity and therefore higher specific activity. They did not catalyze the hydrolysis of pNP-β-mannopyranoside. Interestingly, α-mannosidase of banana fruit acted on β-D-mannan. The enzyme from mango was inhibited only to the extent of about 40% by Hg^{2+}, Cu^{2+}, Zn^{2+} and Mg^{2+} (at 1 μM level) while Cu^{2+}, Fe^{2+} and Hg^{2+} showed significantly higher inhibitory action on α-mannosidase of banana pulp.

A successful attempt on repetitive and proliferative somatic embryogenesis was achieved using nucellar and cotyledonary explants in different genotypes of Alphonso variety. Media composition for further organization of embryogenic callus to embryos, their development, maturation and germination leading to the formation of shoot/root was developed. Each stage of embryogenic tissue, starting from proembryogenic cell mass to fully developed somatic embryo was tested for their amenability for genetic transformation where both stage of the culture and genotype played a crucial role. High frequency transformation was observed after infecting cotyledonary and nucellar explants with *A.tumefaciens* cultured with acetosyringone. The expression of GUS gene in mango serves as a basis for studies

on antisense RNA technology for the major glycosidase, for the improvement of fruit texture and in turn to delay the fruit ripening.

In conclusion, the present study has paved the way for a better understanding of the basic processes involved in fruit ripening in mango cv. Alphonso, with specific reference to the relationship between carbohydrate hydrolysis *in vivo* and the activity of hydrolytic enzymes. Changes in the cell wall polysaccharides of fruits play a major role in the maintenance of fruit texture and in the softening process. Carbohydrate regulation at cell wall level during ripening is important in the context of fruit softening. Specific control of pectin as well as hemicellulose degradation during ripening may be a more promising approach than post harvest preservation. These findings may provide new opportunities to improve the shelf life characteristics of mango through genetic engineering, and possibly such a study might have greater societal implications.

Significant highlights of the present research

1. There is a clear correlation between textural softening, microscopic observation, and changes in biochemical components (starch, pectin, water and alkali soluble polysaccharides, soluble galacturonide, alcohol insoluble solids, physiological loss in weight, pH, total soluble solids, total sugar content and also a climacteric rise in carbohydrate hydrolyzing enzymes) during ripening of mango.

2. Other than EDTA-solubles, CWS, HWS and hemicelluloses are the major polysaccharides that undergo drastic degradation during ripening. This suggests that pectic as well as hemicellulose polysaccharides are implicated in tissue softening.

3. Carbohydrate degradation is accompanied by release of small molecular weight polymers, loss of neutral sugars and concomitant increase in the level of total sugar in alcohol-soluble fraction.

4. A drastic drop in molecular weight along with a concomitant loss of both acidic and neutral sugar residues was noticed in all the polymeric fractions, which indicated extensive depolymerization especially of pectic and hemicellulose polysaccharides during ripening.

5. By methylation analysis (GC-MS), FTIR and NMR, the primary structures of the major CWS (arabinogalactan-type), HWS (arabinogalactan-type) and hemicellulose (xyloglucan-type) polysaccharides were established.

6. Except for PME, all other carbohydrate hydrolases registered a peak in activity at the climacteric stage, while gluconeogenic enzymes showed a steady increase in activity throughout the ripening phase.

7. β-Endomannanase and α-mannosidase were found to be the most active enzymes in mango fruit. Both are implicated in mannan solubilization.

8. The two isoforms of α-mannosidase were resolved by ion exchange chromatography and partially purified by gel permeation chromatography. They differed in their physicochemical characteristics and molecular weight.

9. Repetitive and proliferative somatic embryogenesis was achieved using nucellar and cotyledonary explants in different genotypes of Alphonso variety.

10. Expression of GUS gene via *Agrobacterium tumefaciens* mediated transformation in mango serves as a basis for studies on antisense RNA technology.

Bibliography

1. AACC, American Association of Cereal Chemists. (2000). Visco amylograph. Approved methods of the AACC 22-10.

2. Abbott, J. A., Watada, A. E. and Massie, D. R. (1984). Sensory and instrument measurement of apple texture. *J. Amer. Soc. Hort. Sci.* **109**: 221-228.

3. Abu-Sarra, A. F. and Abu-Goukh, A. A. (1992). Changes in pectinesterase, polygalacturonase and cellulase activity during mango fruit ripening. *J. Hort. Sci.* **67**: 561-568.

4. Agrawal, K. M. and Bahl, O. P. (1968). Glycosidases of Phaseolus vulgaris. II. Isolation and general properties. *J. Biol. Chem.* **243**: 103-111.

5. Ahmed, A. E. R. and Labavitch, J. M. (1980a). Cell wall metabolism in ripening fruit. I. Cell wall changes in ripening ' Bartlett' pears. *Plant Physiol.* **65**: 1009-1013.

6. Ahmed, A. E. R. and Labavitch, J. M. (1980b). Cell wall metabolism in ripening fruit. II. Changes in carbohydrate-degrading enzymes in ripening 'Bartlett' pears. *Plant Physiol.* **65**: 1014-1016.

7. Ahmed, E. M. and Dennison, R. A. (1971). Texture profile of irradiated mangoes and peaches. *J. Texture Studies.* **2**: 489-496.

8. Aina, J. O. and Oladunjoye, O. O. (1993). Respiration, pectolytic activity and textural changes in ripening African mango (*Irvingia gabonensis*) fruits. *J. Sci. Food Agric.* **63**: 451-454.

9. Aitkin, S., Horgan, K. J. and Thorpe, T. A. (1981). Influence of explant selection on shoot forming capacity of juvenile tissue of *Pinusradiata*. *Can. J. For. Res.* **11**: 112-117.

10. Albersheim, P. (1975). The walls of growing plant cells. *Sci. Am.* **232**: 80-95.

11. Albright, L. M., Leroux, B., Yanofsky, M. F., Ma, D. and Nester, E. W. (1987). Processing of the T-DNA of *Agrobacterium tumefaciens* generates a single-stranded linear DNA intermediate. *J. Bacteriol.* **169**: 1046-1055.

12. Ali, Z. M., Armugam, S. and Lazan, H. (1995). β-Galactosidase and its significance in ripening mango fruit. *Phytochem.* **38**: 1109-1114.

13. Aman, P. and Westerlund, E. (1996). Cell wall polysaccharides: Structural, chemical, and analytical aspects. In: *Carbohydrates in Food*. Eliasson, A-C (ed.). Marcel Dekker, Inc. New York. pp. 191-226.

14. Ammirato, P. V. (1983). Somatic embryogenesis, In: *Handbook of plant cell culture*. Evans, D.A., Sharp, W. R., Ammirato, P. V. and Yamada, Y. (eds.). Vol. **1**. MacMillan, New York. pp. 82-183.

15. Ammirato, P. V. and Steward, F. C. (1971). Some effects of the environment on the development of embryos from cultured free cells. *Bot. Gaz*. **132**: 149-158.

16. Anderson, D. M. W. and Stoddard, J. F. (1966). Studies on uronic acid materials. *Carbohydr. Res.* **2**: 104-114.

17. Anderson, D. M. W., Bell, P.C., and McNab, C.G.A. (1971). An analytical study of some Acacia gum exudates of the series Botrycephalae. *Carbohydr. Res.* **20**: 269-274.

18. AOAC. Official methods of analysis of the Association of Analytical Chemists. (2000) 17th Ed. Method: 932.12.

19. Ara, H., Jaiswal, U. and Jaiswal, V. S. (2000). Plant regeneration from protoplasts of mango (*Mangifera indica* L.) through somatic embryogenesis. *Plant Cell Rep.* **19**: 622-627.

20. Ashraf, M., Khan, N., Ahmed, M. and Elahi, M. (1981). Studies on the pectinesterase activity and some chemical constituents of some Pakistani mango varieties during storage-ripening. *J. Agric. Food Chem.* **29**: 526-528.

21. Aspinall, G. O. (1959). In: *Advances in Carbohydrate chemistry* (Wolfrom, M. L. and Tipson, R. S., (eds.), vol. **14**, p. 448. Academic Press, New York.

22. Aspinall, G. O. (1980). Chemistry of cell wall polysaccharides. In: *The Biochemistry of Plants*. Preiss, J. (ed.). Academic Press, Inc. New York. Vol. **3**. pp. 473-500.

23. Awad, M. and Yang, R. E. (1979). Postharvest variation in cellulase, polygalacturonase and pectinmethylesterase in avocado (*Persea americana* Mill, cv. Fuerte) fruits in relation to respiration and ethylene production. *Plant Physiol*. **64**: 306-308.

24. Bahl, O. P. and Agrawal, K. M. (1969). Glycosidases of Aspergillus niger. I. Purification and characterization of alpha- and beta-galactosidases and beta-N-acetylglucosaminidase. *J. Biol. Chem*. **244**: 2970-2978.

25. Bansal, K. C. (2000). Biotechnology for improving product quality in horticultural crops. In: *Biotechnology in Horticultural and Plantation Crops*. Chadha, K. L, Ravindran. P. N and Leela Sahijram (eds.). Malhotra Publishing House, New Delhi, India. pp. 201-218.

26. Barrett, A. J. and Northcote, D. H. (1965). Apple fruit pectic substances, *Biochem. J.* **94**: 617-627.

27. Barrett, D. M., Garcia, E. and Wayne, J. E. (1998). Textural modification of processing tomatoes. *Crit. Rev. Food Sci. Nutr.* **38**: 173-258.

28. Bartolome, L.G. and Hoff, J. E. (1972). Firming of potatoes: Biochemical effects of preheating. *J. Agric. Food Chem.* **20**: 266-271.

29. BeMiller, J. N. (1986). An introduction to pectins: Structure and properties. In: Chemistry and Function of Pectins. Fishman, M. L and Jen, J. J. (eds.). Amer. Chem. Soc., Washington D.C., pp. 2-12.

30. Ben-Arie, R., Kislev, N. and Frenkel, C. (1979a). Ultrastructural changes in the cell walls of ripening apple and pear fruit. *Plant Physiol.* **64**: 197-202.

31. Ben-Arie, R., Sonego, L. and Frenkel, C. (1979b). Changes in pectic substances in ripening pears. *J. Amer. Soc. Hort. Sci.* **104**: 500-505.

32. Bernfeld, P. (1955). Amylases, a and b. *Methods in Enzymology*, **1**: 149-158.

33. Bhagylakshmi, N., Prabha, T. N., Yashoda, H. M., Prasanna, V., Jagadeesh, B. H and Tharanathan, R. N (2002). Biochemical studies related to textural regulation during ripening of banana and mango fruit. *Acta Hort.* **575**: 717-724.

34. Blake, J. D., Murphy, P. T. and Richards, G. N. (1971). Isolation and A/B classification of hemicelluloses. *Carbohydr. Res.* **16**: 49-57.

35. Blumenkrantz, N. and Asboe-Hansen, G. (1973). New method for quantitative determination of uronic acids. *Anal. Biochem.* **54**: 484-489.

36. Bolten, G. W., Nester, E. W. and Gordon, M. P. (1986). Plant phenolic compounds induce expression of *Agrobacterium tumefaciens* loci needed for virulence. *Science*. **232**: 983-985.

37. Boothby, D. (1983). Pectic substances in developing and ripening plum fruits. *J. Sci. Food Agric.* **34**: 1117-1122.

38. Bouranis, D. L. and Niavis, C. A. (1992). Cell wall metabolism in growing and ripening stone fruits. *Plant Cell Physiol.* **33**: 999-1008.

39. Bradford, M. M. (1976). A rapid and sensitive method for the quantification of microgram quantities of protein utilizing the principle of protein-dye binding. *Anal. Biochem.* **72**: 248-254.

40. Brady, C. J. (1987). Fruit ripening. *Ann. Rev. Plant Physiol.* **38**: 155-178.

41. Brinson, K., Dey, P. M., John, M. A. and Pridham, J. B. (1988). Post-harvest changes in *Mangifera indica* mesocarp cell walls and cytoplasmic polysaccharides. *Phytochem.* **27**: 719-723.

42. Brownleader, M. D., Jackson, P., Mobasheri, A., Pantelides, A. T., Sumar, S., Trevan, M. and Dey, P. M. (1999). Molecular aspects of cell wall modifications during fruit ripening. *Crit. Rev. Food Sci. Nutr.* **39**: 149-164.

43. Burns, J. K. and Baldwin, E. A. (1994). Glycosidase activities in grapefruit flavedo, albedo and juice vesicles during maturation and senescence. *Physiol. Plant.* **90**: 37-44.

44. Button, J. and Kochba, J. (1977). Tissue culture in the citrus industry. In: *Applied and fundamental aspects of plant cell, tissue and organ culture.* Reinert, J. and Bajaj, Y. P. S. (eds.). Springer-Verlag. Berlin-Heidelberg. pp. 70-92.

45. Carey, A. T., Holt, K., Picard, S., Wilde, R., Tucker, G. A., Bird, C. R., Schuch, W. and Seymour, G. B. (1995). Tomato exo-(1-4)-β-D-galactanase. *Plant Physiol.* **108**: 1099-1107.

46. * Carpita, N. C. and Gibeaut, D. M. (1993). Structural models of primary cell walls in flowering plants: consistency of molecular structure with the physical properties of the walls during growth. *Plant J.* **3**: 1-30.

47. Carrington, C. M. S., Greve, C. L. and Labavitch, J. M. (1993). Cell wall metabolism in ripening fruit VI. *Plant Physiol.* **103**: 429-434.

48. Chan, H. T. Jr. and Tam, S. Y. T. (1982). Partial separation and characterization of papaya endo- and exo- polygalacturonase. *J. Food Sci.* **47**: 1478-1483.

49. Chang, C. Y., Tsai, Y. R. and Chang, W. H. (1993). Models for the interactions between pectin molecules and other cell-wall constituents in vegetable tissues. *Food Chem.* **48**: 145-157.

50. Clarke, A. B. and Clarke, B. A. (1987). 'A description of preharvest factors affecting yield in mango (*Mangifera indica* L.) in mangoes' – a review. Commonwealth Science Council.

51. Coimbra, M. A., Barros, A., Barros, M., Rutledge, D. N. and Delgadillo, I. (1998). Multivariate analysis of uronic acid and neutral sugars in whole pectic samples by FT-IR spectroscopy. *Carbohydr. Polym.* **37**: 241-248.

52. Coimbra, M. A., Barros, A., Rutledge, D. N. and Delgadillo, I. (1999). FTIR Spectroscopy as a tool for the analysis of olive pulp cell-wall polysaccharide extracts. *Carbohydr. Res.* **317**: 145-154.

53. Colquhoun, I. J., de Ruiter, G. A., Schols, H. A. and Voragen, A. G. J. (1990). Identification by n. m. r. spectroscopy of oligosaccharides obtained by treatment of the hairy regions of apple pectin with rhamnogalacturonase. *Carbohydr. Res.* **206**: 131-144.

54. Crookes, P. R. and Grierson, D. (1983). Ultrastructure of tomato fruit ripening and the role of polygalacturonase isoenzymes in cell wall degradation. *Plant Physiol.* **72**: 1088-1093.

55. Cruz-Hernandez, A. W., Town, L., Cavallaro, A. S. and Botella (1999). Transient and stable transformation in mango by particle bombardment. Sixth Intl. Mango Symp. Working Abstr., Thailand. pp. 39.

56. * Cutillas-Iturralde, A., Zarra, I. and Lorences, E. P. (1993). Metabolism of cell wall polysaccharides from persimmon fruit: Pectin solubilization during fruit ripening occurs in the apparent absence of polygalacturonase activity. *Physiol Plant.* **89**: 369-375.

57. Dahlqvist, A. (1964). Methods for assay of intestinal disaccharidases. *Anal. Biochem.* **7**: 18-25.

58. Daniel Lane, M., Chang, H. C. and Miller, R. S. (1969). Phosphoenolpyruvate carboxykinase from pig liver mitochondria. *Methods in Enzymology*, **13**: 270-277.

59. Davis, E. A., Derouet, C. and Du Penhoat, C. H. (1990). Isolation and N.M.R. study of pectins from flax (*Linum usitatissimum* L.). *Carbohydr. Res.* **197**: 205-215.

60. * De Veau, E. J. I. (1993). Degradation and solubilization of pectin by β-galactosidases purified from avocado mesocarp. *Physiol Plant.* **87**: 279-285.

61. De Vries J. A., den Uijl, C. H., Voragen, A.G.J., Rombouts, F. M. and Pilnik, W. (1983). Structural features of the neutral side chains of apple pectic substances. *Carbohydr. Polym.* **3**: 193-205.

62. De Vries, J. A., Voragen, A. G. J., Rombouts, F. M. and Pilnik, W. (1984). Changes in the structure of apple pectic substances during ripening and storage. *Carbohydr. Polym.* **4**: 3-14.

63. De Vries, J. A., Voragen, A. G. J., Rombouts, F. M. and Pilnik, W. (1986). Structural studies of apple pectins with pectolytic enzymes. In: *Chemistry and Function of Pectins.* Fishman, M. L and Jen, J. J. (eds.). Amer. Chem. Soc., Washington D.C., pp. 38-48.

64. Debergh, P. C., Aitken–Christie, J., Cohen, D., Grout, B., Von Arnold, S., Zimmerman, R. and Ziv, M. (1992). Reconsideration of the term'vitrification' as used in micropropagation. *Plant Cell Tiss. Org. Cult.* **30**: 135-140.

65. DeWald, S. G., Litz, R. E. and Moore, G. A. (1989a). Optimizing somatic embryo production in mango. *J. Amer. Soc. Hort. Sci.* **114**: 712-716.

66. DeWald, S. G., Litz, R. E. and Moore, G. A. (1989b). Maturation and germination of mango somatic embryos. *J. Amer. Soc. Hort. Sci.* **114**: 712-716.

67. * Dey, P. M. and Dixon, R. A. (1985). Biochemistry of Storage Carbohydrates in Green Plants. Academic Press Inc., London.

68. Dick, A. J. and Labavitch, J. M. (1989). Cell wall metabolism in ripening fruit. IV. Characterization of the pectic polysaccharides solubilized during softening of 'Bartlett' pear fruit. *Plant Physiol.* **89**: 1394-1400.

69. * Dick, A. J., Opuku-Gyanifua, A. and DeMacro, A. C. (1990). Glycosidases of apple fruit: A multifunctional β-galactosidase. *Physiol. Plant.* **80**: 250-256.

70. Doesburg, J. J. (1965). Pectic Substances in Fresh and Processed Fruits and Vegetables. I.B.V.T. communication, Wageningen, The Netherlands.

71. Doner, L. W. (1986). Analytical methods for determining pectin composition. In: *Chemistry and Function of Pectins*. Fishman, M. L and Jen, J. J. (eds.). Amer. Chem. Soc., Washington D.C., pp. 13-21.

72. Doreyappa Gowda, I. N. and Huddar, A. G. (2001). Studies on ripening changes in mango (*Mangifera indica* L.) fruits. *J. Food Sci. Technol.* **38**: 135-137.

73. Dubois, M., Gilles, K. A., Hamilton, J. K., Rebers, P. A. and Smith, F. (1956). Colorimetric method for determination of sugars and related substances. *Anal. Chem.* **28**: 350-356.

74. El-Ansari, M. A., Reddy, K. K., Sastry, K. N. S. and Naymdamma, Y. (1969). Polyphenolic constituents of mango (*Mangifera indica* L.) fruit, Leather Sci. **16**: 13-18.

75. El-Otmani, M and Coggins, C. W. Jr. (1985). Fruit age and growth regulator effect on the quantity and structure of the epiculticular wax of 'Washington' Navel orange fruit. *J. Amer. Soc. Hort. Sci.* **110**: 371-378.

76. El-Zoghbi, M. (1994). Biochemical changes in some tropical fruits during ripening. *Food Chem.* **49**: 33-37.

77. Emons, A. M. C., Mulder, M. M. and Kieft, H. (1993). Pyrolysis mass spectrometry of developmental stages of maize somatic embryos. *Acta Bot Neerlandica.* **42**:319-339.

78. FAO, Production Yearbook, Food and Agricultural Organization, Rome. (1999). Food and Agricultural organization of the United Nations. Rome. Italy.

79. Fares, K., Renard, C. M. G. C., R'zina, Q. and Thibault, J-F. (2001). Extraction and composition of pectins and hemicelluloses of cell walls of sugar beet roots grown in Morocco. *Int. J. Food Sci. Technol.* **36**: 35-46.

80. Femenia, A., Sanchez, E. S., Simal, S. and Rosello, C. (1998). Developmental and ripening-related effects on the cell wall of apricots (*Prunus armeniaca*) fruit. *J. Sci Food Agric.* **77**: 487-493.

81. Filippov, M. P. (1992). Practical infrared spectroscopy of pectic substances. *Food Hydrocolloids* **6**: 115-142.

82. Fils Lycaon, B. and Buret, M. (1991). *Postharvest Biol. Technol.* **1**: 143.

83. Fils-Lycaon, B. and Buret, M. (1990). Loss of firmness and changes in pectic fractions during ripening and overripening of sweet cherry. *Hort. Sci.* **25**: 777-778.

84. Fisher, R. L. and Bennett, A. B. (1991). Role of cell wall hydrolases in fruit ripening. *Ann. Rev. Plant Physiol. Plant Mol. Biol.* **42**: 675-703.

85. Fishman, M. L., Pepper, L., Damert, W. C., Phillips, J. G. and Barford, R. A (1986). A critical reexamination of molecular weight and dimensions for citrus pectins. In: *Chemistry and Function of Pectins.* Fishman, M. L and Jen, J. J. (eds.). Amer. Chem. Soc., Washington D.C. pp. 22-37.

86. Frenkel, C., Klein, I. and Dilley, D. R. (1968). Protein synthesis in relation to ripening of pome fruit. *Plant Physiol.* **43**: 1146-1153.

87. Fry, S. C. (1982). Phenolic components of the primary cell wall. Feruloylated disaccharides of D-galactose and L-arabinose from spinach polysaccharide. *Biochem J.* **203**: 493-504.

88. Fry, S. C. (1986). Cross-linking of matrix polymers in the growing cell walls of angiosperms. *Ann. Rev. Plant Physiol.* **37**: 165-186.

89. Fry, S. C. (1995). Polysaccharide-modifying enzymes in the plant cell wall. *Ann. Rev. Plant Physiol. Plant Mol. Biol.* **46**: 497-520.

90. Fuchs, Y., Pesis, E. and Zauberman, G. (1980). Changes in amylase activity, starch and sugar contents in mango fruit pulp. *Sci. Hort.* **13**: 155-160.

91. Fujimura, T. and Komamine, A. (1975). Mode of action of 2,4-D and zeatin on somatic embryogenesis in a carrot cell suspension culture. *Z. Pflanzenphysiol.* **99**: 1-8.

92. Gamage, T. V. and Rehman, M. S. (1999). Post harvest handling of foods of plant origin. *Handbook of Food Preservation.* In: Rehman, M. S. (ed.). Marcel Dekker Inc., New York. pp. 11-46.

93. Gamborg, O. L., Miller, R. A. and Ojima, K. (1968). Plant cell Cultures. I. Nutrient requirements of suspension cultures of soybean root cells. *Exp. Cell. Res.* **50**: 151-158.

94. George, E. F. (1993). Plant propagation by tissue culture part I. The technology. 2 ed. Edington: Exigetics, 574.

95. Gholap, A. S. and Bandyopadhyay, C. (1975). Comparitive assessment of aromatic principles of ripe Alphonso and Langra mango. *J Food Sci. Technol.* **12**: 202-207.

96. Gibbs, M. and Turner, J. F. (1964). Modern methods in plant analysis, by Peach, K. and Tracey, M. V. Springer-Verlag, Berlin-Gottingen, Heidelberg, Vol. **7**, 525.

97. Giovannoni, J. J., DellaPenne, D., Bennett, A. B. and Fischer, R. L. (1989). Expression of a chimeric polygalacturonase gene in transgenic rin (ripening inhibitor) tomato fruit results in polyuronide degradation but not fruit softening. *Plant Cell.* **1**: 53-63.

98. Gomez-Lim, M. A. (1997). Postharvest physiology. In: *The Mango; Botany, Production and Uses*. Litz, R. E. (ed.). CAB International, Florida. pp. 425-445.

99. Gortner, W. A. (1967). International facets of USDA nutrition research. *J Am Diet Assoc.* **50**: 279-83.

100. Gosh, S. (1960). The content of folic acid and its conjugates in some common Indian fruits. *Science and Culture*. **26**: 287-292.

101. Grant, G. T., Morris, E. R., Rees, D. A., Smith, P. J. C. and Thom, D. (1973). Biological interactions between polysaccharides and divalent cations: The Egg-Box model. *FEBS Letters* **32**: 195-198.

102. Gray, J., Picton, S., Shabbeer, J., Schuch, W. and Grierson, D. (1992). Molecular biology of fruit ripening and its manipulation with antisense genes. *Plant Mol. Biol.* **19**: 69-87.

103. Grierson, D., Tucker, G. and Robertson, N.G. (1981). The molecular bilogy of ripening. In:*Recent advances in the biochemistry of fruit and vegetables.* Friend, J. and Rhods, M. J. C. (eds.). Academic press. New York. Pp. 149-160.

104. Gross, K. C. (1984). Fractionation and partial characterization of cell walls from normal and non-ripening mutant tomato fruit. *Physiol. Plant.* **62**: 25-32.

105. Gross, K. C. and Sams, C. E. (1984). Changes in cell wall neutral sugar composition during fruit ripening: A Species survey. *Phytochem.* **23**: 2457-2461.

106. Gross, K. C. and Wallner, S. J. (1979). Degradation of cell wall polysaccharides during tomato fruit ripening. *Plant Physiol.* **63**: 117-120.

107. Gross, K. C., Watada, A. E., Kang, M. S., Kim, S. D., Kim, K. S. and Lee, S. W. (1986). Biochemical changes associated with the ripening of hot pepper fruit. *Physiol. Plant.* **66**: 31-36.

108. Gruppen, H., Hoffmann, R. A., Kormelink, F. J., Voragen, A. G., Kamerling, J. P., Vliegenthart, J. F. (1992). Characterisation by ^{1}H NMR spectroscopy of enzymically derived oligosaccharides from alkali-extractable wheat-flour arabinoxylan. *Carbohydr Res.* **233**: 45-64.

109. Hagerman, A. E. and Austin, P. J. (1986). Continuous spectrophotometric assay for plant pectin methyl esterase. *J. Agric. Food Chem.* **34**: 440-444.

110. Hakomori, S. I. (1964). A rapid permethylation of glycolipid, and polysaccharide catalyzed by methylsulfinyl carbanion in dimethyl sulfoxide. *J. Biochem.* (Tokyo) **55**: 205-208.

111. Hammerschlag, F. A., Owens, L. D. and Smigoki, A. C. (1989). *Agrobacterium*-mediated transformation of peach cells derived from mature plants that were propagated *in vitro*. *J. Amer. Soc. Hort. Sci.* **114**: 508-510.

112. Hassid, W. Z. and Neufeld, E. F. (1964). Quantitative determination of starch in plant tissues. *Methods Carbohydr. Chem.* **4**: 33-46.

113. Hayashi, T. and Maclachlan, G. (1984) Pea xyloglucan and cellulose. III. Metabolism during lateral expansion of pea epicotyl cells. *Plant Physiol.* **76**: 739-742.

114. Hegde, S. and Maness, N. O. (1996). Sugar composition of pectin and hemicellulose extracts of peach fruit during softening over two harvest seasons. *J. Amer. Soc. Hort. Sci.* **121**: 1162-1167.

115. Hegde, S. and Maness, N. O. (1998). Changes in apparent molecular mass of pectin and hemicellulose extracts during peach softening. *J. Amer. Soc. Hort. Sci.* **123**: 445-456.

116. Heredia, A. E. R., Guillen, R., Jimenez, A. and Fernandez Bolanos, J. (1993). *Z. Lebensn. Untersch. Forsch.* **196**: 147.

117. Hobson, G. E. (1968). Cellulase activity during the maturation and ripening of tomato fruit. *J. Food Sci.* **33**: 588-592.

118. Hobson, G. E. (1981). Enzymes and texture changes during ripening. In: *Recent Advances in the Biochemistry of Fruits and Vegetables*. Friend, J. and Rhodes, M. J. C., (eds.). Academic Press, London, pp. 123-132.

119. Hobson, G.E. and Grierson, D. (1993). Tomato. In: *Biochemistry of fruit ripening*. G.B. Seymour *et al*. (eds.). Chapman and Hall, London, pp. 405-442.

120. Hoffmann, R. A., Roza, M., Matt, J., Kamerling, J. P. and Vliegenthart, J. F. G. (1991). *Carbohydr. Polym.* **15**: 415-430.

121. Hoskins, D. D. and Mackenzie, C. G. (1961). Solubilization and Electron Transfer Flavoprotein Requirement of Mitochondrial Sarcosine Dehydrogenase and Dimethylglycine Dehydrogenase. *J. Biol. Chem.* **236**: 177-183.

122. Huber, D. J. (1983a). Polyuronide degradation and hemicellulose modifications in ripening tomato fruit. *J. Amer. Soc. Hort. Sci.* **108**: 405-409.

123. Huber, D. J. (1983b). The role of cell wall hydrolases in fruit softening. *Hort. Rev.* **5**: 169-219.

124. * Huber, D. J. (1984). Strawberry fruit softening: The potential roles of polyuronides and hemicelluloses. *J. Food Sci.* **49**: 1310-1315.

125. Huber, D. J. and Lee, J. H. (1986). Comparative analysis of pectins from pericarp and locular gel in developing tomato fruit. In: *Chemistry and Functions of Pectins*. Fishman, M and Jen, J. (eds.). Amer. Chem. Soc., Washington D.C., USA. pp. 141-156.

126. Huber, D. J. and O'Donoghue, E. M. (1993). Polyuronides in avocado (*Persea americana*) and tomato (*Lycopersicon esculentum*) fruits exhibit markedly different patterns of molecular weight downshifts during ripening. *Plant Physiol.* **102**: 473-480.

127. Huisman, M. M. H., Schols, H. A. and Voragen, A. G. J. (1996). Changes in cell wall polysaccharides from ripening olive fruits. *Carbohydr. Polym.* **31**: 123-133.

128. Hulme, A. C. (1970). In: *Biochemistry of fruits and their products.* Vols. **1** and **2**, Academic Press. Inc., London.

129. Hulme, A. C. (1971). The mango. In: *The Biochemistry of Fruits and their Products*. Vol. 2. Hulme, A. C. (ed.). Academic Press, London. pp. 233-254.

130. Hultin, H.O. and Levine, A.S. (1965). Pectin methyl esterase in the ripening banana. *J. Food Sci.* **30**: 917-921.

131. Hunter, G. L. K., Bucek, W. A. and Radfort, T. (1974). Volatile components of canned Alphonso mango. *J. Food Sci.* **39**: 900-903.

132. Imoto, T. and Yagishita, K. (1971). A simple activity measurement of lysozyme. *Agric. Biol. Chem.* **35**: 1154 -1156.

133. Isherwood, F. A. (1970). Hexosans, pentosans and Gums. In: The Biochemistry of Fruits and their Products. Vol. I. Hulme, A. C. (ed.). Academic Press, London. pp. 33-52.

134. Ishii, T. and Matsunaga, T. (2001). Pectic polysaccharide rhamnogalacturonan II is covalently linked to homogalacturonan. *Phytochem.* **57**: 969-974.

135. Iyer, C. P. A. (1991). Recent Advances in varietal improvement in mango. *Acta Horticulturae*. **291**: 109-132.

136. Jackman, R. L. and Stanley, D. W. (1995). Perspectives in the textural evaluation of plant foods. *Trends Food Sci. Technol.* **6**: 187-194.

137. Jain, N. L. (1961). Chemistry and Technology of mango. *Rev. Food Technology*. **3**: 131-135.

138. Jain, N. L., Krishnamurthy, G. V. and Lal, G. C. (1959). Non-volatile organic acids in unripe pickling mangoes and salted mango slices by paper chromatography. *Food Sci.* **3**: 115-118.

139. Jansson, P. E., Kenne, L., Liedgren, H., Lindberg, B. and Longren, J. (1976). A practical guide to the methylation analysis of carbohydrates. *Univ. Stockholm Chem. Commun.* **8**: 1-25.

140. Jefferson, R. A. (1987). Assaying chimeric genes in plants: The GUS gene fusion system. *Plant Mol. Biol. Rep.* **5**: 387-405.

141. Jimenez, A., Rodriguez, R., Fernandez-caro, I., Guillen, R., Fernandez-Bolanos, J. and Heredia, A. (2001). Olive fruit cells wall:

Degradation of Pectic polysaccharides during ripening. *J. Agric. Food Chem.* **49:** 409-415.

142. Johansen, D. A. (1940). *Plant Microtechnique*. McGraw Hill Co., New York.

143. John, M. A. and Dey, P. M. (1986). Postharvest changes in fruit cell wall. *Adv. Food Res.* **30**: 139-193.

144. Jungalwala, F. B. and Cama, H. R. (1963). Carotenoids in mango (*Mangifera indica*) fruit, *Indian J. Chem.* **1**: 36-41.

145. Kacurakova, M., Capek, P., Sasinkova, V., Wellner, N. and Ebringerova, A. (2000). FT-IR study of plant cell wall model compounds: Pectic polysaccharides and hemicelluloses. *Carbohydr. Polym.* **43**: 195-203.

146. Kader, A. A. (1980). Prevention of ripening in fruits by use of controlled atmosphere. *Food Technol.* **34**: 51-54.

147. Kader, A. A., Zagory, D. and Kerbel, E. L. (1989). Modified atmosphere packaging of fruits and vegetables. *Crit. Rev. Food Sci. Nutr.* **28**: 1-30.

148. Kalra, S. K., Tandon, D. K. and Singh, B. P. (1995). Mango. In: *Handbook of Fruit Science and Technology. Production, Composition, Storage and Processing.* Salunkhe, D. K., Kadam, S. S. (eds.). Marcel Dekker, Inc. New York, pp. 123-169.

149. Kamada, H. and Harada, H. (1979). Studies on organogenesis in carrot tissue cultures: II. Effects of amino acids and inorganic nitrogenous compounds on somatic embryogenesis. Z. *Pflanzenphysiol.* **91**: 453-463.

150. Keenan, M. H. J., Belton, P. S., Matthew, J. A. and Howson, S. J. (1985). A ^{13}C-n. m. r. study of sugar-beet pectin. *Carbohydr. Res.* **138**: 168-170.

151. Kertesz, Z. I. (1951). *The Pectic Substances*. Interscience Publishers Inc. New York.

152. Kikuchi, A., Satoh, S. and Fujii, T. (1992). Analysis of plant pectic substances by electrophoresis on cellulose acetate membrane. *Biosci. Biotech. Biochem.* **56**: 1144-1145.

153. Kintner, P. K. and Van Buren, J. P. (1982). Carbohydrate Interference and its correction in pectin analysis using the m-hydroxydiphenyl method. *J. Food Sci.* **47**: 756-759, 764.

154. Kiyosue, T., Satoh, S., Kamada, H. and Harada, H. (1993). Somatic embryogenesis in higher plants. *J. Plant Res.* **3**: 17-28.

155. Knee, M. (1973). Polysaccharide changes in cell walls of ripening apples. *Phytochem.* 12: 1543-1549.

156. Knee, M. (1978). Properties of polygalacturonate and cell cohesion in apple fruit cortical tissue. *Phytochem.* **17**: 1257-1260.

157. Knee. M., Fielding. A. H., Archer, S. A. and Laborda, F (1975). Enzymic analysis of cell wall structure in apple fruit cortical tissue. *Phytochem.* **14**: 2213-2222.

158. Knight, R. J. Jr. (1997). Important mango cultivars and their descriptors. In: *The Mango; Botany, Production and Uses*. Litz, R. E. (ed.). CAB International, Florida. pp. 545-565.

159. Kobata, A. (1979). Use of endo- and exoglycosidases for structural studies of glycoconjugates. *Anal. Biochem.* **100**: 1-14.

160. Kochba, J. P. and Spiegel-Roy. (1977) Cell and tissue culture for breeding and developmental studies of Citrus. Hort. Sci. **12**: 110-114.

161. Koh, T. H. and Melton, L. D. (1994). Analysis of papaya cell wall polysaccharides. *ASEAN Food J.* **9**: 101-106.

162. Kokini, J. L. and Chou, T. C. (1993). Comparison of the conformation of tomato pectins with apple and citrus pectins. *J. Texture Studies* **24**: 117-137.

163. * Kojima, K., Sakurai. N. and S. Kuraishi (1994). Fruit softening in banana: correlation among stress-relaxation parameters, cell wall components and starch during ripening. *Physiol. Plant.* **90**: 772-778.

164. Komari, T., Saito, Y., Nakakido, F., Kumashiro, T. (1989). Efficient selection of somatic hybrids in *Nicotiana tabacum* L. using a combination of drug-resistance markers introduced by transformation. *Theor. Appl. Genet.* **77**: 547-552.

165. Krall, S. M. and McFeeters, R. F. (1998). Pectin hydrolysis: effect of temperature, degree of methylation, pH and calcium on hydrolysis rates. *J. Agric. Food Chem.* **46**: 1311-1315.

166. Krikorian, A. D., Cronauer-Mitra, S. S. and Fitter Corbin, M. S. F. (1988). Protoplast culture of perennials. *Scientia Horticulturae* **37**: 277-293.

167. Krishnamurty, S., Patwardhan, M. V. and Subramanyam, H. (1971). Biochemical changes during ripening of the mango fruit. *Phytochem.* **10**: 2577-2581.

168. Lakshminarayan, S. (1980). Mango. In: *Tropical and subtropical fruits: Composition, Properties and Uses*. Nagy, S. and Shaw, P. E. (eds). AVI Publishing, Westport. p. 184-257.

169. Lakshminarayana, S., Subhadra, N. V. and Subramanyam, H. (1970). Some aspects of developmental physiology of mango fruit. *J. Hort. Sci.* **45**: 133-142.

170. Lang, C. and Dornenburg, H. (2000). Perspectives in the biological function and the technogical application of polygalacturonases. *Appl. Microbiol. Biotechnol.* **53**: 366-375.

171. Larkin, P. J. and Scowcroft, W. R. (1981). Somaclonal variation- a novel source of variability from cell cultures for plant improvement. *Theor. Appl. Genet.* **60**: 197-214.

172. Lazan, H., Ali, Z. M., Wah, L. K., Voon, J. and Chaplin, G. R. (1986). The potential role of polygalacturonase in pectin degradation and softening of mango fruit. *ASEAN Food J.* **2**: 93-98.

173. Lazo, G. R., Stein, P. A. and Ludwig, R. A. (1991). A DNA transformation-competent *Arabidopsis* genomic library in *Agrobacterium*. *Bio/Technology.* **9**: 963-967.

174. Leley, V. K., Narayan, N. and Daji, J. A. (1943). *Indian J. Agri. Sci.*. **13**: 291.

175. Li, Y. T. and Li, S. C. (1968). Studies on glycosidases in Jack bean meal. II. Separation of various glycosidases by isoelectric focusing. *J. Biol. Chem.* **243**: 3994-3996.

176. Li, Y. T. and Li, S. C. (1997), Biosynthesis and Catabolism of Glycosphingolipids, *J. Biol. Chem.* **52:** 235-286

177. Lindsey, K., Gallois, P. and Eady, C. (1991) Regeneration and transformation of sugarbeet by *Agrobacterium tumefaciens*. In: *Plant Tissue Culture Manual*, (ed. K. Lindsey), Kluwer Academic Publishers, Dordrecht B. **7**: 1-13.

178. Litz, R. E. (1984). *In vitro* somatic embryogenesis from nucellar callus of monoembryogenic mango. *Hort. Sci.* **19**: 715-717.

179. Litz, R. E. (1986a). Mango (*Mangifera indica* L.), p. 267-273. In: Bajaj, Y.P.S. (ed.). Biotechnology in agriculture and forestry. Vol. **1**. Trees. Springer-Verlag, Heidelberg, F.R.G.

180. Litz, R. E., (1986b). Effect of osmotic stress on somatic embryogenesis in *Carica* suspension cultures. *J. Amer. Soc. Hort. Sci.* **111**: 969-972.

181. Litz, R. E. (1988). *In vitro* somatic embryogenesis and plantlet regeneration from leaf callus of the tropical tree *Euphorian langan*. Stend. *J. Plant Physiol.* **132**: 190-194.

182. Litz, R. E. and Conover, R. A. (1982). *In vitro* somatic embryogenesis and plant regeneration from *Carica papaya* L. ovular callus. *Plant Sci. Lett.* **26**: 153-158.

183. Litz, R. E., Knight, R .J. and Gazit, S. (1984). *In vitro* somatic embryogenesis from *Mangifera indica* L. callus. *Scientia Hort.* **22**: 233-240.

184. Litz, R. E., Knight, R. K. and gazit, S. (1982). Somatic embryos from cultured ovules of *Mangifera indica* L. *Plant Cell Rep.* **1**: 264-266.

185. Litz, R. E., Mathews, H., Moon, P. A., Pliego-Alfaro, F., Yurgalevitch, C. and Dewald, S. G. (1993). Somatic embryos of mango (*Mangifera indica* L.) In: *SYNSEEDS: Applications of Synthetic Seeds to Crop Improvement.* (Redenbaugh, K. (ed). CRC Press, Boca Raton. Florida. USA. pp 409-425.

186. Liu, X., Shiomi, S., Nakatsuka, A., Yasutaka, K., Nakamura, R. and Inaba, A. (1999). Characterization of ethylene biosynthesis associated with ripening in banana fruit. *Plant Physiol.* **121**: 1257-1265.

187. Lizada. C. (1993). Mango. In: *Biochemistry of Fruit Ripening*. Seymour, G. B., Taylor, J. E., Tucker, G. A. (eds.) Chapman and Hall, London. pp. 255-271.

188. Lurie, S., Levin, A., Greve, C. and Labavitch, J. M. (1994). Pectic polymer changes in nectarines during normal and abnormal ripening. *Phytochem.* **36**: 11-17.

189. Mac Dougall, A. J., Brett, G. M., Morris, V. J., Rigby. N. M., Ridout. M. J. and Ring, S. G. (2001). The effect of peptide-pectin interactions on the gelation behaviour of a plant cell wall pectin. *Carbohydr. Res.* **335**: 115-126.

190. Machida, Y., Usami, S., Yamamoto, A., Niwa, Y. and Takebe, I. (1986). Plant-inducible recombination between the 25 bp border sequences of T-DNA in *Agrobacterium tumefaciens*. *Mol. Gen. Genet.* **204**: 374-382.

191. Maclachlan, G. and Brady, C. (1994). Endo-1,4-β-glucanase, xyloglucanase and xyloglucan endo-transglycosylase activities verses potential substrates in ripening tomato. *Plant physiol.* **105**: 965-974.

192. MacLeod, A. J. and Gonzalez, D. T. N. (1982). Volatile flavor components of mango fruit. *Phytochem.* **21**: 2523-2527.

193. McCann, M.C., Wells, B. and Roberts, K. (1990). Direct visualization of cross-links in the primary plant cell wall. *J. Cell. Sci.* **96**: 323-334.

194. Madhusudhan, B., Susheelamma, N. S. and Tharanathan, R. N. (1993). Studies on swet potatoes. II. Isolation and characterization of starch. *Staerke*. **45**: 8-12.

195. Mann, S. S., Singh, R. N. and Pandey, R. M. (1974). Maturity studies in Dashehari and Langra cultivars of mango, Haryana. *J. Hort. Sci*. **3**: 97-103.

196. Mante, S., Morgens, P. H., Scorza, R., Cordts, J. M. and Callahan, A. M. (1991). *Agrobacterium*-mediated transformation of plum (*Prunus domestica* L.) hypocotyl slices and regeneration of transgenic plants. *Bio Technology* **9**: 853-857.

197. Markwalder, H. U. and Neukom, H. (1976). Diferulic acid as a possible cross-link in hemicelluloses from wheat germ. *Phytochem*. 15 , 836-837.

198. Marsilio, V., Lanza, B., Campestre, C. and De Angelis, M. (2000). Oven-dried table olives: textural properties as related to pectic composition. *J. Sci. Food Agric*. **80**: 1271-1276.

199. Martin-Cabrejas, M. A., Waldron, K. W., Selvendran, R. R., Parker, M. L. and Moates, G. K. (1994). Ripening-related changes in the cell walls of Spanish pear (*Pyrus communis*). *Physiol. Plant.* **91**: 671-679.

200. Mathews, H., Bharathan, N., Litz, R. E., Narayanan, K. R., Rao, P. S. and Bhatia, C. R. (1990). The promotion of *Agrobacterium* mediated transformation in *Atropa belladonna* L. by Acetosyringone. *Plant Physiol*. **136**: 404-409.

201. Mathews, H., Litz, R. E., Wilde, H. D. and Wetzstein, H. Y. (1993). Genetic transformation of mango. *Acta Hort*. **341**: 93-97.

202. Mathews, H., Litz, R. E., Wilde, H. D., Merkle, S., and Wetzstein, H. Y. (1992). Stable integration and expression of β-glucuronidase and NPT II genes in mango somatic embryos. *In Vitro Cell. Dev. Biol.* 28P: 172-178.

203. Mathlouthi, M. and Koenig, J. L. (1986). Vibrational spectra of carbohydrates. *Adv. Carbohydr. Chem. Biochem.* **44**: 7-89.

204. Matta, K. L. and Bahl, O. P. (1972). Glycosidases of Aspergillus niger. IV. Purification and characterization of α-mannosidase. *J. Biol. Chem*. **247**: 1780-1787.

205. McKelvy, J. F. and Lee, Y. C. (1969). Microheterogeneity of the carbohydrate group of aspergillus oryzae alpha-amylase. *Arch. Biochem. Biophys*. **132**: 99-110.

206. McCann, M.C., Wells, B. and Roberts, K. (1990). Direct visualization of cross-links in the primary plant cell wall. *J. Cell. Sci.* **96**: 323-334.

207. McCleary. B. V. and Matheson, N. K. (1974). Alpha-D-galactosidase activity and galactomannan and galactosyl sucrose oligosaccharide in germinating legume seeds. *Phytochem.* **13**: 1747-1757.

208. McCollum, T. G., Huber, D. J. and Cantliffe, D. J. (1989). Modification of polyuronides and hemicellulose during muskmelon fruit softening. *Physiol. Plant.* **76**: 303-308.

209. * McCormick, (1991). The preembryo as potential: a reply to John A. Robertson. *Kennedy Inst Ethics J.* **1**: 303-5.

210. McGranahan, G. H., Leslie, C. A., Uratsu, S. L., Martin, L. A. and Dandekar, A. M. (1988). *Agrobacterium*-mediated transformation of walnut somatic embryos and regeneration of transgenic plants. *Bio/Technology*. **6**: 800-804.

211. McNeil, M., Darvill, A. G., Fry, S. and Albersheim, P. (1984). Structure and function of the primary cell walls of plants. *Ann. Rev. Biochem.* **53**: 625-663.

212. Medlicott, A. P., Sigrist, S. M. M. Reynolds, S. B. and Thompson, A. K. (1986). Effect of ethylene and acetylene on mango fruit ripening. *Ann. Appl. Biol.* **111**: 439-444.

213. Miller, G. L. (1959). Use of dinitrosalicylic acid reagent for determination of reducing sugar. *Anal. Biochem.* **31**: 426-428.

214. Missang, C. E., Renard, C. M. G. C., Baron, A. and Drilleau, J-F. (2001a). Cell wall polysaccharides of bush butter (*Dacryodes edulis* (Don, G and Lam, H. J.) fruit pulp and their evolution during ripening. *J. Sci. Food Agric.* **81**: 773-780.

215. Missang, C. E., Renard, C. M. G. C., Baron, A. and Drilleau, J-F. (2001b). Changes in the pectic fraction of bush butter (*Dacryodes edulis* (Don, G and Lam, H. J.) fruit pulp during ripening. *J. Sci. Food Agric.* **81**: 781-789.

216. Mitcham, E. J. and McDonald, R. E. (1992). Cell wall modification during ripening of 'Keitt' and 'Tommy Atkins' mango fruit. *J. Amer. Soc. Hort. Sci.* **117**: 919-924.

217. Mitcham, E. J., Lynn, A. J. and Prescott, D. M. (1992). Analysis of a scrambled gene: the gene encoding alpha-telomere-binding protein in Oxytricha nova. *Genes Dev.* **6**: 788-800.

218. Monsalud, M. J., Mathews, H., Litz, R. E. and Gray, D. J. (1995). Control of hyperhydricity of mango somatic embryos. *Plant Cell, Tissue and Organ Culture*. **42**: 195-206.

219. Mort, A. J., Moerschbacher, B. M., Pierce, M. L. and Maness, N. O. (1991). Problems encountered during the extraction, purification, and chromatography of pectic fragments, and some solutions to them. *Carbohydr. Res*. **215**: 219-227.

220. Muda, P., Seymour, G. B., Errington, N. and Tucker, G. A. (1995). Compositional changes in cell wall polymers during mango fruit ripening. *Carbohydr. Polym.* **26**: 255-260.

221. Mukherjee, S. K. (1997). Introduction: Botany and Importance. In: *The Mango; Botany, Production and Uses*. Litz, R. E. (Ed.). CAB International, Florida. pp. 1-19.

222. Mullins, M. G., Tang, F. C. A. and Facciotti, D. (1990). *Agrobacterium*-mediated genetic transformation of grapevines: transgenic plants of *Vitis rupestris* Scheele and buds of *Vitis vinifera* L. *Bio/Technology*. **8**: 1041-1045.

223. Murashige, J. and Skoog, F. (1962). A revised medium for rapid growth and bioassays with tobacco tissue cultures. *Physiol.Plant*. **15**: 473-497.

224. Muyonga, J. H., Ramteke, R. S. and Eipeson, W. E. (2001). Prehydration steaming changes – physicochemical properties of unripe banana flour. *J. Food Process Preserv*. **25**: 35-47.

225. Nakagawa, H., Enomoto, N., Asakawa, M. and Uda, Y. (1988). *Agric. Biol. Chem.* **52**: 2223.

226. Nakagawa, Y. and Takahashi, N. (1977). α-Mannosidase from pineapple fruit: partial purification and action on glycopeptides. *Agri. Biol. Chem.* **41**: 455-460.

227. Neal, G. E. (1965). Changes occurring in the cell walls of strawberries during ripening. *J. Sci. Food Agric.* **16**: 604-611.

228. Nehra, N. S., Chibbar, R. N.. Kartha, K. K.. Datla, R. S. S., Crosby, W. L. and Stushnoff, C. (1990) *Agrobacterium*-mediated transformation of strawberry calli and recovery of transgenic plants. *Plant Cell Reports***. 9**: 10-13.

229. Newman, R. H. and Redgwell, R. J. (2002). Cell wall changes in ripening kiwifruit: ^{13}C solid state NMR characterization of relatively rigid cell wall polymers. *Carbohydr. Polym.* **49**: 121-129.

230. Nogata, Y., Ohta, H. and Voragen, A. G. J. (1993). Polygalacturonase in strawberry fruit. *Phytochem.* **34**: 617– 620.

231. Nonogaki, H. and Morohashi, Y. (1996). An Endo-β-mannanase develops exclusively in the micropylar endosperm of tomato seeds prior to radicle emergence. *Plant Physiol.* **110**: 555-559.

232. Nunan, K. J., Sims, I. M., Bacic, A., Robinson, S. P. and Fincher, G. B. (1998). Changes in cell wall composition during ripening of grape berries. *Plant Physiol.* **118**: 783-792.

233. Nwanekezi, E. C., Alawuba, O. C. G. and Mkpolulu, C. C. M. (1994). Characterization of pectic substances from selected tropical fruits. *J. Food Sci. Technol.* **31**: 159-161.

234. O'Donoghue, E. M., Somerfield, S. D., De Vre, L. A. and Heyes, J. A. (1997). Developmental and ripening-related effects on the cell wall of Pepino (*Solanum muricatum*) fruit. *J. Sci. Food Agric.* **73**: 455-463.

235. O'Neill, M. A., Warrenfeltz, D., Kates, K., Pellerin, P., Doco, T., Darvill, A. G. and Albersheim, P. (1996). Rhamnogalacturonan-II, a pectic polysaccharides in the walls of growing plant cell, forms a dimer that is covalently cross-linked by a borate ester. *in vitro* conditions for the formation and hydrolysis of the dimer. *J. Biol. Chem.* **271**: 22923-22930.

236. Ochoa, S., Mehler, A. H., and Kornberg, A. (1948). Biosynthesis of dicarboxylic acid by CO_2 fixation: I. Isolation and properties of an enzyme from pigeon liver catalyzing the reversible oxidative decarboxylation of L-malic acid. *J. Biol. Chem.* **24**: 111-115.

237. Oesterveld, A., Beldman, G., Schols, H, A. and Voragen, A. G. J. (2000). Characterization of arabinose and ferulic acid rich pectic polysaccharides and hemicelluloses from sugar beet pulp. *Carbohydr. Res.* **328**: 185-197.

238. Ohtani, O. and Misaki, A. (1983). Purification and characterization of β-D-galactosidase and α-D-mannosidase from papaya (*Carica papaya*) seeds. *Agric. Biol. Chem.* **47**: 2441-2451.

239. Olle, D., Lozano, Y. and Brillouet, J-M. (1996). Isolation and characterization of soluble polysaccharides and insoluble cell wall material of the pulp from four mango (*Mangifera indica*. L) cultivars. *J. Agric. Food Chem.* **44**: 2658-2662.

240. Padmini. S. and Prabha, T. N. (1997). Biochemical changes during acetylene-induced ripening in mangoes (var. Alphonso). *Trop. Agric.* **74**: 265-271.

241. Pandey, R. M., Rao, M. M. and Singh, R. N. (1974). Biochemical changes in developing mango fruit (*Mangifera indica* L.), cv. Dashehari, *Prog. Hort.* **5**: 47-53.

242. Pang, S. Z. and Sanford, J. C. (1988). *Agrobacterium*-mediated gene transfer in papaya. *J. Amer. Soc. Hort. Sci.* **113**: 287-291.

243. Pantastico, E. B., Lam, L. R., Ketsa, S., Yuniarti, Y. and Kosittrakul. S. (1984). Mango - fruit development, post harvest physiology and marketing in ASEAN. In: *ASEAN Food Handling Bureau*, Mendoza, D. B. Jr. and Wills, R. B. H. (eds.). Kuala Lumpur, pp. 41-43.

244. Pasqualetto, P. L., Zimmerman, R. H. and Fordham, I. (1986). Gelling agent and growth regulator effects on shoot vitrification of 'Gala' apple *in vitro*. *J. Amer. Soc. Hort. Sci.* **111**: 976-980.

245. Pathak, N. and Sanwal, G. G. (1998). Multiple forms of polygalacturonase from banana fruits. *Phytochem.* **48**: 249-255.

246. Pathak, S. R. and Sarada, J. R. (1974). Lipids of mango (*Mangifera* indica .). *Curr. Sci.*. **43**: 716-719.

247. Peleg, M. (1979). Evaluation by instrumental methods of the textural properties of some tropical fruits. *J. Texture Studies* **10**: 45-65.

248. Pesis, E., Fuchs, Y. and Zauberman, G. (1978). Cellulase activity and fruit softening in avocado. *Plant Physiol.* **61**: 416-419.

249. Pharr, D. M., Sox, H. N. and nesbitt, W. B. (1976). Cell wall-bound nitrophenylglycosidases of tomato fruits. *J. Amer. Soc. Hort. Sci.* **101**: 397-400.

250. * Piechulla, K., Hinz, K. H. and Mannheim, W. (1985). Genetic and phenotypic comparison of three new avian Haemophilus-like taxa and of Haemophilus paragallinarum Biberstein and White 1969 with other members of the family Pasteurellaceae Pohl 1981.*Avian Dis.* **29**: 601-612.

251. Pierik, R. L. M. (1988). Handicaps for the large scale commercial application of micropropagation. *Acta Hort.* **230**: 63-71.

252. Pilnik. W. and Voragen, A. G. J. (1970). Pectic substances and other uronides. In: *The Biochemistry of Fruits and their Products*. Hulme, A. C. (ed.). Vol. I. Academic Press, London. pp. 53-87.

253. Pino, J., Rosado, A. and Sanchez, R. (1989). Volatile components of three cultivars of mango from cuba, *Nahrung* **33**: 709-712.

254. Polle, A. Y., Ovodova, R. G., Shashkov, A. S. and Ovodov, Y. S. (2002). Some structural features of pectic polysaccharide from tansy, *Tanacetum vulgare*. L. *Carbohydr. Polym.* **49**: 337-344.

255. Potrykus I. (1990). Gene transfer to cereals: an assessment. *Bio/Technology*. **8**: 535-542.

256. Prabha, T. N. and Bhagyalakshmi, N. (1998). Carbohydrate metabolism in ripening banana fruit. *Phytochem.* **48**: 915-919.

257. Prabha, T. N., Yashoda, H. M., Prasanna, V., Jagadeesh, B. H. and Bimba Jain, M. V., (2000). Carbohydrate metabolism in relation to textural softening during fruit ripening. *Trends Carbohydr. Chem.* **6**: 89-95.

258. Pressey, R. (1983). β-Galactosidase in ripening tomatoes. *Plant Physiol.* **71**: 132-135.

259. Pressey, R. (1986a). Extraction and assay of tomato polygalacturonases. *Hort. Sci.* **21**: 490-492.

260. Pressey, R. (1986b). Polygalacturonases in higher plants. In: *Chemistry and Function of Pectins*. Fishman, M. L and Jen, J. J. (eds.). Amer. Chem. Soc., Washington D.C. pp. 157-174.

261. Pressey, R. (1989). Endo-β-mannanase in tomato fruit. *Phytochem*. **28**: 3277-3280.

262. Pressey, R. and Avants, J. K. (1973). Separation and characterization of endopolygalacturonase and exopolygalacturonase from peaches. *Plant Physiol.* **52**: 252-256.

263. Pressey, R. and Avants, J. K. (1976). Pear polygalacturonases. *Phytochem*. **15**: 1349-1351.

264. Pressey, R. and Himmelsbach, D. S. (1984). ^{13}C-N.m.r. spectrum of a D-galactose-rich polysaccharide from tomato fruit. *Carbohydr. Res.* **127**: 356-359.

265. Priya Sethu, K. M. and Prabha, T. N. (1997). α-Mannosidase from *Capsicum annum*. *Phytochemistry.* **42**: 961-966.

266. Priya sethu, K. M., Prabha, T. N. and Tharanathan, R. N. (1996). Post-harvest biochemical changes associated with the softening phenomenon in *Capsicum annuum* fruits. *Phytochem.* **42**: 961-966.

267. Purseglove, J. W. (1972). Tropical Crops: Monocotyledons 1. Longman Group Limited., London. *Acta Hort*. **24**: 107.

268. Purseglove, J. W. (1974). *Tropical crops: Dicotyledons*. Vols. 1 and 2. ELBS and Longman.

269. Quintana, E. G., Nanthachai, P., Hiranpradit, H., Mendoza Jr, D. B. and Kesta, S. (1984). 'Changes in mango during growth and maturation'. In: *Mango: Fruit development, post-harvest physiology*

and marketing in ASEAN. Mendoza Jr, D. B. and Wills, R. B. H. (eds.). AFHB, Malaysia. p. 21.

270. Racker, E. (1962). Fructose-1,6-diphosphatase from spinach leaves. *Methods Enzymol.* **5**: 272-280.

271. Raghuvanshi, S. S. and Srivatsava, A. (1995). Plant regeneration of *Mangifera indica* using liquid shaker culture to reduce phenolic excudation. *Plant Cell, Tissue and Organ Culture.* **41**: 83-85.

272. Rangan, T. S., Murashige, T. and Bitters, W.P. (1968). *In vitro* initiation of nucellar embryos in monoembryonic Citrus. *HortScience*. **3**: 226-227.

273. Ranganna, S. (1977). In "*Mannual of Analysis of Fruits and Vegetable Products*". McGraw Hill Publishers, New Delhi, pp. 106-107.

274. Ranwala, A. P., Suematsu, C. and Masuda, H. (1992). The role of β-galactosidases in the modification of cell wall components during muskmelon fruit ripening. *Plant Physiol.* **100**: 1318-1325.

275. Rauvala, H. (1979). Use of triphenylmethane as an indicator of complete methylation of glycolipids and glycopeptides. *Carbohydr. Res.,* **72**: 257-260.

276. Redgwell, R. J., Melton, L. D. and Brasch, D. J. (1988). Cell-wall polysaccharides of kiwifruit (Actinidia deliciosa): chemical features in different tissue zones of the fruit at harvest. *Carbohydr. Res.* **182**: 241-258.

277. * Redgwell, R. J., Fischer, M., Kendal, E. and MacRae, E. A. (1997a). Galactose loss and fruit ripening: high-molecular weight arabinogalactans in the pectic polysaccharides of fruit cell walls. *Planta.* **203**: 174-181.

278. * Redgwell, R. J., MacRae, E. A., Hallet, I., Fischer, M., Perry, J. and Harker, R. (1997b). *In vivo* and *in vitro* swelling of cell walls during fruit ripening. *Planta* **203**: 162-173.

279. Redgwell, R. J., Melton, L. D. and Brasch, D. J. (1990). Cell-wall changes in kiwifruit following postharvest ethylene treatment. *Phytochem.* **29**: 399-407.

280. Redgwell, R. J., Melton, L. D. and Brasch, D. J. (1991). Cell-wall polysaccharides of kiwifruit (*Actinidia deliciosa*): Effect of ripening on the structural features of cell-wall materials. *Carbohydr. Res.* **209**: 191-202.

281. Redgwell, R. J., Melton, L. D. and Brasch, D. J. (1992). Cell wall dissolution in kiwifruit (*Actinidia deliciosa*). Solubilization of pectic polymers. *Plant Physiol.* **98**: 71-81.

282. Renard, C. M. C. G. and Thibault, J. F. (1993). Structure and properties of apple and sugar–beet pectins extracted by chelating agents. *Carbohydr. Res*. **244**: 99-114.

283. * Renard, C. M. C. G., Crepeau, M. J. and Thibault, J. F. (1999). Glucuronic acid directly linked to galacturonic acid in the rhamnogalacturonan backbone of beet pectins. *Eur. J. Biochem*. **266**: 566-574.

284. Rexova-Benkova, L. and Markovic. O. (1976) Pectic enzymes. *Adv. Carbohydr. Chem. Biochem*. **33**: 323-385.

285. Rhodes, M. J. C. (1980). The maturation and ripening of fruits. In: *Senescence in Plants*. Thimann, K. V. (Ed.). CRC Press, Inc. Boca Raton, Florida. pp. 157-205.

286. Rinaudo, M., Milas, M. and Dung, P.L. (1993). Characterization of chitosan, influence of ionic strength and degree of acetylation on chain expansion. *International Journal of Biological macromolecules*, **15**: 281-285.

287. Rizvi, A. F. and Tong, C. H. (1997). Fractional conversion for determining texture degradation kinetics of vegetables. *J. Food Sci*. **62**: 1-7.

288. Roe, B. and Bruemmer, J. H. (1981). Changes in pectic substances and enzymes during ripening and storage of 'Keitt' mangoes. *J. Food Sci.* **46**: 186-189.

289. Rose, J. K. C., Hadfield, K. A., Labavitch, J. M. and Bennett, A. B. (1998). Temporal sequence of cell wall disassembly in rapidly ripening melon fruit. *Plant Physiol*. **117**: 345-361.

290. * Ross, G. S., Redgwell, R. J. and MacRae, E. A. (1993). Kiwi fruit β-galactosidase: Isolation and activity against kiwifruit fruit cell wall polysaccharides. *Planta.* **189**: 499-506.

291. Ross, G. S., Wegrzyn, T., MacRae, E. A. and Redgwell, R. J. (1994). Apple β-galactosidase. Activity against cell wall polysaccharides and characterization of a related cDNA clone. *Plant Physiol*. **106**: 521-528.

292. Russel, P. L. and Juliano, B. O. (1983). Differential scanning calorimetry of rice starches. *Staerke*. **35**: 382-386.

293. Sagar, V. R., Khurdiya, D. S. and Balakrishnan, K. A (1999). Quality of dehydrated ripe mango slices as affected by packaging material and mode of packaging. *J. Food Sci. Technol.* **36**: 67-70.

294. Sakai, T., Sakamoto, T., Hallaert, J. and Vandamme, E. J. (1993). Pectin, pectinase and protopectinase: Production, properties and application. *Adv. Appl. Microbiol.* **39**: 213-294.

295. Sakurai, N. and Nevins, D. J. (1993) Changes in physical properties and cell wall polysaccharides of tomato (Lycopersicon esculentum) pericarp tissues. *Physiol. Plant.* **89**: 681-686.

296. Salimath, P. V. and Tharanathan, R. N. (1982). Carbohydrates of field bean (*Dolichos lablab*). *Cereal Chem.* **59**: 430-435.

297. Salunkhe, D. K. and Desai, B. B. (1984). Postharvest biotechnology of fruits. Vols. I and II. CRC Press, Boca Raton, FL, 168 p.23. FL, 147 p.24.

298. Satyan, H. S. and Patwardhan, M. V. (1984). Organic acid metabolism during ripening of fruits. *Indian J. Biochem. Biophys.* **20**: 311-314.

299. Saulnier, L., Brillouet, J. M. and Joseleau, J. P. (1988). Structural studies of pectic substances from the pulp of grape berries. *Carbohydr. Res.* **182**: 63-78.

300. Sawardeker, J. S., Sloneker, J. H. and Jeanes, A. (1965). Quantitative determination of monosaccharides as their alditol acetates by gas liquid chromatography. *Anal. Chem.* **37**: 1602-1604.

301. Schell, J. (1987 a). Transgenic plants as tools to study the molecular organization of plant genes. *Science.* **237**: 1176-1183.

302. Schell, J. (1987 b). Plant improvements by gene transfer. *In.* Gustav Fischer (ed.). *Bio Technology* **1**: 61-65. Stuttgart.

303. Schols, H. A., Posthumus, M. A. and Voragen, A. G. J. (1990). Structural features of hairy regions of pectins isolated from apple juice produced by the liquefaction process. *Carbohydr. Res.* **206**: 117-129.

304. Schuch, R., Justiniano, E., Schulz, M., Datz, S., Dittner, P. F., Giese, J. P., Krause, H. F., Schone, H., Vane, R. and Shafroth, S. (1991). Population of highly excited intermediate resonance states by electron transfer and excitation. *Phys. Rev. A.* **43**:5180-5183.

305. Selvaraj, Y. and Kumar, R. (1989). Studies on fruit softening enzymes and polyphenol oxidase activity in ripening mango (*Mangifera indica* L.) fruit. *J. Food Sci. Technol.* **26**: 218-222.

306. Selvaraj, Y., Kumar, R. and Pal, D. K. (1989). Changes in sugars, organic acids, amino acids, lipid constituents and aroma characteristics of ripening mango (*Mangifera indica* L.) fruit. *J. Food Sci. Technol.* **26**: 308-313.

307. Selvendran, R. R. (1975). Analysis of cell wall material from plant tissues: Extraction and purification. *Phytochem.* **14**: 1011-1017.

308. Selvendran, R. R. (1985). Developments in the chemistry and biochemistry of pectic and hemicellulosic polymers. *J. Cell Sci.* (Suppl.) **2**: 51-88.

309. Selvendran, R. R. and O'Neil, M. A. (1987). Isolation and analysis of cell walls from plant material. *Methods Biochem. Anal.,* **32**: 25-153.

310. Selvendran, R. R., March, J. F. and Ring, S. G. (1979). Determination of aldoses and uronic acid content of vegetable fiber. *Anal. Biochem.* **96**: 282-292.

311. Seymour, G. B. and Tucker, G. A. (1993). Avocado. In: *Biochemistry of fruit ripening*. G.B. Seymour et al. (eds.). Chapman and Hall, London, pp. 53-81.

312. Seymour, G. B., Wainwright, H. and Tucker, G. A. (1989). *Aspects of Applied Biology*. **20**: 93.

313. Seymour, G. B, Taylor, J. E and Tucker, G. A. (1993) (eds.) *Biochemistry of Fruit Ripening*. Chapman and Hall, pp. 1-454.

314. * Seymour, G. B. and Gross, K. C. (1996). Cell wall disassembly and fruit softening. *Postharvest News and Information* **7**: 45N-52N.

315. Seymour, G. B. and Harding, S. E. (1987). Analysis of the molecular size of tomato (*Lycopersicon esculentum* Mill.) fruit polyuronides by gel filtration and low speed sedimentation equilibrium. *Biochem. J.* **245**: 463-466.

316. Seymour, G. B., Colquhoun, I. J., Dupont, M. S., Parsley, K. R. and Selvendran, R. R. (1990). Composition and structural features of cell wall polysaccharides from tomato fruits. *Phytochem.* **29**: 725-731.

317. Seymour, G. B., Harding, S. E., Taylor, A. J., Hobson, G. E. and Tucker, G. A. (1987). Polyuronide solubilization during ripening of normal and mutant tomato fruit. *Phytochem.* **26**: 1871-1875.

318. Sharaf, A., Ahmed, F. A. and El-Saadany, S. S. (1989). Biochemical changes in some fruits at different ripening stages. *Food Chem*. **31 (1)**:19-26.

319. Shashirekha, M. S. and Patwardhan, M. V. (1976). Changes in aminoacids, sugars and non-volatile organic acids in a ripening mango fruit (*Mangifera indica* Badami variety) *Lebensm. Wissens. Technol.* **9**: 369-370.

320. Sheikholeslam, S. N. and Weeks, D. P. (1987). Acetosyringone promotes high efficiency transformation of *Arabidopsis thaliana* explants by *Agrobacterium tumefaciens*. *Plant Mol. Biol.* **8**: 291-298.

321. Shetty, K. and McKersie, B. D. (1993). Proline, thioproline and potassium mediated stimulation of somatic embryogenesis in alfalfa (Medicago sativa L.). *Plant Sci.* **88**: 185-193.

322. Shewfelt, R. L. (1986). Postharvest treatment for extending the shelf life of fruits and vegetables. *Food Technol.* **40**: 70-80, 89.

323. Siddappa, G. S. and Bhatia, B. S. (1954). The identification of sugars in fruits by paper chromatography. *Indian J. Hort.* **11**: 104-107.

324. Siddiqui, I. R. and Wood, P. J. (1971). DEAE-Cellulose carbonate form. A useful medium for fractionating polysaccharides. *Carbohydr. Res.* **16**: 452-454.

325. Singh, L. B. (1960). *The Mango*. Leonard Hill, London, Second impression.

326. Singh, R. N. (1990). *Mango*. Indian Council Agricultural Research, New Delhi, India.

327. Sirisomboon, P., Tanaka, M., Fujitha, S. and Kojima, T. (2000). Relationship between the texture and pectin constituents of Japanese pear. *J. Texture Studies.* 31: 679-690.

328. Smith, B. G. and Harris, P. J. (1995). Polysaccharide composition of unlignified cell walls of pineapple (*Ananas comosus* L. Merr.) fruit. *Plant Physiol.* **107**: 1399-1409.

329. Smith, C. J. (1999). Carbohydrate biochemistry. In: *Plant Biochemistry and Molecular Biology*. Lea, P. J and Leegood, R. C. (eds.). II edition. John Willey & Sons. New York. pp. 81-118.

330. Smith, C. J. S., Watson, C. F., Ray, J., Bird, C. R., Morris, P. C., Schuch, W. and Grierson, D. (1988). Antisense RNA inhibition of polygalacturonase gene expression in transgenic tomatoes. *Nature.* **334**: 724-726.

331. Snaith, S. M. and Levvy, G. A. (1973). In: *Advances in carbohydrate chemistry and biochemistry*. Tipson, R. S. and Horton, D. (eds). Academic Press. Inc., pp 401-445.

332. Sobotka, F. E. and Stelzig, D. A. (1974). An apparent cellulase complex in tomato (*Lycopersicon esculentum*) fruit. *Plant Physiol.* **53**: 759-763.

333. Sofiari, E., Raemakers, C. J. J. M., Bergervoes, J. E. M., Jacobsen, E. and Vissez, R. G. F. (1998). Plant regeneration from protoplast isolated from friable embryogenic callus of cassava. *Plant Cell Rep*. **18**: 159-165.

334. Spencer, J. L., Morris, M. P. and Kennard, W. C. (1956). Vitamin C concentration in developing and mature fruits of mango. *Plant Physiol.* **31**: 79-82.

335. * Stahl, A. (1933). Changes in composition of Florida avocados in relation to maturity. Bulletin of the University of Florida, *Agricultural experimental station.* **259**: 1-61.

336. Stachel, S. E., Timmerman, B. and Zambryski, P (1987). Activation of *Agrobacterium tumefaciens vir* gene expression generates multiple single-stranded T-strand molecules from the pTiA 6 T-region: requirement for 5' *vir* D gene products. *EMBO J.* **6**: 857-863.

337. Stevens, B. J. H. and Selvendran, R. R. (1984). Structural features of cell- wall polymers of the apple. *Carbohydr. Res.* **135**: 155-166.

338. Steward, F. C., Israel, H. W., Mott, R. L., Wilson, H. J. and Krikorian, A. D. (1975). Observations on growth and morphogenesis in cultured cells of carrot (*Daucus carota* L.). Phil. Trans. R. Soc. London, Ser. B. **273**: 33-53.

339. Stewart, D., Iannetta, P. P. M. and Davies, H. V. (2001). Ripening-related changes in raspberry cell wall composition and structure. *Phytochem.* **56**: 423-428.

340. Still, D. W. and Bradford, K. J. (1997). Endo-β-mannanase activity from individual tomato endosperm caps and radicle tips in relation to germination rates. *Plant Physiol.* **113**: 21-29.

341. Stolle-Smits, T., Beekhuizen, J. G., Van Dijk, C., Voragen, A. G. J. and Recourt, K. (1997). Changes in pectic and hemicellulosic polymers of green beans (*Phaseolus vulgaris* L.) during industrial processing. *J. Agric. Food Chem.* **45**: 4790–4799.

342. Strasser, G. R. and Amado, R. (2002). Pectic substances from red beet (*Beta vulgaris* conditiva) Part-II. Structural characterization of rhamnogalacturonan II. *Carbohydr. Polym.* **48**: 263-269.

343. Subramanyam, H., Krishnamurthy, S. and Parpia, H. A. B. (1975). Physiology and biochemistry of mango fruit. *Adv. Food Res.* **21**: 223-305.

344. Suvarnalatha, G. and Prabha, T. N. (1999). α-D- Mannosidase from *Lycopersicon esculentum* II. *Phytochem.* **50**: 1111-1115.

345. Swanson, M. A. (1955). Glucose-6-phosphatase from liver. *Methods Enzymol.* **2**: 541-543.

346. * Talbott, L. D. and Ray, P. M. (1992). Molecular size and separability features of pea cell wall polysaccharides. *Plant Physiol.* **98**: 357-368.

347. Tandon, D. K. and Kalra, S. K. (1983). Changes in sugars starch and amylase activity during development of mango fruit cv. Dashehari. *J. Hort. Sci.* **58**: 449-454.

348. Tandon, D. K. and Kalra, S. K. (1984). Pectin changes during the development of mango fruit cv Dashehari. *J. Hort. Sci.* **59**: 283-286.

349. Taussky, H. H. and Shorr, E. (1953). A microcalorimetric method for the determination of inorganic phosphate. *J. Biol. Chem.* **202**: 675-685.

350. Taylor, R. L. and Conrad, H. E. (1972). Stoichiometric depolymerization of polyuronides and glycosaminoglycuronans to monosaccharides following reduction of their carbodiimide-activated carboxylic groups. *Biochem.* **11**: 1383-1388.

351. Teasdale, R. D. (1987). Micronutrients. In: *Cell and Tissue Culture in Forestry.* Bonga, J. M. and Durzan, D. J. (Eds.). Vol **1.** Martinus Nijhoff, Dordrecht. pp.17-36.

352. Thakur, B. R., Singh, R. K. and Handa, A. K. (1997). Chemistry and uses of pectin- A review. *Crit. Rev. Food Sci. Nutr.* **37**: 47-73.

353. Tharanathan, R. N. (1995). Starches – The polysaccharides of high abundance and usefulness. *J. Sci. Indus. Res.* **34**: 452-458.

354. Tharanathan, M. and Tharanathan, R. N. (2001). Resistant starch in wheat-based products: Isolation and characterization. *J. Cereal Sci.* **34**: 73-84.

355. Tharanathan, R. N., Muralikrishna, G., Salimath, P. V and Raghavendra Rao, M. R. (1987). Plant carbohydrates- an overview. *Proc. Ind. Acad. Sci. (Plant Sci.)* **97**: 81-155.

356. Themmen, A. P. N., Tucker, G. A. and Grierson, D. (1982). Degradation of isolated tomato cell walls by purified polygalacturonase *in vitro*. *Plant Physiol.* **69**: 122-124.

357. Thomas, M. and Thibault, J. F. (2002). Cell wall polysaccharides in the fruits of Japanese quince (*Chaenomeles japonica*): extraction and preliminary characterization. *Carbohydr. Polym.* **49**: 345-355.

358. Tieman, D. M., Harriman, R. W., Ramamohan, G. and Handa, A. K. (1992). An antisense pectin methylesterase gene alters pectin chemistry and soluble solids in tomato fruit. *Plant Cell.* **4**: 667-679.

359. Ting, I. P. (1968). CO_2 metabolism in Corn roots III. Inhibition of P-enolpyruvate carboxylase by L-malate. *Plant Physiol.* **43**: 1919-1924.

360. Tjiptono, P., Lam, P. E. and Mendoza, D. B. Jr. (1984). Status of the mango industry in ASEAN in mango. ASEAN Food Handling Bureau, pp. 1-11.

361. Tong, C. B. S. and Gross, K. C. (1988). Glycosyl-linkage composition of tomato fruit cell wall hemicellulosic fractions during ripening. Physiol. *Plant.* **74**: 365-370.

362. Tucker, G. A. (1993). Introduction. In: *Biochemistry of Fruit Ripening*. Seymour, G. B., Taylor, J. E., Tucker, G. A. (eds.). Chapman and Hall, London. pp. 1-51.

363. Tucker, G. A. and Grierson, D. (1987). Fruit ripening. In: *The Biochemistry of Plants*. Davies, D. (Ed.). Vol. **12.** Academic Press Inc., New York, pp. 265-319.

364. Tucker, G. A. and Seymour, G. (1991). Cell wall degradation during mango fruit ripening. *Acta Hort*. **291**: 454-460.

365. Uematsu, C., Murase, M., Ichikawa, H. and Imamura, J., (1991). *Agrobacterium*-mediated transformation and regeneration of kiwi fruit. *Plant Cell Rep*. **10**: 286-290.

366. Van Buren, J. P. (1979). The chemistry of texture in fruits and vegetables. *J. Texture Studies* **10**: 1-23.

367. Vardi, A., Bleeichmsn, S. and Aviv, D. (1990). Genetic transformation of *Citrus* protoplasts and regeneration of transgenic plants. *Plant Sci.* **69**: 99-206.

368. Vasil, I. K. (1990). The realities and challenges of plant biotechnology. *Bio Technology.* **8**:296-301.

369. Vidal, S., Williams, P., O'Neill, M. A. and Pellerin, P. (2001). Polysaccharides from grape berry cell walls. Part I: tissue distribution and structural characterization of the pectic polysaccharides. *Carbohydr. Polym*. **45**: 315-323.

370. Visser, R. G., Stolte, A. and Jacobsen, E. (1991). Expression of a chimaeric granule-bound starch synthase-GUS gene in transgenic potato plants. *Plant Mol Biol.* **17**: 691-699.

371. Voragen, A. G. J., Pilnik, W., Thibault, J. F., Axelos, M. A. V. and Renard, C. M. C. G. (1995). Pectins. In: *Food Polysaccharides and their Applications*. Stephen, A M (ed.). Marcel Dekker, Inc. New York. pp. 287-339.

372. Wade, N. L., Kavanagh, E. E., Hokley, D. G. and Brady, C. J. (1992). Relationship between softening and the polyuronides in ripening banana fruit. *J. Sci. Food Agric.* **60**: 61- 68.

373. Waldron, K. W., Smith, A. C., Parr, A. J., Ng. A. and Parker, M. L. (1997). New approaches to understanding and controlling cell separation in relation to fruit and vegetable texture. *Trends Food Sci. Technol.* **8**: 213-221.

374. Wallner, S. J. (1978). Apple fruit β-galactosidase and softening in storage. *J. Amer. Soc. Hort. Sci.* **103**: 364-366.

375. Wallner, S. J. and Bloom, H. L. (1977). Characteristics of tomato cell wall degradation *in vitro*. Implications for the study of fruit-softening enzymes. *Plant Physiol.* **60**: 207-210.

376. Wallner, S. J. and Walker, J. E. (1975). Glycosidases in cell wall-degrading extracts of ripening tomato fruits. *Plant Physiol.* **55**: 94-98.

377. Wang, K., Stachel, S. E., Timmerman, B., Van Montagu, M. and Zambryski, P. C. (1987). Site specific nick in the T-DNA border sequence as a result of *Agrobacterium* vir gene expression. *Science*. **235**: 587-591.

378. Wang, Y. C. and Janick, J. (1984). Inducing precocious germination in asexual embryos of cacao. *HortScience*. **19**: 839-841.

379. * Wardlaw and Leonard (1936). The storage of West Indian mangoes. *Low Temp. Res. Sta. Mem.* **3**: 1.

380. Watkins, C. B., Haki, J. M. and Frenkel, C. (1988). Activities of polygalacturonase, α-D-mannosidase, and α-D- and β-D-galactosidase in ripening tomato. *Hort. Sci.* **23**: 192-194.

381. * Wetherell, D. F. (1984). Enhanced adventive embryogenesis resulting from plasmolysis of cultured wild carrot cells. *Plant cell Tissue. Org. cult.* **3**: 221-227.

382. * Whitaker, J. R. (1984). Pectic substances, pectic enzymes and haze formation in fruit juices. *Enzym. Microb. Technol.* **6**: 341-349.

383. Williams, E. S. and Maheswaran, B. (1986). Somatic embryogenesis: factors influencing coordinated behavior of cells as an embryogenic group. *Ann. Bot.* **57**: 443-462.

384. Wong, D. W. S. (1995). Pectic enzymes. In: *Food Enzymes. Structure and Mechanisms.* Chapman and Hall, New York. pp. 212-236.

385. * Yamaki, S. and Kakiuchi, N. (1979). Changes in hemicellulose-degrading enzymes during development and ripening of Japanese pear fruit. *Plant and Cell Physiol.* **20**: 301-309.

386. * Yamaki, S. and Matsuda, K. (1977). Changes in the activities of some wall degrading enzymes during development of Japanese pear fruit (*pyrus serotina* Rehder var. culta Rehder). *Plant Cell Physiol.* **18**: 81-93.

387. Yamaki, S., Kajiura, I., Omura, M. and Matsuda, K. (1977). Watercore in Japanese pear. III Changes in the activities of some enzymes relating to the degradation of cell walls and the accumulation of sugar. *Scientia Horticulturae*. **6**: 45-53.

388. Yang, S. F. (1985). Biosynthesis and action of ethylene. *Hort.Sci.* **20**: 41-45.

389. York, W. S., Darvill, A. G., McNeil, M., Stevenson, T. T. and Albersheim, P. (1985). Isolation and characterization of plant cell walls and cell wall components. *Methods Enzymol.* **118**: 3-40.

390. Yoshihisa, T., Oshumi, Y. and Anraku, Y. (1988). Solubilization and purification of α-mannosidase, a marker enzyme of vacuolar membranes in *Sacchromyces cerevisiae. J. Biol. Chem*. **263**: 5158.

391. Yu, L., Reitmeier, C. A. and Love, M. H. (1996). Strawberry texture and pectin content as affected by electron beam irradiation. *J. Food Sci*. **61**: 844-846.

392. * Zainal, Z., Tucker, G. A. and Lycett, G. W. (1996). A *rab11*-like gene is developmentally regulated in ripening mango (*Mangifera indica* L.) fruit. *Biochem. Biophys. Acta* **1314**: 187-190.

393. Zhan, D., Janssen, P. and Mort, A. J. (1998). Scarcity or complete lack of single rhamnose residues interspersed within the homogalacturonan regions of citrus pectin. *Carbohydr. Res.* **308**: 373-380.

394. * Ziv, M. (1991). Quality of micropropagated plants-vitrification. *In vitro Cell Dev. Biol.* **27**: 64-69.

* Original reprints were not referred to.